EPIDEMIOLOGY AND INTEGRATED MANAGEMENT OF BACTERIAL LEAF SPOT CAUSED BY *PSEUDOMONAS SYRINGAE* PV. *APTATA* IN TABLE BEET AND SWISS CHARD SEED PRODUCTION IN WESTERN WASHINGTON

By

MARILEN NAMPIJJA

A dissertation submitted in partial fulfillment of
the requirements for the degree of

DOCTOR OF PHILOSOPHY

WASHINGTON STATE UNIVERSITY
Department of Plant Pathology

May 2025

To the Faculty of Washington State University:

The members of the Committee appointed to examine the dissertation of MARILEN NAMPIJJA find it satisfactory and recommend that it be accepted.

Lindsey J. du Toit, Ph.D., Chair

Achour Amiri, Ph.D.

Gary Chastagner, Ph.D.

David Weller, Ph.D.

ACKNOWLEDGMENTS

I would like to express my heartfelt gratitude to my advisor, Lindsey du Toit, for your unwavering guidance and support throughout my PhD journey and during the writing of this dissertation. I am deeply appreciative of the diverse skillset I have gained in laboratory, greenhouse, and field research under your mentorship. Your expertise and encouragement have been instrumental in shaping my growth as a researcher. To my PhD Committee Members, Achour Amiri, Gary Chastagner, and David Weller, it has been an honor working with you. I am truly grateful for your constructive feedback, thoughtful insights, and willingness to provide guidance whenever I sought your input. Your support has greatly enriched my academic and professional development.

I extend my sincere appreciation to the United States Department of Agriculture National Institute of Food and Agriculture Specialty Crop Research Initiative (USDA-NIFA-SCRI) Project No. 2019-51181-30019 for funding my research. Your generous financial support allowed me to complete my PhD without financial burden, for which I am truly grateful. I am also deeply thankful to Dick and Marcia Morrison Seed Production Pathology & Seed Health Fellowship, Alfred Mark Christianson Memorial Fellowship, Pacific Seed Association Scholarship, American Phytopathological Society Raymond J. Tarleton Student Fellowship, and the Washington State University Department of Plant Pathology for their generosity and belief in my work.

I am incredibly fortunate to have collaborated with Dr. Carolee Bull (Pennsylvania State University) and Dr. Neha Potnis (Auburn University) through the USDA-NIFA-SCRI Grant. Your guidance and support in various aspects of my research have been invaluable. I am also grateful to Dr. Jonathan Jacobs (Ohio State University) for introducing me to confocal

microscopy, and to Dr. Nikki Galatti (Western Washington University) for granting me access to the microscopy facility to conduct my research. Special thanks to the Vegetable Seed Pathology Team, especially Mike Derie, for his guidance throughout my research. Tomasita Villarroel and Babette Gundersen, I am deeply appreciative of your support in various aspects of my work.

To my husband, Garon Galloway, words cannot fully express my gratitude for your unwavering support throughout my PhD, especially during the most critical moments of completing my dissertation. You have been my biggest supporter during my lowest points and my greatest cheerleader in moments of success. To my wonderful children, Etienne Bugingo and Eleana Galloway, you have been a source of joy and comfort, bringing light into my life even during the most demanding times. To the entire Galloway family, your support and encouragement throughout my PhD journey mean the world to me, and I am profoundly grateful.

Finally, I extend my deepest gratitude to my mother, Rose Namutebi Bagundidde, for her unwavering love, sacrifices, and constant guidance. To my late father, Joseph Bagundidde (rest in eternal peace), I owe so much of who I am today to the values you instilled in me from childhood. Your wisdom and guidance continue to inspire me, and I hold you dearly close to my heart. Memories of you are still fresh and I think about you every day. To my siblings, thank you for being a pillar of support and encouragement throughout my life. I would not wish for any other siblings besides you. Your belief in me has been a constant source of strength, and for that, I am forever grateful.

EPIDEMIOLOGY AND INTEGRATED MANAGEMENT OF BACTERIAL LEAF SPOT CAUSED BY *PSEUDOMONAS SYRINGAE* PV. *APTATA* IN TABLE BEET AND SWISS CHARD SEED PRODUCTION IN WESTERN WASHINGTON

Abstract

by Marilen Nampijja, Ph.D.
Washington State University
May 2025

Chair: Lindsey du Toit

Bacterial leaf spot (BLS), caused by *Pseudomonas syringae* pv. *aptata* (Psa), has become more prevalent in table beet (*Beta vulgaris* subsp. *vulgaris* Condivita Group) and Swiss chard (*Beta vulgaris* subsp. *vulgaris* Cicla Group) seed production in the Pacific Northwest (PNW). This disease has caused significant economic losses due, in part, to increased demand for seed to plant baby leaf beet and Swiss chard crops which have become more popular as a result of the convenience and perceived health of these leafy green products. The PNW region of the United States produces up to 40% of the global supply of beet and chard seed (Western Washington Seed Advisory Committee, *personal communication*). Psa is a seedborne and seed transmitted pathogen that is characterized by testing positive for levan production; negative for oxidase, pectinolytic activity, and arginine dihydrolase production; and positive for tobacco hypersensitivity (+---+) LOPAT reaction. The objectives of this study were to: 1(i) determine the prevalence and genetic diversity of Psa in table beet and Swiss chard seed crops in western Washington, and (ii) identify genetic factors that differentiate strains of *P. syringae* pv. *aptata*

pathogenic to beet and chard from non-pathogenic strains of *P. syringae*, and that differentiate strains pathogenic to beet and chard vs. beet only; (2) investigate the colonization of table beet and Swiss chard plants by Psa in the vegetative and reproductive growth stages; and 3 (i) determine the location of infection of table beet and Swiss chard seed by Psa, (ii) evaluate hot water and bleach seed treatments for management of seedborne Psa, and (iii) evaluate potential use of decortication for control of seedborne Psa. BLS was present in 72% of the beet and chard seed crops surveyed in 2020 but absent in all seed crops surveyed in 2021 and 2023. Pathogenicity tests on beet and chard seedlings demonstrated variation in virulence among Psa isolates from the beet and chard crops surveyed, with some isolates more virulent on beet than chard. A wide diversity of Psa strains was detected in surveys of beet and chard seed crops, based on multi-locus sequence analysis (MLSA) and whole-genome sequencing (WGS) of 38 strains. However, non-pathogenic isolates of *P. syringae* of these crops also grouped with pathogenic isolates, with genetic evidence of possible horizontal gene transfer between pathogenic and non-pathogenic isolates. Of 192 isolates, there were 25 from table beet seed crops, and one isolate from a table beet fresh market crop that were 100% identical to the pathotype strain CFBP $1617^{PT}$of Psa based on MLSA. Based on WGS, Type III effectors of the Psa strains are located in the pathogenicity island comprised of the conserved effector locus (CEL), the hypersensitivity response and pathogenicity (*hrp*)/HR and conserved genes(*hrc*), and the exchangeable effector locus (EEL), with the EEL being the most variable of these three loci among strains. Greenhouse trials were completed with two strains of Psa tagged with a green fluorescent protein (GFP), GFP-Pap009, which causes BLS on table beet and Swiss chard; and GFP-Pap014, which causes BLS on table beet only. Both strains colonized both the epidermis and apoplast of inoculated table beet and Swiss chard leaves, contrary to the hypothesis that

Pap014 is non-pathogenic on Swiss chard if it can only colonize the epidermis, not the apoplast, of chard leaves. However, GFP-Pap009 was recovered at significantly greater populations (~500-fold) than GFP-Pap014 by 72 h after inoculation. Confocal microscopy revealed that Psa colonization is concentrated along the guard cells of stomata and the walls of spongy mesophyll cells in the apoplast, indicating that stomata may be important entry points for infection. A table beet seed crop field trial was inoculated with a rifampicin resistant strain of Psa (rif-Pap010) in each of three years (2021-2023) to monitor development of Psa and BLS in the seed crop. Fluctuating environmental conditions over the duration of each season had a significant impact on Psa population and BLS development. The amount of rif-Pap010 recovered from samples in each table beet seed crop trial varied over the duration of the trial. The rif-Pap010 population increased following each inoculation but declined when conditions remained dry. In 2021, seedborne rif-Pap010 was detected on the harvested seed compared to the 2022 harvested table beet seed at ~200-fold greater population (mean of $Log_{10}4.9 \pm 0.1$ vs. $Log_{10}2.5 \pm 0.4$ CFU/g seed), respectively. The recovery of rif-Pap010 population from each of three asymptomatic weed hosts, lambsquarters (*Chenopodium album*), pigweed (*Amaranthus retroflexus*) and ladysthumb (*Persicaria maculosa*), also varied widely over the trial duration, but demonstrated that weeds could serve as reservoirs for the pathogen in seed crops. Rif-Pap010 was only recovered from the pericarps, not the embryos, of the seed lots harvested from the inoculated beet seed crop field trials in 2021, 2022, and 2023. Chlorine seed treatment (1.2% NaOCl for 5, 15, 25, 35 minutes) eradicated rif-Pap010 from the 2021 seed lot at all durations of treatment but not from the 2023 seed lot. Evaluation of hot water seed treatments using the 2021 and 2023 harvested seed lots from the field trials revealed that treatment at 55℃ for 40 or 50 minutes eradicated rif-Pap010 without affecting seed quality (germination) adversely. Although treatment

at 60℃ was highly effective for eradication of Psa at all durations, treatment for >30 minutes reduced seed germination. For the decortication trial with 2021 seed lot, the highest amount of rif-Pap010 was recovered from the powder removed from the seed by decortication of the table beet seed samples (log_{10}4.9 ± 0.0 CFU/g powder) recovered compared to (log_{10}4.7 ± 0.1 CFU/g seed for the non-decorticated seed), and (log_{10}3.9 ± 0.1 CFU/g seed) for the decorticated seeds. This study unravels some of the complexities of the epidemiology, genetic diversity, and management of Psa in table beet seed production in the Pacific Northwest USA.

TABLE OF CONTENTS

Page

LIST OF TABLES

Page

LIST OF FIGURES

Page

Dedication

To my parents Rose Namutebi Bagundidde and Joseph Bagundidde (late). You have been a pillar of strength throughout my life. I will forever be grateful for your unconditional love and support.

CHAPTER ONE: PREVALENCE AND GENETIC DIVERSITY OF *PSEUDOMONAS SYRINGAE* PV. *APTATA* IN TABLE BEET AND SWISS CHARD SEED PRODUCTION IN WASHINGTON STATE

Introduction

Amaranthaceae plants include Swiss chard (*Beta vulgaris* subsp. *vulgaris* Cicla Group), table beet (*Beta vulgaris* subsp. *vulgaris* Condivita Group), sugar beet (*Beta vulgaris* subsp. *vulgaris* Altissima Group), Mangel-wurzel (*Beta vulgaris* var. *macrorhiza*), spinach (*Spinacia oleracea*), lambsquarters (*Chenopodium album*), quinoa (*Chenopodium quinoa*), and other genera and species (Harveson et al. 2009; Nottingham 2004). Previously, these and related species were classified in Chenopodiaceae (goosefoot family) (Nottingham 2004). All subspecies of *B. vulgaris* are biennial, requiring two years for seed production (du Toit 2007; Harveson et al. 2009; Schrader and Mayberry 2003). The seed crops require photothermal induction for bolting (transition from vegetative to reproductive growth), i.e., both vernalization and long day length. Vernalization requirements include exposure of roots to cold enough temperatures (0 to 15°C) for 5 to 20 weeks to induce bolting (Abo-Elwafa et al. 2006; du Toit 2007; Kockelmann et al. 2010; Mutasa-Göttgens et al. 2010; Navazio et al. 2010). The maritime Pacific Northwest (PNW), encompassing western Oregon and western Washington, is the only region in the United States with suitable environmental conditions for production of beet and chard seed crops (du Toit 2007). Approximately 95% of the table beet and Swiss chard seed crops grown in the United States are produced in this region. The winters are cold enough for vernalization to trigger bolting, but not so cold as to kill overwintering plants. This, coupled with the reasonably dry summers with low relative humidity, creates optimal conditions for production of beet and chard

seed crops (du Toit 2007; Organic Seed Alliance 2016; Rackham 2002; Schreiber and Ritchie 1995). Other regions of the world where beet and chard seed production occur include Chile, northern Europe, New Zealand, and South Africa (Jacobsen 2009).

Pseudomonas syringae pv. *aptata* causes bacterial leaf spot of all *B. vulgaris* subspecies (Jacobsen 2009). The bacterium is motile with polar, multitrichous flagella, and can either be fluorescent or non-fluorescent on King's B agar medium (King et al. 1954; Lelliott et al. 1966; Safni et al. 2016). The bacterium is also positive for levan and negative for pectolytic activity, oxidase, and arginine dihydrolase production; and causes a hypersensitive response when injected into tobacco leaves. Therefore, this bacterium belongs to LOPAT group 1 of *P. syringae* isolates, with a + - - - + profile (Lelliott et al. 1966).

Bacterial leaf spot symptoms include dark brown to black lesions that range from 2 to 3 mm in diameter, or larger when lesions coalesce, each with a distinct brown to black border (Crane 2023; Derie et al. 2016; Jacobsen 2009; Koike et al. 2003). Lesions become dry, light brown to tan, and paper thin during dry conditions (Jacobsen 2009; Koike et al. 2003; Nampijja et al. 2021; Walker 1952). *P. syringae* pv. *aptata* can infect leaves, stems, or petioles via hydathodes, stomata, and wounds (Jacobsen 2009; Nikolić et al. 2018). The pathogen can spread in wind-blown, aerosolized infected plant particles, and is splash-dispersed. The bacterium can persist as an epiphyte on a number of plant species without causing symptoms (Riffaud and Morris 2002). *P. syringae* pv. *aptata* is readily seedborne and seed transmitted in beet and chard (Jacobsen 2009)

P. syringae pv. *aptata* has been reported in various parts of the world, including the European Union (Belgium, France, Hungary, Italy, the Netherlands), Republic of Serbia, Switzerland, United Kingdom, Asia (Iran, India, Japan, and South Korea), Australia, New

Zealand, and United States (Arabi et al. 2006; Hill 1979; Jacobsen 2009; Janse 1979; Nikolić et al. 2018; Stojšin et al. 2015; Walker 1952). In the United States, *P. syringae* pv. *aptata* has been reported to cause bacterial leaf spot in Arizona, California, Colorado, Georgia, Kentucky, Montana, North Dakota, Nebraska, Oregon, and Washington (Arabiat et al. 2016; Bradbury 1986; Derie et al. 2016; Dutta et al. 2024; Harveson et al. 2009; Khan et al. 2023; Koike et al. 2003; Nampijja et al. 2021). Other plant species can be colonized symptomatically or asymptomatically by *P. syringae* pv. *aptata*, including corn (*Zea mays* subsp. *mays*), cantaloupe (*Cucumis melo* var. *cantalupensis*), squash (*Cucurbita moschata*), oat (*Avena sativa*), tomato (*Solanum lycopersicum*), soybean (*Glycine max*), lettuce (*Lactuca sativa*), pepper (*Capsicum* spp.), onion (*Allium cepa*), and sunflower (*Helianthus annuus*) (Jacobsen 2009; Koike et al. 2003; Morris et al. 2000; Sedighian et al. 2014; Tymon and Inglis 2017).

Over the past several decades, bacterial leaf spot has gained greater economic importance in table beet and Swiss chard seed production due to the rising demand for seed to plant the expanding acreage of baby leaf beet and chard crops (Crane 2023). This increase in baby leaf production is driven partly by increased public awareness of the nutritional benefits of vegetables and the convenience of pre-packaged salads (Lin et al. 2003). In baby leaf chard and beet crops, incidences of bacterial leaf spot and other foliar diseases as low as 5% can lead to rejection of entire crops because of the difficulty of sorting symptomatic leaves (Crane 2023; Derie et al. 2016). The risk of bacterial leaf spot is particularly high in baby leaf crops because the dense plantings (7 to 9 million seed/ha), overhead irrigation, and sequential plantings create a highly conducive environment for seed transmission of *P. syringae* pv. *aptata* and development of bacterial leaf spot. Derie et al. (2016) carried out field trials in western Washington in 2015 to evaluate thresholds for seed transmission of *P. syringae* pv. *aptata*. Seedborne infection levels as

low as 10^2 CFU/g seed resulted in seed transmission and bacterial leaf spot development. In subsequent field trials in the same region in 2020 and 2021 (Crane 2023), the threshold for seedborne inoculum that resulted in ≥5% severity of bacterial leaf spot ranged from 0 to ~6 x 10^4 CFU/g seed, depending on prevailing environmental conditions, i.e., planting non-infected seed under favorable conditions (wet and cool) may be essential to ensure baby leaf crops do not develop bacterial leaf spot.

Gaulke and Goldman (2022) demonstrated that the table beet cv. Touchstone Gold and Swiss chard cv. Rainbow were the most resistant to bacterial leaf spot of 21 table beet and Swiss chard cultivars, 5 table beet breeding lines, and 26 plant introduction (PI) lines screened in greenhouse conditions, when inoculated with a single strain of *P. syringae* pv. *aptata*. However, studies have shown wide variation in virulence among strains of *P. syringae* pv. *aptata* to beet and chard, e.g., Nikolić et al. (2018), and that some strains are pathogenic only to beet, not chard (Nampijja et al. 2023; Safni et al. 2016). In addition, some isolates of the bacterial leaf spot pathogen differ genetically from the pathotype strain of *P. syringae* pv. *aptata* (Nikolić et al. 2018; Safni et al. 2016), complicating efforts to characterize and diagnose the pathogen efficiently. Currently, there are no rapid diagnostic tools, such as PCR assays, that can be used to detect and differentiate *P. syringae* pv. *aptata* strains that cause bacterial leaf spot from non-pathogenic strains of *P. syringae*, both of which are common in regions of beet and chard production, and in beet and chard seed lots (Derie et al. 2016; Safni et al. 2016). Furthermore, there can be wide differences in prevalence of bacterial leaf spot among seasons, e.g., the disease was not detected in a survey of beet and chard seed crops in western Washington in 2015, a very warm and dry season (L. du Toit, *unpublished data*).

Determining the core phylogeny of *P. syringae* is critical for understanding the genetic relationships and evolutionary history of this highly diverse bacterial species, which includes strains with varying pathogenic potential (Bull et al. 2015; Derie et al. 2016; Safni et al. 2016). This is because pathovar nomenclature may not be a reliable approach to identify and classify these strains. Therefore, understanding the diversity of these strains at the genome level using genome-based phylogenies is needed (Bull et al. 2015). Identifying the core genome shared among strains enables conserved genes that are responsible for essential functions, including virulence and environmental adaptation, to be distinguished readily. This aids in elucidating how strains of *P. syringae* may have evolved to be able to infect specific host plants and develop resistance to the immune systems of those plants (Vinatzer et al. 2005). Moreover, core phylogenetic analyses can uncover patterns of genetic diversification and the emergence of new pathogenic lineages, providing potentially valuable insights for disease management and the development of targeted resistance strategies.

The type III secretion system (T3SS**)** is a specialized protein delivery system used by many Gram negative bacterial plant pathogens, including *P. syringae*, to inject virulence factors known as effectors directly into plant host cells (Alfano and Collmer 2004). T3SS effectors **(**T3SSEs**)** are the proteins secreted through the T3SS into host cells, where they interfere with host signaling pathways, disrupt immune responses, and create favorable conditions for bacterial survival and proliferation (Vinatzer et al. 2005; Vinatzer et al. 2006). The conserved effector locus **(**CEL), hypersensitivity response (HR) and pathogenicity locus (*hrp*)/ HR and conserved gene clusters (*hrc*), and exchangeable effector locus (EEL) house many T3SSE genes. The CEL contains effectors that are found commonly across *P. syringae* strains, which suggests a fundamental role in virulence and adaptation to host plants (Alfano et al. 2000). The *hrp*/*hrc*

locus encodes essential components of the T3SS machinery, directly enabling the secretion of T3SSEs into plant cells (Alfano and Collmer 2004). Without a functional *hrp*/*hrc* locus, *P. syringae* is unable to infect host plants. The EEL is a more dynamic region, with variation in effector content among strains of *P. syringae*, likely as a result of horizontal gene transfer (Alfano et al. 2000).

Alfano et al. (2000) demonstrated how studying the CEL, *hrp*/*hrc*, and the EEL involved in pathogenesis of strains of *P. syringae* can provide direct information about the functional role of these loci, enhancing our understanding of the mechanisms of pathogenesis of strains to specific plants that may not be provided by core genome phylogenetic analyses. The EEL contributes to the ability of pathogens to evolve and diversify their pathogenicity profiles. Detailed studies of the CEL, *hrp*/*hrc*, and EEL in strains of the bacterial leaf spot pathogen vs. non-pathogenic strains from the same environments may help identify key effectors critical for virulence in *P. syringae* pv. *aptata*, and the ability to overcome plant defenses. Studying these regions in conjunction with phylogenetic data could allow for a more comprehensive understanding of the diversity of *P. syringae* pv. *aptata* isolates, facilitating identification of virulence factors that are conserved or unique among isolates. This is especially important in the context of developing resistant cultivars or other targeted treatment methods such as RNA interference-based gene silencing to block the expression of key effectors, clustered regularly interspaced short palindromic repeats (CRISPR) associated protein-mediated disruption of virulence genes, or the use of small-molecule inhibitors that specifically interfere with T3SS function (Gosavi et al. 2020; Lv et al. 2022; Zhang et al. 2021).

In addition to the *hrp* pathogenicity island, other T3SSEs are dispersed in the genome, and the presence of specific T3SSEs has been associated with the ability of *P. syringae* strains to

cause symptoms on particular plant species (Jamir et al. 2004). For example, some strains of *P. syringae* harbor effectors that are specialized for targeting plant defenses, while others lack these effectors, resulting in altered pathogenic profiles. The identification and comparison of these effectors among strains can help reveal the genetic factors responsible for differences in virulence, potentially providing valuable information for developing molecular diagnostic tools for target pathogens, and strategies to control bacterial diseases in crops (Jamir et al. 2004; Vinatzer et al. 2006).

The objectives of this study were to: i) determine the prevalence and genetic diversity of *P. syringae* pv. *aptata* in table beet and Swiss chard seed crops in western Washington, and ii) identify genetic factors that differentiate strains of *P. syringae* pv. *aptata* pathogenic to beet and chard from non-pathogenic strains of *P. syringae*, and that differentiate strains pathogenic to beet and chard vs. beet only. This will facilitate development of molecular diagnostic tools to differentiate pathogenic from non-pathogenic strains, and enable rapid quantification of the pathogen in infected beet and chard seed lots for determining the need for management practices such as seed treatments (Crane 2023).

Materials and Methods

Prevalence of *P. syringae* pv. *aptata* in table beet and Swiss chard seed crops in western Washington. A survey was completed in each of 2020, 2021, and 2023 to assess the prevalence of *P. syringae* pv. *aptata* in table beet and Swiss chard seed crops in western Washington. In 2020, the survey was conducted in Skagit, Snohomish, and San Juan Counties. From June to August 2020, one Swiss chard seed crop and 10 table beet seed crops were surveyed for symptoms of bacterial leaf spot. All but two of the crops were surveyed twice. The

first survey was carried out at early anthesis on 15 (Field A), 17 (B and C), 19 (D and E), and 23 June (F to H); and on 7 (I) and 14 July (J) (Fig. 1.1A). The second survey was completed at mid- to late flowering and seed set on 6 (Field A), 10 (B), 13 (C and D), 11 (E), and 28 (F to I) August (Fig. 1.1A). Field L was only surveyed once, on 27 August, at full seed set. Up to 20 leaves with suspect bacterial leaf spot symptoms, if observed, were collected in a transect across each field at the first sampling. During the second sampling, up to 20 symptomatic leaves were sampled from the edges of each field as the seed crops were too dense to walk through without causing excessive damage to plants. For each field surveyed, one leaf was collected per plant, a photo taken of the leaf, and placed on ice in a cooler. In addition, samples of leaves or whole plants were received in late spring 2020 from 2 table beet (VSP20-068 and VSP20-077-1) and 3 Swiss chard (VSP20-065, VSP20-086, and VSP20-094) fresh market crops in Skagit Co. and San Juan Co. that had symptoms of bacterial leaf spot. Symptomatic leaf samples were examined with dissecting (Leica MZ 12.5, Wetzlar, Germany) and compound (Leica DMLB) microscopes (up to 100x and 640x magnification, respectively).

In 2021, the survey was carried out in 11 table beet seed crops in Skagit Co. following the methods used in 2020, with the first survey at early flowering on 18 (Fields M and N) and 25 (O and P) June; and 1 (Q and R), 2 (S and T), and 8 (U, V, W) July. The second survey was carried out at late flowering and seed set on 13 (M and N), 15 (O and P), and 23 (Q and R) July; and 5 (S and T) and 13 (U, V, and W) August (Fig. 1.1B).

In 2023, the survey was carried out in three Swiss chard seed crops and nine table beet seed crops in Skagit and Snohomish Counties, following the methods described for the 2020 survey, except that each crop was surveyed three times at 3- to 4-week intervals from late May through August. The first survey of each crop was at early bolting on 23 (Fields AA and AC), 24

(AB and AD), and 25 (AE to AG) May; and 1 June (AH to AL). The second survey was at late flowering to early anthesis on 26 (Fields AA and AC), 28 (AB), 29 (AD to AF), and 30 (AG) June; and 19 July (AH to AL). The third survey was during seed set on 7 (Fields AA and AC), 9 (AB), 23 (AD to AF), and 30 (AH to AL) August (Fig. 1.1C and 1.1D). Daily relative humidity, and minimum and maximum daily air temperatures (°C) from 1 May to 1 September were obtained each season from the AgweatherNet station at the Washington State University (WSU) Mount Vernon Northwestern Washington Research and Extension Center (NWREC) as an average representation for the region in which seed crops were surveyed to evaluate the potential influence of weather conditions on development of bacterial leaf spot.

For each field from which symptomatic samples were collected, a 1-cm^2 section was cut from the margin of healthy and symptomatic tissue from each leaf or seed stalk sample (Fig. 1.2A). Each section was surface-sterilized in 0.6% NaOCl for 30 s, triple-rinsed in sterilized deionized water, macerated, and the suspension streaked onto MKBC agar medium (Mohan and Schaad 1987). Creamy-white, flat colonies with entire margins, typical of *P. syringae*, were subcultured onto King's B agar medium (King et al. 1954) and subcultured another three times to obtain purified isolates. In total, 99 suspect *P. syringae* isolates were collected from the first survey and 57 isolates in the second survey of seed crops in 2020 (Fig. 1.3). An additional 30 isolates were obtained from the fresh market crop samples received in 2020.

In 2021, none of the seed crops surveyed had symptoms typical of bacterial leaf spot at either sampling time, and bacterial streaming was not observed microscopically on the few foliar samples with suspect symptoms sampled, only the presence of black pycnidia with hyaline, aseptate spores typical of *Phoma betae* (Harveson et al. 2009). Therefore, bacterial isolations were not done for any of the samples collected in 2021, a season with record high summer

temperatures for western Washington and an extended summer period without any precipitation compared to 2020 (Fig. 1.3 and 1.4) (AgweatherNet 2023). Similarly, symptoms of bacterial leaf spot were not observed, and *P. syringae* pv. *aptata* was not isolated from any of the seed crops in the first, second, or third surveys of beet and chard seed crops in 2023. Conditions that season were mostly dry and warm from early spring through August (Fig. 1.5). Symptomatic fresh market beet or chard samples were not received from growers in western Washington in 2021 or 2023.

In addition to the symptomatic samples from seed crops and fresh market table beet and Swiss chard crops in 2020, suspect *P. syringae* pv. *aptata* colonies were quantified from the remnant seed of the seed lots used to plant two of the five fresh market table beet crops and one fresh market Swiss chard crop that had developed bacterial leaf spot symptoms, to determine if the bacterial leaf spot outbreak in each crop may have resulted from planting infected seed. Similarly, samples of table beet seed harvested from 6 of the 11 seed crops surveyed in 2020 (Fields A to E and L) were provided by the seed companies for whom the lots were produced to determine if bacterial leaf spot symptoms observed in those crops might be associated with infection of the seed harvested from the crops. In addition, samples of two beet seed lots (SP VSP20-077 and SP VSP20-094) and one chard seed lot (SP VSP20-65) received by the Vegetable Seed Pathology Program at the WSU Mount Vernon NWREC in the summer of 2020 were assayed for *P. syringae* pv. *aptata*.

For each seed lot, a modified seed wash dilution plating assay based on that described by Mohan and Schaad (1987) was used to isolate and quantify *P. syringae*. Briefly, a 10,000-seed subsample, depending on the amount of seed provided for each lot, was soaked in 1,800 ml of 0.85% saline with three drops of Tween 20 in a sterile poly bag (22.9 cm x 30.5 cm, 6 Mil flat;

Uline, Pleasant Prairie, Wisconsin), and held at room temperature (22 ± 1°C) for 4 h with manual agitation for 2 min every hour. The bag of seed was then placed on a rotary shaker at 150 rpm for 10 min. The seed rinsate was decanted and diluted serially (10-fold) four times. Three 100-µl aliquots of each dilution spread onto MKBC agar medium. In addition, an aliquot of each dilution was spiked with 10^5 CFU/ml of strain Pap009 of *P. syringae* pv. *aptata* to ensure the pathogen could be detected if present in the seed wash (assessment of any inhibitors in each seed lot that might affect detection). A 10^5 CFU/ml concentration of isolate Pap009 also was plated directly onto MKBC agar medium for calibration when reading the seed wash dilution plates. The plates were incubated at 27°C for 7 days. Suspect *P. syringae* pv. *aptata* colonies that developed on the plates were subcultured onto King's B agar medium. Putative *P. syringae* pv. *aptata* isolates (81 from the 9 seed lots) were then inoculated into Medium 523 broth (Kado and Heskett 1970), incubated overnight on a rotary shaker at 200 rpm, and stored at -80°C in 15% glycerol.

Putative *P. syringae* isolates obtained from the survey and seed lots were each subjected to an oxidase test, because *P. syringae* is oxidase negative (Kovács 1956). Oxidase negative isolates were then subjected to a tobacco hypersensitivity test to determine if each isolate might be a plant pathogen (Braun-Kiewnick and Sands 2001). For each isolate, a bacterial suspension grown overnight in Medium 523 broth on a shaker was adjusted to 10^8 CFU/ml, and a 1-ml aliquot infiltrated into the abaxial surface of a tobacco leaf. The leaf was examined 24 h after infiltration for a hypersensitive (necrotic) reaction. Isolates that were oxidase negative and tobacco hypersensitive were then subjected to multi-locus sequence analysis (MLSA) to determine the genetic diversity of the isolates based on the DNA sequences of four housekeeping genes: *gapA*, encoding glyceraldehyde-3-phosphate dehydrogenase; *gltA* (also known as *cts*),

encoding citrate synthase; *gyrB*, encoding DNA gyrase; and *rpoD*, encoding sigma factor 70, as described by Hwang et al. (2005) and detailed below.

Sources of inoculum other than infected seed. Crop residues remaining after harvest of seed crops, volunteer seedlings that developed in spring 2021 from seed that shattered during harvest of two seed crops in fall 2020, rainwater, and irrigation water were examined as potential sources of *P. syringae* pv. *aptata*.

***Seed crop residues*.** To examine the potential for *P. syringae* pv. *aptata* to survive on seed crop residues after harvest and through the winter in western Washington, 10 pieces of table beet seed crop residues were collected in March 2021 (spring) from each of Fields A, H, and I from the 2020 survey. Symptoms of bacterial leaf spot had been observed in each of these crops, and *P. syringae* pv. *aptata* was isolated from samples collected in each field. Each residue section was washed thoroughly under running tap water for 1 min. Three small pieces (each ~5 mm^3) were removed from each piece of residue with a scalpel, and soaked in sterilized, deionized water for 30 min. An inoculating loop was used to streak the residue rinsate onto MKBC agar medium in triplicate.

***Volunteers*.** In addition, 12 volunteer table beet seedlings that had leaf spots were collected in each of Fields A and H in March 2021. The volunteer seedlings grew from seed that had shattered during swathing of each seed crop in 2020. Using the isolation method described above, 10 suspect *P. syringae* pv. *aptata* isolates were obtained from lesions on cotyledons and/or true leaves from the symptomatic volunteers in Field A, and three from Field H. However, isolates from field H were atypical of *P. syringae* based on colony morphology, so no further characterization was carried out with these isolates. (Supplementary Table 1.1).

White to cream-colored colonies typical of *P. syringae* pv. *aptata* isolated from the residues and volunteers were subcultured and then tested for oxidase activity and tobacco hypersensitivity. Isolates that were oxidase negative and positive for tobacco hypersensitivity were subjected to pathogenicity tests on beet and chard seedlings, as described below, to confirm the identity as *P. syringae* pv. *aptata,* and included in MLSA described below to assess genetic diversity of the *P. syringae* pv. *aptata* isolates (Fig. 1.9).

Rainwater. To assess whether rainwater could be a source of inoculum of *P. syringae* pv. *aptata* in western Washington, five 20-liter plastic buckets that had been surface-disinfected with 70% alcohol and rinsed thoroughly, were each attached to a T-post 20 cm above the ground to catch rainwater and avoid splashing of soil from the ground into the buckets. The buckets were set 50 m away from a table beet seed crop trial at the WSU Mount Vernon NWREC (see Chapter 2) in June 2023. Sterile poly bags (22.9 cm x 30.5 cm, 6 Mil flat) were used to collect four subsamples of rainwater from each of the buckets following substantial rainfall on 25 July. The rainwater samples were stored temporarily at 4°C. A 250 ml aliquot of rainwater from each of the five buckets was mixed thoroughly, centrifuged at 8,500 rpm for 10 min, 200 ml of the supernatant discarded, and the remaining 50 ml agitated manually and passed through a sterile, nitrous cellulose filter (0.22-µm pore diameter) (Morris et al. 2008). Each filter was then placed in 5 ml of the corresponding rainwater filtrate and placed on a rotary shaker at 200 rpm for 3 min. A 10-fold dilution series was prepared and a 100-µl aliquot of each dilution plated onto MKBC agar medium. The plates were incubated at 25°C for 7 days. Suspect *P. syringae* colonies were counted, and CFU/ml calculated. A subset of five suspect isolates from a total of 10 was tested for pathogenicity on table beet and chard seedlings, as described below.

Irrigation water. To test whether *P. syringae* pv. *aptata* could be present in some of the sources of irrigation water used by seed growers in Skagit Co., five subsamples of 1,000 ml were drawn from irrigation water sources for three of the seed crops surveyed for bacterial leaf spot in 2023, using the same sterile poly bags used for rainwater samples, and the water stored at 4°C. A 250 ml aliquot of water collected from each field was processed as described above, and aliquots of 100 µl plated onto MKBC agar medium. Twelve suspect *P. syringae* isolates from irrigation water were subjected to oxidase and tobacco hypersensitivity tests. Only two were oxidase negative and caused tobacco hypersensitivity, and were tested for pathogenicity on beet and chard, as described below.

Pathogenicity tests. The putative *P. syringae* pv. *aptata* isolates obtained from symptomatic foliage and seed stalks in the table beet and Swiss chard seed crops, as well as those obtained from symptomatic volunteer table beet seedlings that grew from shattered seed following harvest of the seed crop in Field A, isolates from three seed lots used to plant the fresh market table beet and Swiss chard crops that developed bacterial leaf spot, isolates from the seed lots harvested from six of the symptomatic seed crops surveyed in 2020, and the isolates from irrigation water were tested for pathogenicity to table beet and/or Swiss chard. Seed of the table beet cv. Red Ace and Swiss chard cv. Silverado were planted in 6-packs (TLC Polyform, Inc., Salem, OR) filled with RediEarth propagation mix (SunGro Horticulture, Agawam, MA), with 2 seeds/cell. The plants were maintained in a greenhouse at 22 to 27ºC with supplemental lighting for 10 h/day, and fertigated daily with 20-20-20 fertilizer (Everris, Dublin, OH) injected at a final nitrogen concentration of 200 ppm. Seedlings were thinned to 1/cell. Thrips were managed with weekly, broadcast applications of *Beauveria bassiana* (Botanigard 22WP; Lam International Corp., Butte, MT) applied at 2.4 g/liter, spinosad (Entrust; Dow Agrosciences, Indianapolis, IN)

applied at 0.17 g/liter, or imidacloprid (Leverage 2.0; Bayer, Kansas City, MO) applied at 1.3 ml/liter, with products rotated weekly to minimize the risk of insecticide resistance developing in the thrips population. Up to nine putative *P. syringae* pv. *aptata* isolates and two positive control strains, Pap009 (pathogenic on both table beet and Swiss chard) and Pap014 (pathogenic on table beet but not Swiss chard) (Safni et al. 2016), were evaluated in each pathogenicity trial. A bacterial suspension of each isolate was produced in Medium 523 broth overnight on a rotary shaker at 200 rpm and 25ºC, and adjusted to 10^7 CFU/ml. A 10-ml aliquot of each bacterial suspension, to which 0.06 g of Carborundum (silicon carbide) was added, was used to inoculate two beet plants and chard plants, by dipping a Q-tip into the suspension and wiping the Q-tip gently over the upper and lower surfaces of each of two fully-expanded leaves/plant. Plants inoculated with phosphate buffer and Carborundum served as the negative control treatment in each trial. Each trial was arranged in a randomized complete block design (RCBD) with two replications per isolate and host combination. To quantify virulence of the isolates tested, severity of bacterial leaf spot was rated on a scale of 0 to 100% of the inoculated leaf surface area (Fig. 1.6) 7 days post inoculation (one rating/plant) (Fig. 1.7 and Fig. 1.8).

Multi-locus sequence analysis. To determine the genetic diversity of 134 isolates of *P. syringae* pv. *aptata* and 58 other isolates of *P. syringae* obtained from the beet and chard seed lots, seed crops, and fresh market crops surveyed, DNA was extracted from each isolate by suspending a colony grown on KB agar medium into 100 µl of sterilized, deionized water, and heating the suspension at 95°C for 15 min. Each suspension was then centrifuged for 2 min at 14,000 rpm. A 30 µl total volume of PCR mix per isolate was prepared that included: 3 µl of 10X buffer, 3.6 µl of 25 µM $MgCl_2$, 0.6 µl of 10 µM dNTPs, 0.2 µl of Taq DNA polymerase, 20.3 µl of nuclease-free water, 2 µl of template DNA, and 0.15 µl of 100 µM of each of the

forward and reverse primers, as detailed by Hwang et al. (2005) for each of four housekeeping genes: *gapA*, *gltA*, *gyrB*, and *rpoD*. PCR thermocycling included heating the mix at 95°C for 3 min; followed by 19 cycles at 95 and 72°C for 30 seconds each; and then at 95, 58, and 72°C for 30 s each for denaturation, annealing, and extension, respectively; and a final extension cycle at 72°C for 5 min (Hwang et al. 2005; Sarkar and Guttman 2004). Amplified DNA of each gene for each isolate was run on a 1% agarose gel, and purified using ExosapIT (ThermoFischer Scientific, Boston, MA) following the manufacturer's protocol. The DNA concentration for each gene of each isolate was measured using a Qubit fluorometer with a Quant-iT dsDNA BR Assay Kit (Invitrogen, Waltham, MA). The purified PCR products were sequenced by Elim Biopharmaceuticals (Hayward, CA) using the forward primer for most amplified products or, for 20 isolates for which the forward primer did not amplify correctly, the reverse primer. The resulting sequences of each gene were trimmed: *gapA* to 476 bp, *gyrB* to 507 bp, *gltA* to 529 bp, and *rpoD* to 498 bp, based on reference sequences obtained from the Plant Associated and Environmental Microbes Database (PAMDB) (Almeida et al. 2010). Sequences of these four genes were concatenated in Geneious Prime 2023 to a length of 2,010 bp and aligned using the MAFT plugin (Katoh and Standley 2013) in Geneious Prime 2023. A phylogenetic tree was constructed using Bayesian analysis with MrBayes plugin in Geneious Prime 2023 (Huelsenbeck and Ronquist 2001), using the model HKY85 with 1,000 pseudoreplicates to determine the genetic relationship among these strains. The four housekeeping gene sequences of the pathotype strain of *P. syringae* pv. *lachrymans* CFBP^{PT} 6463 were used as the outgroup (Fig. 1.9).

Detecting recombination events is valuable to understanding the complex evolutionary relationships among bacterial isolates. Traditional phylogenetic trees assume a strictly bifurcating structure, which cannot accurately capture the non-tree-like relationships introduced

by recombination (Yan et al. 2008). Therefore, we used the neighbor-net method in the SplitsTree software to analyze the concatenated sequences of the four housekeeping genes, similar to what was used to generate Fig. 1.10 to detect and display conflicting evolutionary signals in the form of reticulations (web-like patterns) for pathogenic isolates of *P. syringae* pv. *aptata*. This provided visual evidence of recombination by the presence of reticulate networks that represent shared genetic material among lineages (Fig. 1.11).

Whole genome sequencing. A subset of 36 isolates of *P. syringae* representative of fields and sources of inoculum in the 2020 survey, as well as fresh market table beet and Swiss chard crops, and the two positive control strains (Pap009 and Pap014), were subjected to whole genome sequencing (WGS). The isolates included 20 that were pathogenic on beet and chard, 8 pathogenic on beet only, and 8 non-pathogenic isolates. Genomic DNA was extracted from each isolate using the Wizard Genomic DNA Purification Kit (Promega, Madison, WI). Purified genomic DNA was checked for quality and the concentration estimated using a Qubit and by running a sample of each extract on a 1% agarose gel. The purified genomic DNA samples were sent for WGS at SeqCenter (Pittsburgh, PA). Illumina sequencing libraries were prepared using the tagmentation-based and PCR-based Illumina DNA prep kit and custom Integrated DNA Technologies (IDT) 10 bp unique dual indices (UDI) with a target inset size of 320 bp. Additional DNA fragmentation or size selection steps were not performed. Illumina sequencing was performed on an Illumina NextSeq 2000 platform (Microbial Genome Sequencing Center, Pittsburgh, PA) for all the isolates except the two control strains, Pap009 and Pap014, which were sequenced later using an Illumina NovaSeq 6000 sequencer. The sequencing was conducted in multiplexed flow-cell runs, producing 2 x 151 bp paired-end reads. Demultiplexing, quality control, and adapter trimming were performed with bcl-convert (v 4.1.5)

(Illumina Sequencing Systems). Sequencing statistics are included in Supplementary Table 1.2. The reads were assembled using SPAdes (Prjibelski et al. 2020). Contigs of <500 bp and with regions of coverage ≤2 were removed. Bowtie2 (Langmead and Salzberg 2012) was used for sequence alignment, and the module Pilon was used for improved draft genome assembly (Walker et al. 2014). Assemblies were assessed for completeness and contamination using CheckM (Parks et al. 2014).

Core genome phylogeny. The core genes in the genomes of 28 pathogenic and 8 non-pathogenic isolates from table beet and Swiss chard, as well as 38 reference strains of *Pseudomonas* obtained from the National Center for Biotechnology Information (NCBI), were compared using OrthoFinder v2.5.2 to identify orthogroups using the original algorithm as described by Emms and Kelly (2015; 2019). The identified orthogroups were used to infer unrooted gene trees using the BLAST-based hierarchical clustering algorithm DendroBLAST (Kelly and Maini 2013). This set of unrooted gene trees was used with the STAG algorithm to identify the closest pair of genes from those species to infer an unrooted species tree (Emms and Kelly 2018). The species tree was then visualized using FigTree (http://tree.bio.ed.ac.uk/software/figtree/) (Fig. 1.12).

CEL, *hrp*/*hrc*, and EEL sequence comparison. To gain insight into potential causes of differences in pathogenicity among *P. syringae* isolates recovered from table beet and/or Swiss chard seed and fresh market crops vs. non-pathogenic isolates, the nucleotide sequences of the CEL, *hrp*/*hrc*, and EEL of *P. syringae* pv. *tomato* DC3000 (PRJNA359), the causal agent of bacterial leaf speck of tomato (Alfano et al. 2000), were compared with these sequences of 28 isolates of *P. syringae* pv. *aptata*, 5 non-pathogenic isolates of *P. syringae*, and 3 isolates non-pathogenic to beet and chard from the survey that were identified as *P. viridiflava* based on

WGS, and 2 publicly available genomes in the NCBI database for *P. syringae* pv. *aptata*, i.e., P16 (PRJNA701181) and P21(PRJNA731657), that caused bacterial leaf spot of sugar beet (Ranković et al. 2023). These sequences were obtained from the WGS. Only sequences with ≥70% nucleotide identity and ≥70% coverage were included in the analysis. Gene clusters were generated in Clinker with a minimum identity alignment of 0.3% (Gilchrist and Chooi 2021) (Fig. 1.13).

T3SSEs. In an attempt to differentiate genetically the pathogenic isolates of *P. syringae* from non-pathogenic isolates, and differentiate the isolates pathogenic on beet and chard vs. those pathogenic on beet only, the nucleotide sequences of T3SSEs representing all T3SSE families were compared using the genomes of 30 isolates of *P. syringae aptata* pv. *aptata*, 5 isolates of *P. syringae*, and 3 isolates of *P. viridiflava* from the beet and chard survey, along with reference strains P16 and P21, using Blastn (V2.15.0) with ≥80% identity to the T3SSE sequences in *P. syringae* pv. *tomato* strain DC3000, and ≥90% coverage (Fig. 1.14). A metadata file was compiled using these conditions, (Supplementary Table 1.3).

Data analysis. Prevalence was calculated as the percentage of leaf samples positive for *P. syringae* pv. *aptata* out of the total leaf samples collected from each table beet seed crop. The percentage severity of bacterial leaf spot on inoculated table beet and Swiss chard seedlings was determined by calculating the mean and standard error.

Results

Survey results. Bacterial leaf spot was observed in some of the table beet and/or Swiss chard seed crops surveyed in 2020 but not in any of the seed crops surveyed in 2021 or 2023. In 2020, 5 of the 10 seed crops surveyed tested positive for *P. syringae* pv. *aptata* in the first survey

(table beet Fields A, H, F, and J, and the Swiss chard Field I), and 7 of the 10 fields surveyed the second time tested positive (table beet Fields A, B, C, G, F, and H, and the Swiss chard Field I). In total, 8 of the seed crops tested positive for *P. syringae* pv. *aptata* in one or both of the 2020 surveys (Fig. 1.3A). Fields D and E were asymptomatic in both surveys, and Field L was asymptomatic (only surveyed once). Rainfall totaled 129.4 mm from 1 May to 15 June 2020, when the first survey was carried out (Fig. 1.3B), whereas rainfall during the same period in 2021 totaled about half of that, 69.8 mm (Fig. 1.4A); and only 43.9 mm over the same period in 2023 (Fig. 1.5A). The second survey in 2020 was conducted from 6 to 28 August. Rainfall totaled 48.3 mm from 16 June to 11 July 2020, with no rain recorded again until 6 August, and 17 mm of rain from 6 August to 1 September (Fig. 1.3B). In 2021, no rain occurred from 16 June to 5 August, and totaled only 2.5 mm from 6 August to 1 September 2023 (Fig. 1.4A). Only 2.5 mm of rain was recorded from 21 June to 6 August 2023, with another 7.4 mm from 7 August to 1 September (Fig. 1.5A).

In each year of the survey, relative humidity (RH) was highly variable from 1 May to 1 September. In 2020, RH averaged 76.1 ± 1.0% from 1 May to 28 June when the first survey was carried out, and minimum and maximum air temperatures averaged 9.2 ± 0.3 and 18.9 ± 0.4°C, respectively, over that period (Fig. 1.3C). Over the same period in 2021, RH was less than in 2020, averaging 74.2 ± 0.8%, while minimum and maximum air temperature averaged 8.5 ± 0.4 and 20.1 ± 0.6°C, respectively. 2021 was one of the warmest seasons on record for western Washington with the temperature reaching 35.7°C on 28 June (Fig. 1.4B). In 2023, RH was less than in 2020 and 2021, averaging 68.7 ± 1.2%, and minimum and maximum air temperatures averaged 10.7 ± 0.2 and 21.9 ± 0.6°C, respectively, over the first and second surveys (Fig. 1.5B**)**. From 29 June to 14 August, the average minimum and maximum temperatures were 10.8 ±

0.3°C and 22.0 ± 0.4°C in 2020, 11.9 ± 0.3°C and 24.6 ± 0.4°C in 2021, and 13.7 ± 0.2°C and 26.8 ± 0.4°C in 2023, respectively. Relative humidity (RH) during this period averaged 76.9 ± 0.8% in 2020, 75.2 ± 0.7% in 2021 and 64.2 ± 1.0% in 2023. From 14 August to 1 September, minimum and maximum temperatures averaged 10.4 ± 0.7°C and 23.6 ± 0.7°C in 2020, 9.6 ± 0.7°C and 24.2 ± 0.5°C in 2021, and 14.2 ± 0.5°C and 26.1 ± 1.1°C in 2023, respectively; and RH averaged 76.4 ± 1.0% in 2020, 77.3 ± 1.0% in 2021, and 68.4 ± 2.0% in 2023.

In the first 2020 survey, leaf samples from table beet and/or Swiss chard seed crop fields with symptoms of bacterial leaf spot differed in the incidence of bacterial leaf spot samples from Fields A, H, and J with more bacterial leaf spot (90, 94, and 89% incidence, respectively) compared to Fields F and I (55 and 50%, respectively) (Fig. 1.3A). None of the leaf samples from Fields B, C, D, E, and G tested positive for *P. syringae* pv. *aptata* (Fig. 1.3A). Similarly, the incidence of bacterial leaf spot varied among fields in the second survey of 2020. Overall, the percentage of leaf samples that tested positive for *P. syringae* pv. *aptata* was 29.6% less than in the first survey. However, three fields tested positive for *P. syringae* pv. *aptata* in the second survey that were negative in the first survey, i.e., Fields B, C, and G (Fig. 1.3A). As in the first survey, Fields A and H had the greatest incidence of samples infected with *P. syringae* pv. *aptata*: 43% of 14 samples from Field A, and 69% of 16 samples from Field H. For the remaining five seed crops that tested positive, 31% of 14 samples from Field F were infected, as well as 25% of 4 samples from Field G, 17% of 12 samples from Field I, and 25% of 4 samples from each of Fields B and C. The pathogen was not isolated from Fields D, E, and L in the second survey, similar to the first survey.

Pathogenicity tests. The pathogenicity of *P. syringae* isolates recovered from table beet and/Swiss chard seed crops in the first and second surveys of 2020 differed on seedlings of the

table beet cv. Red Ace and Swiss chard cv. Silverado. Interestingly, most of the *P. syringae* pv. *aptata* isolates recovered from seed crops in the first survey caused more severe bacterial leaf spot than those recovered during the second survey. For example, the severity of symptoms ranged from 1.71 ± 0.5 to 12.7 ± 2.5% (mean ± standard error from two replicate plants per isolate) on table beet, and 1.3 ± 0.8 to 9.0 ± 4.1% on Swiss chard seedlings for 87 isolates tested from the first survey, but only from 0.2 ± 0.2 to 1.9 ± 0.6% on table beet, and 0 to 1.0 ± 0.7% on Swiss chard for 25 isolates tested from the second survey (Fig. 1.7). There were also differences in severity of bacterial leaf spot symptoms caused by the isolates recovered from different seed crops (Fig. 1.7). Severity of symptoms caused by isolates recovered from leaf samples in Field A during the first and second surveys averaged 12.5 ± 2.6 and 1.6 ± 0.7% on table beet, and 7.5 ± 0.2 and 1.0 ± 0.7% on Swiss chard, respectively (Fig. 1.7). In contrast, pathogenic isolates were not recovered from Field B in the first survey, but 4 isolates recovered in the second survey caused mild bacterial leaf spot symptoms on table beet (0.2 ± 0.2% severity), and were not pathogenic on Swiss chard (Fig. 1.7B). Pathogenic isolates were not recovered from Field C during the first survey, while isolates recovered during the second survey caused very mild symptoms, 0.8 ± 0.8% severity on table beet and 0.2 ± 0.2% severity on Swiss chard (Fig. 1.7B). Bacterial leaf spot severity caused by isolates recovered from Field F in the first and second surveys averaged only 1.7 ± 0.5 and 1.3 ± 0.5% on table beet, respectively, 1.1 ± 0.5% on Swiss chard, and no symptoms on Swiss chard in the second survey (Fig. 1.7). Pathogenic isolates were not recovered from Field G in the first survey, while isolates in the second survey caused 0.9 ± 0.9% severity on table beet and were not pathogenic on Swiss chard. Isolates from the first survey of Field H caused 12.7 ± 2.4% severity of symptoms on table beet and 8.8 ± 2.9% on Swiss chard compared to 1.9 ± 0.6% on table beet and 0.6 ± 0.6% on Swiss chard for isolates

from the second survey. For Field I, bacterial isolates from the first survey caused 5.0 ± 1.9% severity of symptoms on table beet and 9.0 ± 4.1% on Swiss chard vs. 1.1 ± 0.8 and 1.0 ± 0.7% on beet and Swiss chard in the second survey, respectively. Isolates from the first survey of Field J caused 8.3 ± 1.8% severity of bacterial leaf spot on table beet and 1.5 ± 0.7% on Swiss chard (Fig. 1.7A). That field was only surveyed once.

Isolates of *P. syringae* recovered from the seed lots used to plant three fresh market beet and chard crops that developed bacterial leaf spot in 2020, including one isolate from SPVSP20-065, one from SPVSP20-077, and seven from SPVSP20-094, did not cause bacterial leaf spot on table beet or Swiss chard seedlings, whereas isolates recovered from leaves of the symptomatic fresh market crops, including three from VSP20-065, two from each of VSP20-068, VSP20-077, and VSP20-086, and 21 from VSP20-094, caused severity of symptoms ranging from 4.6 ± 2.2 to 16.4 ± 3.5% on table beet and 0 to 12.3 ± 5.2% on Swiss chard (Fig. 1.8).

Severity of symptoms caused by seven isolates of *P. syringae* obtained from table beet seed harvested from Field A (Field A hsd) surveyed in 2020 averaged 1.9 ± 0.6% on table beet and 0.9 ± 0.3% on Swiss chard. Bacterial leaf spot severity caused by 10 isolates obtained from table beet volunteer seedlings that grew from shattered seed in Field A averaged 5.5 ± 0.8% on table beet and 4.8 ± 1.1% on Swiss chard. The three suspect isolates recovered from volunteer seedlings that grew from shattered seed in Field H were not characteristic of *P. syringae* based on colony morphology and, therefore, were not tested for pathogenicity on table beet and Swiss chard. Also, isolates recovered from seed crop residues collected from Fields A, H, and I were not characteristic of *P. syringae* and were not tested for pathogenicity. A subset of 11 isolates recovered from irrigation water and 5 from rainwater did not cause bacterial leaf spot symptoms on table beet or Swiss chard.

***P. syringae* diversity based on MLSA.** The phylogenetic tree based on concatenated sequences of *gapA*, *gyrB*, *gltA*, and *rpoD* for 134 pathogenic and 58 non-pathogenic isolates showed two major clades comprised of isolates recovered from symptomatic leaf samples from table beet seed crops, fresh market crops, volunteer table beet seedlings, seed lots, and reference strains (Fig. 1.9). Clade 1 had greater genetic diversity, with 4 major subclades supported by bootstrap values ≥70%. In contrast, Clade 2 consisted primarily of non-pathogenic isolates, with only two isolates pathogenic to table beet and Swiss chard, and four isolates pathogenic to table beet only. Within Clade 1, the pathogenic isolates differed in host specificity, with some pathogenic to both table beet and Swiss chard and others pathogenic to table beet only. Isolates from a single field were not genetically monomorphic. Rather than clustering by field, strains were dispersed across the phylogeny, indicating that diverse genotypes coexisted within fields. This was particularly evident in Fields A, H, F, I and J, as well as the fresh market crops VSP20-094 and VSP20-077. Also isolates from different samples were distributed across multiple subclades. Overall, isolates from a single field belonged to >2 distinct MLSA haplotypes, demonstrating that multiple genetic variants of *P. syringae* pv. *aptata* can co-occur in a given field. Regarding the relationship among isolates from fresh market crops, table beet and Swiss chard seed crops, and volunteer table beet seedlings, the clustering patterns of these groups did not always form distinct clades. Some isolates from fresh market crops clustered with isolates from table beet and Swiss chard seed crops, while others grouped with volunteers, suggesting potential movement of strains among these environments. Similarly, the host did not consistently determine clustering patterns. Isolates pathogenic to both table beet and Swiss chard were distributed across multiple subclades.

Within Clade 1, the 4 major subclades represent broad genetic relationships. Subclade 1, for example, consisted of 62 isolates from fresh market crops (VSP20-094, VSP20-077, and VSP20-086), table beet seed crops Fields A, H, and I, volunteer table beet seedlings (VB-A) from Field A, and seed lot VSP21-003a. Subclade 2 consisted of the pathotype strain *P. syringae* pv. *aptata* CFBP^{PT} and strain DSM5022 of *P. syringae* pv. *aptata*, which grouped with 11 isolates from Field A, 7 from Field H, one from Field I, 8 from Field J, 7 from Field A seed lot, and one from VSP21-003a seed lot. Subclade 3 comprised both pathogenic and non-pathogenic isolates, with no clear distinction between isolates pathogenic on table beet and Swiss chard from those pathogenic on table beet only. Subclade 4 consisted of non-pathogenic isolates that clustered with isolates of *P. syringae* pv. *syringae*. These findings suggest that, while the MLSA provides insights into genetic diversity, this analysis does not differentiate pathogenic from non-pathogenic isolates or distinguish isolates pathogenic to both table beet and Swiss chard from those affecting table beet only.

Genetic diversity among pathogenic isolates of *P. syringae pv. aptata*. Among the *P. syringae* pv. *aptata* isolates that caused bacterial leaf spot, the majority recovered during the first survey were pathogenic on both table beet and Swiss chard. In contrast, most isolates from the second survey were pathogenic on table beet only (Fig. 1.7). For these pathogenic isolates, the MLSA of the four housekeeping genes identified a total of 15 clades (Fig. 1.10). Clade 1 included 34 isolates pathogenic on table beet and Swiss chard, and 2 isolates pathogenic on beet only. Within this clade, 4 isolates originated from Field A, six from Field H, and three from Field I, collected during the first survey. Additionally, 2 isolates were recovered during the second survey from Field A, one from Field F, and two from Field I. This clade also included 10 isolates

from volunteer table beet plants in Field A, 19 from the fresh market crop VSP20-094, and 1 each from the fresh market crops VSP20-065 and VSP20-077.

Clade 2 of the MLSA for pathogenic isolates consisted of a single isolate from Field A that was pathogenic on both table beet and Swiss chard. Clade 3 included 5 isolates, all pathogenic on both beet and chard, 4 from 2 fresh market crops, and 1 from Field H. Clade 4 consisted of a single isolate pathogenic on table beet only. Clade 5 comprised 6 isolates pathogenic on table beet only, all from table beet seed lot VSP21-0031. Clade 6 contained 2 isolates from seed lot VSP21-0031 that were pathogenic on table beet only. Clade 7 included 19 isolates pathogenic on both table beet and Swiss chard, and 16 isolates pathogenic on table beet only. This clade included the pathotype strain of *P. syringae* pv. *aptata* CFBP^{PT} and *P. syringae* pv. *aptata* DSM5022. Ten isolates within this clade were from Field A, eight from Field J, 2 from Field H, and one from Field I, all collected during the first survey. Additionally, 2 isolates from Field A and 5 from Field H were recovered in the second survey. This clade also included 7 isolates from the seed lot harvested from Field A, 1 from the table beet seed lot VSP21-0031, and 1 from the fresh market crop VSP20-077.

Clade 8 contained 1 isolate pathogenic on table beet only. Clade 9 consisted of 3 isolates pathogenic on table beet and Swiss chard and a single isolate pathogenic on table beet only, recovered from fresh market crops VSP20-065 and VSP20-068, and a single isolate pathogenic to table beet only from Field J. Clades 10 through 12 each contained a single isolate that was pathogenic on table beet only, recovered from table beet seed lot VSP21-003a, Field A, and Field I, respectively. Clade 13 comprised 8 isolates that were pathogenic to table beet only and 1 isolate pathogenic to both table beet and Swiss chard. Five of these were from the first survey of Field F, the remaining 3 were from the second survey of Field F. An additional isolate from the

Field A first survey, was also in this clade. Clade 14 contained 7 isolates pathogenic to table beet only and 3 pathogenic to beet and chard, and clustered with *P. syringae* pv. *aptata* strain 604 and *P. syringae* pv. *aptata* strain G733. This clade also included two isolates from Field A, three from Field F, and two from Field H. Clade 15 consisted of 2 isolates pathogenic on both table beet and Swiss chard, and 3 isolates pathogenic on table beet only. Four of these isolates were from the fresh market crop VSP21-0031 and a single isolate from Field H. MLSA of the pathogenic isolates shows that *P. syringae* pv. *aptata* is diverse genetically, even isolates from the same field are genetically diverse.

Recombination among pathogenic isolates of *P. syringae pv. aptata*. The phylogenetic network of pathogenic isolates built with the neighbor-net tree for four housekeeping genes identified five major clusters with different evolutionary signals (Fig. 1.11). Each cluster represents a unique haplotype group in which individual isolates are closely related due to minimal recombination with isolates outside that cluster. The reticulations near the center of the tree, especially for isolates in clusters 3 and 4, indicated areas with potential recombination events or gene flow, i.e., haplotypes with shared genetic material or mixed ancestries. The four isolates in cluster 4 were particularly central, and the reticulations connecting cluster 4 with the other clusters imply that cluster 4 isolates may be intermediary or have exchanged genetic material with isolates in clusters 1, 2, 3, and 5. Shorter branches among isolates within clusters indicate close genetic relationships or recent common ancestry, such as the isolates in clusters 1 and 2 that have relatively short internal branches, suggesting the isolates within each cluster are similar genetically. Longer branches, such as those leading to the isolated points within cluster 5 (e.g., for isolate H37), are more distinct genetically from the core groups, indicating less recent recombination or a more divergent lineage. Cluster 1 consisted mostly of isolates from fresh

market beet and chard crops, 18 from VSP20-094, 2 from VSP20-086, 1 from VSP20-077 as well as isolates from 10 volunteer table beet seedlings from Field A, 5 isolates from Field A, 6 from Field H, and 3 from Field I. Most of the isolates in this cluster were pathogenic on table beet and Swiss chard, with only four pathogenic on table beet only. Clusters 2 and 4 were comprised mostly of isolates from table beet and Swiss chard seed crops (Fields A, F, H, I, and J), with only 5 from fresh market crops (VSP20-065, VSP20-068, and VSP20-077). Cluster 4 consisted of one isolate from Field A and 3 isolates from Field F. Cluster 5, a very distinct cluster from other clusters, consisted of 4 isolates from VSP20-003a and 2 from Field H. Two of these isolates were pathogenic on table beet and Swiss chard, and four were pathogenic on table beet only.

Core genome phylogeny. The core phylogeny based on WGS of isolates of *P. syringae* pv. *aptata* and other *Pseudomonas* isolates obtained from table beet and Swiss chard seed crops revealed distinct clustering patterns that reflect genetic diversity and evolutionary relationships among the strains (Fig. 1.12). Isolates associated with table beet and Swiss chard seed crops collected during the first survey formed closely related clusters and were all in phylogroup 2b, except for isolates A02, A04, and J05, which were in phylogroup 7 with strains of *P. viridiflava* (clade 13), i.e., these three isolates were identified as *P. viridiflava*, not *P. syringae*, and were not pathogenic on beet or chard. Typically, isolates from the same seed crop or field grouped together. Within phylogroup 2b, isolates of *P. syringae* pv. *aptata* formed four distinct clades. In clade 1, 7 isolates (4 from Field A, 2 from Field J, and a single isolate from VSP20-077, a fresh market crop) were pathogenic on table beet and Swiss chard, and another 7 isolates (2 from Field H, 1 from Field I, 3 from Field J, and a single isolate from VSP20-086, a fresh market crop) were pathogenic on table beet only. Clade 2 consisted of 13 isolates, all pathogenic on both table beet

and Swiss chard (from Fields H and I, VSP20-065, VSP20-077, and VSP20-094), and grouped with Pap009, a positive control strain pathogenic on table beet and Swiss chard, and strain P21 from sugar beet . In contrast, clade 3 comprised only one isolate from Field F that was pathogenic on table beet and Swiss chard, one isolate from Field F pathogenic on table beet only, and three non-pathogenic isolates from Field F, as well as *P. syringae* pv. *atrofaciens* ICMP 4318, and strain P16 that was reported to be weakly virulent on sugar beet (Nikolić et al. 2018; 2023). Clade 4 included 2 isolates pathogenic on table beet only (1 from Field A and Pap014 a control strain) that grouped with *P. syringae* pv. *lapsa* ICMP 3947, and 2 isolates from Field A and 1 from Field I that were non-pathogenic. Based on these results *P. syringae* pv. *aptata* strains in table beet and Swiss chard crops in western Washington in 2020 were diverse genetically, and the core genome phylogeny based on WGS did not differentiate pathogenic isolates from non-pathogenic isolates or distinguish isolates pathogenic to table beet and Swiss chard from those pathogenic to table beet only.

Diversity of isolates based on CEL, *hrp*/*hrc*, and EEL gene sequences. The CEL, *hrp*/*hrc*, and EEL gene cluster of a subset of 36 isolates from this survey, including 29 *P. syringae* pv. *aptata* isolates, 4 *P. syringae* isolates, 3 isolates of *P. viridiflava*, and 3 reference strains (DC3000, P16, and P21), spanned ~48,932 bp. The cluster showed a consistent overall gene structure with noticeable strain-specific variations (Fig. 1.13). Isolates were clustered based on similarity, particularly in the EEL region (clusters 1 to 14). Most of the isolates pathogenic to table beet and Swiss chard, as well as isolates pathogenic to table beet only, and some of the non-pathogenic isolates in clusters 1 to 13 had intact CEL and *hrp*/*hrc* loci. The EEL was the most variable of the loci, but none of the effectors was unique to the beet and chard pathogenic isolates. Additionally, no effectors were present solely in isolates that were pathogenic to both

table beet and Swiss chard, and absent from isolates pathogenic to table beet only. However, isolates within clusters 3, 4, 5, and 8 included 10 moderately virulent isolates and one weakly virulent isolate that were all pathogenic to both table beet and Swiss chard, all of which had duplication of a putative effector annotated as acetyltransferase_14. Clusters 3 and 11 included the most isolates, all of which were either pathogenic on table beet and Swiss chard or table beet only. Isolates in clusters 10, 11, and 12, (6 isolates pathogenic to table beet only, 5 isolates pathogenic to table beet and Swiss chard, and the non-pathogenic isolate A19, had a duplicated UBA-like protein known to be involved in host-pathogen interactions such as stress adaptation in bacteria (Lehmann et al. 2017). Within these three clusters, one isolate was highly virulent, 6 were moderately virulent, and 3 were weakly virulent and pathogenic to table beet only, whereas isolate A19 was non-pathogenic. Isolates in cluster 2 consisted of 2 pathogenic isolates from Field F and one non-pathogenic isolate from Field F, with the pathogenic isolates weakly virulent, one to Swiss chard and table beet, the other to table beet only.

Notably, isolate A12, which was pathogenic to table beet only and recovered from Field A, had effectors that included *avrB-avrC*, sigma 3 and 4 of RNA polymerase, an uncharacterized effector, and porins in the EEL locus that were not present in any other isolate (Fig. 1.13). The *HopA1* effector in the EEL locus was only present in isolates F05, F09, F04, and F16S. Isolate A19, which was not pathogenic, had 10 genes in the EEL locus encoding 4 T3SSEs and phage related genes. Non-pathogenic isolates J04, A02, and J15 were missing the CEL and *hrp*/*hrc* loci. In addition, an effector annotated as CesT, similar to effectors SchM and SchE (Hacker et al. 1997), was present in almost all isolates except the pathogenic isolate A12 and non-pathogenic isolates J04, A02, and J15.

Overall, this CEL, *hrp*/*hrc*, and EEL gene analysis did not differentiate pathogenic from non-pathogenic isolates, or those pathogenic on table beet and Swiss chard from those pathogenic on table beet only. Furthermore, the presence of *hrp*/*hrc* in non-pathogenic isolates indicates the *hrp*/*hrc* locus is not suitable for differentiating pathogenic from non-pathogenic isolates.

Presence or absence of T3SSE. The WGS analysis revealed the presence of T3SSEs, specifically the *hrp* cluster, across 30 isolates of *P. syringae* pv. *aptata*, 5 isolates of *P. syringae*, and 3 isolates of *P. viridiflava* from this survey (Fig. 1.14). Core effectors associated with the *hrp* cluster in these isolates included *AvrE1*, *HopAA1-1/HopAT1a*, and *HopM1*, which were detected in all the pathogenic isolates. Additional effectors, such as *HopI1* and *HopH1*, were identified in 32 pathogenic isolates as well as 5 non-pathogenic isolates. Of the isolates pathogenic on table beet and Swiss chard, 41% had a broader effector repertoire than the non-pathogenic isolates, suggesting a relationship between the number of effectors or repertoire of effectors and pathogenicity to beet and chard (Fig. 1.14). For example, five effectors (*AVRpm1a*, *HopAT1a*, *HopAX1a*, *HopD2d*, and *HopW1e*) were unique to 13 isolates, including 2 highly virulent isolates (Pap009 and H14), 9 moderately virulent isolates (A14, A20, I14, I15, H10, H11, VSP20-77, VSP20-96-K11, and VSP20-86), and 1 weakly virulent isolate (VSP20-65-1), all of which were pathogenic to table beet and Swiss chard, and the reference strain P21 that is highly pathogenic to sugar beet.

All non-pathogenic and pathogenic *P. syringae* isolates possessed at least one allelic variant of the avirulent effector *AVRE1*, and all had *HopAG1a* and *HopAH1h*, except P16, an isolate weakly pathogenic to sugar beet and which possessed the *HopAL1a* effector that was not present in any other isolate (Fig. 1.14). Non-pathogenic isolates A02, J04, and J15 were missing

all but 2 of the 25 effectors, as they only had the two allelic variants of *AvrE* and *HopB*: *AvrE1y* and *HopB2bc*. In contrast, the other five non-pathogenic isolates from the survey (A19, F04, F16S, I05, and I12) possessed at least 15 of the 25 effectors. However, *HopAZ1b* was missing in A19 and F16S, and F04 possessed an allelic variant, *HopAZ1c*. Additionally, A19 lacked *HopB2d*, and *HopBA1a* was absent in I05, I12, and F16S. F04 and F16S had *HopBK1b*, but F04 and F05 were the only isolates missing *HopBF1b*, and I05 had an allelic variant *HopBK1f*. *HopBN1b* was only found in I05 and I12 of the non-pathogenic isolates, but also was found in Pap014 and A12, two weakly virulent isolates on beet and chard. Isolates A19 and F16S lacked *HopI1d* as did Pap014, but carried the allelic variant *HopI1k*, while I12 and F04 had *HopL1a*, as did the weakly virulent isolate F05 (Fig. 1.14). Overall, analysis of the T3SSEs did not differentiate pathogenic from non-pathogenic isolates and isolates, or pathogenic on table beet and Swiss chard from those pathogenic on table beet only.

Discussion

The overall goal of this study was to determine the prevalence and genetic diversity of *P. syringae* pv. *aptata* in table beet and Swiss chard seed production. Bacterial leaf spot was observed in 72% of 11 table beet and Swiss chard seed crops surveyed in 2020 but not in any seed crops surveyed in 2021 or 2023. Development of bacterial leaf spot in 2020 appears to have been influenced by favorable weather conditions, including relatively high and regular rainfall from May to June with mild temperatures, although the pathogen was not detected in 3 of the 11 seed crops surveyed that season. The absence of the pathogen in three seed crops, despite being in the same environmental conditions, may reflect the lack of inoculum in the fields (e.g., stock seed was not infected) and/or the proprietary cultivars grown in those fields may have been more

resistant to bacterial leaf spot. The absence of bacterial leaf spot in any of the seed crops surveyed in 2021 and 2023 appears to reflect the effects of drier and warmer conditions those seasons on disease pressure.

Dry and warm conditions are unfavorable for most bacterial diseases, as moisture is a critical factor influencing pathogen colonization and establishment of infection (Hirano and Upper 2000). These survey results suggest that development of bacterial leaf spot is strongly influenced by environmental conditions, as documented in field trials on this disease (Crane 2023; Derie et al. 2016). A similar survey of 12 beet and Swiss chard seed crops in western Washington in 2015 resulted in no detection of bacterial leaf spot, a year that was particularly dry and warm for western Washington, similar to 2021 and 2023 (L. du Toit, *unpublished data*). Furthermore, Derie et al. (2016) observed mild symptoms of bacterial leaf spot in baby leaf Swiss chard trials established with naturally infected seed during the drier spring conditions of 2015 in western Washington compared to a trial completed in cooler and wetter conditions in the fall of 2015 with the same seed lot. Similarly, development of bacterial leaf spot in four Swiss chard baby leaf crop trials in western Washington in 2020 and 2021 was strongly influenced by the amount of rainfall and timing of rainfall events among the trials, with the most severe symptoms in the trial that occurred during the wettest conditions (Crane et al. 2023).

P. syringae pv. *aptata* was detected in 5 of 10 seed crops in the first survey of beet and chard seed crops completed in 2020 in this study, and in 7 of 10 fields surveyed later that year, with wide variation in incidence among the symptomatic seed crops. In all the fields in which bacterial leaf spot was observed, symptoms occurred in distinct hot spots distributed randomly in the field, which is indicative of seedborne inoculum potentially being the source of infection (Neergaard 1977). Pathogenicity tests of *P. syringae* isolates from the survey demonstrated

variation in virulence among *P. syringae* pv. *aptata* isolates. Most of the isolates recovered during the first survey in 2020 caused more severe symptoms compared to those recovered in the second survey, and the pathogenic isolates tended to cause more severe symptoms on table beet than Swiss chard. For example, isolates from Field A caused an average severity of 12.5 ± 2.6% on table beet and 7.5 ± 0.2% on Swiss chard in the first survey, while isolates from the second survey of that field caused 1.6 ± 0.7% severity on table beet and 1.0 ± 0.7% on Swiss chard. The discrepancy in bacterial leaf spot severity caused by isolates from the first vs. second surveys could be attributed to a population shift in the pathogen, with less virulent isolates dominating later in the season, but this was confounded by differences in conditions at the time of sampling and the timing of pathogenicity testing of the isolates. Isolates recovered in the second survey were tested for pathogenicity in the winter of 2020-21, when there was less intense natural light and drier greenhouse conditions as a result of the heaters operating, which could have affected disease severity ratings compared to isolates from the first survey that were tested for pathogenicity in the summer and autumn. Notably, the positive control strains used in each pathogenicity test, Pap009 and Pap014, showed reduced virulence when tested in greenhouse conditions in the winter compared the summer (*data not shown*), suggesting that environmental factors play a significant role in severity of disease expression.

Volunteer seedlings that developed from the seed that shattered after harvest of the seed crop in Field A had symptoms of bacterial leaf spot, and isolates recovered from the symptomatic seedlings tested positive for pathogenicity, indicating that volunteers can serve as a reservoir of inoculum for the next season if table beet or Swiss chard seed crops are planted in close proximity to the previous year's crops. However, growers of table beet and Swiss chard seed crops in western Washington rotate out of fields for at least five years, which potentially

reduces this risk unless they plant a field immediately adjacent to one that had an infected crop the prior season. Similarly, *P. syringae* pv. *pisi*, the causal agent of pea bacterial blight, was shown to survive for several months on volunteer plants (Grondeau et al. 1996).

P. syringae pv. *aptata* was not recovered from table beet seed crop residues collected from infected fields, indicating that the bacterium may not survive the winters in western Washington on dead stem tissue and crowns remaining on the soil surface. In contrast, the sequential plantings and short rotations typical of baby leaf beet and chard crop production could pose a risk for *P. syringae* pv. *aptata* dispersal from infected crop residues. In pea, *P. syringae* pv. *pisi* can persist for 18 months in crop residues remaining on the soil surface (Hollaway and Bretag 1997).

The lack of detection of *P. syringae* pv. *aptata* in rainwater and irrigation water associated with the beet and chard seed crops surveyed in 2023 in this study suggests that these may not serve as primary reservoirs for the pathogen in western Washington, or that the bacterium may be present at very low levels in these sources of water. These findings contrast with studies that have identified *P. syringae* in atmospheric precipitation, demonstrating potential for long-distance dispersal via rain and aerosols (Monteil et al. 2014; Morris et al. 2008). The lack of detection of *P. syringae* pv. *aptata* in irrigation water sources and rainwater samples could be attributed to several factors, including low inoculum levels, unfavorable environmental conditions, or the transient nature of bacterial populations in water sources (Morris et al. 2013; 2018). Also, these water sources were only tested for one season and to a very limited extent. Studies have shown that *P. syringae* can occur in rainwater, irrigation water, and surface water, which could serve as reservoirs of inoculum (Morris et al. 2013; 2018). However, the detection and persistence of the pathogen in these environments is influenced by

multiple factors, including temperature, nutrient availability, and competition with other microbial communities (Monteil et al. 2014). Further research involving larger sampling efforts or more sensitive detection methods, such as quantitative PCR assays (once primers specific to *P. syringae* pv. *aptata* have been developed), could help clarify whether *P. syringae* pv. *aptata* can persist in water.

The phylogenetic analysis of pathogenic isolates of *P. syringae* pv. *aptata* detected in this seed crop survey, based on a MLSA of four housekeeping genes, showed significant genetic diversity among isolates, underscoring the complex evolutionary relationships among pathogenic and non-pathogenic strains of *P. syringae* associated with beet and chard. The presence of multiple subclades suggests genetic divergence in the populations that may be driven by host adaptation and/or environmental pressures (Vinatzer et al. 2005). The presence of pathogenic and non-pathogenic isolates within the same subclades, particularly subclades 3 and 4 and subclade 1 of Clade 2, indicates that housekeeping genes *gapA*, *gltA*, *gyrB*, and *rpoD* cannot be used to differentiate pathogenic from non-pathogenic isolates of *P. syringae* associated with beet and chard. Also, these genes could not differentiate isolates that are pathogenic on beet and chard from those that are pathogenic on table beet only. The clustering of pathogenic isolates of table beet and Swiss chard with pathogenic reference strains including, *P. syringae* pv. *atrofaciens* and *P. syringae* pv. *lapsa*, demonstrates that the bacteria that cause bacterial leaf spot of beet and chard originate from diverse lineages, as documented in other studies (e.g., Nikolić et al. 2018).

Genetic recombination can play a critical role in the evolution of *P. syringae* pathovars by introducing genetic variations that impact traits such as host specificity and virulence (Yan et al. 2008). The phylogenetic reticulations observed in this study for the pathogenic isolates from beet and chard illustrate the dynamic nature of these bacterial pathogen populations, in which

horizontal gene transfer and recombination may shape the genetic structure and adaptability of isolates (Sarkar and Guttman 2004). Clusters of isolates with denser reticulations, particularly those in clusters 3 and 4 in this study, demonstrated high levels of genetic connectivity with isolates in neighboring clusters, suggesting ongoing or historical recombination events among lineages. The reticulations observed in the SplitsTree analysis of isolates of *P. syringae* pv. *aptata* reinforced previous studies that showed bacterial populations can undergo frequent recombination, creating complex evolutionary relationships. This evolutionary flexibility enables rapid adaptation to new hosts and environments (Sarkar and Guttman 2004). For instance, in *P. syringae* pv. *tomato* DC3000, recombination events were detected and reconstructed among closely related strains, highlighting the role of homologous recombination in reshuffling virulence genes and contributing to adaptability of the pathogen (Yan et al. 2008).

The WGS of *P. syringae* pv. *aptata* isolates from this beet and chard seed crop survey illustrated that the isolates are diverse genetically. Similar to the MLSA, WGS did not differentiate the pathogenic from non-pathogenic isolates, or isolates pathogenic on table beet and Swiss chard from those that are pathogenic on table beet only. Non-pathogenic isolates frequently clustered with pathogenic isolates in the WGS phylogenetic analysis, as did isolates pathogenic on table beet and Swiss chard with isolates pathogenic on table beet only. *P. syringae* isolates are ubiquitous with a very wide range in symptomatic host plants, and can adapt to various ecological niches (Morris et al. 2000; 2008; Sarkar and Guttman 2004). The multiple clades of *P. syringae* pv. *aptata* isolates detected within phylogroup 2b in this beet and chard study suggest that isolates that cause bacterial leaf spot originate from different genetic backgrounds. Similar results have been observed for the same pathogen of sugar beet. Nikolić et al. (2008), demonstrated that *P. syringae* pv. *aptata* isolates from sugar beet are not clonal, but

originate from different lineages. Some of the pathogenic isolates obtained from beet and chard seed crops in this study clustered with known pathogenic reference strains, such as isolates of *P. syringae* pv. *atrofaciens* and *P. syringae* pv. *lapsa*, which indicates the potential for horizontal gene transfer to influence virulence on specific host plants (Yan et al. 2008). The unique placement of the non-pathogenic isolates A02, A04, and J05 from this study in phylogroup 7 with *P. viridiflava* isolates illustrated that these seed crops can be colonized by strains of other *Pseudomonas* species. *Pseudomonas* is the most frequently reported genus in many crops, with species such as *P. viridiflava* acting as pathogens, endophytes, epiphytes, or saprophytes (Lipps and Samac 2022). *P. viridiflava* has been isolated from a wide range of hosts, including vegetable crops, fruit trees, and aromatic herbs. The ability to act as an opportunistic pathogen across different plant species underscores the potential to colonize and persist in various agricultural settings (Lipps and Samac 2022).

Computational analysis of the presence and absence of core T3SSEs in isolates of *P. syringae* pv. *aptata* obtained from the beet and chard survey in western Washington aimed to determine if these effectors maybe associated with virulence and host specificity. The analysis revealed the presence of T3SSEs associated with the *hrp* cluster, a key component of the T3SS machinery responsible for delivering effector proteins into host cells, facilitating infection, and suppressing plant immune responses (Alfano et al. 2000). Several core effectors were identified within the CEL and the EEL associated with the *hrp* cluster. Notable effectors present in these isolates included *AvrE*, *HopAA1-1*/*HopAT1a*, and *HopM1*, all of which have been implicated in pathogenicity and host immune suppression in *P. syringae (*Alfano et al. 2000; Nikolić et al. 2023). These effectors are known to manipulate host cell processes, potentially contributing to the variation in virulence observed across isolates in this study, as has been observed in *P.*

syringae pv. *aptata* strains from sugar beet (Nikolić et al. 2023) and other *P. syringae* pathogens (Alfano et al. 2000; Cunnac et al. 2009; Lindeberg et al. 2012;). All the pathogenic isolates of *P. syringae* pv. *aptata* and the non-pathogenic isolates of *P. syringae* obtained from the beet and chard seed crop survey were categorized within phylogroup 2b, except for three isolates in phylogroup 7, which were identified by WGS as *P. viridiflava*. This suggests a potential evolutionary relationship with effector content and pathogenicity, consistent with prior studies on the genetic diversity of *P. syringae* (Baltrus et al. 2011; Sarkar et al. 2006).

The EEL was the most variable locus of the CEL, *hrp*/*hrc*, EEL regions evaluated for isolates of *P. syringae* pv. *aptata* from this survey, with significant differences in T3SSE detected and the number of T3SSEs. None of the effectors was exclusive to the pathogenic isolates or specific to those pathogenic on both table beet and Swiss chard vs. those pathogenic on table beet only. However, isolate-specific differences were observed within the EEL locus. For instance, the presence and duplication of acetyltransferase_14 (threonine/serine acetyltransferase), *a YopJ*-like effector (Cheong et al. 2014; Lee et al. 2012) in 11 of the pathogenic isolates, may be linked to enhanced virulence, as observed for isolates from clusters 3, 4, 5, and 8 that were all moderately to highly virulent on beet and chard. However, duplication of that gene was inconsistent across the highly virulent isolates, suggesting additional factors, such as toxins or effector redundancy, may contribute to virulence (Baltrus et al. 2011; Nikolić et al. 2023).

Some isolates of *P. syringae* pv. *aptata* from this beet and chard survey, such as A12, exhibited a unique effector profile, including the presence of the effector *AvrB* and unique sigma factors. In contrast, isolate A19, which was non-pathogenic, had a large number of effectors in the EEL locus. The pathogenicity tests in this study were limited to a single cultivar of each host.

We cannot rule out the possibility that the non-pathogenic isolates might be pathogenic on other beet or chard cultivars. This should be evaluated to rule out the possibility of these isolates being pathogenic, and to provide clarification on which effectors might be associated with pathogenicity to beet and chard. The observation of effector variants, like CesT, a known chaperone aiding in the translocation of T3SSEs (Hacker et al. 1997), in both pathogenic and non-pathogenic isolates also suggests that some non-pathogenic isolates may have the potential to be pathogenic under more conducive conditions.

The effectors detected in this study are consistent with previous research showing that pathogenic isolates of *P. syringae* tend to have larger or more diverse effector repertoires than non-pathogenic isolates (Alfano and Collmer 2004). Also, specific combinations of effectors can enhance the pathogenic potential of isolates synergistically (Alfano and Collmer 2004; Nikolić et al. 2023). While this study focused on beet and chard, a narrow host range, the variation in virulence and effector profiles observed suggests a complex relationship between genetic diversity and pathogenicity. This complexity emphasizes the potential value of effector profiling to better understand mechanisms driving host specificity and adaptation. The identification of both the structural components of the T3SS and the associated effector repertoire supports the pathogenic potential of the isolates tested. Functional assays similar to that described by Cheong et al. (2014) would be needed to determine the specific roles of these effectors in the infection process and pathogenicity to table beet and Swiss chard.

Five T3SSE, *AVRpm1a*, *HopAT1a*, *HopAX1a*, *HopD2d*, and *HopW1e*, were unique to 12 of the 30 pathogenic isolates of *P. syringae* in this study on beet and chard. Previous studies have shown that even closely related strains of *P. syringae* can have unique effectors that influence the degree of virulence on different cultivars of the same host (Baltrus et al. 2011). However, these

effectors were absent in other pathogenic isolates, indicating that different isolates may employ different effector combinations for pathogenicity to beet and chard. The absence of some effectors in pathogenic isolates might be explained by the concept of functional redundancy among effectors (Baltrus et al. 2011). *P. syringae* possesses multiple effectors that can target similar host pathways, leading to similar pathogenic outcomes even when specific effectors are missing (Baltrus et al. 2011). Functional redundancy allows for evolutionary flexibility, as isolates can lose or gain effectors while maintaining pathogenic potential. This redundancy can also provide an advantage of enabling isolates to adapt to different hosts or environmental conditions without losing virulence (Baltrus et al. 2011). Such observations have been made with strain T1 of the tomato pathogen *P. syringae* pv. *tomato*, which possesses a distinct effector repertoire compared to *P. syringae* pv. *tomato* DC3000 (Almeida et al. 2009).

Identification of the core T3SS effectors *AvrE*, *HopI*, *HopAA*, and *HopM1* in isolates of *P. syringae* pv. *aptata* from beet and chard in this study underscores the potential role of these effectors at promoting infection of table beet and Swiss chard. These effectors are well characterized in other *P. syringae* pathovars for ability to suppress host immune responses and facilitate bacterial colonization (DebRoy et al. 2004; Jayaraman et al. 2020; Washington et al. 2016). For example, *AvrE* disrupts host vesicle trafficking and immune signaling, promoting water-soaking and chlorosis (Badel et al. 2006; Jayaraman et al. 2020). Similarly, *HopM1* targets vesicle trafficking and destabilizes proteins involved in basal immune responses, enhancing pathogenicity (Nomura et al. 2006). The presence of *HopI* and *HopAA*, which modulate host signaling and chloroplast function, further suggests additional strategies employed by these isolates of *P. syringae* pv. *aptata* to overcome plant defenses (Jelenska et al. 2007).

Interestingly, the pathogenic and non-pathogenic isolates of *P. syringae* from this beet and chard survey possessed at least one allelic variant of the avirulent effector *AvrE1*, and all isolates possessed *HopAG1a* and *HopAH1h*, except for P16, the only isolate to possess *HopAL1*. This highlights the potential for certain effectors to be present in isolates, that may serve roles beyond pathogenicity (Buell et al. 2003). The non-pathogenic isolates A02, J04, and J15 lacked most of the 32 core effectors detected in pathogenic isolates, retaining only *HopB2bc* and *AvrE1y*, which might explain their non-pathogenic nature to beet and chard. Conversely, other non-pathogenic isolates such as A19, F04, F16S, I05, and I12, had at least 15 effectors, demonstrating variability even among non-pathogenic strains. For example, *HopAZ1b* was missing in A19 and F16S, while F04 exhibited the allelic variant *HopAZ1c*, suggesting allelic diversity might play a role in host-pathogen interactions (Lindeberg et al. 2009; Lindeberg et al. 2012). Also, these alleles may have a role in triggering defense response in the host, indicating the possibility of gene-for-gene interactions resulting in non-pathogenicity on the host plants tested. Also, pathogens can have different alleles for these effectors, which may offer clues to resistance genes recognizing specific effectors.

In summary, the findings from this study revealed that bacterial leaf spot was present in 72% of the table beet and Swiss chard seed crops surveyed in western Washington in 2020 but absent in all the seed crops surveyed in 2021 and 2023, likely due to drier and warmer conditions in the latter two seasons. These findings also reinforce previous observations that seed may be a primary source of inoculum for infection of beet and chard crops by *P. syringae* pv. *aptata based* on the hot spots of symptomatic plants in infected seed crops (Crane 2024; Derie et al. 2016; Safni et al. 2016*)*. The MLSA and WGS work in this study revealed that *P. syringae* pv. *aptata* isolates in the primary beet and chard seed production region of the United States are diverse

genetically. Based on the WGS, isolates of *P. syringae* pv. *aptata* were all in phylogroup 2b of *P. syringae*. However, clustering of pathogenic and non-pathogenic isolates within the same subclades, along with high levels of genetic connectivity, highlight the complexity of *P. syringae* populations associated with beet and chard, and the potential role of recombination in their evolution.

Pathogenicity tests demonstrated differences in virulence among *P. syringae* pv. *aptata* isolates from the beet and chard crops surveyed, with some isolates more virulent on table beet than Swiss chard. However, neither MLSA nor WGS differentiated the pathogenic vs. non-pathogenic isolates or isolates pathogenic on beet and chard from those pathogenic on beet only. Effector analysis provided insights into potential virulence factors associated with pathogenicity, identifying core T3SSE such as *AvrE*, *HopM1*, and *HopAA1-1*, which may contribute to host infection. However, no single effector or effector combination was uniquely associated with pathogenicity or plant subspecies specificity. While certain effectors were unique to some pathogenic isolates, others were shared across pathogenic and non-pathogenic isolates, suggesting that functional redundancy or additional factors not yet identified may influence pathogenicity to table beet and chard.

Future research on the bacterial leaf spot pathogen of beet and chard could explore the interactions between T3SS and Type VI secretion systems (T6SS) on the pathogenicity of *P. syringae* pv. *aptata* isolates. These secretion systems include critical virulence factors, with T3SS primarily mediating the delivery of effector proteins into host cells to suppress plant immune responses (Nikolić et al. 2023), while T6SS often play a dual role in interbacterial competition and interaction with host cells (Wang et al. 2021). Emerging evidence suggests complex crosstalk between these two systems that can influence bacterial virulence and fitness

(Nikolić et al. 2023; Wang et al. 2021). For instance, regulatory proteins like *RetS* and *LadS* modulate both T3SS and T6SS in response to environmental signals, potentially affecting pathogenicity (Records and Gross 2010). Investigating these interactions could provide insights into the molecular mechanisms that differentiate pathogenic *P. syringae* pv. *aptata* isolates from non-pathogenic isolates associated with beet and chard plants and seed, contributing to a greater understanding of host-pathogen dynamics, aiding in the development of molecular diagnostic tools, and ultimately contributing to enhanced disease management strategies. In addition, the presence of plasmids in strains of this pathogen should be examined as plasmids are well-known carriers of virulence genes in diverse bacterial plant pathogens, including pathovars of *P. syringae* (Alfano and Collmer 1997).

Acknowledgements

We acknowledge the program of Dr. Neha Potnis for conducting the WGS of isolates of *P. syringae* pv. *aptata* for this study and completing some of the analyses. We thank members of the Vegetable Seed Pathology Program at the WSU Mount Vernon NWREC, including Michael Derie and Tomasita Villaroel, for technical support. This work was funded by the United States Department of Agriculture (USDA) National Institute of Food and Agriculture NIFA Specialty Crops Research Initiative (SCRI) Project No. 2019-51181-30019, the Dick and Marcia Morrison Seed Production Pathology & Seed Health Fellowship, the Alfred Mark Christianson Memorial Fellowship, a Pacific Seed Association Scholarship, and WSU College of Agriculture, Human, and Natural Resource Sciences Hatch Project No. WNP0001.

Literature Cited

Abo-Elwafa, S. F., Abdel-Rahim, H. M., Abou-Salama, A. M., and Teama, E. A. 2006. Sugar beet floral induction and fertility. Effect of vernalization and day-length extension. Sugar Tech. 8:281-287.

AgWeatherNet. 2023. Washington State University. https://weather.wsu.edu/. Accessed 2 Feb. 2023.

Alfano, J. R., and Collmer, A. 1997. The type III (Hrp) secretion pathway of plant pathogenic bacteria: trafficking harpins, *Avr* proteins, and death. J. Bacteriol. 179:5655-5662.

Alfano, J. R., and Collmer, A. 2004. Type III secretion system effector proteins: Double agents in bacterial disease and plant defense. Annu. Rev. Phytopathol. 42:385-414.

Alfano, J. R., Charkowski, A. O., Deng, W. L., Badel, J. L., Petnicki-Ocwieja, T., van Dijk, K., and Collmer, A. 2000. The *Pseudomonas syringae* Hrp pathogenicity island has a tripartite mosaic structure composed of a cluster of type III secretion genes bounded by exchangeable effector and conserved effector loci that contribute to parasitic fitness and pathogenicity in plants. Proc. Natl. Acad. Sci. 97:4856-4861.

Almeida, N. F., Yan, S., Cai, R., Clarke, C. R., Morris, C. E., Schaad, N. W., Schuenzel, E. L., Lacy, G. H., Sun, X., Jones, J. B., Castillo, J. A., Bull, C. T., Leman, S., Guttman, D. S., Setubal, J. C., and Vinatzer, B. A. 2010. PAMDB, a multilocus sequence typing and analysis database and website for plant-associated microbes. Phytopathology 100:208-215.

Almeida, N. F., Yan, S., Lindeberg, M., Studholme, D. J., Schneider, D. J., Condon, B., Liu, H., Viana, C. J., Warren, A., Evans, C., Kemen, E., MaClean, D., Angot, A., Martin, G. B., Jones, J. D., Collmer, A., Setubal, J. C., and Vinatzer, B. A. 2009. A draft genome

sequence of *Pseudomonas syringae* pv. *tomato* T1 reveals a type III effector repertoire significantly divergent from that of *Pseudomonas syringae* pv. *tomato* DC3000. Mol. Plant Microbe Interact. 22:52–62.

Arabi, F., Nikravesh, Z., Babaeizad, V., Rezaeian, V., and Rahimian, H. 2006. Occurrence of bacterial leaf spot and blight of garden beet caused by *Pseudomonas syringae* pv. *aptata* in Iran. Iran. J. Plant Pathol. 42:655-671.

Arabiat, S., Chanda, A. K., Chittem, K., and Khan, M. F. R. 2016. First report of *Pseudomonas syringae* pv. *aptata* causing bacterial blight of sugar beet (*Beta vulgaris*) in Oregon. Plant Dis. 100:2334.

Badel, J. L., Shimizu, R., Oh, H. S., and Collmer, A. 2006. A *Pseudomonas syringae* pv. *tomato* *avrE1*/*hopM1* mutant is severely reduced in growth and lesion formation in tomato. Mol. Plant Microbe Interact. 19:99-111.

Baltrus, D. A., Nishimura, M. T., Romanchuk, A., Chang, J. H., Mukhtar, M. S., Cherkis, K., Roach, J., Grant, S. R., Jones, C. D., and Dangl, J. L. 2011. Dynamic evolution of pathogenicity revealed by sequencing and comparative genomics of 19 *Pseudomonas syringae* isolates. PLoS Path. 7:e1002132.

Bradbury, J. F. 1986. Guide to the Plant Pathogenic Bacteria. CAB International, Wallingford.

Braun-Kiewnick, A., and Sands, D. C. 2001. Gram negative bacteria. Pp. 84-120, In: Laboratory Guide for Identification of Plant Pathogenic Bacteria, Third Edition. N. W. Schaad, J. B. Jones, and W. Chun, editors. American Phytopathological Society, St. Paul.

Buell, C. R., Joardar, V., Lindeberg, M., Selengut, J., Paulsen, I. T., Gwinn, M. L., Dodson, R. J., Deboy, R. T., Durkin, A. S., Kolonay, J. F., Madupu, R., Daugherty, S., Brinkac, L., Beanan, M. J., Haft, D. H., Nelson, W. C., Davidsen, T., Zafar, N., Zhou, L., Liu, J., and

Collmer, A. 2003. The complete genome sequence of the Arabidopsis and tomato pathogen *Pseudomonas syringae* pv. *tomato* DC3000. Proc. Natl. Acad. Sci 100:10181-10186.

Bull, C. T., and Koike, S. T. 2015. Practical benefits of knowing the enemy: modern molecular tools for diagnosing the etiology of bacterial diseases and understanding the taxonomy and diversity of plant-pathogenic bacteria. Annu. Rev. Phytopathol. 53:157-180.

Cheong, M. S., Kirik, A., Kim, J.-G., Frame, K., Kirik, V., and Mudgett, M. B. 2014. *AvrBsT* acetylates Arabidopsis ACIP1, a protein that associates with microtubules and is required for immunity. PLoS Pathog. 10:e1003952.

Crane, A. S. 2023. Seed transmission of *Pseudomonas syringae* pv. *aptata*, and efficacy of bactericides for control of the pathogen in beet and Swiss chard seed production. MS thesis, Washington State University, Pullman. 63 pp.

Cunnac, S., Lindeberg, M., and Collmer, A. 2009. *Pseudomonas syringae* type III secretion system effectors: repertoires in search of functions. Curr. Opin. Microbiol. 12:53-60.

DebRoy, S., Thilmony, R., Kwack, Y. B., Nomura, K., and He, S. Y. 2004. A family of conserved bacterial effectors inhibits salicylic acid-mediated basal immunity and promotes disease necrosis in plants. Proc. Natl. Acad. Sci. 101:9927-9932.

Derie, M. L., Holmes, B. J., Safni, I., Bull, C. T., and du Toit, L. J. 2016. Seedborne inoculum thresholds of *Pseudomonas syringae* pv. *aptata*, causal agent of bacterial leaf spot, in 'baby leaf' Swiss chard crops. Phytopathology 106:S4.142 (Abstr.).

du Toit, L. J. 2007. Crop Profile for Table Beet Seed in Washington. USDA Pest Management Centers. http://www.ipmcenters.org/CropProfiles/docs/WAbeetseed.pdf. Accessed on 23 March 2022.

Dutta, B., Ingram, T., Gitaitis, R. D., Langston, D. B., Brenneman, T., Webster, T. M., and Davis, R. F. 2014. First report of bacterial blight of sugar beet caused by *Pseudomonas syringae* pv. *aptata* in Georgia, USA. Plant Dis. 98:1423.

Emms, D. M., and Kelly, S. 2015. OrthoFinder: solving fundamental biases in whole genome comparisons dramatically improves orthogroup inference accuracy. Genome Biol. 16:157.

Emms, D. M., and Kelly, S. 2018. STAG: species tree inference from all genes. bioRxiv 267914. https://www.biorxiv.org/content/10.1101/267914v1

Emms, D. M., and Kelly, S. 2019. OrthoFinder: phylogenetic orthology inference for comparative genomics. Genome Biol. 20:238.

Gaulke, E., and Goldman, I. L. 2022. Screening table beet and Swiss chard for resistance to *Pseudomonas syringae* pathovar *aptata*. HortSci. 57:1436-1446.

Gilchrist, C. L. M., and Chooi, Y. H. 2021. Clinker & clustermap.js: automatic generation of gene cluster comparison figures. Bioinform. 37:2473-2475.

Gosavi, G., Yan, F., Ren, B., Kuang, Y., Yan, D., Zhou, X., and Zhou, H. 2020. Applications of CRISPR technology in studying plant-pathogen interactions: Overview and perspective. Phytopathology Res. 2:21.

Grondeau, C., Mabiala, A., Ait-Oumeziane, R., and Samson, R. 1996. Epiphytic life is the main characteristic of the life cycle of *Pseudomonas syringae* pv. *pisi*, pea bacterial blight agent. Eur. J. Plant Pathol. 102:353-363.

Hacker, J., Blum-Oehler, G., Mühldorfer, I., and Tschäpe, H. 1997. Pathogenicity islands of virulent bacteria: structure, function and impact on microbial evolution. Mol. Microbiol. 23:1089-1097.

Harveson, R. M., Hanson, L. E., and Hein, G. L. Editors. 2009. Compendium of Beet Diseases and Pests, Second Edition. The American Phytopathological Society, St. Paul.

Hill, C. F. 1979. New plant disease records in New Zealand. N. Z. J. Agric. Res. 22:641-645.

Hirano S. S., and Upper, C. D. 2000. Bacteria in the leaf ecosystem with emphasis on *Pseudomonas syringae* - a pathogen, ice nucleus, and epiphyte. Microbiol. Mol. Biol. Rev. 64:624-653.

Hollaway, G. J., and Bretag, T. W., 1997. Survival of *Pseudomonas syringae* pv. *pisi* in soil and on pea trash and their importance as a source of inoculum for a following field pea crop. Austral. J. Exp. Agric. 37:369-375.

Huelsenbeck, J. P., and Ronquist, F. 2001. MRBAYES: Bayesian inference of phylogenetic trees. Bioinformatics 17:754-755.

Hwang, M. S., Morgan, R. L., Sarkar, S. F., Wang, P. W., and Guttman, D. S. 2005. Phylogenetic characterization of virulence and resistance phenotypes of *Pseudomonas syringae*. Appl. Environ. Microbiol. 71:5182-5191.

Jacobsen, B. J. 2009. Bacterial leaf spot. Pp. 59-60. In: Compendium of Beet Diseases and Pests, Second Edition. R. M. Harveson, L. E. Hanson, and G. L. Hein, editors. The American Plant Pathological Society, St. Paul.

Jamir, Y., Guo, M., Oh, H. S., Petnicki-Ocwieja, T., Chen, S., Tang, X., Dickman, M. B., Collmer, A., and Alfano, J. R. 2004. Identification of *Pseudomonas syringae* type III effectors that can suppress programmed cell death in plants and yeast. Plant J. 37:554-565.

Janse, J. D. 1979. A leaf spot disease of sugar beet caused by *Pseudomonas syringae*. Gewasbescherming 10:121-125.

Jayaraman, J., Yoon, M., Applegate, E. R., Stroud, E. A., and Templeton, M. D. 2020. *AvrE1* and *HopR1* from *Pseudomonas syringae* pv. *actinidiae* are additively required for full virulence on kiwifruit. Mol. Plant Pathol. 21:1467-1480.

Jelenska, J., Yao, N., Vinatzer, B. A., Wright, C. M., Brodsky, J. L., and Greenberg, J. T. 2007. A J domain virulence effector of *Pseudomonas syringae* remodels host chloroplasts and suppresses defenses. Curr. Biol. 17:499-508.

Kado, C. I., and Heskett, M. G. 1970. Selective medium for isolation of *Agrobacterium*, *Corynebacterium*, *Erwinia*, *Pseudomonas*, and *Xanthomonas*. Phytopathology 60:969-976.

Katoh, K., and Standley, D. M. 2013. MAFFT multiple sequence alignment software version 7: improvements in performance and usability. Mol. Biol. Evol. 30:772-780.

Kelly, S., and Maini, P. K. 2013. DendroBLAST: approximate phylogenetic trees in the absence of multiple sequence alignments. PloS One 8:e58537.

Khan, M. F. R., Windels, C. E., and Bradley, C. A. 2023. Cercospora and Bacterial Leaf Spots on Sugarbeet. North Dakota State University/University of Minnesota. https://www.ndsu.edu/agriculture/sites/default/files/2023-11/pp1244.pdf. Accessed 18 Oct. 2024

King, E. O., Ward, M. K., and Raney, D. E. 1954. Two simple media for the demonstration of pyocyanin and fluorescin. J. Lab. Clin. Med. 44:301-307.

Kockelmann, A., Tilcher, R., and Fischer, U. 2010. Seed production and processing. Sugar Tech. 12:267-275.

Koike, S. T., Henderson, D. M., Bull, C. T., Goldman, P. H., and Lewen, R. T. 2003. First report of bacterial leaf spot of Swiss chard caused by *Pseudomonas syringae* pv. *aptata* in California. Plant Dis. 87:1397.

Kovács, N. 1956. Identification of *Pseudomonas pyocyanea* by the oxidase reaction. Nature 178:703.

Langmead, B., and Salzberg, S. L. 2012. Fast gapped-read alignment with Bowtie 2. Nat. Methods 9:357-359.

Lee, A. H.-Y., Hurley, B., Felsensteiner, C., Yea, C., Ckurshumova, W., Bartetzko, V., Wang, P. W., Quach, V., Lewis, J. D., Liu, Y. C., Börnke, F., Angers, S., Wilde, A., Guttman, D. S., and Desveaux, D. 2012. A bacterial acetyltransferase destroys plant microtubule networks and blocks secretion. PloS Pathog. 8:e1002523.

Lehmann, G., Udasin, R. G., Livneh, I., and Ciechanover, A. 2017. Identification of UBact, a ubiquitin-like protein, along with other homologous components of a conjugation system and the proteasome in different gram negative bacteria. Biochem. Biophys. Res. Commun. 483:946-950.

Lelliott, R. A., Billing, E., and Hayward, A. C. 1966. A determinative scheme for the fluorescent plant pathogenic pseudomonads. J. Appl. Bacteriol. 29:470-489.

Lin, B. H., Jayachandran, N. V., Jane, A., and John, C. 2003. Food and Agricultural Commodity Consumption in the United States: Looking Ahead to 2020. USDA Economic Research Service AER-820. https://www.ers.usda.gov/webdocs/publications/42576/19268_aib792-7_1_.pdf?v=0. Accessed 1 Apr. 2024.

Lindeberg, M., Cunnac, S., and Collmer, A. 2009. The evolution of *Pseudomonas syringae* host specificity and type III effector repertoires. Mol. Plant Pathol. 10:767-775.

Lindeberg, M., Cunnac, S., and Collmer, A. 2012. *Pseudomonas syringae* type III effector repertoires: last words in endless arguments. Trends Microbiol. 20:199-208.

Lipps, S. M., and Samac, D. A. 2022. *Pseudomonas viridiflava*: An internal outsider of the *Pseudomonas syringae* species complex. Mol. Plant Pathol. 23:3-15.

Lv, C., Li, Y., Wei, Y., Wang, J., Yu, H., Gao, F., Zhu, C., Jia, X., Tong, M., Dong, P., Gao, Q., and Geng, L. 2022. Research progress on small molecular inhibitors of the type 3 secretion system. Molecules 27:8348.

Mohan, S. K., and Schaad, N. W. 1987. An improved agar plating assay for detecting *Pseudomonas syringae* pv. *syringae* and *Pseudomonas syringae* pv. *phaseolicola* in contaminated bean seed. Phytopathology 77:1390-1395.

Monteil, C. L., Bardin, M., and Morris, C. E. 2014. Features of air masses associated with the deposition of *Pseudomonas syringae* and *Botrytis cinerea* by rain and snowfall. ISME J. 8:2290-2304.

Morris, C. E., Monteil, C. L., and Berge, O. 2013. The life history of *Pseudomonas syringae*: linking agriculture to earth system processes. Annu. Rev. Phytopathol. 51:85-104.

Morris, C. E., Sands, D. C., Vinatzer, B. A., Glaux, C., Guilbaud, C., Buffie`re, A., Yan, S., Dominguez, H., and Thompson, B. M. 2008. The life history of the plant pathogen *Pseudomonas syringae* is linked to the water cycle. ISME J. 2:321-334.

Morris, C., Glaux C., Latour X., Gardan L., Samson R., and Pitrat M., 2000. The relationship of host range, physiology, and genotype to virulence on cantaloupe in *Pseudomonas syringae* from cantaloupe blight epidemics in France. Phytopathology 90:636–646.

Mutasa-Göttgens, E. S., Qi, A., Zhang, W., Schulze-Buxloh, G., Jennings, A., Hohmann, U., Müller, A. E., and Hedden, P. 2010. Bolting and flowering control in sugar beet:

Relationships and effects of gibberellin, the bolting gene B and vernalization. AoB Plant. 2010:plq012.

Nampijja, M., Derie, M. L., and du Toit, L. J. 2021. First report of bacterial leaf spot caused by *Pseudomonas syringae* pv. *aptata* on Swiss chard, *Beta vulgaris* subsp. *vulgaris*, in Arizona. Plant Dis. 105:3738.

Nampijja, M., Jacobs, J., and du Toit, L. 2023. Host colonization by strains of *Pseudomonas syringae* pv. *aptata* with differential pathogenicity on table beet and Swiss chard. Phytopathology 113:S3.31 (Abstr.).

Navazio, J., Colley, M., and Zyskowski, J. 2010. Principles and Practices of Organic Beet Seed Production in the Pacific Northwest. Organic Seed Alliance, Port Townsend.

Neergaard P. 1977. Seed Pathology. Macmillan Press, London.

Newberry, E. A., Ebrahim, M., Timilsina, S., Zlatković, N., Obradović, A., Bull, C. T., Goss, E. M., Huguet-Tapia, J. C., Paret, M. L., Jones, J. B., and Potnis, N. 2019. Inference of convergent gene acquisition among *Pseudomonas syringae* strains isolated from watermelon, cantaloupe, and squash. Front. Microbiol. 10:270.

Nikolić, I., Glatter, T., Ranković, T., Berić, T., Stanković, S., and Diepold, A. 2023. Repertoire and abundance of secreted virulence factors shape the pathogenic capacity of *Pseudomonas syringae* pv. *aptata*. Front. Microbiol. 14:1205257.

Nikolić, I., Stanković, S., Dimkić, I., Berić, T., Stojšin, V., Janse, J., and Popović, T. 2018. Genetic diversity and pathogenicity of *Pseudomonas syringae* pv. *aptata* isolated from sugar beet. Plant Pathol. 67:1194-1207.

Nomura, K., Debroy, S., Lee, Y. H., Pumplin, N., Jones, J., and He, S. Y. 2006. A bacterial virulence protein suppresses host innate immunity to cause plant disease. Science 313:220-223.

Nottingham, S. 2004. Beetroot. Archived from the original (e-book) on 9 Feb. 2012. Accessed on 15 Aug. 2010.

Organic Seed Alliance. 2016. Climatic Considerations for Seed Crops: Guidelines and Field Trainings for Organic and Specialty Vegetable Seed Producers. https://seedalliance.org/. Accessed on 16 Jul. 2024.

Parks, D. H., Imelfort, M., Skennerton, C. T., Hugenholtz, P., and Tyson, G. W. 2015. CheckM: assessing the quality of microbial genomes recovered from isolates, single cells, and metagenomes. Genome Res. 25:1043-1055.

Prjibelski, A., Antipov, D., Meleshko, D., Lapidus, A., and Korobeynikov, A. 2020. Using SPAdes de novo assembler. Curr. Protoc. Bioinf. 70:e102.

Rackham, L. R. 2002. History of Specialty Seed Crop Production in the Pacific Northwest. Willamette Valley Specialty Seed Crops Association, Corvallis.

Ranković, T., Nikolić, I., Berić, T., Popović, T., Lozo, J., Medić, O., and Stanković, S. 2023. Genome analysis of two *Pseudomonas syringae* pv. *aptata* strains with different virulence capacity isolated from sugar beet: Features of successful pathogenicity in the phyllosphere microbiome. Microbiol. Spectr. 11:e0359822.

Records, A. R., and Gross, D. C. 2010. Sensor kinases RetS and LadS regulate *Pseudomonas syringae* type VI secretion and virulence factors. J. Bacteriol. 192:3584-3596.

Riffaud, C. M. H., and Morris, C. E. 2002. Detection of *Pseudomonas syringae* pv. *aptata* in irrigation water retention basins by immuno-fluorescence colony staining. Eur. J. Plant Pathol. 108:539-545.

Safni, I., Ramos-Sepulveda, L., Goldman, P., Derie, M., du Toit, L., Koike, S., Stockwell, V., and Bull, C. 2016. Genetic diversity of *Pseudomonas syringae* causing bacterial leaf spot on table beet (*Beta vulgaris*) and Swiss chard (*Beta vulgaris* subsp. *cicla*). Phytopathology 106:S4.143 (Abstr.).

Sarkar, S. F., and Guttman, D. S. 2004. Evolution of the core genome of *Pseudomonas syringae*, a highly clonal, endemic plant pathogen. Appl. Environ. Microbiol. 70:1999-2012.

Sarkar, S. F., Gordon, J. S., Martin, G. B., and Guttman, D. S. 2006. Comparative genomics of host-specific virulence in *Pseudomonas syringae*. Genetics 174:1041-1056.

Schrader, L. W., and Mayberry, S. K. 2003. Beet and Swiss chard production in California. Univ. California Agric. Nat. Res. No. 8096. https://doi.org/10.3733/ucanr.8096. Accessed 16 Feb. 2024.

Schreiber, A., and Ritchie, L. 1995. Washington Minor Crops. Food and Environmental Quality Laboratory, Washington State University, Richland.

Sedighian, N., Shams-Bakhsh, M., Osdaghi, E., and Khodaygan, P. 2014. Etiology and host range of bacterial leaf blight and necrosis of squash and muskmelon in Iran. Plant Pathol. 96:507-514.

Stojšin, V., Balaž, J., Budakov, D., Stanković, S., Nikolić, I., Ivanović, Ž., and Popović, T. 2015. First report of *Pseudomonas syringae* pv. *aptata* causing bacterial leaf spot on sugar beet in Serbia. Plant Dis. 99:281.

Tymon, L. S., and Inglis, D. A. 2017. Identification and pathogenicity of *Pseudomonas syringae* genomospecies 1 phylogroup 2b causing leaf spots and fruit warts on cucurbits in western Washington U.S. Plant Pathol. 99:713-722.

Vinatzer, B. A., Jelenska, J., and Greenberg, J. T. 2005. Bioinformatics correctly identifies many type III secretion substrates in the plant pathogen *Pseudomonas syringae* and the biocontrol isolate *P. fluorescens* SBW25. Mol. Plant Microbe Interact. 18:877-888.

Vinatzer, B. A., Teitzel, G. M., Lee, M. W., Jelenska, J., Hotton, S., Fairfax, K., Jenrette, J., and Greenberg, J. T. 2006. The type III effector repertoire of *Pseudomonas syringae* pv. s*yringae* B728a and its role in survival and disease on host and non-host plants. Mol. Microbiol. 62:26-44.

Walker, B. J., Abeel, T., Shea, T., Priest, M., Abouelliel, A., Sakthikumar, S., Cuomo, C. A., Zeng, Q., Wortman, J., Young, S. K., and Earl, A. M. 2014. Pilon: an integrated tool for comprehensive microbial variant detection and genome assembly improvement. PloS One 9:e112963.

Walker, J. C. 1952. Diseases and pests. Pp. 190-191, In: Diseases of Vegetable Crops. McGraw-Hill Book Co., Inc., New York.

Wang, N., Han, N., Tian, R., Chen, J., Gao, X., Wu, Z., Liu, Y., and Huang, L. 2021. Role of the type VI secretion system in the pathogenicity of *Pseudomonas syringae* pv. *actinidiae*, the causative agent of kiwifruit bacterial canker. Front. Microbiol. 12:627785.

Washington, E. J., Mukhtar, M. S., Finkel, O. M., Wan, L., Banfield, M. J., Kieber, J. J., and Dangl, J. L. 2016. *Pseudomonas syringae* type III effector *HopAF1* suppresses plant immunity by targeting methionine recycling to block ethylene induction. Proc. Natl. Acad. Sci. 113:E3577-E3586.

Yan, S., Liu, H., Mohr, T. J., Jenrette, J., Chiodini, R., Zaccardelli, M., Setubal, J. C., Vinatzer, B. A. 2008. Role of recombination in the evolution of the model plant pathogen *Pseudomonas syringae* pv. tomato DC3000, a very atypical tomato strain. Appl. Env. Microbiol. 74:3171-3181.

Zhang, R., Xu, W., Shao, S., and Wang, Q. 2021. Gene silencing through CRISPR interference in bacteria: Current advances and future prospects. Front. Microbiol. 12:635227.

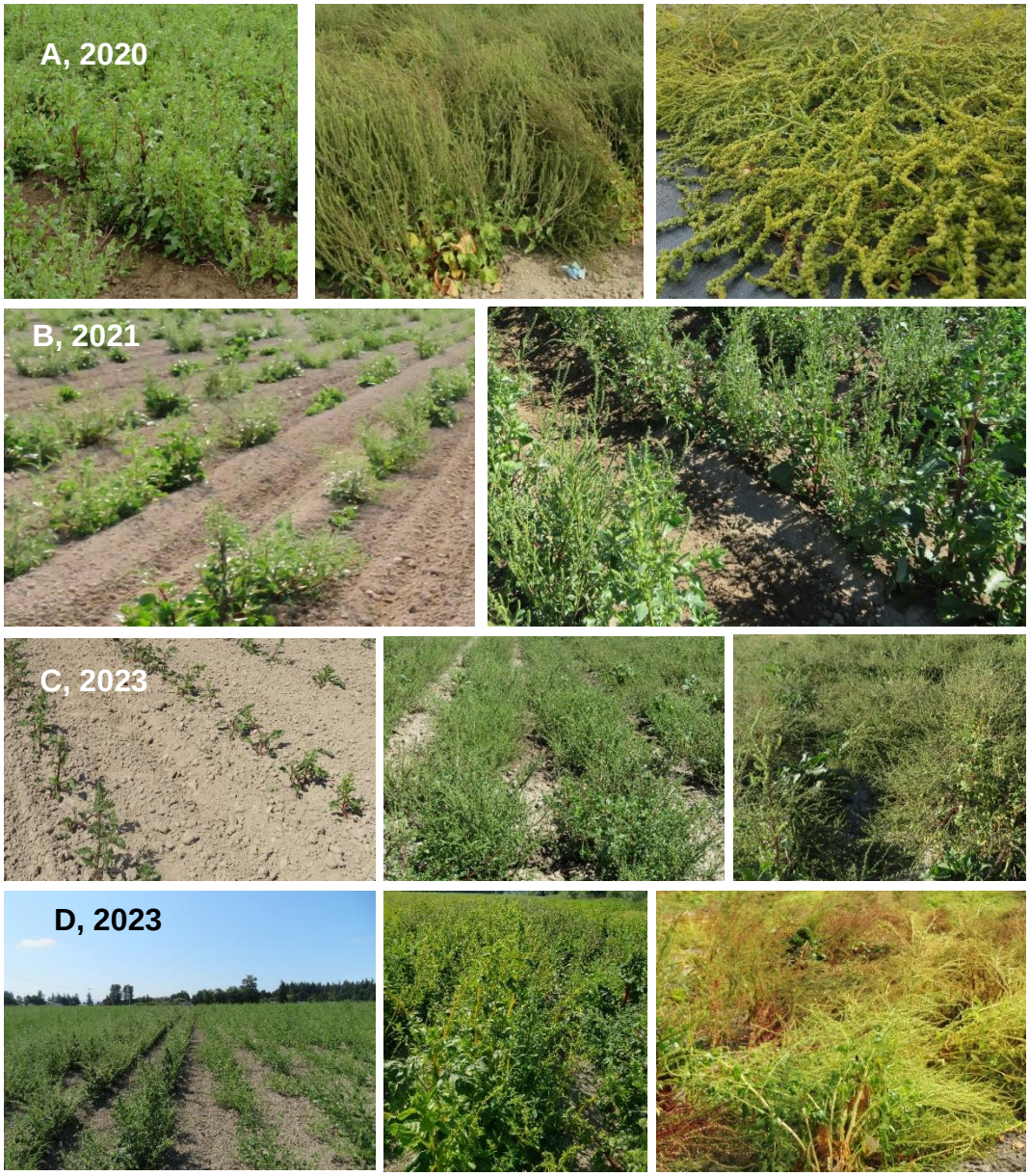

Fig. 1.1. Growth stages of table beet and Swiss chard seed crops in western Washington during surveys for bacterial leaf spot in 2020, 2021, and 2023. From left to right: A) early flowering, pollen shed, and seed set in table beet seed crops in 2020; (B) late bolting to early flowering in table beet seed crops in 2021; (C) early bolting, flowering, and seed set for table beet seed crops in 2023; and D) late bolting, flowering, and seed set in a Swiss chard seed crop in 2023.

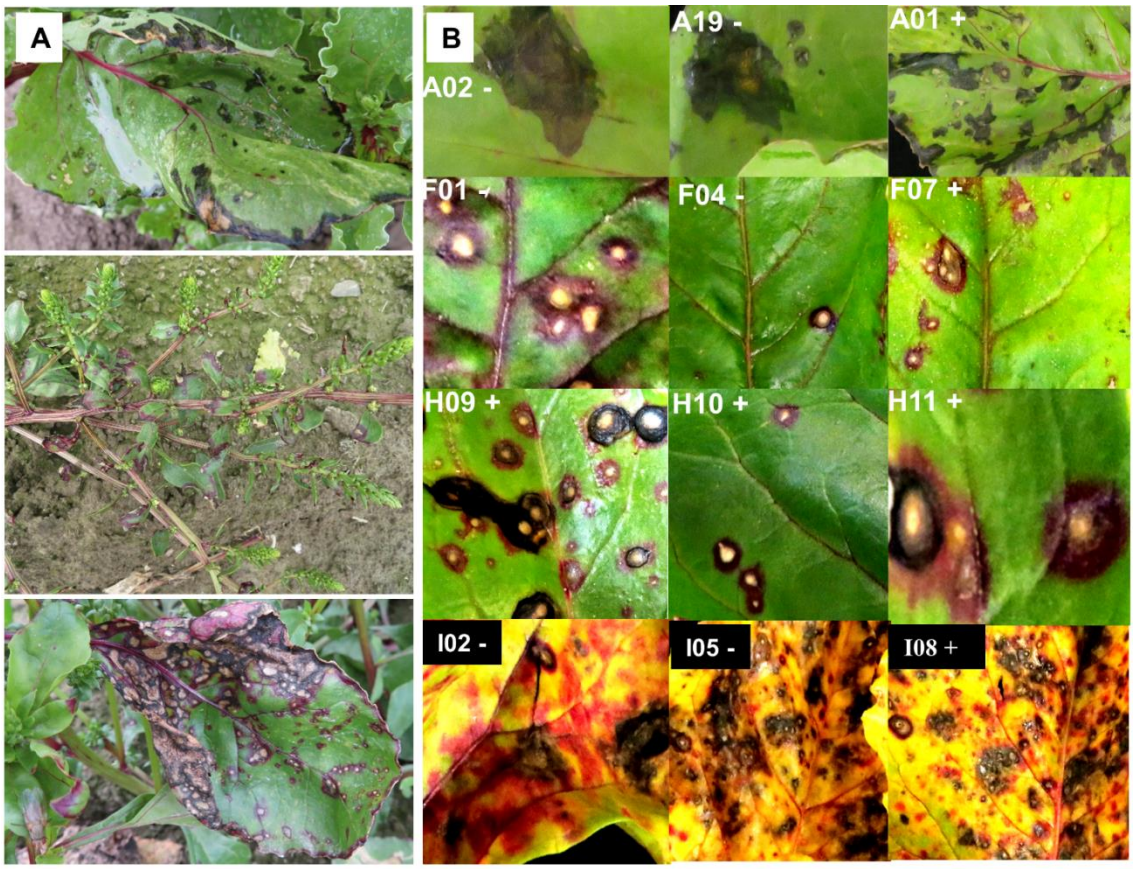

Fig. 1.2. A) Symptoms observed in table beet seed crops surveyed in June 2020 for bacterial leaf spot caused by *Pseudomonas syringae* pv. *aptata*. B) Representative symptoms on leaves collected from table beet seed crops in 2020. A, F, H, and I = fields surveyed; + = samples that tested positive for the bacterial leaf spot pathogen following inoculation of seedlings of the table beet cv. Red Ace and the Swiss chard cv. Silverado with *P. syringae* isolates obtained from these samples; - = leaf samples from which *P. syringae* isolates recovered did not cause symptoms when inoculated onto table beet and Swiss chard seedlings.

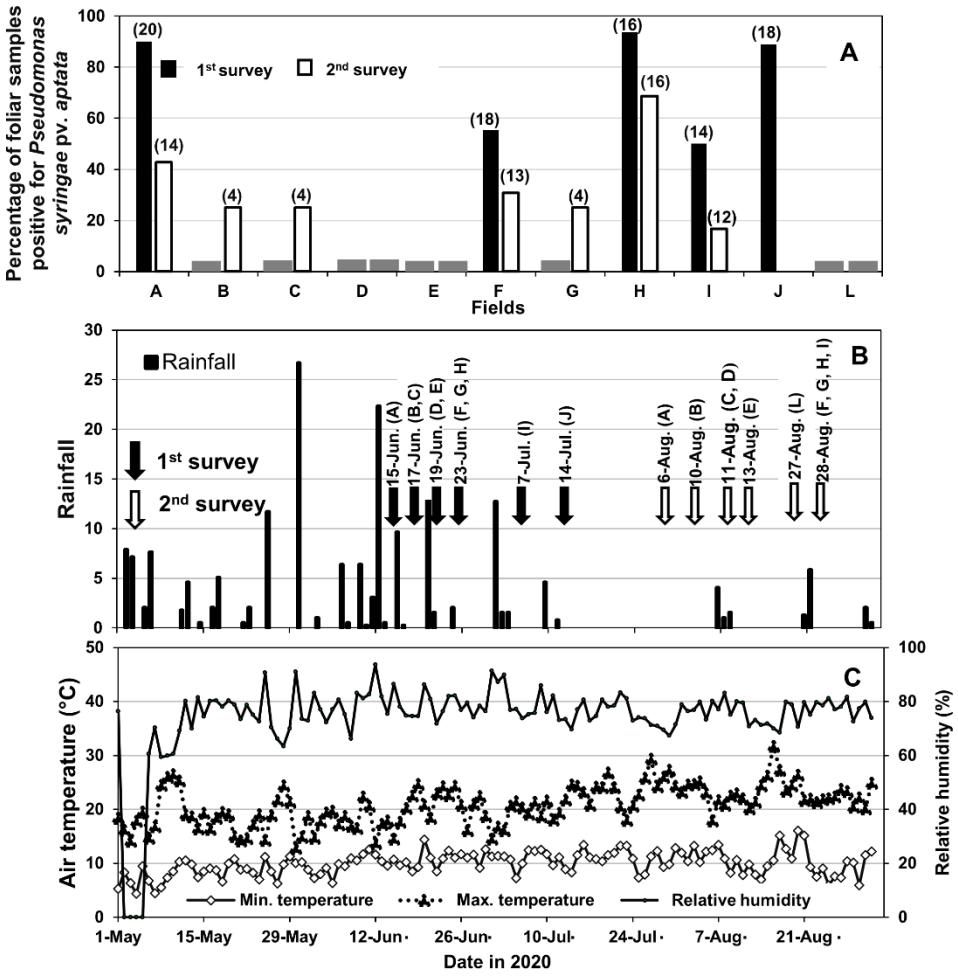

Fig. 1.3. A) Percentage of plants with symptoms of bacterial leaf spot caused by *Pseudomonas syringae* pv. *aptata* during a survey of 10 table beet seed crops (fields A to H, J, and L) and a Swiss chard seed crop (Field I) in western Washington in 2020. The number in parentheses above each bar is the number of symptomatic leaf samples collected in that field. The gray bars indicate fields in which symptoms were not observed for that survey date. There is no field K. B) Amount of rainfall that occurred from 1 May to 1 September 2020 in Skagit Co., WA. Arrows = dates the crops were surveyed, with fields surveyed at each date shown in parentheses. C) Relative humidity (%), and minimum and maximum air temperatures (°C) from 1 May to 1 September 2020 in Skagit Co., obtained from the AgWeatherNet station at the Washington State University Mount Vernon Northwestern Washington Research and Extension Center as a representation of the region in which the seed crops were surveyed.

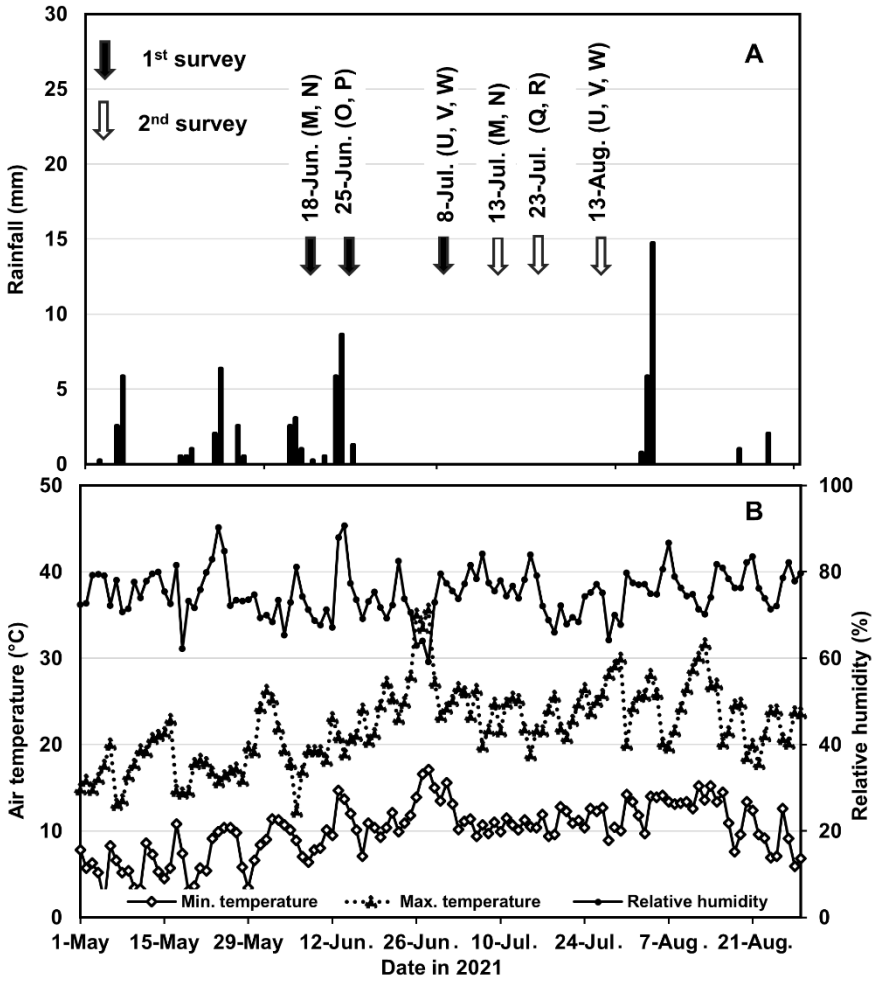

Fig. 1.4. A) Amount of rainfall that occurred from 1 May to 1 September 2021 in Skagit Co., WA. Arrows = dates bacterial leaf spot surveys were completed in table beet and Swiss chard seed crops, with the fields surveyed at each date shown in parentheses. Bacterial leaf spot was not observed in any of the seed crops surveyed in 2021. B) Relative humidity (%), and minimum and maximum air temperatures (°C) from 1 May to 1 September 2021 in Skagit Co., obtained from the AgWeatherNet station at the Washington State University Mount Vernon Northwestern Washington Research and Extension Center as a representation of the region in which seed crops were surveyed.

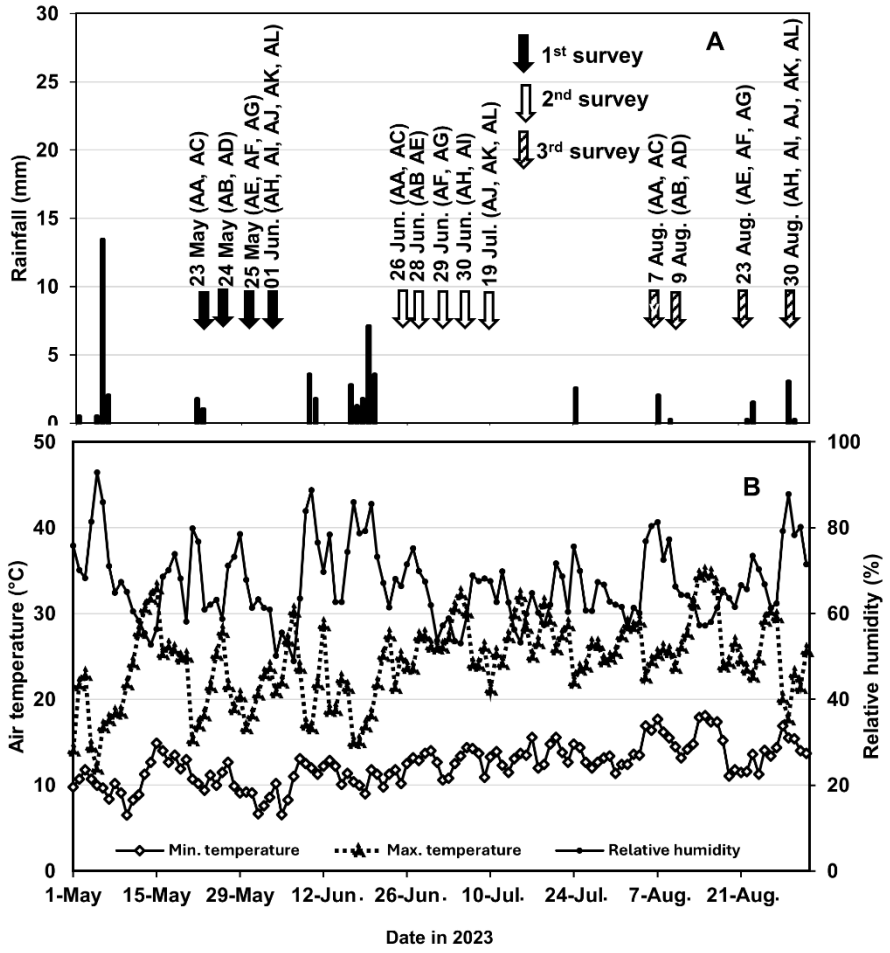

Fig. 1.5. A) Amount of rainfall that occurred from 1 May through 1 September 2023 in Skagit Co., WA. Arrows = dates when table beet and Swiss chard seed crops in western Washington were surveyed for bacterial leaf spot caused by *Pseudomonas syringae* pv. *aptata*, with the specific fields surveyed at each date shown in parentheses. Bacterial leaf spot was not observed in any of the seed crops surveyed in 2023. B) Relative humidity (%), and minimum and maximum air temperatures (°C) from 1 May to 1 September 2023 in Skagit Co., obtained from the AgWeatherNet station at the Washington State University Mount Vernon Northwestern Washington Research and Extension Center in Skagit Co. as a representation of the region in which seed crops were surveyed.

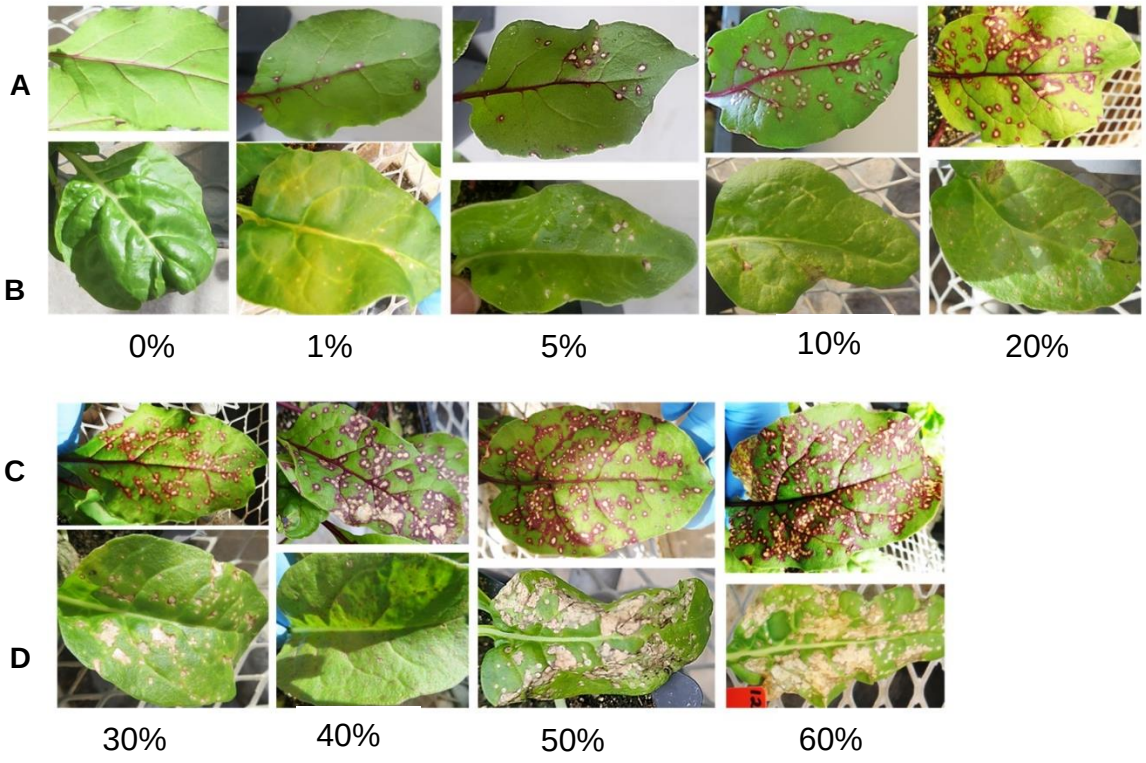

Fig. 1.6. Symptoms of bacterial leaf spot on seedlings of the table beet cv. Red Ace (**A** and **C**) and Swiss chard cv. Silverado (B and D) inoculated with isolates of *Pseudomonas syringae* pv. *aptata*. The percentages indicate the severity rating for bacterial leaf spot assigned to each inoculated leaf based on the surface area with symptoms.

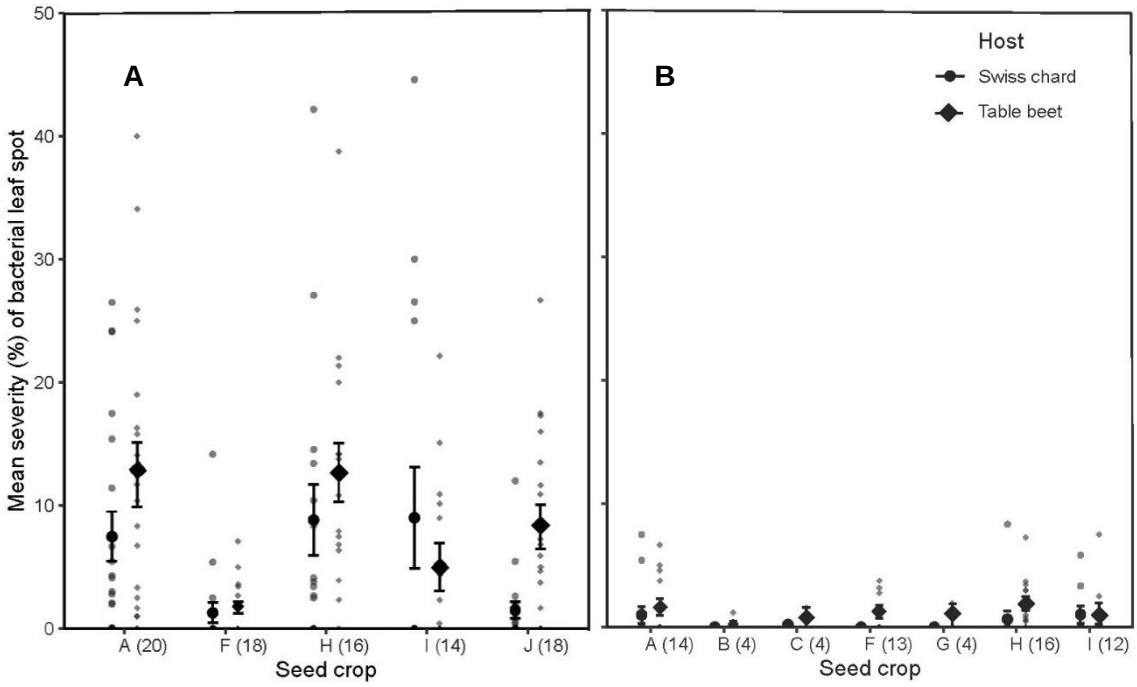

Fig. 1.7. Severity of bacterial leaf spot on seedlings of the Swiss chard cv. Silverado and the table beet cv. Red Ace inoculated with isolates of *Pseudomonas syringae* pv. *aptata* recovered from symptomatic leaves collected in table beet and Swiss chard seed crops during the first (A) and second (B) surveys in western Washington in 2020. Each black circle and diamond shows the mean ± standard error of bacterial leaf spot severity caused by an isolate. Each gray diamond and circle is the data for an individual isolate that caused symptoms. The number of isolates tested from each field is shown in parentheses after the letter code for each seed crop on the x-axes.

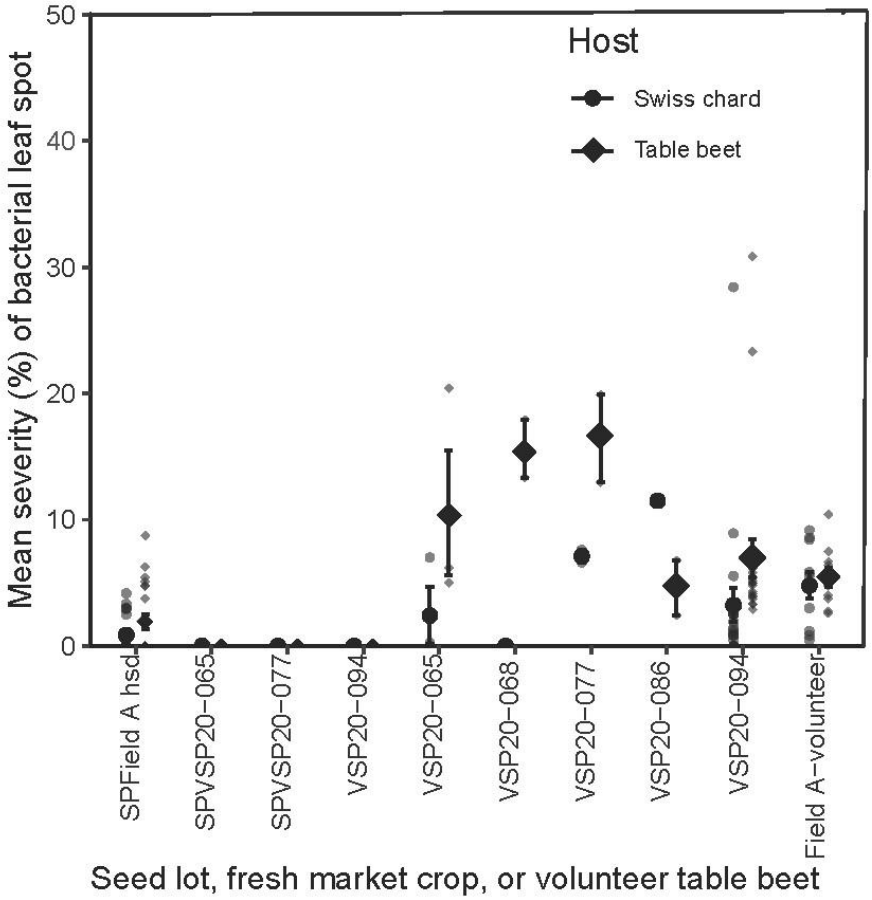

Fig. 1. 8. Severity of bacterial leaf spot on seedlings of the Swiss chard cv. Silverado and the table beet cv. Red Ace inoculated with isolates of *Pseudomonas syringae* pv. *aptata* recovered from: a seed lot harvested from a table beet seed crop surveyed in 2020 (Field A hsd), seed lots used to plant three fresh market beet and chard crops that developed symptoms (SP VSP20-65, SP VSP20-077, and SP VSP20-094), symptomatic leaves of these fresh market beet and chard crops (VSP20-65, VSP20-68, VSP20-077, VSP20-086, and VSP20-094), and table beet volunteer seedlings that grew from shattered seed in field A (Field A volunteer) in Skagit Co., WA. Each black circle and diamond shows the mean ± standard error of bacterial leaf spot severity of isolates from that source. Each gray diamond and circle is the severity rating for an individual isolate. Number of isolates tested: SPField A hsd = 7, SP VSP20-065 = 1, SPVSP20-077 = 1, VSP20-065 = 3, VSP20-068 = 2, VSP20-077 = 2, VSP20-086 = 2, VSP20-094 = 21, and Field A volunteer = 10.

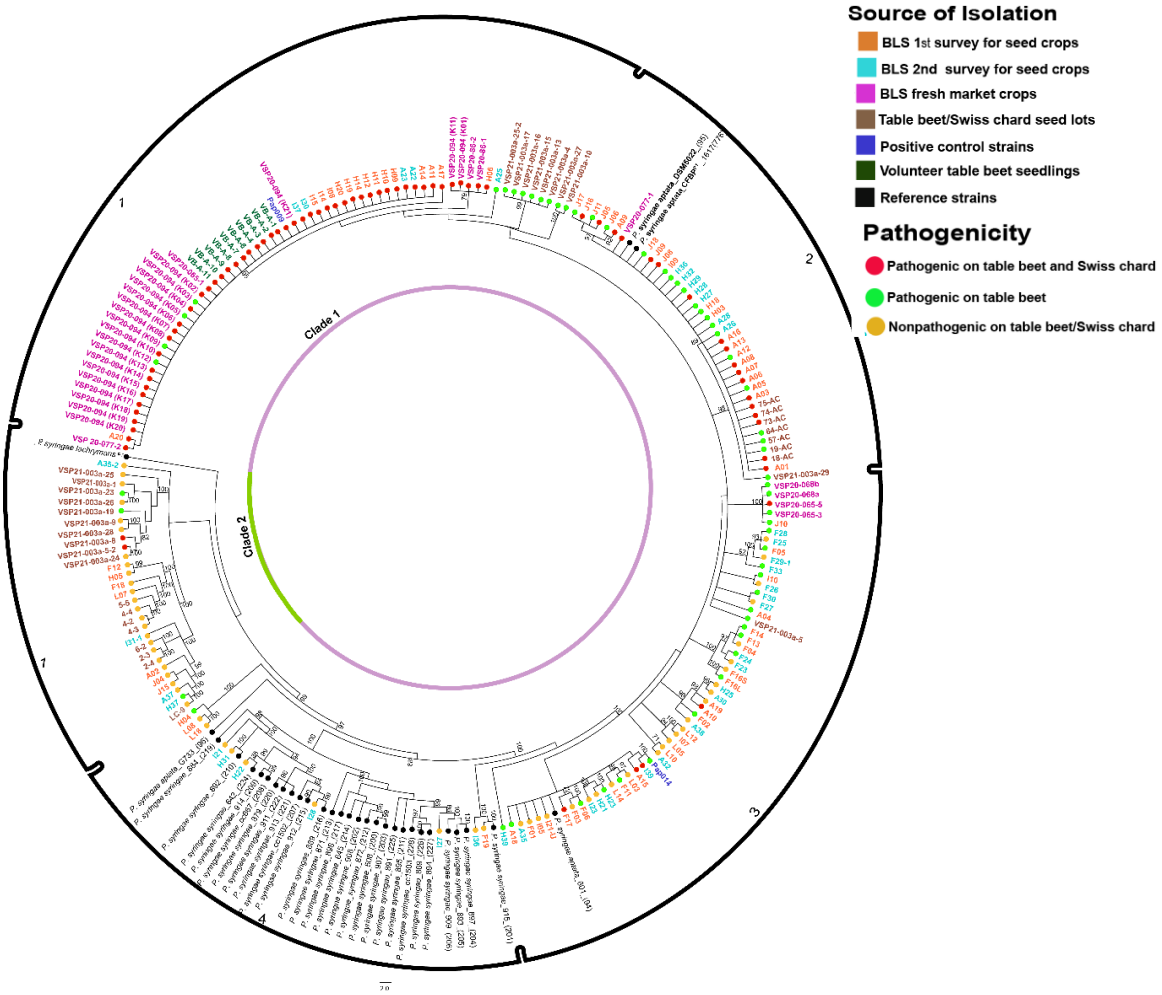

Fig. 1.9. Phylogenetic tree showing the relationship of pathogenic isolates of *Pseudomonas syringae* pv. *aptata* and non-pathogenic isolates obtained from table beet and/or Swiss chard seed crops in 2020, table beet seed harvested in 2020, fresh market beet and chard crops, and seed that was used to plant the fresh market crops compared to isolates of other *P. syringae* pathovars, based on multilocus sequence analysis of the concatenated sequences of four housekeeping genes: *gyrB*, *rpoD*, *gapA*, and *gltA*. Strain CFBP 1617^{PT} is the pathotype strain of *P. syringae* pv. *aptata*. Strain CFBP 6463^{PT} of *P. syringae* pv. *lachrymans* was used as an outgroup. The sequences were aligned using MAFFT version 7.450 (Katoh and Standle 2013) and the phylogenetic tree was constructed using Mr. Bayes (Huelsenbeck and Ronquist 2001) with 1,000 pseudoreplicates and the model HKY85 to estimate the phylogeny in Geneious Prime version 2023. Posterior probabilities on the branches are expressed as percentages. The numbers 1 to 4 in Clade 1, and 1 in Clade 2 between the grooves of the outer black circle represent subclades.

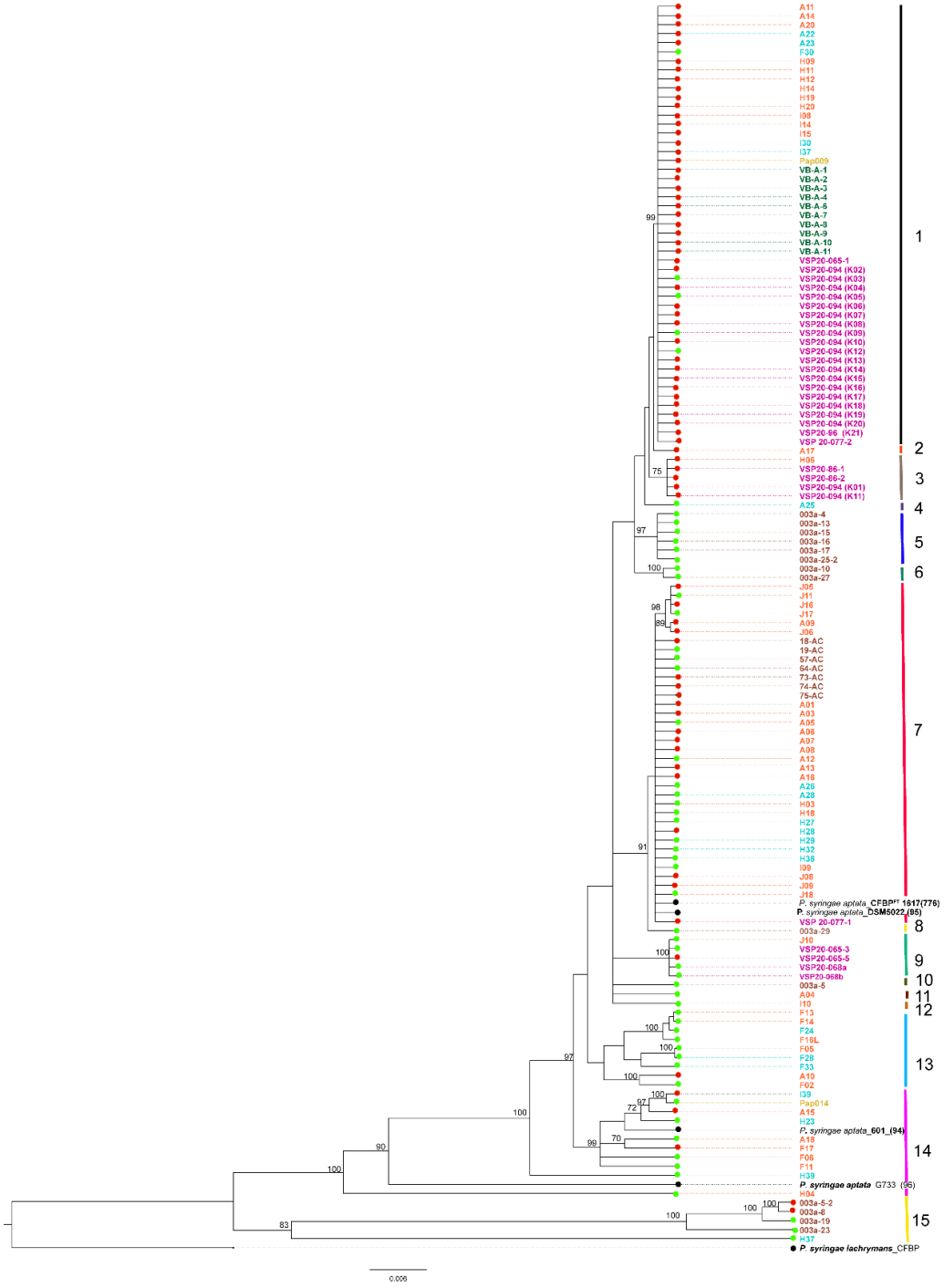

Fig. 1.10. Phylogenetic tree showing the relationship of pathogenic isolates of *Pseudomonas syringae* pv. *aptata* obtained from table beet seed crop fields surveyed in 2020, table beet seed harvested from a seed crop in 2020, and fresh market beet and Swiss chard crops based on multilocus sequence analysis of the concatenated sequences of four housekeeping genes: *gyrB*, *rpoD*, *gapA*, and *gltA*. Strain CFBP 1617^{PT} is the pathotype strain of *P. syringae* pv. *aptata*. Strain CFBP 6463^{PT} of *P. syringae* pv. *lachrymans* is the outgroup. Numbers 1 to 15 represent

clades. Red circles = isolates pathogenic on table beet and Swiss chard; green = isolates pathogenic on table beet only, and black = reference strains. The sequences were aligned using MAFFT version 7.450 (Katoh and Standle 2013) and the phylogenetic tree was constructed using Mr. Bayes (Ronquist et al. 2012) with 1,000 pseudoreplicates and the model HKY85 to estimate the phylogeny in Geneious Prime version 2023. Posterior probabilities on the branches are expressed as percentages, and only percentages ≥70 are shown.

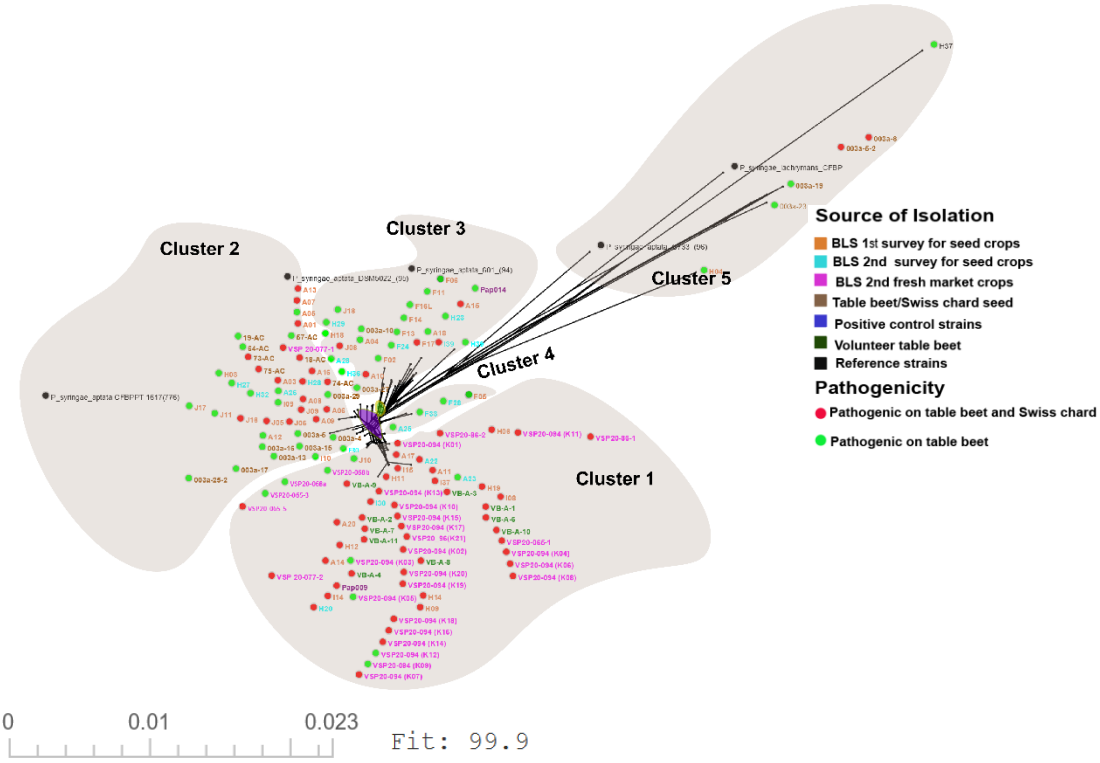

Fig. 1.11. A phylogenetic network among pathogenic isolates of *Pseudomonas syringae* pv. *aptata* obtained from table beet and Swiss chard samples, generated using SplitsTree with default settings, indicating the likelihood of recombination events during the evolutionary history of these isolates. The neighbor-net tree was constructed based on concatenated sequences of four housekeeping genes: *gyrB*, *rpoD*, *gapA*, and *gltA*, from 137 isolates of *P*. *syringae* pv. *aptata* to examine diversity and recombination events among isolates. Clusters 1 to 5 include isolates of the same haplotype. Red circles = isolates pathogenic on table beet and Swiss chard, green = isolates pathogenic on table beet only, and black = reference strains. Strain CFBP 1617^{PT} is the pathotype strain of *P*. *syringae* pv. *aptata*. Strain CFBP 6463^{PT} of *P*. *syringae* pv. *lachrymans* is the outgroup.

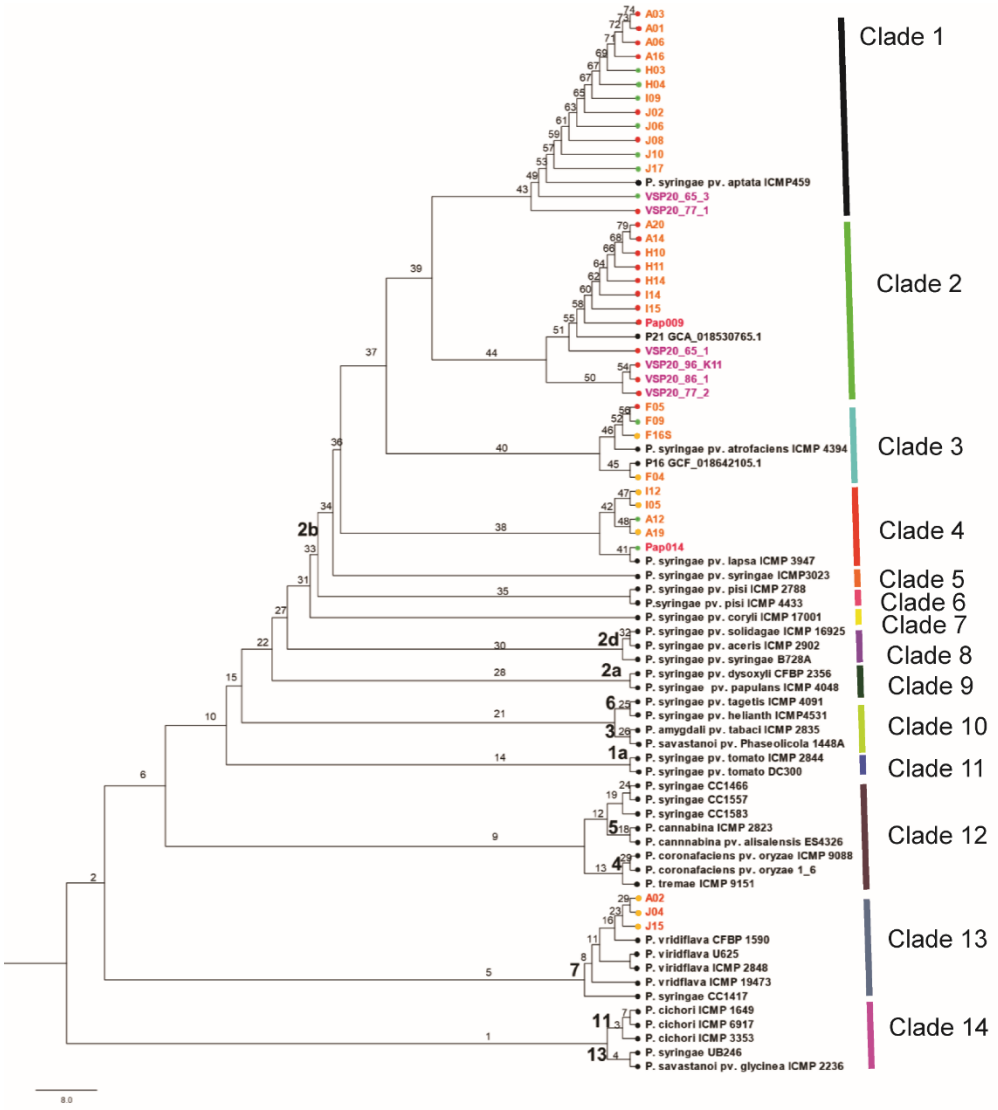

Fig. 1.12. Core phylogeny based on whole genome sequencing of isolates of *Pseudomonas syringae pv. aptata and other Pseudomonas spp. obtained from table beet and Swiss chard crops*, and reference strains, determined using OrthoFinder v2.5.2 to identify orthogroups. Phylogenetic relationships were inferred using DendroBLAST, followed by the STAG algorithm for species tree inference. Node support (%) is indicated on the branches. Isolates of *P. syringae* pv. *aptata* and other *P. syringae* isolates from the table beet and Swiss chard seed crops are indicated in orange. Red circles = isolates pathogenic on table beet and Swiss chard, green = isolates pathogenic on table beet only, dark yellow = isolates non-pathogenic on table beet and Swiss chard, and black = reference strains. The letters in bold on the branches are phylogroups, and the colors on the right represent clades 1 to 14.

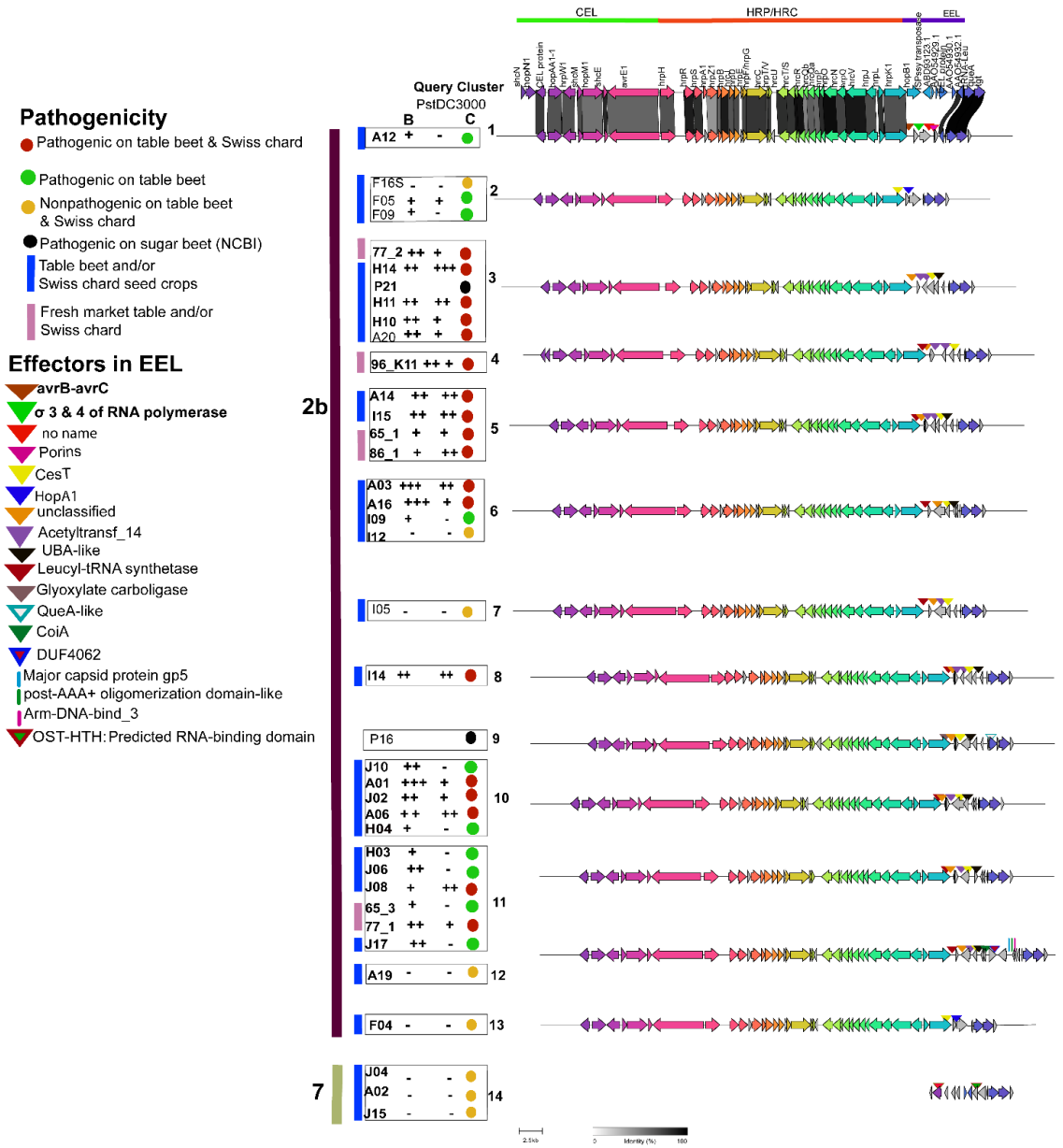
Pathogenicity
Pathogenic on table beet & Swiss chard
Pathogenic on table beet
Nonpathogenic on table beet & Swiss chard
Pathogenic on sugar beet (NCBI)
Table beet and/or Swiss chard seed crops
Fresh market table and/or Swiss chard
Effectors in EEL
avrB-avrC
σ 3 & 4 of RNA polymerase
no name
Porins
CesT
HopA1
unclassified
Acetyltransf_14
UBA-like
Leucyl-tRNA synthetase
Glyoxylate carboligase
QueA-like
CoiA
DUF4062
Major capsid protein gp5
post-AAA+ oligomerization domain-like
Arm-DNA-bind_3
OST-HTH: Predicted RNA-binding domain
CEL
HRP/HRC
EEL
Query Cluster
PstDC3000
B
C
2b
7
A12
F16S
F05
F09
77_2
H14
P21
H11
H10
A20
96_K11
A14
I15
65_1
86_1
A03
A16
I09
I12
I05
I14
P16
J10
A01
J02
A06
H04
H03
J06
J08
65_3
77_1
J17
A19
F04
J04
A02
J15
1
2
3
4
5
6
7
8
9
10
11
12
13
14

Fig. 1.13. Clinker gene cluster comparison of the genomic region comprising the conserved effector locus (CEL), hypersensitivity and pathogenicity (*hrp*)/conserved genes (*hrc*), and exchangeable effector locus (EEL) from whole genome sequences (WGS) of isolates of *Pseudomonas syringae* pv. *aptata* obtained from table beet and Swiss chard seed crops surveyed in western Washington in 2020, and fresh market table beet and Swiss chard crops in western Washington that had symptoms of bacterial leaf spot. The WGS of strains P16 and P21 obtained from sugar beet crops in Serbia were published by Nikolić et al. (2023). The numbers 1 to 14 each indicate a group of isolates in the same gene cluster. B = beet cv. Red Ace, and C = Swiss chard cv. Silverado on which the isolates were tested for pathogenicity. Isolates that caused mean disease severity ratings >30% were considered highly virulent (+++), those that caused 10-30% severity were moderately virulent (++), those that caused <10% severity were weakly virulent (+), and isolates that did not cause symptoms were avirulent (-). 2b and 7 are phylogroups of *P. syringae* (Bull et al. 2015; Newberry et al. 2019). Refer to the main text for details on the survey, pathogenicity tests, and WGS generation. The colored inverted triangles are annotated effectors in the EEL region searched in the Integrated Microbial Genomes and Microbiomes of the Joint Genomic Institute USA Department of Energy platform. The arrows show the direction of transcription.

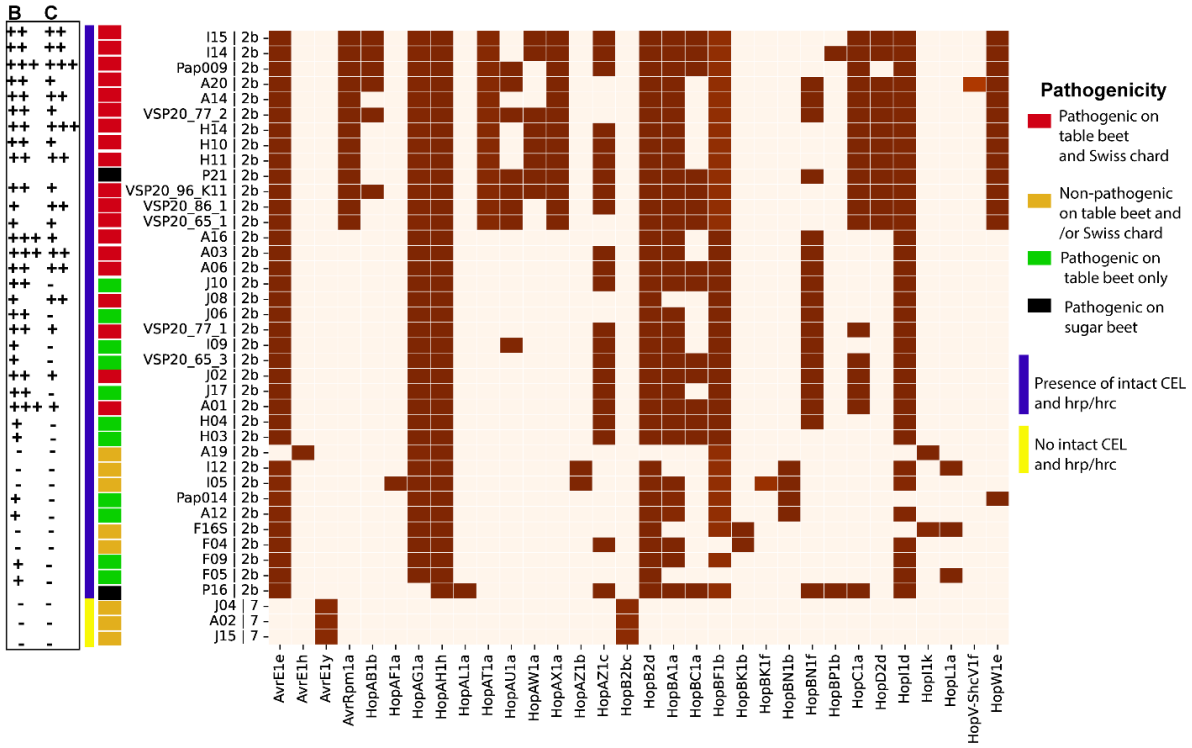

Fig. 1.14. Presence or absence of genes (x-axis) involved in colonization and virulence of bacterial isolates in the *Pseudomonas syringae* complex. A brown square represents the presence of a gene, and a cream-colored square the absence of a gene. 2b and 7 are two of the phylogroups of *P. syringae* (Bull et al. 2015; Newberry et al. 2019). B = table beet cv. Red Ace, and C = Swiss chard cv. Silverado on which the isolates were tested for pathogenicity. Isolates of *P. syringae* obtained from table beet and Swiss chard seed crops with symptoms of bacterial leaf spot, beet and chard seed lots, fresh market crops with symptoms of bacterial leaf spot, or symptomatic volunteer table beet seedlings that caused a mean disease severity on inoculated beet and chard seedlings of >30% were considered highly virulent (+++), 10-30% severity were moderately virulent (++), <10% severity were weakly virulent (+), and no symptoms were avirulent (-). The blue and yellow lines show presence of an intact CEL and *hrp*/*hrc* locus and absence of CEL and *hrp*/*hrc*, respectively, based on Fig. 1.13.

Supplementary Table 1.1. *Pseudomonas syringae* pv. *aptata* isolates and other *Pseudomonas* spp. associated with seed, stems, and leaves of table beet and Swiss chard plants in western Washington

								Virulence		GenBank accession number			
Isolate	**Identity to *P. syringae* pv. *aptata* CFBP^{PT} 1617 based on MLSA (%)**	**Year**	**Geographic origin**	**Source of isolation**	**Fluorescence on KB agar medium**	**Oxidase**	**Tobacco hypersensitivity**	**Table beet cv. Red Ace[a]**	**Swiss chard cv. Silverado[a]**	***gltA***	***gyrB***	***rpoD***	***gapA***
A01	100	2020	Skagit Co., WA	Table beet	Blue	-	+	+++	+	PV552037	PV552038	PV552039	PV552040
A02	85.7	2020	Skagit Co., WA	Table beet	No	-	+	-	-	PV552041	PV552042	PV552043	PV552044
A03	100	2020	Skagit Co., WA	Table beet	Blue	-	+	+++	+	PV552045	PV552046	PV552047	PV552048
A04	99.5	2020	Skagit Co., WA	Table beet	Blue	-	+	+	-	PV552049	PV552050	PV552051	PV552052
A05	100	2020	Skagit Co., WA	Table beet	Blue	-	+	++	-	PV552053	PV552054	PV552055	PV552056
A06	100	2020	Skagit Co., WA	Table beet	Blue	-	+	++	++	PV552057	PV552058	PV552059	PV552060
A07	100	2020	Skagit Co., WA	Table beet	Blue	-	+	++	++	PV552061	PV552062	PV552063	PV552064
A08	100	2020	Skagit Co., WA	Table beet	Blue	-	+	++	++	PV552065	PV552066	PV552067	PV552068
A09	99.7	2020	Skagit Co., WA	Table beet	Blue	-	+	++	++	PV552069	PV552070	PV552071	PV552072
A10	99.2	2020	Skagit Co., WA	Table beet	Blue	-	+	++	+	PV552073	PV552074	PV552075	PV552076
A11	99.1	2020	Skagit Co., WA	Table beet	No	-	+	+	+	PV552077	PV552078	PV552079	PV552080
A12	99.9	2020	Skagit Co., WA	Table beet	Blue	-	+	+	-	PV552081	PV552082	PV552083	PV552084
A13	100	2020	Skagit Co., WA	Table beet	Blue	-	+	+	+	PV552085	PV552086	PV552087	PV552088
A14	99.1	2020	Skagit Co., WA	Table beet	No	-	+	++	++	PV552089	PV552090	PV552091	PV552092
A15	98.7	2020	Skagit Co., WA	Table beet	No	-	+	+	+	PV552093	PV552094	PV552095	PV552096
A16	99.9	2020	Skagit Co., WA	Table beet	No	-	+	+++	+	PV552097	PV552098	PV552099	PV552100
A17	99.3	2020	Skagit Co., WA	Table beet	No	-	+	+	++	PV552101	PV552102	PV552103	PV552104
A18	98.4	2020	Skagit Co., WA	Table beet	Blue	-	+	+	-	PV552105	PV552106	PV552107	PV552108
A19	99.0	2020	Skagit Co., WA	Table beet	Blue	-	+	-	-	PV552109	PV552110	PV552111	PV552112

Isolate	Identity to *P. syringae* pv. *aptata* CFBP^{PT} 1617 based on MLSA (%)	Year	Geographic origin	Source of isolation	Fluorescence on KB agar medium	Oxidase	Tobacco hypersensitivity	Virulence		GenBank accession number			
								Table beet cv. Red Ace[a]	Swiss chard cv. Silverado[a]	*gltA*	*gyrB*	*rpoD*	*gapA*
A20	99.1	2020	Skagit Co., WA	Table beet	No	-	+	++	+	PV552113	PV552114	PV552115	PV552116
A22	98.7	2020	Skagit Co., WA	Table beet	No	-	+	+	+	PV552117	PV552118	PV552119	PV552120
A23	99.1	2020	Skagit Co., WA	Table beet	No	-	+	+	+	PV552121	PV552122	PV552123	PV552124
A25	99.7	2020	Skagit Co., WA	Table beet	No	-	+	+	-	PV552125	PV552126	PV552127	PV552128
A26	100	2020	Skagit Co., WA	Table beet	No	-	+	+	-	PV552129	PV552130	PV552131	PV552132
A28	100	2020	Skagit Co., WA	Table beet	Blue	-	+	+	-	PV552133	PV552134	PV552135	PV552136
A30	99.1	2020	Skagit Co., WA	Table beet	Blue	-	+	-	-	PV552137	PV552138	PV552139	PV552140
A32	99.2	2020	Skagit Co., WA	Table beet	Green	-	+	-	-	PV552141	PV552142	PV552143	PV552144
A35	99.0	2020	Skagit Co., WA	Table beet	Blue	-	+	-	-	PV552145	PV552146	PV552147	PV552148
A35-2	93.6	2020	Skagit Co., WA	Table beet	No	-	+	-	-	PV552149	PV552150	PV552151	PV552152
A37	90.2	2020	Skagit Co., WA	Table beet	No	-	+	-	-	PV552153	PV552154	PV552155	PV552156
A38	99.1	2020	Skagit Co., WA	Table beet	Blue	-	+	-	-	PV552157	PV552158	PV552159	PV552160
F01	99.1	2020	Skagit Co., WA	Table beet	No	-	+	-	-	PV552161	PV552162	PV552163	PV552164
F02	99.1	2020	Skagit Co., WA	Table beet	Blue	-	+	+	-	PV552165	PV552166	PV552167	PV552168
F03	98.8	2020	Skagit Co., WA	Table beet	Blue	-	+	-	-	PV552169	PV552170	PV552171	PV552172
F04	99.0	2020	Skagit Co., WA	Table beet	Blue	-	+	-	-	PV552173	PV552174	PV552175	PV552176
F05	99.1	2020	Skagit Co., WA	Table beet	Blue	-	+	+	-	PV552177	PV552178	PV552179	PV552180
F06	98.9	2020	Skagit Co., WA	Table beet	Blue	-	+	+	-	PV552181	PV552182	PV552183	PV552184
F09	-	2020	Skagit Co., WA	Table beet	Blue	-	+	+	-	-	-	-	-
F11	99.1	2020	Skagit Co., WA	Table beet	No	-	+	+	-	PV552185	PV552186	PV552187	PV552188
F12	90.6	2020	Skagit Co., WA	Table beet	Green	-	+	-	-	PV552189	PV552190	PV552191	PV552192

Isolate	Identity to *P. syringae* pv. *aptata* CFBP^{PT} 1617 based on MLSA (%)	Year	Geographic origin	Source of isolation	Fluorescence on KB agar medium	Oxidase	Tobacco hypersensitivity	Virulence		GenBank accession number			
								Table beet cv. Red Ace[a]	Swiss chard cv. Silverado[a]	*gltA*	*gyrB*	*rpoD*	*gapA*
F13	99.0	2020	Skagit Co., WA	Table beet	No	-	+	+	-	PV552193	PV552194	PV552195	PV552196
F14	99.0	2020	Skagit Co., WA	Table beet	Blue	-	+	+	-	PV552197	PV552198	PV552199	PV552200
F16S	98.8	2020	Skagit Co., WA	Table beet stem	Blue	-	+	-	-	PV552205	PV552206	PV552207	PV552208
F16 L	98.9	2020	Skagit Co., WA	Table beet	Blue	-	+	+	-	PV552201	PV552202	PV552203	PV552204
F17	98.6	2020	Skagit Co., WA	Table beet	Blue	-	+	+	+	PV552209	PV552210	PV552211	PV552212
F18	88.2	2020	Skagit Co., WA	Table beet	Green	-	+	-	-	PV552213	PV552214	PV552215	PV552216
F19	97.4	2020	Skagit Co., WA	Table beet	No	-	+	-	-	PV552217	PV552217	PV552219	PV552220
F23	98.9	2020	Skagit Co., WA	Table beet	Blue	-	+	-	-	PV552221	PV552222	PV552223	PV552224
F24	98.8	2020	Skagit Co., WA	Table beet	Blue	-	+	+	-	PV552225	PV552226	PV552227	PV552228
F25	99.0	2020	Skagit Co., WA	Table beet	No	-	+	-	-	PV552229	PV552230	PV552231	PV552232
F26	99.2	2020	Skagit Co., WA	Table beet	NT	-	+	-	-	PV552233	PV552234	PV552235	PV552236
F27	99.4	2020	Skagit Co., WA	Table beet	Blue	-	+	-	-	PV552237	PV552238	PV552239	PV552240
F28	99.1	2020	Skagit Co., WA	Table beet	No	-	+	+	-	PV552241	PV552242	PV552243	PV552244
F29-1	99.1	2020	Skagit Co., WA	Table beet	Blue	-	-	-	-	PV552245	PV552246	PV552247	PV552248
F30	99.3	2020	Skagit Co., WA	Table beet	Blue	-	+	+	-	PV552249	PV552250	PV552251	PV552252
F33	99.2	2020	Skagit Co., WA	Table beet	Blue	-	+	+	-	PV552253	PV552254	PV552255	PV552256
H03	100	2020	Skagit Co., WA	Table beet	Blue	-	+	+	-	PV552257	PV552258	PV552259	PV552260
H04	94.4	2020	Skagit Co., WA	Table beet	No	-	+	+	-	PV552261	PV552262	PV552263	PV552264
H05	93.4	2020	Skagit Co., WA	Table beet	Green	-	+	-	-	PV552265	PV552266	PV552267	PV552268
H06	99.4	2020	Skagit Co., WA	Table beet	No	-	+	++	+	PV552269	PV552270	PV552271	PV552272
H09	99.0	2020	Skagit Co., WA	Table beet	No	-	+	++	++	PV552273	PV552274	PV552275	PV552276

Isolate	Identity to *P. syringae* pv. *aptata* CFBP^{PT} 1617 based on MLSA (%)	Year	Geographic origin	Source of isolation	Fluorescence on KB agar medium	Oxidase	Tobacco hypersensitivity	Virulence		GenBank accession number			
								Table beet cv. Red Ace[a]	Swiss chard cv. Silverado[a]	*gltA*	*gyrB*	*rpoD*	*gapA*
H10	99.1	2020	Skagit Co., WA	Table beet	No	-	+	++	+	PV552277	PV552278	PV552279	PV552280
H11	99.0	2020	Skagit Co., WA	Table beet	No	-	+	++	++	PV552281	PV552282	PV552283	PV552284
H12	99.1	2020	Skagit Co., WA	Table beet	No	-	+	++	++	PV552285	PV552286	PV552287	PV552288
H14	99.0	2020	Skagit Co., WA	Table beet	No	-	+	++	+++	PV552289	PV552290	PV552291	PV552292
H18	100	2020	Skagit Co., WA	Table beet	No	-	+	+	-	PV552293	PV552294	PV552295	PV552296
H19	99.1	2020	Skagit Co., WA	Table beet	No	-	+	+	+	PV552297	PV552298	PV552299	PV552300
H20	99.1	2020	Skagit Co., WA	Table beet	No	-	+	+	+	PV552301	PV552302	PV552303	PV552304
H21	98.7	2020	Skagit Co., WA	Table beet	Blue	-	+	-	-	PV552305	PV552306	PV552307	PV552308
H22	96.8	2020	Skagit Co., WA	Table beet	Blue	-	+	-	-	PV552309	PV552310	PV552311	PV552312
H23	98.7	2020	Skagit Co., WA	Table beet	Blue	-	+	+	-	PV552313	PV552314	PV552315	PV552316
H25	99.1	2020	Skagit Co., WA	Table beet	Blue	-	+	-	-	PV552317	PV552318	PV552319	PV552320
H27	100	2020	Skagit Co., WA	Table beet	Blue	-	+	+	-	PV552321	PV552322	PV552323	PV552324
H28	99.9	2020	Skagit Co., WA	Table beet	Blue	-	+	+	+	PV552325	PV552326	PV552327	PV552328
H29	100	2020	Skagit Co., WA	Table beet	Blue	-	+	+	-	PV552329	PV552330	PV552331	PV552332
H31	96.5	2020	Skagit Co., WA	Table beet	Blue	-	+	+	-	PV552333	PV552334	PV552335	PV552336
H32	100	2020	Skagit Co., WA	Table beet	Blue	-	+	+	-	PV552337	PV552338	PV552339	PV552340
H36	100	2020	Skagit Co., WA	Table beet	Blue	-	+	+	-	PV552341	PV552342	PV552343	PV552344
H37	89.9	2020	Skagit Co., WA	Table beet	Blue	-	+	+	-	PV552345	PV552346	PV552347	PV552348
H39	98.1	2020	Skagit Co., WA	Table beet	Blue	-	+	+	-	PV552349	PV552350	PV552351	PV552352
I05	98.8	2020	Snohomish Co., WA	Table beet	Blue	-	+	-	-	PV552353	PV552354	PV552355	PV552356
I07	98.9	2020	Snohomish Co., WA	Table beet	Blue	-	+	-	-	PV552357	PV552358	PV552359	PV552360

Isolate	Identity to *P. syringae* pv. *aptata* CFBP^{PT} 1617 based on MLSA (%)	Year	Geographic origin	Source of isolation	Fluorescence on KB agar medium	Oxidase	Tobacco hypersensitivity	Virulence		GenBank accession number			
								Table beet cv. Red Ace[a]	Swiss chard cv. Silverado[a]	*gltA*	*gyrB*	*rpoD*	*gapA*
I08	99.1	2020	Snohomish Co., WA	Table beet	No	-	+	++	+++	PV552361	PV552362	PV552363	PV552364
I09	100	2020	Snohomish Co., WA	Table beet	No	-	+	+	-	PV552365	PV552366	PV552367	PV552368
I10	99.6	2020	Snohomish Co., WA	Table beet	Blue	-	+	+	-	PV552369	PV552370	PV552371	PV552372
I14	99.1	2020	Snohomish Co., WA	Table beet	No	-	+	++	++	PV552373	PV552374	PV552375	PV552376
I15	99.1	2020	Snohomish Co., WA	Table beet	No	-	+	++	++	PV552377	PV552378	PV552379	PV552380
I21-U	98.9	2020	Snohomish Co., WA	Table beet	Blue	-	+	-	-	PV552381	PV552382	PV552383	PV552384
I21	96.9	2020	Snohomish Co., WA	Table beet	Blue	-	-	-	-	PV552385	PV552386	PV552387	PV552388
I23	98.5	2020	Snohomish Co., WA	Table beet	Blue	-	+	-	-	PV552389	PV552390	PV552391	PV552392
I27	96.6	2020	Snohomish Co., WA	Table beet	Blue	-	+	-	-	PV552393	PV552394	PV552395	PV552396
I28	96.8	2020	Snohomish Co., WA	Table beet	No	-	-	-	-	PV552397	PV552398	PV552399	PV552400
I30	99.1	2020	Snohomish Co., WA	Table beet	No	-	+	+	+	PV552401	PV552402	PV552403	PV552404
I31-1	91.9	2020	Snohomish Co., WA	Table beet	No	-	+	-	-	PV552405	PV552406	PV552407	PV552408
I36	97.3	2020	Snohomish Co., WA	Table beet	No	-	+	-	-	PV552409	PV552410	PV552411	PV552412
I37	99.1	2020	Snohomish Co., WA	Table beet	No	-	+	+	+	PV552413	PV552414	PV552415	PV552416
I39	98.9	2020	Snohomish Co., WA	Table beet	Blue	-	+	-	-	PV552417	PV552418	PV552419	PV552420
J02	-	2020	San Juan Co., WA	Table beet	Blue	-	+	++	+	-	-	-	-
J04	90.3	2020	San Juan Co., WA	Table beet	No		+	-	-	PV552421	PV552422	PV552423	PV552424
J05	99.9	2020	San Juan Co., WA	Table beet	Blue	-	+	++	+	PV552425	PV552426	PV552427	PV552428
J06	99.9	2020	San Juan Co., WA	Table beet	No	-	+	++	-	PV552429	PV552430	PV552431	PV552432
J08	100	2020	San Juan Co., WA	Table beet	No	-	+	+	++	PV552433	PV552434	PV552435	PV552436
J09	100	2020	San Juan Co., WA	Table beet	No	-	+	+	+	PV552437	PV552438	PV552439	PV552440

Isolate	Identity to *P. syringae* pv. *aptata* CFBP^{PT} 1617 based on MLSA (%)	Year	Geographic origin	Source of isolation	Fluorescence on KB agar medium	Oxidase	Tobacco hypersensitivity	Virulence		GenBank accession number			
								Table beet cv. Red Ace[a]	Swiss chard cv. Silverado[a]	*gltA*	*gyrB*	*rpoD*	*gapA*
J10	99.5	2020	San Juan Co., WA	Table beet	No	-	+	++	-	PV552441	PV552442	PV552443	PV552444
J11	99.9	2020	San Juan Co., WA	Table beet	No	-	+	+	-	PV552445	PV552446	PV552447	PV552448
J15	89.8	2020	San Juan Co., WA	Table beet	No	-	+	-	-	PV552449	PV552450	PV552451	PV552452
J16	99.9	2020	San Juan Co., WA	Table beet	No	-	+	+	+	PV552453	PV552454	PV552455	PV552456
J17	99.9	2020	San Juan Co., WA	Table beet	No	-	+	++	-	PV552457	PV552458	PV552459	PV552460
J18	100	20	Skagit Co., WA	Table beet	No	-	+	++		PV552461	PV552462	PV552463	PV552464
L03	99.0	2020	Skagit Co., WA	Table beet	Blue	-	+	-	-	PV552465	PV552466	PV552467	PV552468
L05	99.1	2020	Skagit Co., WA	Table beet	Blue	-	+	-	-	PV552469	PV552470	PV552471	PV552472
L07	86.2	2020	Skagit Co., WA	Table beet	Blue	-	+	-	-	PV552473	PV552474	PV552475	PV552476
L08	96.2	2020	Skagit Co., WA	Table beet	Blue	-	+	-	-	PV552477	PV552478	PV552479	PV552480
L10	99.2	2020	Skagit Co., WA	Table beet	Blue	-	+	-	-	PV552481	PV552482	PV552483	PV552484
L12	98.8	2020	Skagit Co., WA	Table beet	Blue	-	+	-	-	PV552485	PV552486	PV552487	PV552488
L14	98.0	2020	Skagit Co., WA	Table beet	Green	-	+	-	-	PV552489	PV552490	PV552491	PV552492
L18	94.3	2020	Skagit Co., WA	Table beet	No	-	+	-	-	PV552493	PV552494	PV552495	PV552496
LC-19	90.0	2021	Skagit Co., WA	Table beet seed lot	No	-	-	-	-	PV552497	PV552498	PV552499	PV552500
Pap009	99.1	2015	OR	Swiss chard	No	-	+	+++	+++	PV552501	PV552502	PV552503	PV552504
Pap014	98.9	2015	Skagit Co., WA	Table beet	Blue	-	+	+	-	PV552505	PV552506	PV552507	PV552508
VB-A-1	99.1	2021	Skagit Co., WA	Volunteer Table beet	No	-	+	+	+	PV552629	PV552630	PV552631	PV552632
VB-A-2	99.1	2021	Skagit Co., WA	Volunteer Table beet	No	-	+	+	+	PV552633	PV552634	PV552635	PV552636
VB-A-3	99.1	2021	Skagit Co., WA	Volunteer Table beet	No	-	+	+	+	PV552637	PV552638	PV552639	PV552640
VB-A-4	99.1	2021	Skagit Co., WA	Volunteer Table beet	No	-	+	++	+	PV552641	PV552642	PV552643	PV552644

Isolate	Identity to *P. syringae* pv. *aptata* CFBP[PT] 1617 based on MLSA (%)	Year	Geographic origin	Source of isolation	Fluorescence on KB agar medium	Oxidase	Tobacco hypersensitivity	Virulence		GenBank accession number			
								Table beet cv. Red Ace[a]	Swiss chard cv. Silverado[a]	*gltA*	*gyrB*	*rpoD*	*gapA*
VB-A-6	99.1	2021	Skagit Co., WA	Volunteer Table beet	No	-	+	+	+	PV552645	PV552646	PV552647	PV552648
VB-A-7	99.1	2021	Skagit Co., WA	Volunteer Table beet	No	-	+	+	+	PV552649	PV552650	PV552651	PV552652
VB-A-8	99.0	2021	Skagit Co., WA	Volunteer Table beet	No	-	+	+	+	PV552653	PV552654	PV552655	PV552656
VB-A-9	98.8	2021	Skagit Co., WA	Volunteer Table beet	No	-	+	+	+	PV552657	PV552658	PV552659	PV552660
VB-A-10	99.1	2021	Skagit Co., WA	Volunteer Table beet	No	-	+	+	+	PV552661	PV552662	PV552663	PV552664
VB-A-11	99.1	2021	Skagit Co., WA	Volunteer Table beet	No	-	+	+	+	PV552665	PV552666	PV552667	PV552668
VSP20-065-1	99.1	2020	San Juan Co., WA	Table beet	No	-	+	+	+	PV552509	PV552510	PV552511	PV552512
VSP20-065-3	99.6	2020	San Juan Co., WA	Table beet	No	-	+	+	-	PV552513	PV552514	PV552515	PV552516
VSP20-065-5	99.6	2020	San Juan Co., WA	Table beet	Blue	-	+	++	+	PV552517	PV552518	PV552519	PV552520
VSP20-068a	99.6	2020	Skagit Co., WA	Table beet	Blue	-	+	++	-	PV552521	PV552522	PV552523	PV552524
VSP20-068b	99.6	2020	Skagit Co., WA	Table beet	Blue	-	+	++	-	PV552525	PV552526	PV552527	PV552528
VSP20-077-1	100	2020	Skagit Co., WA	Table beet	No	-	+	++	+	PV552529	PV552530	PV552531	PV552532
VSP20-077-2	99.2	2020	Skagit Co., WA	Table beet	No	-	+	++	+	PV552533	PV552534	PV552535	PV552536
VSP20-086-1	99.5	2020	San Juan Co., WA	Table beet	No	-	+	+	++	PV552537	PV552538	PV552539	PV552540
VSP20-086-2	99.5	2020	San Juan Co., WA	Table beet	No	-	+	+	++	PV552541	PV552542	PV552543	PV552544
VSP20-094 (K01)	99.4	2020	San Juan Co., WA	Table beet	No	-	+	+++	++	PV552545	PV552546	PV552547	PV552548
VSP20-094 (K02)	99.0	2020	San Juan Co., WA	Table beet	No	-	+	+	+	PV552549	PV552550	PV552551	PV552552
VSP20-094 (K03)	99.1	2020	San Juan Co., WA	Table beet	No	-	+	+	-	PV552553	PV552554	PV552555	PV552556
VSP20-094 (K04)	99.1	2020	San Juan Co., WA	Table beet	No	-	+	+	+	PV552557	PV552558	PV552559	PV552560

Isolate	Identity to *P. syringae* pv. *aptata* CFBP^{PT} 1617 based on MLSA (%)	Year	Geographic origin	Source of isolation	Fluorescence on KB agar medium	Oxidase	Tobacco hypersensitivity	Virulence		GenBank accession number			
								Table beet cv. Red Ace[a]	Swiss chard cv. Silverado[a]	*gltA*	*gyrB*	*rpoD*	*gapA*
VSP20-094 (K05)	99.1	2020	San Juan Co., WA	Table beet	No	-	+	+	-	PV552561	PV552562	PV552563	PV552564
VSP20-094 (K06)	99.1	2020	San Juan Co., WA	Table beet	No	-	+	+	+	PV552565	PV552566	PV552567	PV552568
VSP20-094 (K07)	99.1	2020	San Juan Co., WA	Table beet	No	-	+	+	+	PV552569	PV552570	PV552571	PV552572
VSP20-094 (K08)	99.1	2020	San Juan Co., WA	Table beet	No	-	+	+	+	PV552573	PV552574	PV552575	PV552576
VSP20-094 (K09)	99.1	2020	San Juan Co., WA	Table beet	No	-	+	+	-	PV552577	PV552578	PV552579	PV552580
VSP20-094 (K10)	99.1	2020	San Juan Co., WA	Table beet	No	-	+	+	+	PV552581	PV552582	PV552583	PV552584
VSP20-094 (K11)	99.4	2020	San Juan Co., WA	Table beet	No	-	+	++	+	PV552585	PV552586	PV552587	PV552588
VSP20-094 (K12)	99.1	2020	San Juan Co., WA	Table beet	No	-	+	+	-	PV552589	PV552590	PV552591	PV552592
VSP20-094 (K13)	99.1	2020	San Juan Co., WA	Table beet	No	-	+	+	+	PV552593	PV552594	PV552595	PV552596
VSP20-094 (K14)	99.1	2020	San Juan Co., WA	Table beet	No	-	+	+	+	PV552597	PV552598	PV552599	PV552600
VSP20-094 (K15)	99.1	2020	San Juan Co., WA	Table beet	No	-	+	+	+	PV552601	PV552602	PV552603	PV552604
VSP20-094 (K16)	99.1	2020	San Juan Co., WA	Table beet	No	-	+	+	+	PV552605	PV552606	PV552607	PV552608
VSP20-094 (K17)	99.1	2020	San Juan Co., WA	Table beet	No	-	+	+	+	PV552609	PV552610	PV552611	PV552612
VSP20-094 (K18)	99.1	2020	San Juan Co., WA	Table beet	No	-	+	+	+	PV552613	PV552614	PV552615	PV552616

								Virulence		GenBank accession number			
Isolate	**Identity to *P. syringae* pv. *aptata* CFBP^{PT} 1617 based on MLSA (%)**	**Year**	**Geographic origin**	**Source of isolation**	**Fluorescence on KB agar medium**	**Oxidase**	**Tobacco hypersensitivity**	**Table beet cv. Red Ace[a]**	**Swiss chard cv. Silverado[a]**	***gltA***	***gyrB***	***rpoD***	***gapA***
VSP20-094 (K19)	99.0	2020	San Juan Co., WA	Table beet	No	-	+	+	+	PV552617	PV552618	PV552619	PV552620
VSP20-094 (K20)	99.0	2020	San Juan Co., WA	Table beet	No	-	+	+	+	PV552621	PV552622	PV552623	PV552624
VSP20-094 (K21)	99.1	2020	San Juan Co., WA	Table beet	No	-	+	+	+	PV552625	PV552626	PV552627	PV552628
4_2	88.5	2021	San Juan Co., WA	Table beet seed lot	NT[b]	-	+	-	-	PV552677	PV552678	PV552679	PV552680
4_3	85.5	2021	San Juan Co., WA	Table beet seed lot	NT[b]	-	+	-	-	PV552681	PV552682	PV552683	PV552684
4_4	85.5	2021	San Juan Co., WA	Table beet seed lot	NT[b]	-	+	-	-	PV552685	PV552686	PV552687	PV552688
5_5	85.5	2021	San Juan Co., WA	Table beet seed lot	NT[b]	-	+	-	-	PV552689	PV552690	PV552691	PV552692
6_2	88.9	2021	WA	Swiss chard seed lot	NT[b]	-	+	-	-	PV552693	PV552694	PV552695	PV552696
2_3	88.4	2021	Skagit Co., WA	Table beet seed lot	NT[b]	-	-	-	-	PV552669	PV552670	PV552671	PV552672
2_4	85.5	2021	Skagit Co., WA	Table beet seed lot	NT[b]	-	-	-	-	PV552673	PV552674	PV552675	PV552676
18-AC	100	2021	WA	Table beet seed lot	-	-	+	+	+	PV552697	PV552698	PV552699	PV552700
19-AC	100	2021	WA	Table beet seed lot	-	-	+	+	-	PV552701	PV552702	PV552703	PV552704
57-AC	99.9	2021	WA	Table beet seed lot	-	-	+	+	-	PV552705	PV552706	PV552707	PV552708
64-AC	100	2021	WA	Table beet seed lot	-	+	+	+	-	PV552709	PV552710	PV552711	PV552712
73-AC	100	2021	WA	Table beet seed lot	-	-	+	+	+	PV552713	PV552714	PV552715	PV552716
74-AC	100	2021	WA	Table beet seed lot	-	-	+	+	+	PV552717	PV552718	PV552719	PV552720
75-AC	100	2021	WA	Table beet seed lot	-	-	+	+	+	PV552721	PV552722	PV552723	PV552724
VSP21-003a-1	92.1	2021	WA	Table beet seed lot	NT[b]	-	+	-	-	PV552725	PV552726	PV552727	PV552728
VSP21-003a-4	99.6	2021	WA	Table beet seed lot	NT[b]	-	+	+	-	PV552729	PV552730	PV552731	PV552732
VSP21-003a-5	99.3	2021	WA	Table beet seed lot	NT[b]	-	+	+	-	PV552733	PV552734	PV552735	PV552736

Isolate	Identity to *P. syringae* pv. *aptata* CFBP^{PT} 1617 based on MLSA (%)	Year	Geographic origin	Source of isolation	Fluorescence on KB agar medium	Oxidase	Tobacco hypersensitivity	Virulence		GenBank accession number			
								Table beet cv. Red Ace[a]	Swiss chard cv. Silverado[a]	*gltA*	*gyrB*	*rpoD*	*gapA*
VSP21-003a-8	92.9	2021	WA	Table beet seed lot	NT[b]	-	+	+	+	PV552740	PV552741	PV552742	PV552743
VSP21-003a-9	94.6	2021	WA	Table beet seed lot	NT[b]	-	+	-	-	-	PV552744	PV552745	PV552746
VSP21-003a-10	99.5	2021	WA	Table beet seed lot	NT[b]	-	+	+	-	PV552747	PV552748	PV552749	PV552750
VSP21-003a-13	99.5	2021	WA	Table beet seed lot	NT[b]	-	+	+	-	PV552751	PV552752	PV552753	PV552754
VSP21-003a-15	99.7	2021	WA	Table beet seed lot	NT[b]	-	+	+	-	PV552755	PV552756	PV552757	PV552758
VSP21-003a-16	99.5	2021	WA	Table beet seed lot	NT[b]	-	+	+	-	PV552759	PV552760	PV552761	PV552762
VSP21-003a-17	99.7	2021	WA	Table beet seed lot	NT[b]	-	+	+	-	PV552763	PV552764	PV552765	PV552766
VSP21-003a-19	92.7	2021	WA	Table beet seed lot	NT[b]	-	+	+	-	PV552767	PV552768	PV552769	PV552770
VSP21-003a-23	93.0	2021	WA	Table beet seed lot	NT[b]	-	+	+	-	PV552771	PV552772	PV552773	PV552774
VSP21-003a-24	93.5	2021	WA	Table beet seed lot	NT[b]	-	+	-	-	-	PV552775	PV552776	PV552777
VSP21-003a-25	93.3	2021	WA	Table beet seed lot	NT[b]	-	+	-	-	PV552778	PV552779	PV552780	PV552781
VSP21-003a-VSP21-25-2	99.7	2021	WA	Table beet seed lot	NT[b]	-	+	+	-	PV552782	PV552783	PV552784	PV552785
VSP21-003a-26	92.1	2021	WA	Table beet seed lot	NT[b]	-	+	-	-	PV552786	PV552787	PV552788	PV552789
VSP21-003a-27	99.3	2021	WA	Table beet seed lot	NT[b]	-	+	+	-	PV552790	PV552791	PV552792	PV552793
VSP21-003a-28	94.1	2021	WA	Table beet seed lot	NT[b]	-	+	-	-	-	PV552794	PV552795	PV552796
VSP21-003a-29	99.7	2021	WA	Table beet seed lot	NT[b]	-	+	+	-	PV552797	PV552798	PV552799	PV552800

[a] Six table beet and Swiss chard seedlings (21 to 30 days old) were inoculated with the isolates of *P. syringae* pv. *aptata* and rated for bacterial leaf spot severity 7 days after inoculation. An isolate that caused a mean disease severity >30% was considered highly virulent (+++), 10-30% severity was moderately virulent (++), <10% severity was weakly virulent (+) and no symptoms was avirulent (-).

[b] NT = not tested.

Supplementary Table 1.2. Whole genome sequencing statistics of isolates of *Pseudomonas syringae* pv. *aptata* and other *Pseudomonas* spp. obtained from table beet and Swiss chard seed crops, and fresh market table beet and Swiss chard crops in a survey in western Washington in 2020

Isolate	Genome size	Number of contigs	GC (%)	Number of reads	CheckM score (% completeness)	CheckM score (% contamination)	GenBank Accession number
A01[a]	6,050,697	55	58.9	1,208,401	100	0.10	SAMN46926468
A02 [a]	6,013,690	123	59.3	1,367,579	100	0.10	SAMN46926469
A03 [a]	6,018,541	39	59.0	1,144,062	100	0.10	SAMN46926470
A06 [a]	6,019,942	45	59.0	1,131,367	100	0.10	SAMN46926471
A12 [a]	6,036,772	55	59.0	847,448	99.67	0.10	SAMN46926472
A14 [a]	6,303,234	85	58.8	1,520,144	100	0.10	SAMN46926473
A16 [a]	6,018,275	35	59.0	1,337,531	100	0.10	SAMN46926474
A19 [a]	5,902,374	92	59.1	956,884	100	0.43	SAMN46926475
A20 [a]	6,303,156	71	58.8	1,655,346	100	0.10	SAMN46926476
F04 [a]	6,000,971	82	59.0	1,249,472	100	0.59	SAMN46926477
F05 [a]	5,967,479	65	59.1	1,629,835	100	0.27	SAMN46926478
F09 [a]	5,940,363	74	59.2	1,078,795	100	0.10	SAMN46926479
F16S [a]	6,090,281	59	59.1	1,474,722	100	0.13	SAMN46926480
H03 [a]	5,988,095	49	59.0	1,415,677	100	0.10	SAMN46926481
H04[a]	6,170,542	76	59.0	1,188,898	100	0.43	SAMN46926482
H10 [a]	6,310,562	96	58.8	993,459	100	0.21	SAMN46926483
H11[a]	6,306,854	86	58.8	1,264,482	100	0.10	SAMN46926484
H14[a]	6,306,662	105	58.8	1,381,059	100	0.10	SAMN46926485
I05[a]	5,877,090	63	59.2	1,331,771	100	1.00	SAMN46926486
I09[a]	6,053,518	52	58.9	1,109,139	100	0.10	SAMN46926487
I12[a]	5,889,364	61	59.3	1,457,788	100	0.43	SAMN46926488

Isolate	Genome size	Number of contigs	GC (%)	Number of reads	CheckM score (% completeness)	CheckM score (% contamination)	GenBank Accession number
I14[a]	6,275,338	152	58.8	1,605,585	100	0.10	SAMN46926489
I15[a]	6,277,654	144	58.8	1,570,382	100	0.10	SAMN46926490
J02[a]	5,994,707	44	59.0	1,475,462	100	0.27	SAMN46926491
J04[a]	6,005,267	143	59.3	1,520,621	99.67	0.13	SAMN46926492
J06[a]	6,004,744	41	58.8	1,488,237	100	0.10	SAMN46926493
J08[a]	6,002,947	35	58.8	1,856,027	100	0.10	SAMN46926494
J10[a]	6,002,988	53	58.8	1,211,835	100	0.10	SAMN46926495
J15[a]	5,994,926	140	59.3	1,078,720	99.67	0.21	SAMN46926496
J17[a]	5,996,976	71	59.0	1,100,249	100	0.10	SAMN46926497
Pap009[a]	6,32,0876	67	58.7	1,755,897	100	0.10	SAMN46926498
Pap014[a]	595,9635	29	59.1	1,927,584	100	0.10	SAMN46926499
VSP20-65-1[a]	6,231,565	80	58.8	1,134,561	100	0.75	SAMN46926500
VSP20-63-3[a]	5,997,967	64	59.0	1,219,872	100	0.10	SAMN46926501
VSP20-77-1[a]	5,908,849	77	59.0	1,176,579	100	0.10	SAMN46926502
VSP20-77-2[a]	6,299,971	105	58.8	1,363,938	100	0.13	SAMN46926503
VSP20-86-1[a]	6,238,295	113	58.8	1,500,047	100	0.43	SAMN46926504
VSP20-96-K11[a]	6,349,485	97	58.8	1,205,652	100	0.17	SAMN46926505

a For the rest of the metadata, refer to Supplementary Table 1.1

Supplementary Table 1.3. Metadata of isolates of *Pseudomonas syringae* pv. *aptata*, 5 isolates of *P. syringae*, and 3 isolates of *P. viridiflava* obtained from beet and Swiss chard plants in a seed crop survey in western Washington in 2020, and reference strains P16 and P21, using Blastn (Version 2.15.0) with ≥80% identity to *P. syringae* pv. *tomato* strain DC3000, and ≥90% coverage

Isolate	Query	Subject/ effector	Length of the effector	Alignment length	Mismatches	Gaps	Qstart[a]	Qend[b]	Subj. start[c]	Subj. end[d]	Evalue	Score	Identity	% Coverage
A01	NODE_1_length_664854_cov_7.975176	PttICMP459_HopAH1h_1	1,143	1,143	0	0	555,081	556,223	1	1,143	0	2,111	100	100
	NODE_6_length_278561_cov_8.494279	PttICMP459_HopBA1a_1	720	720	0	0	204,831	205,550	1	720	0	1,330	100	100
	NODE_10_length_175366_cov_7.795913	PttICMP459_HopC1a_1	810	810	0	0	5,801	6,610	1	810	0	1,496	100	100
	NODE_11_length_171747_cov_8.284425	PttICMP459_HopBF1b_1	606	606	0	0	35,655	36,260	1	606	0	1,120	100	100
	NODE_12_length_171078_cov_8.026446	PttICMP459_HopAZ1c_1	666	666	0	0	84,134	84,799	666	1	0	1,230	100	100
	NODE_17_length_121019_cov_8.022764	PttICMP459_HopAG1a_1	2,109	2,109	0	0	79,189	81,297	2,109	1	0	3,895	100	100
	NODE_18_length_115491_cov_7.584229	PttICMP459_HopBN1f_1	888	888	0	0	22,484	23,371	1	888	0	1,640	100	100
	NODE_26_length_87176_cov_7.773381	PttICMP459_HopI1d_1	1,011	1,011	0	0	31,925	32,935	1	1,011	0	1,868	100	100

Isolate	Query	Subject/ effector	Length of the effector	Alignment length	Mismatches	Gaps	Qstart[a]	Qend[b]	Subj. start[c]	Subj. end[d]	Evalue	Score	Identity	% Coverage
	NODE_25_length_87618_cov_8.049136	PttICMP459_AvrE1e_1	5,370	5,370	1	0	46,246	51,615	5,370	1	0	9,912	100	100
	NODE_13_length_164422_cov_8.033963	PttICMP459_HopBC1a_1	762	762	1	0	124,565	125,326	1	762	0	1,402	100	100
	NODE_15_length_144884_cov_8.003468	Pla1,188_1_HopB2d_1	6,069	6,069	36	0	122,018	128,086	1	6,069	0	11,008	99	100
A02	NODE_3_length_178202_cov_8.848457	PvrICMP2,848_AvrE1y_1	5,160	5,162	171	4	118,974	124,133	5,160	1	0	8,560	97	100
	NODE_43_length_53318_cov_9.770017	PprICMP3,956_HopB2bc_1	6,090	6,091	261	2	29,540	35,629	6,090	1	0	9,790	96	100
	NODE_2_length_207981_cov_8.857741	PsaShaanxi_M7_HopV-ShcV1f_1	477	437	83	2	119,100	119,535	41	476	5.23E-89	335	81	92
A03	NODE_1_length_537009_cov_8.410345	PttICMP459_HopBA1a_1	720	720	0	0	526,354	527,073	720	1	0	1,330	100	100
	NODE_2_length_525447_cov_8.087410	PttICMP459_HopBF1b_1	606	606	0	0	170,089	170,694	606	1	0	1,120	100	100
	NODE_4_length_420042_cov_8.043378	PttICMP459_HopBN1f_1	888	888	0	0	195,652	196,539	1	888	0	1,640	100	100
	NODE_9_length_309001_cov_7.945330	PttICMP459_HopAH1h_1	1,143	1,143	0	0	162,035	163,177	1	1,143	0	2,111	100	100

Isolate	Query	Subject/ effector	Length of the effector	Alignment length	Mismatches	Gaps	Qstart[a]	Qend[b]	Subj. start[c]	Subj. end[d]	Evalue	Score	Identity	% Coverage
	NODE_10_length_284638_cov_8.075958	PttICMP459_HopI1d_1	1,011	1,011	0	0	54,268	55,278	1,011	1	0	1,868	100	100
	NODE_11_length_249036_cov_7.947736	PttICMP459_HopAZ1c_1	666	666	0	0	86,265	86,930	1	666	0	1,230	100	100
	NODE_16_length_123554_cov_8.056924	PttICMP459_HopAG1a_1	2,109	2,109	0	0	42,252	44,360	1	2,109	0	3,895	100	100
	NODE_14_length_164735_cov_7.976210	PttICMP459_AvrE1e_1	5,370	5,370	1	0	50,578	55,947	5,370	1	0	9,912	100	100
	NODE_19_length_104618_cov_8.050904	Pla1,188_1_HopB2d_1	6,069	6,069	36	0	76,707	82,775	6,069	1	0	11,008	99	100
	NODE_13_length_182541_cov_7.844053	PsaShaanxi_M7_HopV-ShcV1f_1	477	464	66	1	70,661	71,123	12	475	4.3E-134	484	86	97
A06	NODE_1_length_524820_cov_8.197533	PttICMP459_HopBF1b_1	606	606	0	0	354,843	355,448	1	606	0	1,120	100	100
	NODE_2_length_372841_cov_8.005798	PttICMP459_HopBN1f_1	888	888	0	0	176,289	177,176	888	1	0	1,640	100	100
	NODE_6_length_308951_cov_7.887680	PttICMP459_HopAH1h_1	1,143	1,143	0	0	161,985	163,127	1	1,143	0	2,111	100	100

Isolate	Query	Subject/ effector	Length of the effector	Alignment length	Mismatches	Gaps	Qstart[a]	Qend[b]	Subj. start[c]	Subj. end[d]	Evalue	Score	Identity	% Coverage
	NODE_9_length_208674_cov_8.136871	PttICMP459_HopI1d_1	1,011	1,011	0	0	153,396	154,406	1	1,011	0	1,868	100	100
	NODE_12_length_178812_cov_8.247833	PttICMP459_HopAG1a_1	2,109	2,109	0	0	97,535	99,643	1	2,109	0	3,895	100	100
	NODE_13_length_171058_cov_8.175024	PttICMP459_HopAZ1c_1	666	666	0	0	84,129	84,794	666	1	0	1,230	100	100
	NODE_20_length_138268_cov_8.097835	PttICMP459_HopBC1a_1	762	762	0	0	20,419	21,180	1	762	0	1,408	100	100
	NODE_21_length_125642_cov_8.747066	PttICMP459_HopBA1a_1	720	720	0	0	121,742	122,461	720	1	0	1,330	100	100
	NODE_16_length_160401_cov_7.982549	PttICMP459_AvrE1e_1	5,370	5,370	1	0	46,244	51,613	5,370	1	0	9,912	100	100
	NODE_7_length_247172_cov_8.061313	Pla1,188_1_HopB2d_1	6,069	6,069	36	0	219,501	225,569	6,069	1	0	11,008	99	100
	NODE_11_length_182583_cov_7.856672	PsaShaanxi_M7_HopV-ShcV1f_1	477	464	66	1	70,682	71,144	12	475	4.3E-134	484	86	97
A12	NODE_2_length_495129_cov_5.119828	PlpICMP8,813_HopBN1b_1	897	897	1	0	28,440	29,336	1	897	0	1,652	100	100

Isolate	Query	Subject/ effector	Length of the effector	Alignment length	Mismatches	Gaps	Qstart[a]	Qend[b]	Subj. start[c]	Subj. end[d]	Evalue	Score	Identity	% Coverage
	NODE_8_length_199917_cov_5.384654	Psy0,554_HopAH1h_1	1,143	1,143	5	0	90,414	91,556	1	1,143	0	2,084	100	100
	NODE_14_length_169794_cov_5.302693	PlpICMP8,813_HopAG1a_1	2,151	2,151	16	0	87,015	89,165	1	2,151	0	3,884	99	100
	NODE_5_length_314792_cov_5.385794	PlpICMP8,813_HopB2d_1	6,069	6,069	50	0	121,759	127,827	1	6,069	0	10,931	99	100
	NODE_15_length_159856_cov_5.261180	PsyB64_HopI1d_1	1,014	1,014	13	0	52,348	53,361	1,014	1	0	1,801	99	100
	NODE_1_length_590730_cov_5.203385	PpiICMP2,788_AvrE1e_1	5,376	5,375	77	2	544,207	549,575	2	5,376	0	9,461	98	100
	NODE_7_length_297322_cov_5.118663	PsyHS191_HopBA1a_1	720	720	16	2	74,466	75,183	720	1	0	1,229	98	100
	NODE_3_length_414709_cov_5.389366	PsyFF5_HopBF1b_1	753	746	35	5	373,654	374,391	10	753	0	1,120	94	99
A14	NODE_8_length_208657_cov_9.093799	PttICMP459_HopBN1f_1	888	888	0	0	175,953	176,840	1	888	0	1,640	100	100
	NODE_12_length_181801_cov_8.987362	PttICMP459_HopC1a_1	810	810	0	0	8,274	9,083	810	1	0	1,496	100	100
	NODE_59_length_5313_cov_38.883725	PsyICMP3,688_AvrRpm1a_1	687	687	0	0	2,401	3,087	1	687	0	1,269	100	100

Isolate	Query	Subject/ effector	Length of the effector	Alignment length	Mismatches	Gaps	Qstart[a]	Qend[b]	Subj. start[c]	Subj. end[d]	Evalue	Score	Identity	% Coverage
	NODE_60_length_4146_cov_35.615576	PheICMP3,263_HopD2d_1	1,017	1,017	0	0	2,095	3,111	1,017	1	0	1,879	100	100
	NODE_3_length_318547_cov_8.960511	Pla1,188_1_HopAH1h_1	1,143	1,143	3	0	200,826	201,968	1	1,143	0	2,095	100	100
	NODE_2_length_518409_cov_9.137834	PsyICMP4,917_HopAX1a_1	1,338	1,338	4	0	38,800	40,137	1	1,338	0	2,449	100	100
	NODE_15_length_159367_cov_9.316510	Psy0,538_HopB2d_1	6,069	6,069	22	0	76,600	82,668	6,069	1	0	11,086	100	100
	NODE_4_length_300021_cov_9.698517	PttICMP459_HopBA1a_1	720	720	2	1	287,691	288,409	720	1	0	1,312	100	100
	NODE_1_length_554490_cov_9.239599	PsyCC440_HopW1e_1	2,739	2,739	12	0	461,049	463,787	2,739	1	0	4,992	100	100
	NODE_5_length_294231_cov_9.268517	PsyCC440_AvrE1e_1	5,370	5,370	38	0	203,036	208,405	5,370	1	0	9,707	99	100
	NODE_6_length_275374_cov_9.136750	PttICMP459_HopI1d_1	1,011	1,011	10	0	41,959	42,969	1,011	1	0	1,812	99	100
	NODE_30_length_53819_cov_9.186806	PaflCMP5,011_HopAG1a_1	2,151	2,151	33	0	33,036	35,186	2,151	1	0	3,790	98	100
	NODE_37_length_45916_cov_33.966826	PpdICMP8,902_HopAT1a_1	3,360	3,361	81	1	40,087	43,447	1	3,360	0	5,751	98	100

Isolate	Query	Subject/ effector	Length of the effector	Alignment length	Mismatches	Gaps	Qstart[a]	Qend[b]	Subj. start[c]	Subj. end[d]	Evalue	Score	Identity	% Coverage
	NODE_24_length_81649_cov_9.324894	PsyFF5_HopBF1b_1	753	746	34	5	56,189	56,926	10	753	0	1,125	94	99
	NODE_11_length_194630_cov_8.884984	PsaShaanxi_M7_HopV-ShcV1f_1	477	462	67	1	152,943	153,403	12	473	2.8E-131	475	85	97
A16	NODE_1_length_870987_cov_9.565293	PttICMP459_HopBN1f_1	888	888	0	0	674,435	675,322	888	1	0	1,640	100	100
	NODE_2_length_668313_cov_9.723197	PttICMP459_HopBF1b_1	606	606	0	0	497,620	498,225	1	606	0	1,120	100	100
	NODE_3_length_570108_cov_10.066648	PttICMP459_HopBA1a_1	720	720	0	0	559,453	560,172	720	1	0	1,330	100	100
	NODE_7_length_308666_cov_9.379479	PttICMP459_HopAH1h_1	1,143	1,143	0	0	162,001	163,143	1	1,143	0	2,111	100	100
	NODE_9_length_187083_cov_9.613631	PttICMP459_HopI1d_1	1,011	1,011	0	0	131,806	132,816	1	1,011	0	1,868	100	100
	NODE_10_length_178837_cov_9.732667	PttICMP459_HopAG1a_1	2,109	2,109	0	0	79,195	81,303	2,109	1	0	3,895	100	100
	NODE_12_length_160427_cov_9.375390	PttICMP459_AvrE1e_1	5,370	5,370	1	0	46,270	51,639	5,370	1	0	9,912	100	100
	NODE_18_length_104378_co	Pla1,188_1_HopB2d_1	6,069	6,069	36	0	76,707	82,775	6,069	1	0	11,008	99	100

Isolate	Query	Subject/ effector	Length of the effector	Alignment length	Mismatches	Gaps	Qstart[a]	Qend[b]	Subj. start[c]	Subj. end[d]	Evalue	Score	Identity	% Coverage
	v_9.889891													
	NODE_5_length_393415_cov_9.529721	PsaShaanxi_M7_HopV-ShcV1f_1	477	464	66	1	281,325	281,787	12	475	9.3E-134	484	86	97
A19	NODE_8_length_155854_cov_6.598425	PlpICMP8,813_HopI1k_1	1,014	1,014	1	0	49,592	50,605	1,014	1	0	1,868	100	100
	NODE_1_length_556343_cov_6.127192	Psy0,554_HopAH1h_1	1,143	1,143	5	0	97,364	98,506	1,143	1	0	2,084	100	100
	NODE_2_length_275271_cov_6.229887	PlpICMP8,813_AvrE1h_1	5,373	5,373	46	0	29,778	35,150	5,373	1	0	9,668	99	100
	NODE_12_length_142925_cov_6.541478	PafICMP5,011_HopAG1a_1	2,151	2,151	29	0	87,080	89,230	1	2,151	0	3,812	99	100
	NODE_38_length_54088_cov_6.586201	PsyFF5_HopBF1b_1	753	746	35	5	18,130	18,867	753	10	0	1,120	94	99
A20	NODE_1_length_555066_cov_10.291104	PsyCC440_HopW1e_1	2,739	2,739	12	0	90,698	93,436	1	2,739	0	4,992	99.562	100
	NODE_2_length_518409_cov_10.325975	PsyICMP4,917_HopAX1a_1	1,338	1,338	4	0	38,800	40,137	1	1,338	0	2,449	99.701	100
	NODE_3_length_329988_cov_10.394245	Psy0,538_HopB2d_1	6,069	6,069	22	0	76,691	82,759	1	6,069	0	11,086	99.638	100

Isolate	Query	Subject/ effector	Length of the effector	Alignment length	Mismatches	Gaps	Qstart[a]	Qend[b]	Subj. start[c]	Subj. end[d]	Evalue	Score	Identity	% Coverage
	NODE_4_length_300751_cov_10.923220	PttICMP459_HopBA1a_1	720	720	2	1	12,495	13,213	1	720	0	1,312	99.583	100
	NODE_5_length_294301_cov_10.332704	PsyCC440_AvrE1e_1	5,370	5,370	38	0	203,106	208,475	5,370	1	0	9,707	99.292	100
	NODE_6_length_275374_cov_10.118486	PttICMP459_HopI1d_1	1,011	1,011	10	0	232,406	233,416	1	1,011	0	1,812	99.011	100
	NODE_7_length_272295_cov_10.234521	Pla1,188_1_HopAH1h_1	1,143	1,143	3	0	116,580	117,722	1,143	1	0	2,095	99.738	100
	NODE_10_length_194630_cov_10.084338	PsaShaanxi_M7_HopV-ShcV1f_1	477	462	67	1	152,943	153,403	12	473	2.8E-131	475	85.281	97
	NODE_13_length_181801_cov_10.082874	PttICMP459_HopC1a_1	810	810	0	0	8,274	9,083	810	1	0	1,496	100	100
	NODE_21_length_81649_cov_10.476583	PsyFF5_HopBF1b_1	753	746	34	5	24,724	25,461	753	10	0	1,125	94.102	99
	NODE_26_length_72323_cov_9.777218	PttICMP459_HopBN1f_1	888	888	0	0	39,619	40,506	1	888	0	1,640	100	100
	NODE_33_length_53818_cov_10.286622	PafICMP5,011_HopAG1a_1	2,151	2,151	33	0	18,633	20,783	1	2,151	0	3,790	98.466	100

Isolate	Query	Subject/ effector	Length of the effector	Alignment length	Mismatches	Gaps	Qstart[a]	Qend[b]	Subj. start[c]	Subj. end[d]	Evalue	Score	Identity	% Coverage
	NODE_38_length_50286_cov_36.564286	PpdICMP8,902_HopAT1a_1	3,360	3,361	81	1	40,087	43,447	1	3,360	0	5,751	97.56	100
	NODE_41_length_44872_cov_51.119209	PpdICMP8,902_HopAB1b_1	1,254	1,242	6	0	18,121	19,362	1,254	13	0	2,261	99.517	99
	NODE_55_length_6996_cov_120.915854	PsaTP6_1_HopAU1a_1	2,445	2,339	12	0	4,282	6,620	2,445	107	0	4,253	99.487	96
	NODE_58_length_5309_cov_37.890390	PsyICMP3,688_AvrRpm1a_1	687	687	0	0	2,397	3,083	1	687	0	1,269	100	100
	NODE_60_length_4146_cov_38.770839	PheICMP3,263_HopD2d_1	1,017	1,017	0	0	2,095	3,111	1,017	1	0	1,879	100	100
F04	NODE_7_length_258375_cov_8.203979	PsyCC1,458_HopAH1h_1	1,143	1,143	1	0	154,814	155,956	1	1,143	0	2,106	100	100
	NODE_34_length_58970_cov_7.599596	Psy0,554_HopBA1a_1	720	720	2	0	26,090	26,809	1	720	0	1,319	100	100
	NODE_25_length_75978_cov_8.783668	PsyCC440_HopAG1a_1	2,109	2,109	7	0	39,769	41,877	1	2,109	0	3,856	100	100
	NODE_18_length_104388_cov_8.386789	PsyCC1,543_HopB2d_1	6,069	6,069	40	0	76,720	82,788	6,069	1	0	10,986	99	100
	NODE_20_length_89326_cov_8.083207	Psy0,545_HopAZ1c_1	672	678	0	1	59,707	60,384	1	672	0	1,214	99	101

Isolate	Query	Subject/ effector	Length of the effector	Alignment length	Mismatches	Gaps	Qstart[a]	Qend[b]	Subj. start[c]	Subj. end[d]	Evalue	Score	Identity	% Coverage
	NODE_3_length_345570_cov_8.115434	PlpICMP8,813_HopBK1b_1	201	201	2	0	139,193	139,393	201	1	1.43E-96	361	99	100
	NODE_35_length_56870_cov_8.491338	Pja301,072_AvrE1e_1	5,370	5,370	62	0	23,437	28,806	5,370	1	0	9,574	99	100
	NODE_11_length_142172_cov_8.308311	Pla1,188_1_HopI1d_1	1,011	1,011	13	0	67,884	68,894	1	1,011	0	1,796	99	100
	NODE_29_length_71427_cov_8.103156	PsaShaanxi_M7_HopV-ShcV1f_1	477	464	67	1	23,191	23,653	12	475	7.8E-133	479	85	97
F05	NODE_3_length_551885_cov_11.705480	PpaLMG2,367_HopL1a_1	2,700	2,700	0	0	519,516	522,215	2,700	1	0	4,987	100	100
	NODE_7_length_205461_cov_11.793853	PafICMP4,394_HopB2d_1	6,069	6,069	1	0	47,184	53,252	6,069	1	0	11,202	100	100
	NODE_1_length_656111_cov_11.869183	PafICMP1,852_HopI1d_1	1,011	1,011	1	0	426,580	427,590	1,011	1	0	1,862	100	100
	NODE_20_length_107146_cov_12.006718	PpaLMG2,367_HopAG1a_1	2,109	2,109	5	0	65,244	67,352	2,109	1	0	3,868	100	100
	NODE_17_length_115737_cov_11.648543	PsyCC1,458_HopAH1h_1	1,143	1,143	4	0	108,313	109,455	1,143	1	0	2,089	100	100

Isolate	Query	Subject/ effector	Length of the effector	Alignment length	Mismatches	Gaps	Qstart[a]	Qend[b]	Subj. start[c]	Subj. end[d]	Evalue	Score	Identity	% Coverage
	NODE_4_length_447577_cov_11.643765	Pja301,072_AvrE1e_1	5,370	5,370	34	0	36,975	42,344	5,370	1	0	9,729	99	100
	NODE_6_length_219315_cov_11.235483	PsaShaanxi_M7_HopV-ShcV1f_1	477	462	66	1	47,790	48,250	473	12	6.7E-133	481	85	97
F09	NODE_1_length_552157_cov_7.277847	PttICMP459_HopBA1a_1	720	720	0	0	521,677	522,396	720	1	0	1,330	100	100
	NODE_16_length_118305_cov_7.393102	PafICMP1,852_HopI1d_1	1,011	1,011	1	0	49,578	50,588	1,011	1	0	1,862	100	100
	NODE_18_length_113677_cov_7.407565	PpaLMG2,367_HopAG1a_1	2,109	2,109	5	0	82,747	84,855	2,109	1	0	3,868	100	100
	NODE_17_length_116003_cov_7.057303	PsyCC1,458_HopAH1h_1	1,143	1,143	4	0	6,493	7,635	1	1,143	0	2,089	100	100
	NODE_9_length_216953_cov_7.510585	PsyHS191_HopB2d_1	6,069	6,069	34	0	135,409	141,477	1	6,069	0	11,020	99	100
	NODE_2_length_414973_cov_7.093917	PpiICMP2,788_AvrE1e_1	5,376	5,375	76	1	23,432	28,800	5,376	2	0	9,467	98	100
	NODE_32_length_53698_cov_7.220903	PsyFF5_HopBF1b_1	753	746	35	5	18,130	18,867	753	10	0	1,120	94	99
	NODE_15_length_119158_co	PsaShaanxi_M7_HopV-	477	464	67	1	48,428	48,890	475	12	1.3E-132	479	85	97

Isolate	Query	Subject/ effector	Length of the effector	Alignment length	Mismatches	Gaps	Qstart[a]	Qend[b]	Subj. start[c]	Subj. end[d]	Evalue	Score	Identity	% Coverage
	v_6.899371	ShcV1f_1												
F16S	NODE_3_length_356334_cov_10.045024	Psy0,545_HopAH1h_1	1,143	1,143	0	0	103,733	104,875	1,143	1	0	2,111	100	100
	NODE_4_length_338674_cov_9.949585	PpaLMG2,367_HopL1a_1	2,700	2,700	0	0	255,848	258,547	2,700	1	0	4,987	100	100
	NODE_17_length_122061_cov_10.207604	PpaLMG2,367_HopAG1a_1	2,109	2,109	1	0	38,016	40,124	1	2,109	0	3,890	100	100
	NODE_8_length_227556_cov_9.862797	PsyHS191_HopB2d_1	6,069	6,069	22	0	144,953	151,021	1	6,069	0	11,086	100	100
	NODE_38_length_26688_cov_9.774143	PlpICMP8,813_HopBK1b_1	201	201	1	0	21,950	22,150	1	201	2.4E-99	366	100	100
	NODE_2_length_456769_cov_9.786058	Pja301,072_AvrE1e_1	5,370	5,370	53	0	28,984	34,353	5,370	1	0	9,624	99	100
	NODE_1_length_885479_cov_10.100467	PlpICMP8,813_HopI1k_1	1,014	1,014	21	1	852,546	853,556	1,014	1	0	1,736	98	100
	NODE_34_length_53345_cov_10.197527	PsyFF5_HopBF1b_1	753	746	35	5	18,130	18,867	753	10	0	1,120	94	99
	NODE_16_length_123221_cov_9.534770	PsaShaanxi_M7_HopV-ShcV1f_1	477	464	67	1	74,968	75,430	12	475	1.4E-132	479	85	97

Isolate	Query	Subject/ effector	Length of the effector	Alignment length	Mismatches	Gaps	Qstart[a]	Qend[b]	Subj. start[c]	Subj. end[d]	Evalue	Score	Identity	% Coverage
H03	NODE_1_length_811956_cov_9.625582	PttICMP459_HopBA1a_1	720	720	0	0	526,445	527,164	720	1	0	1,330	100	100
	NODE_3_length_364982_cov_9.533346	PttICMP459_HopBC1a_1	762	762	0	0	312,288	313,049	1	762	0	1,408	100	100
	NODE_8_length_209485_cov_9.672451	PttICMP459_HopBF1b_1	606	606	0	0	135,749	136,354	606	1	0	1,120	100	100
	NODE_11_length_178831_cov_9.597273	PttICMP459_HopAG1a_1	2,109	2,109	0	0	79,189	81,297	2,109	1	0	3,895	100	100
	NODE_12_length_171063_cov_9.457200	PttICMP459_HopAZ1c_1	666	666	0	0	84,134	84,799	666	1	0	1,230	100	100
	NODE_19_length_123166_cov_9.751014	PttICMP459_HopI1d_1	1,011	1,011	0	0	67,874	68,884	1	1,011	0	1,868	100	100
	NODE_21_length_116108_cov_9.155482	PttICMP459_HopAH1h_1	1,143	1,143	0	0	6,638	7,780	1	1,143	0	2,111	100	100
	NODE_16_length_137226_cov_9.815899	PttICMP459_AvrE1e_1	5,370	5,370	1	0	85,612	90,981	1	5,370	0	9,912	100	100
	NODE_32_length_44712_cov_10.425143	Pla1,188_1_HopB2d_1	6,069	6,069	36	0	21,844	27,912	1	6,069	0	11,008	99	100

Isolate	Query	Subject/ effector	Length of the effector	Alignment length	Mismatches	Gaps	Qstart[a]	Qend[b]	Subj. start[c]	Subj. end[d]	Evalue	Score	Identity	% Coverage
H04	NODE_6_length_180933_cov_9.086330	PttICMP459_HopBA1a_1	720	720	0	0	58,469	59,188	1	720	0	1,330	100	100
	NODE_7_length_170876_cov_7.782857	PttICMP459_HopAZ1c_1	666	666	0	0	86,272	86,937	1	666	0	1,230	100	100
	NODE_14_length_142875_cov_7.939152	PttICMP459_HopBC1a_1	762	762	0	0	39,097	39,858	762	1	0	1,408	100	100
	NODE_19_length_123842_cov_7.849671	PttICMP459_HopAG1a_1	2,109	2,109	0	0	42,252	44,360	1	2,109	0	3,895	100	100
	NODE_22_length_116111_cov_7.517666	PttICMP459_HopAH1h_1	1,143	1,143	0	0	108,331	109,473	1,143	1	0	2,111	100	100
	NODE_24_length_110893_cov_7.908492	PttICMP459_HopBF1b_1	606	606	0	0	73,132	73,737	1	606	0	1,120	100	100
	NODE_37_length_71074_cov_7.822952	PttICMP459_HopI1d_1	1,011	1,011	0	0	54,263	55,273	1,011	1	0	1,868	100	100
	NODE_46_length_51148_cov_6.557770	PttICMP459_HopBN1f_1	888	888	0	0	38,362	39,249	1	888	0	1,640	100	100
	NODE_16_length_137146_cov_7.998818	PttICMP459_AvrE1e_1	5,370	5,370	1	0	46,166	51,535	5,370	1	0	9,912	100	100
	NODE_26_length_104378_co	Pla1,188_1_HopB2d_1	6,069	6,069	36	0	21,604	27,672	1	6,069	0	11,008	99	100

Isolate	Query	Subject/ effector	Length of the effector	Alignment length	Mismatches	Gaps	Qstart[a]	Qend[b]	Subj. start[c]	Subj. end[d]	Evalue	Score	Identity	% Coverage
	v_8.496245													
	NODE_8_length_165950_cov_7.489003	PsaShaanxi_M7_HopV-ShcV1f_1	477	464	66	1	111,434	111,896	475	12	3.9E-134	484	86	97
H10	NODE_20_length_96676_cov_6.033724	PttICMP459_HopC1a_1	810	810	0	0	9,384	10,193	810	1	0	1,496	100	100
	NODE_73_length_5309_cov_20.081050	PsyICMP3,688_AvrRpm1a_1	687	687	0	0	2,227	2,913	687	1	0	1,269	100	100
	NODE_76_length_4641_cov_19.104564	PheICMP3,263_HopD2d_1	1,017	1,017	0	0	2,598	3,614	1,017	1	0	1,879	100	100
	NODE_81_length_3560_cov_21.034081	PsaTP6_1_HopAW1a_1	657	657	1	0	489	1,145	657	1	0	1,208	100	100
	NODE_3_length_286901_cov_5.963553	PsyICMP4,917_HopAX1a_1	1,338	1,338	4	0	18,953	20,290	1	1,338	0	2,449	100	100
	NODE_7_length_221423_cov_6.227274	Psy0,538_HopB2d_1	6,069	6,069	21	0	138,754	144,822	1	6,069	0	11,092	100	100
	NODE_4_length_266646_cov_5.989783	Pla1,188_1_HopAH1h_1	1,143	1,143	4	0	110,840	111,982	1,143	1	0	2,089	100	100
	NODE_1_length_615013_cov_5.963193	PttICMP459_HopBA1a_1	720	720	2	1	529,181	529,899	720	1	0	1,312	100	100
	NODE_9_length_176777_cov_6.127693	PsyCC440_HopW1e_1	2,739	2,739	12	0	13,983	16,721	1	2,739	0	4,992	100	100

Isolate	Query	Subject/ effector	Length of the effector	Alignment length	Mismatches	Gaps	Qstart[a]	Qend[b]	Subj. start[c]	Subj. end[d]	Evalue	Score	Identity	% Coverage
	NODE_8_length_211725_cov_5.962107	PsyUS1_HopAZ1c_1	660	660	4	0	127,609	128,268	1	660	0	1,197	99	100
	NODE_16_length_117281_cov_5.898774	PsyCC440_AvrE1e_1	5,370	5,370	38	0	85,827	91,196	1	5,370	0	9,707	99	100
	NODE_37_length_58686_cov_5.675660	PttICMP459_HopI1d_1	1,011	1,011	10	0	41,869	42,879	1,011	1	0	1,812	99	100
	NODE_6_length_229712_cov_6.163286	PafICMP5,011_HopAG1a_1	2,151	2,151	33	0	33,129	35,279	2,151	1	0	3,790	98	100
	NODE_38_length_55797_cov_14.519687	PpdICMP8,902_HopAT1a_1	3,360	3,361	81	1	6,840	10,200	3,360	1	0	5,751	98	100
	NODE_40_length_53715_cov_6.266683	PsyFF5_HopBF1b_1	753	746	34	5	18,123	18,860	753	10	0	1,125	94	99
	NODE_12_length_163077_cov_5.677275	PsaShaanxi_M7_HopV-ShcV1f_1	477	462	67	1	98,355	98,815	473	12	2.3E-131	475	85	97
H11	NODE_11_length_185482_cov_7.704853	PttICMP459_HopC1a_1	810	810	0	0	8,857	9,666	810	1	0	1,496	100	100
	NODE_70_length_5309_cov_22.888074	PsyICMP3,688_AvrRpm1a_1	687	687	0	0	2,227	2,913	687	1	0	1,269	100	100
	NODE_74_length_4138_cov_21.752680	PheICMP3,263_HopD2d_1	1,017	1,017	0	0	2,095	3,111	1,017	1	0	1,879	100	100

Isolate	Query	Subject/ effector	Length of the effector	Alignment length	Mismatches	Gaps	Qstart[a]	Qend[b]	Subj. start[c]	Subj. end[d]	Evalue	Score	Identity	% Coverage
	NODE_36_length_57656_cov_21.925898	PsaTP6_1_HopAW1a_1	657	657	1	0	47,009	47,665	1	657	0	1,208	100	100
	NODE_1_length_430572_cov_7.799842	PsyICMP4,917_HopAX1a_1	1,338	1,338	4	0	162,550	163,887	1	1,338	0	2,449	100	100
	NODE_8_length_221756_cov_8.325914	Psy0,538_HopB2d_1	6,069	6,069	21	0	76,575	82,643	6,069	1	0	11,092	100	100
	NODE_5_length_266555_cov_7.697693	Pla1,188_1_HopAH1h_1	1,143	1,143	4	0	110,840	111,982	1,143	1	0	2,089	100	100
	NODE_13_length_157328_cov_6.770243	PttICMP459_HopBA1a_1	720	720	2	1	86,321	87,039	1	720	0	1,312	100	100
	NODE_4_length_289891_cov_7.781439	PsyCC440_HopW1e_1	2,739	2,739	12	0	273,069	275,807	2,739	1	0	4,992	100	100
	NODE_12_length_166656_cov_7.999243	PsyUS1_HopAZ1c_1	660	660	4	0	83,458	84,117	660	1	0	1,197	99	100
	NODE_18_length_117278_cov_7.648454	PsyCC440_AvrE1e_1	5,370	5,370	38	0	85,827	91,196	1	5,370	0	9,707	99	100
	NODE_20_length_110846_cov_7.532519	PttICMP459_HopI1d_1	1,011	1,011	10	0	67,884	68,894	1	1,011	0	1,812	99	100
	NODE_7_length_22	PaflCMP5,011_	2,151	2,151	33	0	33,018	35,168	2,151	1	0	3,790	98	100

Isolate	Query	Subject/ effector	Length of the effector	Alignment length	Mismatches	Gaps	Qstart[a]	Qend[b]	Subj. start[c]	Subj. end[d]	Evalue	Score	Identity	% Coverage
	9601_cov_7.342771	HopAG1a_1												
	NODE_40_length_50575_cov_16.847031	PpdICMP8,902_HopAT1a_1	3,360	3,361	81	1	1,618	4,978	3,360	1	0	5,751	98	100
	NODE_26_length_81585_cov_8.016831	PsyFF5_HopBF1b_1	753	746	34	5	56,125	56,862	10	753	0	1,125	94	99
	NODE_6_length_257091_cov_7.259924	PsaShaanxi_M7_HopV-ShcV1f_1	477	462	67	1	158,277	158,737	12	473	3.7E-131	475	85	97
H14	NODE_11_length_185507_cov_7.513092	PttICMP459_HopC1a_1	810	810	0	0	8,882	9,691	810	1	0	1,496	100	100
	NODE_76_length_5458_cov_60.948790	PsyICMP3,688_AvrRpm1a_1	687	687	0	0	2,376	3,062	687	1	0	1,269	100	100
	NODE_81_length_4004_cov_49.576219	PheICMP3,263_HopD2d_1	1,017	1,017	0	0	1,022	2,038	1	1,017	0	1,879	100	100
	NODE_48_length_37472_cov_48.343018	PsaTP6_1_HopAW1a_1	657	657	1	0	2,416	3,072	1	657	0	1,208	100	100
	NODE_3_length_294537_cov_7.589997	PsyICMP4,917_HopAX1a_1	1,338	1,338	4	0	26,589	27,926	1	1,338	0	2,449	100	100
	NODE_8_length_193895_cov_7.964148	Psy0,538_HopB2d_1	6,069	6,069	21	0	76,600	82,668	6,069	1	0	11,092	100	100

Isolate	Query	Subject/ effector	Length of the effector	Alignment length	Mismatches	Gaps	Qstart[a]	Qend[b]	Subj. start[c]	Subj. end[d]	Evalue	Score	Identity	% Coverage
	NODE_4_length_257193_cov_7.462113	Pla1,188_1_HopAH1h_1	1,143	1,143	4	0	101,367	102,509	1,143	1	0	2,089	100	100
	NODE_7_length_200443_cov_7.412538	PttICMP459_HopBA1a_1	720	720	2	1	85,115	85,833	1	720	0	1,312	100	100
	NODE_12_length_176799_cov_7.938955	PsyCC440_HopW1e_1	2,739	2,739	12	0	160,079	162,817	2,739	1	0	4,992	100	100
	NODE_13_length_166655_cov_7.611092	PsyUS1_HopAZ1c_1	660	660	4	0	82,539	83,198	1	660	0	1,197	99	100
	NODE_17_length_117281_cov_7.641719	PsyCC440_AvrE1e_1	5,370	5,370	38	0	85,827	91,196	1	5,370	0	9,707	99	100
	NODE_21_length_110846_cov_7.666083	PttICMP459_HopI1d_1	1,011	1,011	10	0	67,884	68,894	1	1,011	0	1,812	99	100
	NODE_5_length_229388_cov_7.806051	PafICMP5,011_HopAG1a_1	2,151	2,151	33	0	194,110	196,260	1	2,151	0	3,790	98	100
	NODE_40_length_51818_cov_32.877309	PpdICMP8,902_HopAT1a_1	3,360	3,361	81	1	45,215	48,575	1	3,360	0	5,751	98	100
	NODE_32_length_67365_cov_8.167762	PsyFF5_HopBF1b_1	753	746	34	5	24,727	25,464	753	10	0	1,125	94	99
	NODE_18_length_114026_co	PsaShaanxi_M7_HopV-	477	462	67	1	49,304	49,764	473	12	1.6E-131	475	85	97

Isolate	Query	Subject/ effector	Length of the effector	Alignment length	Mismatches	Gaps	Qstart[a]	Qend[b]	Subj. start[c]	Subj. end[d]	Evalue	Score	Identity	% Coverage
	v_7.059790	ShcV1f_1												
I05	NODE_3_length_415666_cov_8.722084	PlpICMP8,813_HopBN1b_1	897	897	0	0	6,385	7,281	1	897	0	1,657	100	100
	NODE_7_length_181577_cov_8.953596	PaflCMP5,011_HopAZ1b_1	780	780	0	0	24,190	24,969	780	1	0	1,441	100	100
	NODE_4_length_230165_cov_9.145745	Pav013_HopBA1a_1	720	720	3	0	82,140	82,859	1	720	0	1,314	100	100
	NODE_18_length_127525_cov_9.580614	PlpICMP8,813_HopAG1a_1	2,151	2,151	11	0	46,205	48,355	1	2,151	0	3,912	99	100
	NODE_21_length_116506_cov_8.819778	Psy0,554_HopAH1h_1	1,143	1,143	6	0	7,069	8,211	1	1,143	0	2,078	99	100
	NODE_22_length_103600_cov_9.201444	PlpICMP8,813_HopB2d_1	6,069	6,069	48	0	21,938	28,006	1	6,069	0	10,942	99	100
	NODE_1_length_491815_cov_9.463845	PsyCC1,458_HopAF1a_1	855	855	9	0	113,221	114,075	1	855	0	1,530	99	100
	NODE_2_length_425734_cov_9.072741	PttDSM5,022_AvrE1e_1	5,370	5,370	92	0	403,214	408,583	1	5,370	0	9,407	98	100
	NODE_45_length_22295_cov_9.370489	Psy0,540_HopI1d_1	1,014	1,014	21	0	11,396	12,409	1,014	1	0	1,757	98	100
	NODE_6_length_19	PsyFF5_HopBF1b_1	753	746	35	5	18,143	18,880	753	10	0	1,120	94	99

Isolate	Query	Subject/ effector	Length of the effector	Alignment length	Mismatches	Gaps	Qstart[a]	Qend[b]	Subj. start[c]	Subj. end[d]	Evalue	Score	Identity	% Coverage
	5951_cov_9.357704													
	NODE_13_length_150592_cov_8.619626	PmpICMP568_HopBK1f_1	240	242	17	3	14,439	14,679	1	240	1.36E-88	333	92	101
	NODE_20_length_117296_cov_8.512525	PsaShaanxi_M7_HopV-ShcV1f_1	477	461	67	1	75,389	75,848	12	472	6E-131	473	85	97
I09	NODE_1_length_479765_cov_7.784329	PttICMP459_HopBF1b_1	606	606	0	0	354,762	355,367	1	606	0	1,120	100	100
	NODE_2_length_433446_cov_7.451965	PttICMP459_HopBN1f_1	888	888	0	0	234,822	235,709	888	1	0	1,640	100	100
	NODE_3_length_424150_cov_7.983501	PttICMP459_HopBA1a_1	720	720	0	0	362,900	363,619	720	1	0	1,330	100	100
	NODE_6_length_284701_cov_7.769961	PttICMP459_HopI1d_1	1,011	1,011	0	0	54,304	55,314	1,011	1	0	1,868	100	100
	NODE_7_length_274256_cov_8.051111	PttICMP459_HopAH1h_1	1,143	1,143	0	0	161,996	163,138	1	1,143	0	2,111	100	100
	NODE_13_length_171335_cov_7.877821	PttICMP459_HopAZ1c_1	666	666	0	0	86,265	86,930	1	666	0	1,230	100	100
	NODE_20_length_123581_cov_7.746189	PttICMP459_HopAG1a_1	2,109	2,109	0	0	79,222	81,330	2,109	1	0	3,895	100	100

Isolate	Query	Subject/ effector	Length of the effector	Alignment length	Mismatches	Gaps	Qstart[a]	Qend[b]	Subj. start[c]	Subj. end[d]	Evalue	Score	Identity	% Coverage
	NODE_17_length_137214_cov_7.809909	PttICMP459_AvrE1e_1	5,370	5,370	1	0	46,228	51,597	5,370	1	0	9,912	100	100
	NODE_34_length_44456_cov_8.260191	Pla1,188_1_HopB2d_1	6,069	6,069	36	0	16,794	22,862	6,069	1	0	11,008	99	100
	NODE_33_length_46343_cov_17.639865	PsaTP6_1_HopAU1a_1	2,445	2,339	21	0	40,638	42,976	2,445	107	0	4,204	99	96
	NODE_8_length_268358_cov_7.654078	PsaShaanxi_M7_HopV-ShcV1f_1	477	464	66	1	156,515	156,977	12	475	6.3E-134	484	86	97
I12	NODE_20_length_107457_cov_9.929125	PsyB64_HopAZ1b_1	780	780	1	0	24,262	25,041	780	1	0	1,435	100	100
	NODE_1_length_473395_cov_9.702053	PlpICMP8,813_HopBN1b_1	897	897	3	0	6,480	7,376	1	897	0	1,640	100	100
	NODE_11_length_160165_cov_9.819305	Psy0,554_HopAH1h_1	1,143	1,143	5	0	102,397	103,539	1,143	1	0	2,084	100	100
	NODE_9_length_191411_cov_10.501009	PaflCMP5,011_HopB2d_1	6,069	6,069	44	0	46,624	52,692	6,069	1	0	10,964	99	100
	NODE_13_length_152248_cov_9.670203	PsySM_HopL1a_1	2,700	2,700	25	0	34,091	36,790	2,700	1	0	4,848	99	100
	NODE_34_length_5	PlpICMP8,813_	2,151	2,151	25	0	17,729	19,879	2,151	1	0	3,834	99	100

Isolate	Query	Subject/ effector	Length of the effector	Alignment length	Mismatches	Gaps	Qstart[a]	Qend[b]	Subj. start[c]	Subj. end[d]	Evalue	Score	Identity	% Coverage
	6446_cov_10.950674	HopAG1a_1												
	NODE_39_length_47579_cov_10.388898	Pav013_HopI1d_1	1,014	1,014	14	0	14,727	15,740	1,014	1	0	1,796	99	100
	NODE_19_length_108498_cov_10.037086	PpiICMP2,788_AvrE1e_1	5,376	5,375	80	1	85,983	91,351	2	5,376	0	9,444	98	100
	NODE_5_length_274955_cov_10.808993	PsyFF5_HopBF1b_1	753	746	35	5	136,410	137,147	10	753	0	1,120	94	99
	NODE_3_length_353036_cov_9.813975	PsaShaanxi_M7_HopV-ShcV1f_1	477	464	68	1	222,298	222,760	475	12	1.8E-130	473	85	97
I14	NODE_15_length_129552_cov_8.000425	PsaShaanxi_M7_HopV-ShcV1f_1	477	462	67	1	59,041	59,501	473	12	1.8E-131	475	85	97
	NODE_29_length_81585_cov_8.751099	PsyFF5_HopBF1b_1	753	746	34	5	56,125	56,862	10	753	0	1,125	94	99
	NODE_54_length_27323_cov_28.655758	PpdICMP8,902_HopAT1a_1	3,360	3,361	81	1	17,124	20,484	1	3,360	0	5,751	98	100
	NODE_13_length_144805_cov_8.533336	PaflCMP5,011_HopAG1a_1	2,151	2,151	33	0	33,018	35,168	2,151	1	0	3,790	98	100

Isolate	Query	Subject/ effector	Length of the effector	Alignment length	Mismatches	Gaps	Qstart[a]	Qend[b]	Subj. start[c]	Subj. end[d]	Evalue	Score	Identity	% Coverage
	NODE_24_length_104796_cov_8.512501	PttICMP459_HopI1d_1	1,011	1,011	10	0	61,922	62,932	1	1,011	0	1,812	99	100
	NODE_51_length_39384_cov_8.465598	PsyCC440_AvrE1e_1	5,370	5,370	38	0	5,280	10,649	1	5,370	0	9,707	99	100
	NODE_7_length_191324_cov_8.250595	PsyUS1_HopAZ1c_1	660	660	4	0	127,610	128,269	1	660	0	1,197	99	100
	NODE_67_length_13427_cov_73.719549	PpdICMP8,902_HopAB1b_1	1,254	1,242	6	0	11,011	12,252	1,254	13	0	2,261	100	99
	NODE_10_length_176905_cov_8.538896	PsyCC440_HopW1e_1	2,739	2,739	13	0	160,083	162,821	2,739	1	0	4,987	100	100
	NODE_18_length_126416_cov_12.864739	PttICMP459_HopBA1a_1	720	720	2	1	11,100	11,818	1	720	0	1,312	100	100
	NODE_1_length_281547_cov_8.571981	Psy0,538_HopB2d_1	6,069	6,069	21	0	163,053	169,121	6,069	1	0	11,092	100	100
	NODE_31_length_79565_cov_8.273597	PttICMP459_HopBP1b_1	1,236	1,236	3	1	21,481	22,715	1,236	1	0	2,259	100	100
	NODE_8_length_183814_cov_8.300288	PsyICMP4,917_HopAX1a_1	1,338	1,338	4	0	162,521	163,858	1	1,338	0	2,449	100	100
	NODE_2_length_273284_cov_8.200994	Pla1,188_1_HopAH1h_1	1,143	1,143	3	0	154,471	155,613	1	1,143	0	2,095	100	100

Isolate	Query	Subject/ effector	Length of the effector	Alignment length	Mismatches	Gaps	Qstart[a]	Qend[b]	Subj. start[c]	Subj. end[d]	Evalue	Score	Identity	% Coverage
	NODE_101_length_2977_cov_76.595856	PsaTP6_1_HopAW1a_1	657	657	1	0	436	1,092	657	1	0	1,208	100	100
	NODE_14_length_142133_cov_8.425179	Pla1,188_1_HopBC1a_1	762	762	0	0	129,114	129,875	1	762	0	1,408	100	100
	NODE_56_length_25016_cov_7.905661	PttICMP459_HopC1a_1	810	810	0	0	15,326	16,135	1	810	0	1,496	100	100
	NODE_86_length_5294_cov_47.180763	PsyICMP3,688_AvrRpm1a_1	687	687	0	0	2,382	3,068	1	687	0	1,269	100	100
	NODE_92_length_4331_cov_41.324929	PheICMP3,263_HopD2d_1	1,017	1,017	0	0	1,221	2,237	1	1,017	0	1,879	100	100
I15	NODE_10_length_149429_cov_8.392607	Pla1,188_1_HopBC1a_1	762	762	0	0	11,069	11,830	1	762	0	1,408	100	100
	NODE_29_length_74435_cov_8.244025	PttICMP459_HopC1a_1	810	810	0	0	8,882	9,691	810	1	0	1,496	100	100
	NODE_93_length_5458_cov_40.890452	PsyICMP3,688_AvrRpm1a_1	687	687	0	0	2,397	3,083	1	687	0	1,269	100	100
	NODE_101_length_4134_cov_37.083604	PheICMP3,263_HopD2d_1	1,017	1,017	0	0	2,095	3,111	1,017	1	0	1,879	100	100
	NODE_112_length_1997_cov	PsaTP6_1_HopAW1a_1	657	657	1	0	853	1,509	1	657	0	1,208	100	100

Isolate	Query	Subject/ effector	Length of the effector	Alignment length	Mismatches	Gaps	Qstart[a]	Qend[b]	Subj. start[c]	Subj. end[d]	Evalue	Score	Identity	% Coverage
	_64.890909													
	NODE_37_length_59629_cov_7.979950	Pla1,188_1_HopAH1h_1	1,143	1,143	3	0	36,060	37,202	1	1,143	0	2,095	100	100
	NODE_8_length_155285_cov_8.389326	PsyICMP4,917_HopAX1a_1	1,338	1,338	4	0	127,751	129,088	1,338	1	0	2,449	100	100
	NODE_7_length_166501_cov_8.676933	Psy0,538_HopB2d_1	6,069	6,069	21	0	21,277	27,345	6,069	1	0	11,092	100	100
	NODE_46_length_45076_cov_16.418630	PttICMP459_HopBA1a_1	720	720	2	1	33,446	34,164	720	1	0	1,312	100	100
	NODE_6_length_176426_cov_8.476282	PsyCC440_HopW1e_1	2,739	2,739	13	0	14,001	16,739	1	2,739	0	4,987	100	100
	NODE_72_length_16969_cov_63.559494	PpdICMP8,902_HopAB1b_1	1,254	1,242	6	0	14,553	15,794	1,254	13	0	2,261	100	99
	NODE_21_length_109545_cov_8.212643	PsyUS1_HopAZ1c_1	660	660	4	0	45,928	46,587	1	660	0	1,197	99	100
	NODE_2_length_294771_cov_8.563015	PsyCC440_AvrE1e_1	5,370	5,370	38	0	203,065	208,434	5,370	1	0	9,707	99	100
	NODE_15_length_130198_cov_8.578384	PttICMP459_HopI1d_1	1,011	1,011	10	0	105,695	106,705	1	1,011	0	1,812	99	100
	NODE_12_length_1	PafICMP5,011_	2,151	2,151	33	0	109,563	111,713	1	2,151	0	3,790	98	100

Isolate	Query	Subject/ effector	Length of the effector	Alignment length	Mismatches	Gaps	Qstart[a]	Qend[b]	Subj. start[c]	Subj. end[d]	Evalue	Score	Identity	% Coverage
	44730_cov_8.621585	HopAG1a_1												
	NODE_59_length_28688_cov_26.340079	PpdICMP8,902_HopAT1a_1	3,360	3,361	81	1	17,125	20,485	1	3,360	0	5,751	98	100
	NODE_27_length_81585_cov_8.810111	PsyFF5_HopBF1b_1	753	746	34	5	24,724	25,461	753	10	0	1,125	94	99
	NODE_3_length_251863_cov_8.234992	PsaShaanxi_M7_HopV-ShcV1f_1	477	462	67	1	98,439	98,899	473	12	3.6E-131	475	85	97
J02	NODE_1_length_750967_cov_10.379707	PttICMP459_HopBA1a_1	720	720	0	0	284,899	285,618	1	720	0	1,330	100	100
	NODE_2_length_491591_cov_10.715584	PttICMP459_HopBF1b_1	606	606	0	0	354,783	355,388	1	606	0	1,120	100	100
	NODE_6_length_271806_cov_10.207307	PttICMP459_HopAH1h_1	1,143	1,143	0	0	108,632	109,774	1,143	1	0	2,111	100	100
	NODE_11_length_187254_cov_10.510471	PttICMP459_HopI1d_1	1,011	1,011	0	0	131,984	132,994	1	1,011	0	1,868	100	100
	NODE_12_length_171520_cov_10.332511	PttICMP459_HopAZ1c_1	666	666	0	0	86,265	86,930	1	666	0	1,230	100	100

Isolate	Query	Subject/ effector	Length of the effector	Alignment length	Mismatches	Gaps	Qstart[a]	Qend[b]	Subj. start[c]	Subj. end[d]	Evalue	Score	Identity	% Coverage
	NODE_13_length_169993_cov_10.329177	PttICMP459_HopC1a_1	810	810	0	0	168,757	169,566	810	1	0	1,496	100	100
	NODE_22_length_123548_cov_10.496220	PttICMP459_HopAG1a_1	2,109	2,109	0	0	42,252	44,360	1	2,109	0	3,895	100	100
	NODE_26_length_70110_cov_10.759613	PttICMP459_HopBN1f_1	888	888	0	0	53,313	54,200	888	1	0	1,640	100	100
	NODE_21_length_137242_cov_10.498385	PttICMP459_AvrE1e_1	5,370	5,370	1	0	46,256	51,625	5,370	1	0	9,912	100	100
	NODE_5_length_280515_cov_10.353428	PttICMP459_HopBC1a_1	762	762	1	0	116,613	117,374	762	1	0	1,402	100	100
	NODE_32_length_44710_cov_10.621178	Pla1,188_1_HopB2d_1	6,069	6,069	37	0	21,844	27,912	1	6,069	0	11,003	99	100
J04	NODE_8_length_131865_cov_9.846961	PvrICMP2,848_AvrE1y_1	5,160	5,162	175	4	72,640	77,799	5,160	1	0	8,538	97	100
	NODE_58_length_38851_cov_10.295062	PprICMP3,956_HopB2bc_1	6,090	6,090	249	0	15,108	21,197	6,090	1	0	9,867	96	100
	NODE_3_length_188591_cov_9.606392	PsaShaanxi_M7_HopV-ShcV1f_1	477	442	79	4	99,717	100,156	37	476	1.31E-94	353	81	93

Isolate	Query	Subject/ effector	Length of the effector	Alignment length	Mismatches	Gaps	Qstart[a]	Qend[b]	Subj. start[c]	Subj. end[d]	Evalue	Score	Identity	% Coverage
J06	NODE_1_length_748995_cov_9.708919	PttICMP459_HopBN1f_1	888	888	0	0	195,666	196,553	1	888	0	1,640	100	100
	NODE_2_length_524994_cov_10.780474	PttICMP459_HopBF1b_1	606	606	0	0	354,769	355,374	1	606	0	1,120	100	100
	NODE_3_length_407376_cov_10.607374	PttICMP459_HopBA1a_1	720	720	0	0	121,750	122,469	720	1	0	1,330	100	100
	NODE_8_length_284655_cov_11.032412	PttICMP459_HopI1d_1	1,011	1,011	0	0	229,392	230,402	1	1,011	0	1,868	100	100
	NODE_9_length_271776_cov_9.865558	PttICMP459_HopAH1h_1	1,143	1,143	0	0	162,003	163,145	1	1,143	0	2,111	100	100
	NODE_12_length_178831_cov_10.670500	PttICMP459_HopAG1a_1	2,109	2,109	0	0	79,189	81,297	2,109	1	0	3,895	100	100
	NODE_15_length_137237_cov_10.459026	PttICMP459_AvrE1e_1	5,370	5,370	1	0	85,618	90,987	1	5,370	0	9,912	100	100
	NODE_19_length_104632_cov_11.807138	Pla1,188_1_HopB2d_1	6,069	6,069	36	0	76,707	82,775	6,069	1	0	11,008	99	100
J08	NODE_1_length_1167466_cov_13.182926	PttICMP459_HopBN1f_1	888	888	0	0	970,928	971,815	888	1	0	1,640	100	100

Isolate	Query	Subject/ effector	Length of the effector	Alignment length	Mismatches	Gaps	Qstart[a]	Qend[b]	Subj. start[c]	Subj. end[d]	Evalue	Score	Identity	% Coverage
	NODE_2_length_920105_cov_13.682433	PttICMP459_HopAH1h_1	1,143	1,143	0	0	810,332	811,474	1	1,143	0	2,111	100	100
	NODE_3_length_524746_cov_13.701765	PttICMP459_HopBF1b_1	606	606	0	0	169,381	169,986	606	1	0	1,120	100	100
	NODE_7_length_284656_cov_13.452133	PttICMP459_HopI1d_1	1,011	1,011	0	0	54,255	55,265	1,011	1	0	1,868	100	100
	NODE_15_length_123548_cov_13.550093	PttICMP459_HopAG1a_1	2,109	2,109	0	0	42,252	44,360	1	2,109	0	3,895	100	100
	NODE_14_length_137204_cov_13.427650	PttICMP459_AvrE1e_1	5,370	5,370	1	0	85,618	90,987	1	5,370	0	9,912	100	100
	NODE_8_length_247155_cov_13.551217	Pla1,188_1_HopB2d_1	6,069	6,069	36	0	21,627	27,695	1	6,069	0	11,008	99	100
J10	NODE_2_length_387007_cov_8.813508	PttICMP459_HopBA1a_1	720	720	0	0	283,899	284,618	720	1	0	1,330	100	100
	NODE_5_length_301583_cov_8.219976	PttICMP459_HopBC1a_1	762	762	0	0	116,798	117,559	762	1	0	1,408	100	100
	NODE_7_length_264460_cov_7.947566	PttICMP459_HopAH1h_1	1,143	1,143	0	0	101,382	102,524	1,143	1	0	2,111	100	100

Isolate	Query	Subject/ effector	Length of the effector	Alignment length	Mismatches	Gaps	Qstart[a]	Qend[b]	Subj. start[c]	Subj. end[d]	Evalue	Score	Identity	% Coverage
	NODE_10_length_197940_cov_5.941601	PttICMP459_HopBN1f_1	888	888	0	0	36,262	37,149	1	888	0	1,640	100	100
	NODE_12_length_187131_cov_8.726979	PttICMP459_HopI1d_1	1,011	1,011	0	0	54,255	55,265	1,011	1	0	1,868	100	100
	NODE_14_length_171063_cov_8.053786	PttICMP459_HopAZ1c_1	666	666	0	0	84,134	84,799	666	1	0	1,230	100	100
	NODE_18_length_122962_cov_8.266626	PttICMP459_HopAG1a_1	2,109	2,109	0	0	79,938	82,046	2,109	1	0	3,895	100	100
	NODE_21_length_107433_cov_7.061292	PttICMP459_HopBF1b_1	606	606	0	0	35,655	36,260	1	606	0	1,120	100	100
	NODE_9_length_225229_cov_8.081763	PttICMP459_AvrE1e_1	5,370	5,370	1	0	85,618	90,987	1	5,370	0	9,912	100	100
	NODE_37_length_44724_cov_9.354172	Pla1,188_1_HopB2d_1	6,069	6,069	36	0	21,858	27,926	1	6,069	0	11,008	99	100
	NODE_13_length_182612_cov_8.149294	PsaShaanxi_M7_HopV-ShcV1f_1	477	464	66	1	111,471	111,933	475	12	4.3E-134	484	86	97
J15	NODE_5_length_174027_cov_7.161461	PvrICMP2,848_AvrE1y_1	5,160	5,162	173	4	114,805	119,964	5,160	1	0	8,549	97	100
	NODE_3_length_22	PprICMP3,956_	6,090	6,090	274	0	214,809	220,898	1	6,090	0	9,729	96	100

Isolate	Query	Subject/ effector	Length of the effector	Alignment length	Mismatches	Gaps	Qstart[a]	Qend[b]	Subj. start[c]	Subj. end[d]	Evalue	Score	Identity	% Coverage
	8741_cov_7.387675	HopB2bc_1												
	NODE_2_length_246480_cov_7.199612	PsaShaanxi_M7_HopV-ShcV1f_1	477	441	84	2	167,322	167,761	476	37	1.72E-89	337	80	92
J17	NODE_2_length_372454_cov_7.649013	PttICMP459_HopBA1a_1	720	720	0	0	284,890	285,609	1	720	0	1,330	100	100
	NODE_3_length_341375_cov_9.588393	PttICMP459_HopBN1f_1	888	888	0	0	84,211	85,098	1	888	0	1,640	100	100
	NODE_8_length_172294_cov_7.379974	PttICMP459_HopBF1b_1	606	606	0	0	35,486	36,091	1	606	0	1,120	100	100
	NODE_9_length_171063_cov_7.392796	PttICMP459_HopAZ1c_1	666	666	0	0	84,134	84,799	666	1	0	1,230	100	100
	NODE_10_length_170010_cov_7.060506	PttICMP459_HopC1a_1	810	810	0	0	428	1,237	1	810	0	1,496	100	100
	NODE_16_length_140238_cov_7.021597	PttICMP459_HopAH1h_1	1,143	1,143	0	0	37,715	38,857	1	1,143	0	2,111	100	100
	NODE_20_length_123542_cov_7.379419	PttICMP459_HopAG1a_1	2,109	2,109	0	0	42,246	44,354	1	2,109	0	3,895	100	100
	NODE_26_length_87180_cov_7.218281	PttICMP459_HopI1d_1	1,011	1,011	0	0	31,925	32,935	1	1,011	0	1,868	100	100

Isolate	Query	Subject/ effector	Length of the effector	Alignment length	Mismatches	Gaps	Qstart[a]	Qend[b]	Subj. start[c]	Subj. end[d]	Evalue	Score	Identity	% Coverage
	NODE_17_length_137255_cov_7.393749	PttICMP459_AvrE1e_1	5,370	5,370	1	0	85,618	90,987	1	5,370	0	9,912	100	100
	NODE_22_length_104399_cov_7.616877	Pla1,188_1_HopB2d_1	6,069	6,069	37	0	21,623	27,691	1	6,069	0	11,003	99	100
Pap009	NODE_10_length_198549_cov_28.839474	PttICMP459_HopC1a_1	810	810	0	0	189,517	190,326	1	810	0	1,496	100	100
	NODE_16_length_161144_cov_31.850398	Pla1,188_1_HopBC1a_1	762	762	0	0	22,840	23,601	1	762	0	1,408	100	100
	NODE_31_length_72349_cov_107.613446	PthNCPPB2,598_HopAU1a_1	2,196	2,196	0	0	28	2,223	1	2,196	0	4,056	100	100
	NODE_42_length_30141_cov_137.356173	PsyICMP3,688_AvrRpm1a_1	687	687	0	0	15,095	15,781	687	1	0	1,269	100	100
	NODE_4_length_319415_cov_29.153004	Pla1,188_1_HopAH1h_1	1,143	1,143	3	0	200,652	201,794	1	1,143	0	2,095	100	100
	NODE_6_length_289792_cov_32.694976	PsyICMP4,917_HopAX1a_1	1,338	1,338	4	0	162,471	163,808	1	1,338	0	2,449	100	100
	NODE_3_length_361598_cov	Psy0,538_HopB2d_1	6,069	6,069	21	0	169,640	175,708	1	6,069	0	11,092	100	100

Isolate	Query	Subject/ effector	Length of the effector	Alignment length	Mismatches	Gaps	Qstart[a]	Qend[b]	Subj. start[c]	Subj. end[d]	Evalue	Score	Identity	% Coverage
	_40.676788													
	NODE_21_length_124896_cov_26.585512	PttICMP459_HopBA1a_1	720	720	2	1	114,549	115,267	720	1	0	1,312	100	100
	NODE_12_length_176790_cov_37.085353	PsyCC440_HopW1e_1	2,739	2,739	13	0	160,102	162,840	2,739	1	0	4,987	100	100
	NODE_40_length_37645_cov_167.452912	PpdICMP8,902_HopAB1b_1	1,254	1,242	6	0	18,669	19,910	1,254	13	0	2,261	100	99
	NODE_11_length_191215_cov_30.865579	PsyUS1_HopAZ1c_1	660	660	4	0	62,997	63,656	660	1	0	1,197	99	100
	NODE_2_length_384278_cov_35.412948	PsyCC440_AvrE1e_1	5,370	5,370	38	0	293,480	298,849	5,370	1	0	9,707	99	100
	NODE_17_length_154312_cov_38.727020	PttICMP459_HopI1d_1	1,011	1,011	10	0	111,488	112,498	1	1,011	0	1,812	99	100
	NODE_13_length_175108_cov_38.722061	PaflCMP5,011_HopAG1a_1	2,151	2,151	33	0	139,991	142,141	1	2,151	0	3,790	98	100
	NODE_35_length_55382_cov_96.033795	PpdICMP8,902_HopAT1a_1	3,360	3,361	81	1	40,037	43,397	1	3,360	0	5,751	98	100

Isolate	Query	Subject/ effector	Length of the effector	Alignment length	Mismatches	Gaps	Qstart[a]	Qend[b]	Subj. start[c]	Subj. end[d]	Evalue	Score	Identity	% Coverage
	NODE_27_length_81485_cov_45.018843	PsyFF5_HopBF1b_1	753	746	34	5	24,674	25,411	753	10	0	1,125	94	99
	NODE_7_length_251763_cov_27.819597	PsaShaanxi_M7_HopV-ShcV1f_1	477	462	67	1	98,389	98,849	473	12	3.6E-131	475	85	97
Pap014	NODE_3_length_777710_cov_39.868628	PlpICMP8,813_HopBN1b_1	897	897	0	0	296,173	297,069	1	897	0	1,657	100	100
	NODE_1_length_994255_cov_46.375063	PsyCC457_HopW1e_1	2,739	2,739	3	0	185,559	188,297	1	2,739	0	5,042	100	100
	NODE_12_length_116464_cov_41.974843	Psy0,554_HopAH1h_1	1,143	1,143	6	0	7,015	8,157	1	1,143	0	2,078	99	100
	NODE_6_length_364593_cov_48.513462	PlpICMP8,813_HopB2d_1	6,069	6,069	41	0	170,218	176,286	1	6,069	0	10,981	99	100
	NODE_13_length_103176_cov_48.361012	PlpICMP8,813_HopAG1a_1	2,151	2,151	26	0	84,708	86,858	1	2,151	0	3,829	99	100
	NODE_4_length_489297_cov_40.371066	PsyHS191_HopBA1a_1	720	720	15	0	416,218	416,937	1	720	0	1,247	98	100
	NODE_2_length_856937_cov	PpiH5E3_AvrE1e_1	5,370	5,371	129	2	365,469	370,838	5,370	1	0	9,191	98	100

Isolate	Query	Subject/ effector	Length of the effector	Alignment length	Mismatches	Gaps	Qstart[a]	Qend[b]	Subj. start[c]	Subj. end[d]	Evalue	Score	Identity	% Coverage
	_45.605965													
	NODE_9_length_229535_cov_50.838389	PsyFF5_HopBF1b_1	753	746	35	5	78,706	79,443	10	753	0	1,120	94	99
P16	JAHCZG010000007.1	PttICMP459_HopC1a_1	810	810	0	0	16,923	17,732	1	810	0	1,496	100	100
	JAHCZG010000020.1	PttICMP459_HopBC1a_1	762	762	0	0	80,307	81,068	762	1	0	1,408	100	100
	JAHCZG010000024.1	Pja301,072_HopBP1b_1	1,236	1,236	0	0	58,045	59,280	1	1,236	0	2,283	100	100
	JAHCZG010000058.1	PttICMP459_HopBA1a_1	720	720	0	0	510	1,229	1	720	0	1,330	100	100
	JAHCZG010000081.1	PttICMP459_HopBN1f_1	888	888	0	0	1,251	2,138	888	1	0	1,640	100	100
	JAHCZG010000013.1	Pja301,072_AvrE1e_1	5,370	5,370	2	0	130,255	135,624	5,370	1	0	9,906	100	100
	JAHCZG010000015.1	PsyBRIP34,881_HopAL1a_1	2,040	2,040	1	0	104,021	106,060	2,040	1	0	3,762	100	100
	JAHCZG010000016.1	PsyCC1,458_HopAH1h_1	1,143	1,143	1	1	102,215	103,356	1,143	1	0	2,098	100	100
	JAHCZG010000001.1	PsyBRIP34,881_HopI1d_1	1,014	1,014	5	0	232,437	233,450	1	1,014	0	1,845	100	100
	JAHCZG010000003.1	PsyCC1,543_HopB2d_1	6,069	6,069	44	0	184,527	190,595	6,069	1	0	10,964	99	100
	JAHCZG010000026.1	PsyCC440_HopAZ1c_1	672	625	7	0	70,564	71,188	48	672	0	1,116	99	93

Isolate	Query	Subject/ effector	Length of the effector	Alignment length	Mismatches	Gaps	Qstart[a]	Qend[b]	Subj. start[c]	Subj. end[d]	Evalue	Score	Identity	% Coverage
	JAHCZG010000006.1	PsyFF5_HopBF1b_1	753	746	33	6	105,607	106,343	753	10	0	1,123	94	99
	JAHCZG010000008.1	PsaShaanxi_M7_HopV-ShcV1f_1	477	464	67	1	9,643	10,105	475	12	1.9E-132	479	85	97
P21	JAHDT000015.1	PttICMP459_HopBN1f_1	888	888	0	0	71,878	72,765	1	888	0	1,640	100	100
	JAHDT000027.1	Pla1,188_1_HopBC1a_1	762	762	0	0	66,163	66,924	762	1	0	1,408	100	100
	JAHDT000036.1	PttICMP459_HopC1a_1	810	810	0	0	52,827	53,636	1	810	0	1,496	100	100
	JAHDT000050.1	PsyICMP3,688_AvrRpm1a_1	687	687	0	0	2,729	3,415	687	1	0	1,269	100	100
	JAHDT000084.1	PheICMP3,263_HopD2d_1	1,017	1,017	0	0	1,224	2,240	1	1,017	0	1,879	100	100
	JAHDT000056.1	PsaTP6_1_HopAW1a_1	657	657	1	0	20,062	20,718	1	657	0	1,208	100	100
	JAHDT000002.1	PsyICMP4,917_HopAX1a_1	1,338	1,338	4	0	127,632	128,969	1,338	1	0	2,449	100	100
	JAHDT000001.1	Psy0,538_HopB2d_1	6,069	6,069	21	1	246,494	252,561	6,069	1	0	11,084	100	100
	JAHDT000009.1	PttICMP459_HopBA1a_1	720	720	2	1	42,540	43,258	720	1	0	1,312	100	100
	JAHDT000066.1	Pla1,188_1_HopAH1h_1	1,143	1,143	4	1	15,057	16,198	1,143	1	0	2,082	100	100
	JAHDT000045.1	PsyCC440_HopW1e_1	2,739	2,739	12	0	28,374	31,112	2,739	1	0	4,992	100	100

Isolate	Query	Subject/ effector	Length of the effector	Alignment length	Mismatches	Gaps	Qstart[a]	Qend[b]	Subj. start[c]	Subj. end[d]	Evalue	Score	Identity	% Coverage
	JAHDT00 00062.1	PsaTP6_ 1_HopA U1a_1	2,445	2,339	12	0	2,924	5,262	2,445	107	0	4,253	99	96
	JAHDT00 00016.1	PsyUS1_ HopAZ1 c_1	660	660	4	0	23,734	24,393	660	1	0	1,197	99	100
	JAHDT00 00018.1	PsyCC4 40_AvrE 1e_1	5,370	5,370	38	0	26,086	31,455	5,370	1	0	9,707	99	100
	JAHDT00 00003.1	PttICMP 459_Hop I1d_1	1,011	1,011	10	0	232,495	233,505	1	1,011	0	1,812	99	100
	JAHDT00 00051.1	PafICM P5,011_ HopAG1 a_1	2,151	2,151	33	0	33,118	35,268	2,151	1	0	3,790	98	100
	JAHDT00 00053.1	PpdICM P8,902_ HopAT1 a_1	3,360	3,361	81	1	27,186	30,546	1	3,360	0	5,751	98	100
	JAHDT00 00028.1	PsyFF5_ HopBF1 b_1	753	746	34	6	56,211	56,947	10	753	0	1,118	94	99
	JAHDT00 00030.1	PsaShaa nxi_M7_ HopV-ShcV1f_ 1	477	462	67	1	9,628	10,088	473	12	1.1E-131	475	85	97
	NODE_3_ length_31 8125_cov _6.224517	Pla1,188 _1_Hop BC1a_1	762	762	0	0	307,816	308,577	762	1	0	1,408	100	100
	NODE_24 _length_9 5346_cov _6.416913	PttICMP 459_Hop C1a_1	810	810	0	0	86,492	87,301	1	810	0	1,496	100	100
	NODE_64 _length_5 979_cov_ 29.962064	PsyICM P3,688_ AvrRpm 1a_1	687	687	0	0	2,897	3,583	687	1	0	1,269	100	100
	NODE_69 _length_4 138_cov_ 22.706308	PheICM P3,263_ HopD2d _1	1,017	1,017	0	0	1,028	2,044	1	1,017	0	1,879	100	100

Isolate	Query	Subject/ effector	Length of the effector	Alignment length	Mismatches	Gaps	Qstart[a]	Qend[b]	Subj. start[c]	Subj. end[d]	Evalue	Score	Identity	% Coverage
	NODE_5_length_272162_cov_6.291374	Pla1,188_1_HopAH1h_1	1,143	1,143	3	0	116,334	117,476	1,143	1	0	2,095	99.738	100
	NODE_4_length_302893_cov_6.283678	PsyICMP4,917_HopAX1a_1	1,338	1,338	4	0	139,392	140,729	1,338	1	0	2,449	99.701	100
	NODE_1_length_394497_cov_6.522421	Psy0,538_HopB2d_1	6,069	6,069	21	0	218,788	224,856	6,069	1	0	11,092	99.654	100
	NODE_13_length_164173_cov_8.419370	PttICMP459_HopBA1a_1	720	720	2	1	12,495	13,213	1	720	0	1,312	99.583	100
	NODE_7_length_249233_cov_6.195527	PsyCC440_HopW1e_1	2,739	2,739	12	0	232,413	235,151	2,739	1	0	4,992	99.562	100
	NODE_61_length_6808_cov_144.780721	PsaTP6_1_HopAU1a_1	2,445	2,339	12	0	377	2,715	107	2,445	0	4,253	99.487	96
	NODE_18_length_141431_cov_6.342821	PsyCC440_AvrE1e_1	5,370	5,370	38	0	85,808	91,177	1	5,370	0	9,707	99.292	100
	NODE_6_length_262431_cov_6.281391	PttICMP459_HopI1d_1	1,011	1,011	10	0	28,939	29,949	1,011	1	0	1,812	99.011	100
	NODE_17_length_144748_cov_6.466523	PafICMP5,011_HopAG1a_1	2,151	2,151	33	0	109,563	111,713	1	2,151	0	3,790	98.466	100
	NODE_39_length_45064_cov	PpdICMP8,902_HopAT1a_1	3,360	3,361	81	1	40,087	43,447	1	3,360	0	5,751	97.56	100

Isolate	Query	Subject/ effector	Length of the effector	Alignment length	Mismatches	Gaps	Qstart[a]	Qend[b]	Subj. start[c]	Subj. end[d]	Evalue	Score	Identity	% Coverage
	_19.056301													
	NODE_26_length_81585_cov_6.376341	PsyFF5_HopBF1b_1	753	746	34	5	56,125	56,862	10	753	0	1,125	94.102	99
VSP20-65-3	NODE_2_length_373656_cov_8.375371	PttICMP459_HopBF1b_1	606	606	0	0	354,929	355,534	1	606	0	1,120	100	100
	NODE_4_length_282595_cov_8.058322	PttICMP459_HopAH1h_1	1,143	1,143	0	0	108,382	109,524	1,143	1	0	2,111	100	100
	NODE_6_length_212419_cov_7.923827	PttICMP459_HopBN1f_1	888	888	0	0	15,911	16,798	1	888	0	1,640	100	100
	NODE_11_length_171063_cov_8.171123	PttICMP459_HopAZ1c_1	666	666	0	0	84,134	84,799	666	1	0	1,230	100	100
	NODE_12_length_169993_cov_8.026597	PttICMP459_HopC1a_1	810	810	0	0	428	1,237	1	810	0	1,496	100	100
	NODE_18_length_125484_cov_9.220690	PttICMP459_HopBA1a_1	720	720	0	0	66,297	67,016	720	1	0	1,330	100	100
	NODE_20_length_123581_cov_8.278201	PttICMP459_HopAG1a_1	2,109	2,109	0	0	79,222	81,330	2,109	1	0	3,895	100	100
	NODE_21_length_123144_cov_8.349602	PttICMP459_HopI1d_1	1,011	1,011	0	0	67,874	68,884	1	1,011	0	1,868	100	100

Isolate	Query	Subject/ effector	Length of the effector	Alignment length	Mismatches	Gaps	Qstart[a]	Qend[b]	Subj. start[c]	Subj. end[d]	Evalue	Score	Identity	% Coverage
	NODE_14_length_137265_cov_8.438828	PttICMP459_AvrE1e_1	5,370	5,370	1	0	85,618	90,987	1	5,370	0	9,912	100	100
	NODE_13_length_138484_cov_7.961491	PttICMP459_HopBC1a_1	762	762	1	0	20,926	21,687	1	762	0	1,402	100	100
	NODE_41_length_44705_cov_8.926870	Pla1,188_1_HopB2d_1	6,069	6,069	37	0	16,794	22,862	6,069	1	0	11,003	99	100
	NODE_10_length_182582_cov_7.987739	PsaShaanxi_M7_HopV-ShcV1f_1	477	464	66	1	111,450	111,912	475	12	4.3E-134	484	86	97
VSP20-77-1	NODE_6_length_264548_cov_7.815635	PttICMP459_HopAH1h_1	1,143	1,143	0	0	101,382	102,524	1,143	1	0	2,111	100	100
	NODE_8_length_206187_cov_7.908109	PttICMP459_HopBF1b_1	606	606	0	0	170,097	170,702	606	1	0	1,120	100	100
	NODE_9_length_200518_cov_7.977893	PttICMP459_HopBN1f_1	888	888	0	0	198,870	199,757	888	1	0	1,640	100	100
	NODE_12_length_171065_cov_7.987896	PttICMP459_HopAZ1c_1	666	666	0	0	84,129	84,794	666	1	0	1,230	100	100
	NODE_18_length_118468_cov_8.523597	PttICMP459_HopBA1a_1	720	720	0	0	114,568	115,287	720	1	0	1,330	100	100
	NODE_22_length_9	PttICMP459_HopAG1a_1	2,109	2,109	0	0	42,252	44,360	1	2,109	0	3,895	100	100

Isolate	Query	Subject/ effector	Length of the effector	Alignment length	Mismatches	Gaps	Qstart[a]	Qend[b]	Subj. start[c]	Subj. end[d]	Evalue	Score	Identity	% Coverage
	3674_cov_8.018622													
	NODE_31_length_71074_cov_8.006625	PttICMP459_HopI1d_1	1,011	1,011	0	0	15,802	16,812	1	1,011	0	1,868	100	100
	NODE_55_length_16250_cov_6.488805	PttICMP459_HopC1a_1	810	810	0	0	10,423	11,232	810	1	0	1,496	100	100
	NODE_15_length_137146_cov_8.007211	PttICMP459_AvrE1e_1	5,370	5,370	1	0	85,618	90,987	1	5,370	0	9,912	100	100
	NODE_41_length_44462_cov_8.554641	Pla1,188_1_HopB2d_1	6,069	6,069	36	0	21,594	27,662	1	6,069	0	11,008	99	100
	NODE_10_length_182569_cov_7.528458	PsaShaanxi_M7_HopV-ShcV1f_1	477	464	66	1	111,427	111,889	475	12	4.3E-134	484	86	97
VSP20-77-2	NODE_25_length_74442_cov_8.406701	PttICMP459_HopC1a_1	810	810	0	0	64,752	65,561	1	810	0	1,496	100	100
	NODE_59_length_24223_cov_6.414094	PttICMP459_HopBN1f_1	888	888	0	0	21,369	22,256	888	1	0	1,640	100	100
	NODE_70_length_11966_cov_45.184306	PsyICMP3,688_AvrRpm1a_1	687	687	0	0	1,502	2,188	687	1	0	1,269	100	100
	NODE_88_length_4223_cov_40.008057	PheICMP3,263_HopD2d_1	1,017	1,017	0	0	2,095	3,111	1,017	1	0	1,879	100	100
	NODE_89_length_3	PsaTP6_1_HopAW1a_1	657	657	1	0	513	1,169	657	1	0	1,208	100	100

Isolate	Query	Subject/ effector	Length of the effector	Alignment length	Mismatches	Gaps	Qstart[a]	Qend[b]	Subj. start[c]	Subj. end[d]	Evalue	Score	Identity	% Coverage
	584_cov_66.848713													
	NODE_2_length_473759_cov_7.594679	PsyICMP4,917_HopAX1a_1	1,338	1,338	4	0	433,196	434,533	1,338	1	0	2,449	100	100
	NODE_8_length_193881_cov_8.094279	Psy0,538_HopB2d_1	6,069	6,069	21	0	76,600	82,668	6,069	1	0	11,092	100	100
	NODE_5_length_257328_cov_7.599383	Pla1,188_1_HopAH1h_1	1,143	1,143	4	0	154,691	155,833	1	1,143	0	2,089	100	100
	NODE_1_length_542876_cov_7.856061	PttICMP459_HopBA1a_1	720	720	2	1	9,680	10,398	1	720	0	1,312	100	100
	NODE_3_length_405697_cov_7.678376	PsyCC440_HopW1e_1	2,739	2,739	12	0	388,991	391,729	2,739	1	0	4,992	100	100
	NODE_58_length_26775_cov_65.838487	PpdICMP8,902_HopAB1b_1	1,254	1,242	6	0	220	1,461	13	1,254	0	2,261	100	99
	NODE_86_length_4321_cov_108.415355	PsaTP6_1_HopAU1a_1	2,445	2,339	12	0	1,607	3,945	2,445	107	0	4,253	99	96
	NODE_4_length_294248_cov_7.631652	PsyCC440_AvrE1e_1	5,370	5,370	38	0	85,827	91,196	1	5,370	0	9,707	99	100
	NODE_32_length_58680_cov_6.656175	PttICMP459_HopI1d_1	1,011	1,011	10	0	41,863	42,873	1,011	1	0	1,812	99	100
	NODE_22_length_83966_cov_7.533141	PafICMP5,011_HopAG1a_1	2,151	2,151	33	0	48,781	50,931	1	2,151	0	3,790	98	100

Isolate	Query	Subject/ effector	Length of the effector	Alignment length	Mismatches	Gaps	Qstart[a]	Qend[b]	Subj. start[c]	Subj. end[d]	Evalue	Score	Identity	% Coverage
	NODE_40_length_50286_cov_27.170578	PpdICMP8,902_HopAT1a_1	3,360	3,361	81	1	40,087	43,447	1	3,360	0	5,751	98	100
	NODE_30_length_60342_cov_7.702234	PsyFF5_HopBF1b_1	753	746	34	5	34,870	35,607	10	753	0	1,125	94	99
	NODE_17_length_100181_cov_7.474314	PsaShaanxi_M7_HopV-ShcV1f_1	477	462	67	1	46,230	46,690	473	12	1.4E-131	475	85	97
VSP20-86-1	NODE_13_length_157210_cov_7.346740	PttICMP459_HopC1a_1	810	810	0	0	148,356	149,165	1	810	0	1,496	100	100
	NODE_19_length_127284_cov_7.511557	Pla1,188_1_HopBC1a_1	762	762	0	0	9,549	10,310	1	762	0	1,408	100	100
	NODE_77_length_5185_cov_82.671807	PsyICMP3,688_AvrRpm1a_1	687	687	0	0	2,401	3,087	1	687	0	1,269	100	100
	NODE_79_length_4250_cov_75.798933	PheICMP3,263_HopD2d_1	1,017	1,017	0	0	1,028	2,044	1	1,017	0	1,879	100	100
	NODE_2_length_318408_cov_7.022832	Pla1,188_1_HopAH1h_1	1,143	1,143	3	0	116,334	117,476	1,143	1	0	2,095	100	100
	NODE_12_length_167453_cov_7.541775	PsyICMP4,917_HopAX1a_1	1,338	1,338	4	0	26,589	27,926	1	1,338	0	2,449	100	100
	NODE_25_length_104466_co	Psy0,538_HopB2d_1	6,069	6,069	21	0	76,600	82,668	6,069	1	0	11,092	100	100

Isolate	Query	Subject/ effector	Length of the effector	Alignment length	Mismatches	Gaps	Qstart[a]	Qend[b]	Subj. start[c]	Subj. end[d]	Evalue	Score	Identity	% Coverage
	v_8.740797													
	NODE_20_length_124977_cov_6.800833	PttICMP459_HopBA1a_1	720	720	2	1	9,661	10,379	1	720	0	1,312	100	100
	NODE_9_length_177149_cov_7.669968	PsyCC440_HopW1e_1	2,739	2,739	12	0	14,092	16,830	1	2,739	0	4,992	100	100
	NODE_84_length_3449_cov_361.979530	PsaTP6_1_HopAU1a_1	2,445	2,339	12	0	760	3,098	2,445	107	0	4,253	99	96
	NODE_6_length_191107_cov_7.424416	PsyUS1_HopAZ1c_1	660	660	4	0	83,458	84,117	660	1	0	1,197	99	100
	NODE_21_length_119912_cov_7.838118	PsyCC440_AvrE1e_1	5,370	5,370	38	0	28,736	34,105	5,370	1	0	9,707	99	100
	NODE_26_length_97832_cov_7.819528	PttICMP459_HopI1d_1	1,011	1,011	10	0	67,884	68,894	1	1,011	0	1,812	99	100
	NODE_15_length_144832_cov_8.187768	PaflCMP5,011_HopAG1a_1	2,151	2,151	33	0	109,563	111,713	1	2,151	0	3,790	98	100
	NODE_46_length_45063_cov_47.729749	PpdICMP8,902_HopAT1a_1	3,360	3,361	81	1	1,618	4,978	3,360	1	0	5,751	98	100
	NODE_39_length_53715_cov_8.213947	PsyFF5_HopBF1b_1	753	746	34	5	34,856	35,593	10	753	0	1,125	94	99

Isolate	Query	Subject/ effector	Length of the effector	Alignment length	Mismatches	Gaps	Qstart[a]	Qend[b]	Subj. start[c]	Subj. end[d]	Evalue	Score	Identity	% Coverage
	NODE_10_length_171861_cov_6.926974	PsaShaanxi_M7_HopV-ShcV1f_1	477	462	68	1	18,460	18,920	473	12	1.1E-129	470	85	97
VSP20-96-K11	NODE_7_length_185493_cov_5.750316	PttICMP459_HopC1a_1	810	810	0	0	175,803	176,612	1	810	0	1,496	100	100
	NODE_18_length_139002_cov_5.204292	Pla1,188_1_HopBC1a_1	762	762	0	0	21,267	22,028	1	762	0	1,408	100	100
	NODE_73_length_5812_cov_58.640809	PsyICMP3,688_AvrRpm1a_1	687	687	0	0	2,397	3,083	1	687	0	1,269	100	100
	NODE_79_length_4183_cov_46.313609	PheICMP3,263_HopD2d_1	1,017	1,017	0	0	2,095	3,111	1,017	1	0	1,879	100	100
	NODE_57_length_17033_cov_78.818881	PsaTP6_1_HopAW1a_1	657	657	1	0	2,416	3,072	1	657	0	1,208	100	100
	NODE_25_length_109455_cov_5.296511	Pla1,188_1_HopAH1h_1	1,143	1,143	3	0	101,496	102,638	1,143	1	0	2,095	100	100
	NODE_12_length_155269_cov_5.534523	PsyICMP4,917_HopAX1a_1	1,338	1,338	4	0	26,182	27,519	1	1,338	0	2,449	100	100
	NODE_4_length_252469_cov_6.065934	Psy0,538_HopB2d_1	6,069	6,069	21	0	169,800	175,868	1	6,069	0	11,092	100	100
	NODE_20_length_129342_co	PttICMP459_HopBA1a_1	720	720	2	1	117,869	118,587	720	1	0	1,312	100	100

Isolate	Query	Subject/ effector	Length of the effector	Alignment length	Mismatches	Gaps	Qstart[a]	Qend[b]	Subj. start[c]	Subj. end[d]	Evalue	Score	Identity	% Coverage
	v_22.469667													
	NODE_9_length_176850_cov_5.343770	PsyCC440_HopW1e_1	2,739	2,739	12	0	160,130	162,868	2,739	1	0	4,992	100	100
	NODE_52_length_25256_cov_70.551634	PpdICMP8,902_HopAB1b_1	1,254	1,242	6	0	22,186	23,427	1,254	13	0	2,261	100	99
	NODE_74_length_5638_cov_193.924696	PsaTP6_1_HopAU1a_1	2,445	2,339	12	0	377	2,715	107	2,445	0	4,253	99	96
	NODE_11_length_166657_cov_5.548394	PsyUS1_HopAZ1c_1	660	660	4	0	83,458	84,117	660	1	0	1,197	99	100
	NODE_24_length_119916_cov_5.599429	PsyCC440_AvrE1e_1	5,370	5,370	39	0	28,735	34,104	5,370	1	0	9,701	99	100
	NODE_15_length_149732_cov_5.423061	PttICMP459_HopI1d_1	1,011	1,011	10	0	41,953	42,963	1,011	1	0	1,812	99	100
	NODE_6_length_200239_cov_5.008075	PafICMP5,011_HopAG1a_1	2,151	2,151	33	0	33,036	35,186	2,151	1	0	3,790	98	100
	NODE_42_length_44571_cov_29.970007	PpdICMP8,902_HopAT1a_1	3,360	3,361	81	1	40,086	43,446	1	3,360	0	5,751	98	100
	NODE_31_length_81585_cov_5.587076	PsyFF5_HopBF1b_1	753	746	34	5	56,125	56,862	10	753	0	1,125	94	99

Isolate	Query	Subject/ effector	Length of the effector	Alignment length	Mismatches	Gaps	Qstart[a]	Qend[b]	Subj. start[c]	Subj. end[d]	Evalue	Score	Identity	% Coverage
	NODE_22_length_127772_cov_5.049222	PsaShaanxi_M7_HopV-ShcV1f_1	477	462	67	1	28,958	29,418	12	473	1.8E-131	475	85	97

[a] **Qstart is** the starting position of the alignment within the query sequence.
[b] **Qend is the** ending position of the alignment within the query sequence.
[c] **Subj. start is** the starting (**Subj. start**).
[d] **Subj. end** is the ending positions of the alignment within the subject effector sequence.

CHAPTER TWO: COLONIZATION OF TABLE BEET AND SWISS CHARD BY *PSEUDOMONAS SYRINGAE* PV. *APTATA*

Introduction

Swiss chard (*Beta vulgaris* subsp. *vulgaris* Cicla Group), table beet (*Beta vulgaris* subsp. *vulgaris* Condivita Group), and sugar beet (*Beta vulgaris* subsp. *vulgaris* Altissima Group) belong to Amaranthaceae (Nottingham 2004). Previously, these and related species were classified in Chenopodiaceae (goosefoot) family which has since been placed in Amaranthaceae. Some of the species within Amaranthaceae include Mangel-wurzel (*B. vulgaris* var. *macrorrhiza*), spinach (*Spinacia oleracea*), lambsquarters (*Chenopodium album*), quinoa (*Chenopodium quinoa*), and many others (Harveson et al. 2009). Beet, Swiss chard, and sugar beet grow best at 15 to 19°C and are produced for various purposes, including fresh market, frozen, canned and, in the case of sugar beet, for sugar production (Harveson et al. 2009; Navazio et al. 2010). For example, leaves and roots harvested from fresh market beet and chard crops are included in salads and other value-added products such as juices and dietary supplements (Chancia et al. 2021; Harveson et al. 2009; Pethybridge et al. 2024).

All subspecies of *B. vulgaris* are biennial, i.e., they require two years to complete the reproductive growth stage (Harveson et al. 2009; Navazio et al. 2010; Schrader and Mayberry 2003). These crops require photothermal induction for bolting, i.e., both vernalization and long day length to transition from vegetative to reproductive growth. Vernalization entails the exposure of roots to cold enough temperatures (0 to 15°C) for 5 to 20 weeks to induce bolting (Abo-Elwafa et al. 2006; du Toit 2007; Kockelmann et al. 2010; Mutasa-Göttgens et al. 2010; Navazio et al. 2010). Therefore, beet and Swiss chard seed production is limited to regions of the

world that have the specific environmental conditions required to induce bolting, including Argentina, Brazil, Chile, Denmark, New Zealand, Peru, South Africa, and the United States. In the United States, the maritime region of the Pacific Northwest (PNW), i.e., western Oregon and Washington, is the only region with suitable climatic conditions for production of table beet, sugarbeet, and Swiss chard seed crops (du Toit 2007). Approximately 95% of the table beet and Swiss chard seed crops grown in the United States are produced in this region, where winters are cold enough for vernalization but not too cold to kill overwintering plants, and summers are reasonably dry with low relative humidity that is optimal for ripening and drying of seed crops while minimizing the risk of seed colonization by fungal and bacterial pathogens (du Toit 2007; Organic Seed Alliance 2016; Rackham 2002; Schreiber and Ritchie 1995).

Over the past two to three decades, there has been a rise in demand for leafy vegetables, driven, in part, by an increase in public awareness of the nutritional benefits associated with vegetable consumption, and the convenience of bagged baby leaf salads (Lin et al. 2003). Fresh market table beet and Swiss chard crops grown as baby leaf crops are harvested as soon as 20 to 40 days after planting at 7 to 9 million seed/ha (Crane 2023; Nottingham 2004). The short crop duration, limited crop rotations, and dense populations grown with sprinkler (overhead) irrigation create highly favorable conditions for foliar fungal and bacterial pathogens of beet, chard, spinach and other species grown for baby leaf salads. In baby leaf crops, incidences of foliar symptoms as low as 5% can lead to rejection of entire crops by packers because of the difficulty of sorting symptomatic leaves (Crane 2023; Nottingham 2004).

Pseudomonas syringae pv. *aptata* is a seedborne and seed transmitted pathogen that causes bacterial leaf spot of table beet, sugar beet, and Swiss chard (Jacobsen 2009). Symptoms caused by *P. syringae* pv. *aptata* most often develop during prolonged cool to warm and wet (10

to 25°C) conditions (Brown and Jamieson 1913; Jacobsen 2009). Bacterial leaf spot symptoms include dark brown to black lesions on leaves, which become dry, light brown to tan, and paper thin during dry conditions (Jacobsen 2009; Koike et al. 2003; Morris et al. 2008; Nampijja et al. 2021). Lesions range from 2 to 3 mm in diameter, each with a distinct brown to black border (Crane 2023; Derie et al. 2016; Koike et al. 2003; Riffaud and Morris 2002). Lesions usually are water-soaked and coalesce under extended wet conditions, giving infected leaves a blighted appearance (Walker 1952). Like most foliar bacterial pathogens, *P. syringae* pv. *aptata* can infect leaves, stems, or petioles via hydathodes and stomata as well as wounds (Jacobsen 2009; Nikolić et al. 2018). Brown to black, necrotic lesions also can appear on cotyledons and seed stalks. *P. syringae* pv. *aptata* can spread in wind-blown, aerosolized particles, and splash-dispersed by irrigation water or rain. The bacterium can also persist as an epiphyte without causing symptoms of bacterial leaf spot (Riffaud and Morris 2002).

P. syringae pv. *aptata* occurs worldwide, including the European Union (Belgium, France, Hungary, Italy, and the Netherlands), Republic of Serbia, Switzerland, United Kingdom, Iran, India, Japan, South Korea, Australia, New Zealand, and the United States (Arabi et al. 2006; Hill 1979; Jacobsen 2009; Janse 1979; Nikolić et al. 2018; Stojšin et al. 2015; Walker 1952). In the United States, *P. syringae* pv. *aptata* has been reported in Arizona, California, Colorado, Georgia, Kentucky, Montana, North Dakota, Nebraska, Oregon, and Washington (Arabiat et al. 2016; Bradbury 1986; Derie et al. 2016; Koike et al. 2003; Nampijja et al. 2021). *P. syringae* pv. *aptata* can colonize other hosts such as cantaloupe (*Cucumis melo* var. *cantalupensis*), squash (*Cucurbita moschata*), oat (*Avena sativa*), corn (*Zea mays* subsp. *mays*), pepper (*Capsicum* spp.), tomato (*Solanum lycopersicum*), lettuce (*Lactuca sativa*), soybean

(*Glycine max*), onion (*Allium cepa*), and sunflower (*Helianthus annuus*) (Jacobsen 2009; Koike et al. 2003; Morris et al. 2000; Sedighian et al. 2014; Tymon and Inglis 2017).

Over the past two decades, bacterial leaf spot periodically has become more prevalent in table beet and Swiss chard seed production in the PNW (Puget Sound Growers' Association, *Personal communication*), reducing the supply of clean certified seed. This has resulted in significant economically losses due, in part, to increased demand for seed to plant the increasing acreage of baby leaf beet and Swiss chard crops, as the PNW region of the United States accounts for up to 40% of the global supply of beet and chard seed (Rackam 2002; Schreiber and Ritchie 1995; Western Washington Seed Advisory Committee, *personal communication*). Because these seed crops can only be grown in about a half-dozen regions of the world that have the appropriate climatic conditions, beet and chard seed trade is increasingly global. Nonetheless, producers in the United States have to compete with other regions of the world to produce high quality, pathogen-free seed (du Toit 2007). Based on the risk of beet and Swiss chard seed crops becoming infected with *P. syringae* pv. *aptata*, there is a need to increase our understanding of the pathogen ecology, epidemiology and management in biennial table beet and Swiss chard seed crops.

To understand the epidemiology and management options for bacterial pathogens, populations of the pathogens typically are monitored over multiple seasons using direct sampling and testing methods (Hirano and Upper 2000). This has improved our understanding of host-pathogen interactions and the influence of abiotic factors, such as environmental conditions, on these diseases. For example, various *P. syringae* pathovars as well as isolates of pathogenic *Xanthomonas* spp. have been monitored in crops by quantifying the pathogen from plant samples that were plated onto semi-selective media (Crosse 1959; Cuppels and Elmhirst 1999; Donati et

al. 2020; du Toit et al. 2005; Hirano and Upper 2000; King et al. l954). In addition, antibiotic-resistant mutants of bacterial pathogens, capable of growing on media amended with the antibiotic to which they are resistant, have been employed to study the ecology of plant pathogenic bacteria. For example, rifampicin-resistant strains of *Xanthomonas phaseoli* pv. *phaseoli* (formerly known as *Xanthomonas phaseoli*) and *Xanthomonas citri* pv. *fuscans* (formerly known as *Xanthomonas fuscans*) were generated to monitor these pathogens in common bean (*Phaseolus vulgaris*) under field conditions (Weller and Saettler 1978). Similarly, this approach has been utilized in various ecological studies, including generation of streptomycin-resistant strains of *Erwinia amylovora,* causal agent of fire blight of pome fruit trees, to investigate the pathogen population dynamics under greenhouse conditions (Gowda and Goodman 1970; Lewis and Goodman 1965). Pathogens also have been tagged with fluorescent proteins, such as the green fluorescent protein (GFP) and mCherry protein, to monitor colonization in planta as well as understand where the pathogens localize on plants, by employing non-destructive advanced imaging techniques such as laser scanning confocal microscopy to visualize the pathogens in real-time (Cerutti et al. 2017; Kubheka et al. 2013; Wang et al. 2007).

Strains of bacterial pathogens can differ in the host-pathogen response they incite on different cultivars and/or subspecies of hosts, e.g., sugar beet (Nikolić et al. 2018; Ranković et al. 2023). Some strains of *P. syringae* pv. *aptata* cause bacterial leaf spot on beet and Swiss chard, while other strains only cause symptoms on beet (Ranković et al. 2023; Safni et al. 2016). The objectives of this study were to determine the population dynamics and patterns of colonization of table beet and Swiss chard plants by *P. syringae* pv. *aptata* in both vegetative and reproductive growth stages. GFP-tagged strains of *P. syringae* pv. *aptata* were generated and

used to examine colonization of the epidermis and apoplast of leaves of table beet and Swiss chard seedlings in an attempt to understand why some *P. syringae* pv. *aptata* strains cause symptoms on both table beet and Swiss chard while other strains cause symptoms only on table beet. In addition, a rifampicin-resistant strain of *P. syringae* pv. *aptata* was used to examine colonization and symptom development during the reproductive growth stages of table beet seed crops in field trials in western Washington in 2021, 2022, and 2023.

Materials and Methods

Colonization during vegetative growth. *P. syringae* pv. *aptata* strain Pap009, which is pathogenic on table beet and Swiss chard, and strain Pap014, which is pathogenic on table beet but not Swiss chard, were isolated originally from Swiss chard and table beet seed grown in Washington (Safni et al. 2016). These strains were selected to examine why the two isolates cause differential disease responses on table beet vs. Swiss chard, and tagged with a GFP (J. Jacobs and E. Bernal, The Ohio State University, Columbus, OH). Pap009 and Pap014 were grown overnight in 40 ml nutrient broth (NB) on a shaker at 200 rpm at room temperature. Each suspension of competent bacterial cells (cells capable of taking up foreign DNA) was then centrifuged at 4,000 rpm at room temperature in 50 ml conical tubes for 10 minutes. The supernatant was decanted, the cell pellet was suspended in 10 ml of 10% glycerol, and the resultant pellet was resuspended in 5 ml of 10% glycerol followed by centrifugation at 4,000 rpm at room temperature, with the supernatant decanted. The cells of each bacterial strain were resuspended in 2 ml of 10% glycerol in a 2 ml Eppendorf tube, centrifuged at 6,000 rpm, and the supernatant decanted. The bacterial pellet was suspended again in 200 µl of 10% glycerol, and 2 µg of a GFP plasmid (pGFP vector, Takara Bio, Inc., San Jose, CA) added to the 200 µl

suspension of competent cells, mixed gently, and incubated on ice for 2 minutes. The cells were transferred to an electroporation cuvette and electroporated (2.5 V, 5.4 milliseconds). After transformation, 950 µl of NB was added to the cuvette and the suspension mixed gently. A 900-µl aliquot of the bacterial suspension was transferred to a new 1.5 ml Eppendorf tube and incubated for 3 h at 28°C on a shaker at 200 rpm. The electroporated cells were centrifuged at 5,000 rpm for 10 minutes, and the supernatant discarded. The bacterial pellet was resuspended in 200 µl of sterile water, plated onto nutrient agar (NA) medium amended with kanamycin (50 µg ml^{-1}), and incubated at 27°C. Individual transformed colonies with transformed cells were identified by a bright green glow under long wave ultraviolent (UV) light, and subcultured onto NA medium amended kanamycin (50 µg ml^{-1}). The GFP-tagged strains are referred to as GFP-Pap009 and GFP-Pap014.

To ensure that the virulence of GFP-Pap009 and GFP-Pap014 was comparable to that of the wild-type strains, a pathogenicity trial was set up in a randomized complete block design with three replications of each inoculation treatment, i.e., Pap009, Pap014, GFP-Pap009, GFP-Pap014 and a non-inoculated control treatment. Leaves of three 21-week-old seedlings of table beet cv. Red Ace and Swiss chard cv. Silverado were each rub inoculated with 10^7 CFU/ml of each bacterial strain on the adaxial and abaxial surfaces. Each replication consisted of six seedlings per host plant, with one seedling in each cell of a 6-pack flat (TLC Polyform, Inc., Salem, OR). Each of 30 6-pack flats was filled with propagation mix (SunGro Potting Medium, Agawam, MA), and 15 packs planted with seed of the table beet cv. Red Ace, and the other 15 flats with seed of the Swiss chard cv. Silverado (two seeds per cell). Plants were maintained in a greenhouse at 22 to 26°C, and seedlings thinned to one per cell. Plants were fertigated with 20-20-20 fertilizer (Everris, Dublin, OH) injected at a final nitrogen concentration of 200 ppm.

Thrips were managed with weekly broadcast applications of *Beauveria bassiana* (Botanigard 22WP; Lam International Corp., Butte, MT) applied at 2.4 g/liter, spinosad (Entrust; Dow Agrosciences, Indianapolis, IN) applied at 0.17 g/liter, or imidacloprid (Leverage 2.0; Bayer, Kansas City, MO) applied at 1.3 ml/liter, with products rotated weekly to minimize development of insecticide resistance in the thrips population. Symptoms of bacterial leaf spot were rated 7 days post inoculation.

Once the virulence of the GFP-tagged isolates was confirmed, an experiment was set up to test the hypothesis that the differential response of beet and chard to infection by *P. syringae* pv. *aptata* strains Pap009 and Pap014 results from the ability of Pap009 to colonize both the epidermis and apoplast of both table beet and Swiss chard plants, whereas Pap014 can only colonize the epidermis of chard, but both the leaf surface and apoplast of table beet plants. The trial was a 2 x 3 x 3 factorial treatment design with two host plants (table beet cv. Red Ace and Swiss chard cv. Silverado), three inoculation treatments (GFP-Pap009, GFP-Pap014, and a water control treatment), and three sampling times (24, 48, and 72 h after inoculation). The experiment was arranged in a randomized complete block design with two replications of the 18 treatment combinations. Each replication consisted of six seedlings per host plant, with one seedling in each cell of a 6-pack flat. Six-packs filled with RediEarth propagation mix were planted with seed of the table beet cv. Red Ace or seed of the Swiss chard cv. Silverado, and the plants maintained in the greenhouse as described above.

GFP-Pap009 and GFP-Pap014 were inoculated into medium 523 broth (Kado and Heskett 1970), and incubated overnight on a gyratory shaker (200 rpm, 25°C). Each bacterial suspension was adjusted to 10^7 CFU/ml, 0.06 g Carborundum added, and 10 ml of the suspension inoculated onto the relevant plants by rubbing the suspension gently on both surfaces

of each of two leaves per plant using a cotton swab dipped in inoculum. The inoculated leaves were sampled from each plant 24, 48, and 72 h after inoculation. Severity of bacterial leaf spot was rated each day of sampling by estimating the percentage of each inoculated leaf area with bacterial leaf spot symptoms (0 – 100%).

To quantify epiphytic and internal colonization of the leaves by GFP-Pap009 and GFP-Pap014, the fresh weight of leaves sampled from each plant was measured at each sampling time, and a 0.9 mm-diameter leaf disk removed from each of six plants per replication of each treatment combination using a cork borer sterilized by dipping in 95% alcohol and flamed. The entire leaf was then surface-sterilized in 0.6% NaOCl for 30 s, triple-rinsed in 50 ml of deionized water, and blotted dry with sterilized paper towels in a laminar flow hood. A second disk was then removed from each of the surface-sterilized leaves, and the leaf weighed again. Six leaf disks sampled prior to surface-sterilization, and six disks sampled after surface-sterilization of leaves of each replicate 6-pack of each treatment combination were placed into a BIOREBA universal extraction bag (BIOREBA AG, Reinach, Switzerland) and ground with a pestle in 1 ml of 0.0125 M phosphate buffer. The population of GFP-Pap009 and GFP-Pap014 was quantified at each sampling period by dilution-plating each ground leaf disk suspension onto NA medium supplemented with kanamycin (50 µg/ml). The plates were incubated at 27°C in the dark for 7 days, and the colonies counted to calculate CFU/g fresh tissue.

Colonization of the epidermis and apoplast of table beet and Swiss chard leaves by GFP-Pap009 and GFP-Pap014 at each sampling period also was visualized for six beet and six chard plants for each inoculation treatment using a Sterallis 8 Leica confocal laser scanning microscope (Leica, Wetzlar, Germany) at Western Washington University, Bellingham, WA. Imaging was done by mounting a 1.0 cm × 0.5 cm piece of tissue from each leaf disk in 100 µl of

deionized water in a glass Petri dish. Fluorescent images were taken at 250× at a speed of 600 Hz, and excitations of 488 and 561 nm to excite the GFP-tagged *P. syringae* pv. *aptata* and the chloroplasts, respectively. Confocal microscope images were processed in Fiji (Walter et al. 2010).

The entire trial was repeated with three replications and addition of a 96-h post-inoculation sampling time based on results of the first trial, to see if the later sampling time reflected differences in GFP-Pap009 vs. GFP-Pap014 development on beet and chard leaves. This resulted in a 2 x 3 x 4 factorial treatment design. In trial 2, 12 leaves were sampled from each of the six-packs per plant for each treatment combination, and the initial weight of the leaves measured. Six of the leaves were surface-sterilized as described for the first trial, while the other six leaves were not surface-sterilized. A disk was removed from both the surface-sterilized and non-surface-sterilized leaves for each replication of each treatment combination. The rest of the procedure was completed as described for the first trial. Confocal imaging was not done for trial 2 because images from the first trial showed no differences in leaf surface vs. apoplast colonization of beet vs. chard by GFP-Pap009 and GFP-Pap014.

Colonization during reproductive growth. Vernalized transplants of the same proprietary, open-pollinated, table beet cultivar were obtained from a seed grower in Skagit Co., WA in each of March 2021, April 2022, and April 2023 to plant a table beet seed crop trial each year at the Washington State University (WSU) Mount Vernon Northwestern Washington Research and Extension Center (NWREC) in Skagit Co, WA. Each year 3.36 kg/ha of agricultural limestone flour (97 Oregon lime score, 97% calcium carbonate, Northwest Lime Co., Mount Vernon, WA) was applied to the field trial site prior to planting, using a 1.8-m-wide Gandy drop spreader (Gandy, Owatonna, MN), and incorporated by mulching to raise the soil

pH from 6.0, 5.8, and 5.6 in 2021, 2022, and 2023, respectively, by approximately 0.5 units. RoNeet (cycloate) broadcast at 6.3 liters/ha along with 46-0-0 urea in 2021 and 2022, and with 38-0-0-7.3 in 2023, and incorporated by mulching for weed control. In 2021, the vernalized seedlings were first transplanted into 4.6-cm-diameter pots (1 seedling/pot) and maintained in a greenhouse at 22 to 26°C for a month until the trial site was ready for transplanting. In 2022 and 2023, the vernalized seedlings were transplanted directly into the field site. Seedlings were transplanted manually on 12 April 2021, 16 April 2022, and 3 May 2023. The table beet cultivar used each year was the same as the nearest commercial table beet seed crop to avoid unwanted cross-pollination with the grower's seed crops. The trial measured 25 m × 4 m, 61 m × 3 m, and 70 m × 3 m in 2021, 2022, and 2023, respectively, with five rows of transplants in 2021, and four rows in each of 2022 and 2023. The inter-row spacing was 1.1 m and the intra-row spacing was 0.3 m each year. Plants were irrigated as needed using hand-line sprinklers.

Generation of rifampicin-resistant strains of *P. syringae* pv. *aptata*. A rifampicin-resistant selection of strain Pap010 of *P. syringae* pv. *aptata* (rif-Pap010), produced by C. Bull, Pennsylvania State University in 2019-20, was used to inoculate the trial each year. To generate rif-Pap010, Pap010 was grown overnight in 50 ml aliquots of NB on a shaker at 150 rpm, centrifuged (4,000 rpm, 10 minutes, 4°C), the supernatant discarded, and the pellet resuspended in 1 ml of sterile water. Aliquots (100 µl) of the cell suspension were spread onto NA amended with 30% rifampicin (v/v). Variants that grew on the medium were then subcultured onto NA medium amended with 60% rifampicin, and the process repeated with NA amended with 100% rifampicin.

To ensure that growth rates of the rifampicin-resistant variants were not significantly affected by the *rpoB* mutation that confers this resistance, the growth rate of each variant was

compared to that of the wild type Pap010 strain. Each variant was streaked alongside Pap010 onto NA medium and yeast dextrose carbonate (YDC) agar medium (Schaad et al. 2001), and incubated for 3 days at 28°C. Variant isolates that did not differ significantly from Pap010 in colony morphology and size were grown overnight in NB. The following day, 5 ml of each suspension was added to 125 ml of sterile NB and growth rate measured at an optical density (OD) of 600 nm every 30 min during the logarithmic phase of growth over the course of 3.5 h. Rifampicin-resistant strains with growth rates that did not differ significantly from the wild type, as tested using a student's T test (*data not shown*), were assessed again using the same method but with 1/10 tryptic soy agar (TSA) medium and 1/10 tryptic soy broth (Mac Faddin 1985). Variant strains that still showed no significant difference in growth rate compared to that of Pap010 were preserved in 15% glycerol at -80°C. One of the variants, M10 (rif-Pap010), was used for the field trials after verifying the strain was still pathogenic on table beet cv. Red Ace and Swiss chard cv. Silverado as described above (*data not shown*).

Colonization of table beet during reproductive growth. ***2021 trial***. Inoculum for the 2021 field trial was produced by plating 100 µl of rif-Pap010, grown in medium 523 broth overnight on a shaker at 200 rpm, onto King's B agar medium (King et al. 1954), and incubating the plates for 48 h at 27°C in the dark. The bacterial lawn on each plate was transferred to 60 ml of deionized water using a sterilized glass rod, and the suspension adjusted to 10^8 CFU/ml (OD_{600} = 0.3). A total of 12 liters of inoculum was applied to plants in the trial at each inoculation (360 liters inoculum/ha) using a CO_2-pressurized backpack sprayer (5438907, IMI Cornelius, Italy) operated at 30 psi with three 8003 nozzles (XR11003, TeeJet, Glendale Heights, IL) spaced 0.15 m apart on a 0.5-m-long boom. The table beet seed crop was inoculated in the

evenings five times at approximately 2-week intervals from 18 June to 30 August 2021 (Fig. 2.2A).

2022 trial. In the 2022 trial, rif-Pap010 was grown in medium 523 broth on a shaker at 200 rpm for 16 h, and the suspension adjusted to 10^8 CFU/ml. Inoculations were carried out similarly to the 2021 trial, using the same volume of inoculum with the same CO_2-pressurized backpack sprayer for the first and second inoculations on 24 May and 6 June (Fig. 2.2B and 2.2C). For each of the final three inoculations on 5 July, and 2 and 30 August, 27 liters of rif-Pap010 inoculum were applied using a tractor-mounted boom sprayer with four 8003 nozzles spaced 0.5 m apart on a 2-m-long boom to avoid walking through the trial and damaging the dense canopy of the seed crop during full bloom and seed set. The tractor was operated at 18 rpm, and driven along each side of the trial to apply 374 liters of inoculum/ha.

2023 trial. In the 2023 trial, inoculum was prepared as described for the 2022 trial except that, for the first inoculation, 1 liter of inoculum was applied to the seedlings on 1 May using a spray bottle, before transplanting 230 vernalized seedlings on 3 May, to maximize coverage of the plants by rif-Pap010 and establish the pathogen on the plants early in the trial. Thereafter, the trial was inoculated on 11 July, 31 August, and 7 September (Fig. 2.2D and Fig. 2.5) using the tractor-mounted spray boom described for the 2022 trial.

Monitoring colonization of plants by rif-Pap010. ***2021 trial*****.** After each inoculation in the 2021 trial, a 20-g sample of tissue, including leaves attached to the main stem, seed stalks, and flowers or seed, was collected from each of three plants from each of five areas of the trial. The samples were collected 12 h, and again 1, 2, 7, and 14 days after the first inoculation, and then 1, 2, 7, and 14 days after each subsequent inoculation. The 14-day samples were not collected after the last inoculation on 30 August because the seed crop was ready to be swathed.

At each sampling time, three table beet plants also were sampled from the nearest grower's table beet seed crop of the same proprietary cultivar, located ~ 400 m away, that had not been inoculated and had not tested positive for *P. syringae* pv. *aptata* in a 2021 survey of beet and chard seed crops for bacterial leaf spot (Chapter 1). These served as negative control samples. The severity of bacterial leaf spot was estimated for each sample based on the percentage of sampled foliage with symptoms, and the incidence of sampled leaves with symptoms was calculated as a percentage of the 72 leaves collected each time.

At each sampling in 2021, the collected tissue was assayed to estimate the epiphytic and endophytic populations of rif-Pap010, except for samples collected after the fourth (final) inoculation on 30 August, when only the total population was quantified since the samples consisted almost entirely of seeds and seed stalks. To estimate the epiphytic population size of *P. syringae* pv. *aptata,* each sample was rinsed in 300 ml of 0.0125M phosphate buffer on a rotary shaker (170 rpm, 15 minutes) at room temperature, and the rinsate used to quantify rif-Pap010 by dilution plating, as detailed below. To estimate the endophytic rif-Pap010 population, each sample was surface-sterilized in 200 ml of 0.6% NaOCl for 30 s after the rinse step described above, and then triple-rinsed in 50 ml of sterilized, deionized water. Each sample was then cut into ~20 mm^2 pieces using scissors sterilized with 70% ethyl alcohol between samples, and the cut tissue shaken in 300 ml of 0.0125M phosphate buffer at 170 rpm for 30 minutes at room temperature. A 100-µl aliquot of each of the epiphytic leaf rinses and each of the cut tissue rinses was used to generate four 10-fold dilutions in 0.0125 M sterilized phosphate buffer, and 0.1 ml aliquots of each dilution plated onto NA medium amended with rifampicin (82.3 µg ml^{-1}) and nystatin (66.6 µg ml^{-1}). Plates were incubated at 27^{o}C for 7 days, and colonies typical of rif-Pap010 counted to quantify CFU for each sample. The plant tissue was then dried at 56°C to

calculate CFU/g dry foliage (leaves, flowers and seed). The endophytic and epiphytic populations were added to calculate total population size of rif-Pap010/g dry tissue.

***2022 trial*.** In the 2022 trial, four plants were sampled from each of the four rows 1, 7, 14, and 21 days after each of the inoculations on 24 May, 7 June, 5 July, and 2 August. In addition, 200 table beet plants in the trial were rated for severity of bacterial leaf spot prior to each inoculation from 18 June to 27 July by estimating the area of the canopy of each plant with symptoms. In addition, the area of each of 96 leaves sampled randomly each time was rated for bacterial leaf spot symptoms prior to each inoculation, from 18 June to 16 August, to assess disease severity on a per leaf basis. Also, the incidence of 200 plants with bacterial leaf spot (percentage of plants with symptoms) was assessed as well as the incidence of the 96 sampled leaves with symptoms. The amount of rif-Pap010 on each leaf/seed stalk sample was then quantified by cutting the tissue into small (0.5-cm-long) pieces, rinsing each sample in 300 ml of 0.0125 M phosphate buffer on a gyratory shaker at 170 rpm for 30 minutes at room temperature, and plating a series of each rinsate onto NA medium, as described for the 2021 trial, except that cycloheximide was added (200 mg/liter) instead of nystatin to provide greater inhibition of fungal growth on nutrient agar medium. The total rif-Pap010 population size was calculated for each sample at each sampling time instead of assaying the endophytic and epiphytic population separately.

***2023 trial*.** The 2023 trial was sampled 7, 14, and 21 days after the first inoculation on May 1; and 7, 14, 21, and 28 days after the second inoculation on 11 July. No samples were taken after the third and fourth inoculations on 31 August and 9 September, respectively, because the seed crop was close to being swathed. These inoculations were done to increase the chances of generating a rif-Pap010 infected seed lot for calculating hot water and bleach seed treatments

for control of seedborne *P*. *syringae* pv. *aptata* (Chapter 3). Severity and incidence of bacterial leaf spot were rated on 27 June; 4, 19, and 26 July; and 1 and 15 August as described for the 2022 trial. The trial was rated only once after the second inoculation because canopy closure made it impossible to walk through the trial without damaging plants. The population size of rif-Pap010 was quantified for each sample as described for the 2022 trial.

Weeds in 2021 and 2022 trials. In the 2021 trial, foliage (leaves, flowers and seed) from lambsquarters (*Chenopodium album*) (1 plant from each of the 5 rows) were collected randomly from 13 July and 19 August, and likewise samples from pigweed (*Amaranthus retroflexus*) were collected from 18 to 19 August even though symptoms were not observed on these weeds. In the 2022 trial, lambsquarters, ladysthumb (*Persicaria maculosa*), and pigweed samples were collected from four replicate areas of the trial from 22 June through 31 August.

Swathing and harvest. In 2021, the plants were swathed manually onto Remay on 7 September, dried for two weeks, and then threshed manually. The harvested seed was cleaned and sized (20-mm diameter sieve) using a seed clipper (M-2B, A. T. Ferrel-Ross & Co., Saginaw, MI) and a draper. In 2022, the plants were swathed manually onto Remay on 19 September, dried for a week, and threshed using a plot thresher (LPT-MRB, Allan Machine Company, Lucas, IA). The harvested seed was cleaned and sized using an Eliminator 224 (Commodity Traders International, Trilla, IL) and cleaned further using a belt grader (Harashima Electric Industry Co. Ltd, Chome Sakura Prefecture, Japan). For the 2023 trial, swathing and threshing were completed on 13 September and 7 October, respectively, and the seed cleaned and sized as described for the 2022 trial.

For each trial, three replicate samples of 10,000 harvested seeds were tested to quantify rif-Pap010 colonization of the seed, following the seed wash assay described by Mohan and

Schaad (1987), with modifications. Briefly, each 10,000-seed subsample was soaked in 1,800 ml of 0.85% saline in 22.9 cm x 30.5 cm 6 Mil flat, sterile poly bags to which three drops of Tween 20 were added. The seeds were incubated in the bags at room temperature for 4 h with manual agitation every hour. Each bag of seed was then placed on a gyratory shaker operated at 150 rpm for 10 minutes. The seed rinsate was then decanted, diluted 10-fold four times, and three 100-µl aliquots of each dilution plated onto plates of NA medium amended with 100 µM rifampicin and 200 mg of cycloheximide/liter (rif-NA) (Weller and Saettler 1978). The remaining volume (600 µl) of each dilution was spiked with 10^5 CFU of rif-Pap010/ml and incubated for 30 minutes to assess whether rif-Pap010 could be detected if present in the seed wash (spiked positive control samples). In addition, 100 µl of rif-Pap010 was plated onto rif-NA medium directly as a standard for calibration to count rif-Pap010 colonies from the seed wash dilution plates. The plates were incubated at 27°C for 7 days and colonies were counted to calculate CFU rif-Pap010/g seed.

Weather conditions. Rainfall (mm), relative humidity (%), and minimum and maximum air temperature (°C) were obtained from the AgweatherNet (https://weather.wsu.edu/) station at the WSU Mount Vernon NWREC over the duration of each trial. Spearman's correlation coefficient (ρ) was calculated for the weather variables in relation to CFU rif-Pap010 recovered at each sampling time/g dry tissue, and incidence and severity of bacterial leaf spot at each rating, as well as CFU rif-Pap010/g seed harvested. Also, correlations of incidence and severity of bacterial leaf spot with CFU rif-Pap010/g dry tissue and CFU rif-Pap010/g seed were calculated. Correlations were calculated using R Statistical Software (Version 4.3.0).

Data analyses for colonization during vegetative growth. Analyses of variance (ANOVA) were calculated with block, host, strains, and sampling time after inoculation as the sources of variation for the vegetative colonization trials. Blocks (replications) were treated as a

random effect while host, strains, and time were fixed effects. ANOVA and means separation of log_{10}CFU/g tissue for GFP-Pap009 and GFP-Pap014 were calculated using Tukey's honestly significant difference (HSD) at (P <0.05) in (R version 4.3.0) for each trial.

Results

Pathogenicity and virulence of GFP-Pap009 and GFP-Pap014 vs. wild type.

Inoculation of table beet and Swiss chard seedlings with GFP-Pap009 caused an average bacterial leaf spot severity rating of 10.8 ± 1.1 and 14.7 ± 1.8%, respectively, whereas the wild-type strain of Pap009 caused an average severity rating of 21.7 ± 2.8 and 8.9 ± 2.8%, respectively. In addition, GFP-Pap014 caused an average severity rating on table beet of 1.2 ± 0.2% and no symptoms on Swiss chard seedlings, while the wild-type strain of Pap014 caused an average severity rating of 0.9 ± 0.1% on table beet and no symptoms on Swiss chard. Therefore, GFP-tagging of Pap009 and Pap014 did not appear to have a significant effect on pathogenicity or virulence of either strain on table beet or Swiss chard.

Colonization during vegetative growth. ***Trial 1*****.** In Trial 1, non-inoculated control plants of table beet and Swiss chard remained asymptomatic for the duration of the trial, and *P. syringae* pv. *aptata* was not recovered from these control plants. Therefore, the control plants were excluded from the ANOVA and means comparisons. Symptoms of bacterial leaf spot were not observed 24, 48, or 72 h after inoculation of table beet and Swiss chard seedlings with GFP-Pap009 and GFP-Pap014. However, *P. syringae* pv. *aptata* was recovered from leaf disks of both table beet and Swiss chard plants 24, 48, and 72 h after inoculation with each GFP strain of *P. syringae* pv. *aptata*. Based on the ANOVA, there was no significant main effect of host or inoculation, and no significant interaction of these two factors on the amount of *P. syringae* pv.

aptata recovered from non-sterilized and surface-sterilized leaf tissue (Table 2.1). However, the sampling time post-inoculation was significant at $P = 0.069$ for the population of *P. syringae* pv. *aptata* recovered from the surface-sterilized table beet and Swiss chard leaves, and less slightly significant ($P = 0.100$) for the non-surface-sterilized leaves. Also, there was a significant interaction between inoculation and sampling time post-inoculation for the amount of pathogen recovered from surface-sterilized leaves ($P = 0.041$), but this interaction was less significant for the non-surface sterilized leaves ($P = 0.115$). The two-way interaction between host and sampling time, and the three-way interaction of host-by-inoculation-by-time were not significant, regardless of whether the leaf tissue was surface-sterilized or not prior to sampling and quantification of *P. syringae* pv. *aptata* (Table 2.1).

Based on the significant interaction of inoculation treatment (GFP strain) with sampling time, the data were analyzed separately based on sampling time after inoculation (Table 2.2). The host plant inoculated (table beet vs. Swiss chard) did not affect the amount of *P. syringae* pv. *aptata* recovered from surface-sterilized and non-surface-sterilized leaves 24, 48, or 72 h after inoculation (Table 2.2). However, the strain of the pathogen (GFP-Pap009 vs. GFP-Pap014) had a significant effect on amount of *P. syringae* pv. *aptata* recovered from non-surface-sterilized leaves 48 and 72 h post-inoculation ($P = 0.018$ and 0.049, respectively), but only at 72 h post-inoculation for surface-sterilized leaves ($P = 0.020$) (Table 2.2). There was no significant interaction of host with inoculation on the amount of *P. syringae* pv. *aptata* recovered.

By 24 h after inoculation, the mean population size of *P. syringae* pv. *aptata* recovered from non-surface-sterilized leaves was similar for plants inoculated with GFP-Pap014 and GFP-Pap009 ($\log_{10}5.70 \pm 0.37$, and $\log_{10}5.85 \pm 0.06$ CFU/g tissue, respectively) (Table 2.3). However, 48 h after inoculation, significantly more *P. syringae* pv. *aptata* was recovered from

non-surface-sterilized leaves of plants inoculated with GFP-Pap009 vs. GFP-Pap014 (P = 0.018), with $\log_{10}$7.12 ± 0.025 vs. $\log_{10}$5.52 ± 0.32 CFU/g tissue, respectively. This difference persisted at 72 h after inoculation (P = 0.049) with $\log_{10}$6.92 ± 0.21 and $\log_{10}$5.72 ± 0.31 CFU/g tissue, respectively demonstrating greater population development of GFP-Pap009 than GFP-Pap014 on both beet and chard leaves. For surface-sterilized leaves, there were no significant differences in the amount of *P. syringae* pv. *aptata* recovered from plants 24 and 48 h after inoculation with the two strains (average of $\log_{10}$ 5.58 vs. $\log_{10}$ 5.33 for GFP-Pap014 vs. GFP-Pap009, respectively, at both sampling times), but by 72 h after inoculation, the amount of pathogen recovered from surface-sterilized leaves of table beet and Swiss chard seedlings was significantly greater (P = 0.020) for plants inoculated with GFP-Pap009 ($\log_{10}$6.85 ± 0.31 CFU/g tissue) than with GFP-Pap014 ($\log_{10}$5.47 ± 0.13 CFU/g tissue). Therefore, it took 24 h longer to detect differences in populations of GFP-Pap009 vs. GFP-Pap014 internally in leaves (surface-sterilized) vs. externally (non-surface-sterilized).

Trial 2. Similar to Trial 1 results, symptoms of bacterial leaf spot were not observed on the non-inoculated control plants of table beet and Swiss chard, and *P. syringae* pv. *aptata* was not recovered from these control plants. Therefore, the control plants were excluded from the ANOVA and means comparisons. Symptoms of bacterial leaf spot were first observed on table beet seedlings 48 h after inoculation with GFP-Pap009 at a low average severity of 1.2 ± 1.2%. By 72 h after inoculation, symptoms were observed on both table beet and Swiss chard seedlings inoculated with GFP-Pap009, at an average severity rating of 4.9 ± 3.2 and 3.1 ± 1.9%, respectively. Symptoms also were observed on table beet seedlings inoculated with GFP-Pap014 by 72 h post-inoculation, at an average severity 1.7 ± 0.9%, but not on Swiss chard seedlings inoculated with this strain. By 96 h after inoculation, severity of bacterial leaf spot was 13.2 ±

5.1% for table beet and 7.1 ± 2.0% for Swiss chard seedlings inoculated with GFP-Pap009, and 0.5 ± 0.3% on table beet seedlings vs. 0% on Swiss chard seedlings inoculated with GFP-Pap014.

Based on the ANOVA, there was no significant main effect of host (beet vs. chard) or inoculation (GFP-Pap009 vs -Pap014), and no significant interaction of these two factors on the population size of *P. syringae* pv. *aptata* recovered from non-surface-sterilized or surface-sterilized leaf disks (Table 2.1). However, the main effect of time of sampling (24, 48, 72, or 96 h post-inoculation) was significant for surface-sterilized leaves $P = 0.089$, and the interaction of inoculation (bacterial strain) with time of sampling was significant for both surface-sterilized leaves ($P = 0.005$), and non-surface-sterilized leaves ($P = 0.041$). The three-way interaction of host-by-inoculation-by-time was not significant, regardless of whether leaf disks were surface-sterilized or not prior to quantifying *P. syringae* pv. *aptata* colonization. Based on the significant two-way interaction of inoculation-by-time, the data were analyzed separately by time of sampling post-inoculation.

For the ANOVAs by sampling time, there was no significant main effect of host (Swiss chard vs. table beet) on the amount of *P. syringae* pv. *aptata* recovered from non-surface-sterilized or surface-sterilized leaf disks 24, 48, 72, or 96 h post-inoculation (Table 2.2). However, the bacterial strain had a significant main effect on the amount of pathogen recovered 48 and 96 h post-inoculation for non-surface-sterilized leaf disks; and at 48, 72, and 96 h post inoculation for surface-sterilized leaf disks (Table 2.2). There was no significant interaction of host plant and strain for any of the sampling times for non-surface-sterilized and surface-sterilized leaves. The amount of *P. syringae* pv. *aptata* recovered from the non-surface sterilized leaves averaged $\log_{10}5.45 \pm 0.2$ by 24 h post-inoculation for the two strains. By 48 h after

inoculation, recovery averaged $\log_{10}7.34 \pm 0.17$ and $\log_{10}5.46 \pm 0.26$ CFU/g tissue for plants inoculated with GFP-Pap009 and GFP-Pap014, respectively, i.e., there was almost 100-fold greater recovery of the former strain. This difference persisted to 96 h post-inoculation, when the mean population recovered from non-surface-sterilized leaf disks of plants inoculated with GFP-Pap009 and GFP-Pap014 averaged $\log_{10}7.77 \pm 0.11$ and $\log_{10}5.02 \pm 0.9$ CFU/g, respectively. For surface-sterilized leaves, the mean population of *P. syringae* pv. *aptata* recovered from plants inoculated with GFP-Pap009 and GFP-Pap014 was $\log_{10}4.8 \pm 0.4$ CFU/g tissue at 24 h post-inoculation, with no difference between the two strains. However, by 48 h post-inoculation, recovery of *P. syringae* pv. *aptata* averaged $\log_{10}6.98 \pm 0.43$ and $\log_{10}5.62 \pm 0.2$ CFU/g leaves for GFP-Pap009 and GFP-Pap014, respectively. By 72 h post-inoculation, the pathogen was recovered at $\log_{10}7.00 \pm 0.13$ and $\log_{10}4.27 \pm 0.21$ CFU/g leaves, respectively; and by 96 h, averaged $\log_{10}7.58 \pm 0.04$ and $\log_{10}4.87 \pm 1.04$ CFU/g leaves, respectively, from surface-sterilized leaves (Table 2.3).

Using confocal microscopy imaging 24 h after inoculation, the control plants of table beet and Swiss chard inoculated with water and Carborundum did not show a cyan GFP signal, while table beet and Swiss chard plants inoculated with GFP-Pap009 and GFP-Pap014 showed a very weak or no signal on the leaf disk abaxial epidermis surfaces and in the apoplast around the spongy mesophyll cells. By 48 h after inoculation, the GFP signal had increased visually on both the epidermis and in the apoplast of table beet and Swiss chard plants inoculated with each strain. GFP-tagged bacterial cells tended to be concentrated around the guard cells of stomata and along the walls of spongy mesophyll cells in the apoplast (Fig. 2.1C and 2.1D). For leaf samples collected 72 h after inoculation, there was further increase in the GFP signal observed

around guard cells of stomata and on epidermal cells (predominantly along the cell walls of adjacent epidermal cells), as well as in the apoplast around spongy mesophyll cells.

Colonization during reproductive plant growth. In the 2021, 2022, and 2023 beet seed crop field trials examining colonization and persistence of *P. syringae* pv. *aptata* in the reproductive growth stages, inoculation of plants with rif-Pap010 successfully resulted in development of bacterial leaf spot symptoms. However, the incidence and severity of symptoms differed among trials and over the duration of each trial. In all three years, plants were asymptomatic prior to the first inoculation. Bacterial leaf spot symptoms were first observed on 13 July 2021, 18 June 2022, and 27 June 2023, 7, 25, and 56 days after the first inoculation, respectively.

2021 trial. In the 2021 trial, following the first inoculation on 6 July, the incidence of bacterial leaf spot on leaves sampled 7 d later was 48.8 ± 8.9% and remained relatively stable over the trial duration (Fig. 2.2A), fluctuating between 62.2 ± 9.3% on 28 July and 46.7 ± 6.9% on 29 July. The incidence of symptomatic leaves increased slightly after each inoculation (Fig. 2.2A). The severity of bacterial leaf spot symptoms on individual leaf samples was only 1.3 ± 0.3% on July 13, a week after the first inoculation, but increased slightly to 4.9 ± 2.1% by 20 July (Fig. 2.2A). Severity of symptoms remained low over the duration of the trial, averaging fluctuating between 2.9 ± 0.6% on 29 July and 5.5 ± 2.3% on 3 August (Fig. 2.2A).

2022 trial. Following the first inoculation on 24 May in the 2022 trial, the incidence of plants with bacterial leaf spot increased rapidly to 57.7 ± 11.3% by 22 June, 4 weeks later (Fig. 2.2B), but then dropped to 41.5 ± 3.8% a week later. Following the second inoculation on 5 July, there was a sharp increase in disease incidence to 81.5 ± 9.7% of plants rated on 6 July, followed by a further increase to 99.0 ± 2.4% of plants on 13 July, and then a decrease to 79.0 ± 6.0% on

20 July (Fig. 2.2B). The severity of bacterial leaf spot symptoms followed a similar trend, starting at 2.8 ± 0.5% on 22 June, decreasing to 0.9 ± 0.1% on 29 June, and increasing to 5.0 ± 2.0% on 6 July following the second inoculation, with a further increase to 15.3 ± 2.4% by 13 July and a slight decrease to 11.0 ± 2.0% on 20 July (Fig. 2.2B). When incidence was rated on a leaf basis rather than plant basis, bacterial leaf spot symptoms averaged 17.8 ± 6.4% of leaves evaluated on 29 June and increased rapidly to 60.4 ± 9.8% by 6 July, 78.1 ± 1.5% by 13 July, and 87.5 ± 5.2% by 20 July (Fig. 2.2C). Thereafter, incidence of symptomatic leaves dropped gradually over the next month to 64.6 ± 2.0% by 16 August (Fig. 2.2C). The severity of bacterial leaf spot on these leaves averaged only 0.4 ± 0.1% on 29 June, following the first two inoculation, and then increased gradually over the next month to reach 10.8 ± 2.1% by 27 July. Similar to the incidence ratings, severity of bacterial leaf spot on leaves decreased steadily thereafter to 7.6 ± 1.9% on 3 August, then to 2.1 ± 0.6% by 10 August, with a slight increase to 4.5 ± 1.9% on 16 August following the final inoculation on 2 August (Fig. 2.2C).

2023 trial. In the 2023 trial, the incidence of bacterial leaf spot on individual leaves averaged 11.1 ± 7.2% on 27 June, 56 days after the first inoculation, and increased slightly thereafter to 17.5 ± 5.5% on 4 July, and to 20.8 ± 7.8% following the second inoculation on 19 July. Thereafter, the incidence decreased, fluctuating between, 5.0 ± 0.4% on 1 August and 12.5 ± 7.2% on 15 August (Fig. 2.2D). The severity of bacterial leaf spot remained very low throughout the trial fluctuating between 0.1 ± 0.1% on 27 June and 0.5 ± 0.3% on 15 August (Fig. 2.2D).

Recovery of rif-Pap010 during reproductive plant growth stages. ***2021 trial***. In the 2021 trial, rif-Pap010 was recovered at every sampling time, but the population size of CFU recovered fluctuated widely over the duration of the trial, from $\log_{10}3.5 \pm 0.3$ to $\log_{10}5.1 \pm 0.2$

CFU/g tissue (Fig. 2.3A). The population size of rif-Pap010 recovered after the first inoculation on 18 June ranged from $\log_{10}3.5 \pm 0.3$ to $\log_{10}4.0 \pm 0.5$ CFU/g tissue, from 19 June to 7 July when the average minimum and maximum air temperatures were 15.9 ± 1 and 34.8 ± 0.6℃, respectively, with 62 ± 1.5% RH and no rainfall (Fig. 2.3A and 2.3B**)**. Similar dry conditions persisted after the second inoculation on 6 July, with a wide fluctuation in populations of rif-Pap010. Following the third inoculation on 27 July and 21.3 mm of rainfall on 5 to 10 August, there was a thousand-fold increase in rif-Pap010 recovered, peaking at $\log_{10}4.6$ CFU/g tissue on 10 Aug. After the fourth inoculation on 17 August, recovery of rif-Pa010 peaked again at 4.6 CFU/g tissue on 24 August, but declined 100-fold within a week to 3.1 CFU/g. The average population size of rif-Pa010 recovered from seed harvested from the trial was $\log_{10}4.9 \pm 0.1$ CFU/g seed (Fig. 2.3A).

2021 was a relatively warm and dry season for Skagit Co. No rainfall occurred from prior the first inoculation until 4 August 2021, after which rainfall totaled 73.7 mm from 4 August to 22 September, when the seed crop was threshed (Fig. 2.3A). Minimum and maximum air temperatures fluctuated widely from 19 June to 3 August, averaging 11.6 ± 0.3 and 25.0 ± 0.5℃, respectively, while RH averaged 73.9 ± 0.8% (Fig. 2.3B**)**. The air temperature reached 35.7℃ on 28 June, and 2021 was the hottest summer season on record for western Washington (AgweatherNet). For the latter half of the season, from 4 August to 22 September, minimum and maximum air temperatures averaged 10.3 ± 0.4 and 22.1 ± 0.5℃, respectively, while RH averaged 78.4 ± 0.7% (Fig. 2.3B). The correlation of rif-Pap010 CFU/g tissue with daily RH over the duration of the field trial was not significant ($r = 0.28$, $P = 0.2772$), and likewise for the population size of pathogen recovered vs. minimum and maximum air temperatures ($r = -0.16$ at $P = 0.5306$ and $r = -0.15$, $P = 0.5595$, respectively) (Fig. 2.3B). Interestingly, the mean CFU

recovered was negatively correlated with both incidence and severity of bacterial leaf spot (r = -0.73, *P* = 0.1611 and r = -0.84, *P* = 0.0810, respectively) probably reflecting the very wide fluctuations in the population size of CFU rif-Pap010 recovered among individual samples and sampling times compared to the more consistent incidence and severity ratings over the duration of the trial.

2022 trial. In the 2022 field trial, conditions were wet and cool from 25 May to 15 June with a total rainfall of 4.0 mm, average RH of 81.1 ± 1.0%, and average minimum and maximum temperatures of 10.8 ± 0.2 and 18.1 ± 0.5°C, in contrast to the same period in the 2021 trial (Fig. 2.4A and 2.4B). However, the weather turned dry and warm after 14 June 2022, with total rainfall from 28 June to 3 July of only 8.6 mm (Fig. 2.4A and 2.4B). Rif-Pap010 was not recovered 24 h after the first inoculation on 24 May. However, 6 days later, rif-Pap010 was recovered at a low population of $\log_{10}$1.8 ± 0.5 CFU/g tissue. After the second inoculation on 7 June, the amount of rif-Pap010 increased rapidly from $\log_{10}$1.0 ± 0.4 CFU/g tissue 24 h after inoculation to $\log_{10}$ 4.1 ± 0.3 CFU rif-Pap010/g tissue 7 days post-inoculation, and then fluctuated between $\log_{10}$2.3 ± 0.4 CFU/g tissue 21 days after the second inoculation and a peak of $\log_{10}$5.2 ± 0.2 CFU/g tissue on 16 August, with increases in recovery after a rain event on 5 July and after inoculations on 5 July and 2 August. Conditions were dry from 6 July until swathing of the seed crop on 16 September, with only 3.1 ± 2.5 mm of rain 75.7 ± 0.5% RH, and an average maximum air temperature 24.0 ± 0.4°C. The amount of rif-Pap010 recovered from three samples of 10,000 table beet seed averaged $\log_{10}$2.5 ± 0.4 CFU/g seed.

As in the 2021 trial, the amount of rif-Pap010 recovered over the sampling times in the 2022 trial was not significantly correlated with daily RH (r = -0.17 at *P* = 0.5328) but was positively correlated with minimum air temperature (r = 0.43 at *P* = 0.1080) and maximum air

temperature (r = 0.55 at *P* = 0.0325) (Fig. 2.4B). In contrast to the 2021 trial, the mean CFU rif-Pap010 detected in the 2022 trial was positively correlated with the mean incidence and severity of bacterial leaf spot (r = 0.84 at *P* = 0.0089 and r = 0.65 at *P* = 0.0780, respectively).

2023 trial. The 2023 table beet seed crop trial characterized by alternating periods of rainfall and dry conditions (Fig. 2.5A). From 1 May to 15 June, rainfall totaled 28.2 mm, and minimum maximum temperatures, and RH averaged mean ± SE for min temperature 20.6 ± 0.7°C, and 72.3 ± 1.5%, respectively. Rif-Pap010 was recovered at $\log_{10}$2.7 ± 0.5 CFU/g tissue on 20 June, 48 days following the first inoculation on 1 May (Fig. 2.5A). Subsequently, there was a ~100-fold decrease in rif-Pap010 recovered on 27 June and 4 July. Eight days after the second inoculation on 11 July, the amount of rif-Pap010 recovered increased approximately 1000-fold to $\log_{10}$4.2 ± 0.5 CFU/g tissue, and then fluctuated between $\log_{10}$ 3.6 ± 0.6 and $\log_{10}$ 5 ± 0.5, followed by a decline to ~$\log_{10}$3.2 CFU/g dry tissue by22 August (Fig. 2.5A). The amount rif-Pap010 recovered from the harvested seed averaged $\log_{10}$3.5 ± 0.0 CFU/g seed.

Rainfall in the 2023 trial totaled 50.3 mm, while minimum and maximum air temperature and RH averaged 10.0 ± 0.2°C, 22.3 ± 0.3°C, and 74.5 ± 0.7%, respectively, over the trial duration. The amount of rif-Pap010 recovered was not significantly correlated with RH (r = -0.17, *P* = 0.6598), minimum air temperature (r = 0.42, *P* = 0.2652), maximum air temperature (r = 0.19 at *P* = 0.6186) or incidence and severity of bacterial leaf spot (r = -0.23 at *P* = 0.6598 and r = 0.32 at *P* = 0.5399, respectively) in the 2023 trial (Fig. 2.5B).

Colonization of weeds in the 2021 and 2022 trials. Symptoms of bacterial leaf spot were not observed on weeds growing in the 2021 and 2022 field trials. The population size of rif-Pap010 detected on lambsquarters in the 2021 trial from 13 July to 19 August averaged $\log_{10}$3.9 ± 0.4 CFU/g tissue, and averaged $\log_{10}$4.4 ± 0.8 CFU/g tissue for pigweed samples collected on 18 to

19 August, even though symptoms were not observed on these weeds. In the 2022 trial, the amount of rif-Pap010 recovered from lambsquarters weeds sampled varied widely across the weekly sampling periods from 22 June to 31 August (Fig. 2.6). The pathogen was not recovered from lambsquarters samples collected on 29 June, 20 July, and 16 August 2022, but was recovered at all seven other sampling times, and fluctuated from $\log_{10}0.5 \pm 0.5$ to $\log_{10} 4.0 \pm 0.5$ CFU/g tissue. Similarly, the amount of rif-Pap010 recovered from ladysthumb plants in the 2022 trial from 20 July to 31 August varied widely from 0 to $\log_{10}3.4 \pm 0.4$ CFU/g tissue, with the pathogen recovered at four of the seven sampling times (Fig. 2.6). In addition, rif-Pap010 was recovered from pigweed samples at each of six sampling times from 27 July to 31 August varied widely ranging from $\log_{10}0.6 \pm 0.6$ to $\log_{10}3.9 \pm 0.1$ CFU/g tissue (Fig. 2.6).

Discussion

One of the objectives of this was to address why some strains of *P. syringae* pv. *aptata*, such as Pap009, cause symptoms on table beet and Swiss chard, while other strains, such as Pap014, cause symptoms only on table beet. The hypothesis that Pap014 might only colonize the epidermis, and not the apoplast, of chard plants was proven incorrect, as both GFP-Pap009 and GFP-Pap014 from both the epidermis and the apoplast of Swiss chard and beet plants. However, although results from both trials showed no significant differences between GFP-Pap009 and GFP-Pap014 populations detected 24 h post-inoculation, GFP-Pap009 was recovered at significantly greater populations than GFP-Pap014 48 h after inoculation, from non-surface-sterilized leaf tissue in both trials, and from surface-sterilized leaf tissue in one of the two trials. By 72 h post-inoculation, the population of GFP-Pap009 was much greater than that of GFP-Pap014 (approximately 20-fold and 500-fold greater than GFP-Pap014 in Trials 1 and 2,

respectively). When sampling was extended to 96 h in Trial 2, the population of GFP-Pap009 strain remained ~500-fold greater than that of GFP-Pap014 for surface-sterilized leaves and comparable results were observed for the non-surface-sterilized leaves in both trials.

These findings suggest that Pap009 is able to develop to a greater population density on both table beet and Swiss chard leaves than Pap014 which may account for the lower virulence of Pap014 than Pap009 on beet, and the inability of Pap014 to cause symptoms on chard. Lindemann et al. (1984) showed that an epiphytic population of *P. syringae* pv. *syringae* exceeding $\log_{10}4$ cells per leaflet was required to cause symptoms of bacterial brown spot on snap beans (*Phaseolus vulgaris*). GFP-Pap009 was detected above this threshold by 72 h, post-inoculation, which might explain why this strain was able to cause bacterial leaf spot symptoms on table beet and Swiss chard, whereas Pap014 could only cause mild symptoms on table beet and no symptoms on Swiss chard. Further investigation is needed to understand the underlying host-pathogen interactions that drive these differences in colonization of beet and chard by these two strains, as has been documented for other strains of *P. syringae* pv. *aptata* (Nikolic et al. 2023; Safni et al 2016).

Nikolić et al. (2023) revealed that strains of *P. syringae* pv. *aptata* weakly virulent on sugar beet secrete Type III secretion system effectors (T3SSs) in larger quantities compared to moderately and highly virulent strains. These T3SSs included *AvrE1*, *AvrRpm1*, *HopI1*, *HopZ3*, *HopAZ1*, *HopAA1*, and *HopBA1*, as well as hairpins, which play a role in host effector-triggered immunity involved in the hypersensitivity response (Choi et al. 2013; La Flamme et al. 2020). Moreover, Nikolic et al. (2023) showed that moderately and highly virulent strains also tended to produce a variety of other T3SSs, such as *HopAU1*, *HopAW1*, *HopAH1*, and *AvrRpm1*, in relatively lower quantities than weakly virulent strains. In addition, even though weakly,

moderately, and highly virulent strains of *P. syringae* pv. *aptata* all secrete Type VI secretion system effectors (T6SSs) such as *Hcp1* and the *VgrG* tip protein, moderately and highly virulent strains secreted additional variants of *Hcp1* and secreted *VgrG* and *Rhs* in larger quantities (Nikolić et al. 2023). The differences in quantity of T3SSs and T6SSs secretomes among weakly and highly virulent strains likely also influences the host range of these strains (Nikolić et al. 2023). Future studies should examine if the differential pathogenicity on table beet and Swiss chard by Pap009 and Pap104 is associated with differences in the quantity and spectrum of T3SSs and T6SSs secretomes.

In this study, confocal microscopy was used to gain insights into the colonization patterns and early pathogenesis of GFP-Pap009 and GFP-Pap014 on table beet and Swiss chard plants. The prevalence of GFP-Pap009 and GFP-Pap014 cells around the guard cells of stomata on the epidermis, and along the walls of spongy mesophyll cells in the apoplast, indicates that stomata serve as a primary entry point for colonization of both beet and chard leaves by *P. syringae* pv. *aptata*. This is consistent with the behavior of many other bacterial and fungal foliar plant pathogens that exploit stomata and other natural openings to gain entry into plant tissues (Melotto et al. 2006). The GFP signal detected in the apoplast suggests this is a critical area for proliferation of *P. syringae* pv. *aptata* in beet and chard leaves. The apoplast provides a conducive environment for bacterial growth as it is rich in nutrients and relatively protected from plant cellular immune responses (Rico and Preston 2008).

The presence of *P. syringae* pv. *aptata* cells on the epidermis and the clustering along the junctions of adjacent epidermal cells and around guard cells of bacterial cells suggests the early stages of biofilm formation. Biofilms are crucial for bacterial survival and pathogenicity, providing protection against environmental stresses and the host immune responses (Costerton et

al. 1999). Biofilms also enhance bacterial resistance to antimicrobial agents, making them more challenging to eradicate (Danhorn and Fuqua 2007). Biofilm formation is known to be an important aspect of pathogenesis in *P. syringae*, facilitating persistent colonization and infection of host plants (Monier and Lindow 2004). Therefore, the early evidence of biofilm formation by GFP-Pap009 and GFP-Pap014 in this study indicated transitioning of the strains from initial colonization to more stable, persistent infections. Overall, this study revealed that strain Pap014 of *P. syringae* pv. *aptata*, which causes bacterial leaf spot on table beet but not Swiss chard, can colonize both the epidermis and apoplast of both hosts similar to Pap009, contrary to the original hypothesis.

This study also aimed to investigate colonization of table beet plants by *P. syringae* pv. *aptata* during reproductive growth stages to understand what influences the bacterial population and symptom development. In each of three field trials with a beet seed crop, inoculation with rif-Pap010 was successful as the pathogen was recovered from plants at every sampling period in each trial. However, the incidence and severity of bacterial leaf spot varied widely in each trial, which appeared to reflect the weather conditions each season. In the 2021 table beet seed crop trial, the incidence of bacterial leaf spot on individual leaves ranged from 48 to 62%, while severity of the disease on individual leaves remained very low throughout the season. This is likely because rif-Pap010 did not reach sufficient populations for severe symptom expression. The population reached $\log_{10}5$ CFU/g tissue only once in this trial, as was $\leq \log_{10} 3$ CFU/g tissue at 8 of the 17 sampling times. The unseasonably warm and dry conditions in the summer of 2021 were unfavorable for development of *P. syringae* pv. *aptata*. In the 2022 trial, the incidence and severity of bacterial leaf spot was greater than in 2021, due to the wet and cool conditions in May and June. In the 2023 trial, the beginning of the 2023 season was characterized by

occasional rains, followed by a dry period, which was associated with a lower incidence and severity of bacterial leaf spot compared to the 2021 and 2022 trial because conditions became dry and warm mid-season with occasional rains. These results suggest that bacterial leaf spot development is strongly influenced by environmental conditions, similar to what has been documented in other studies. For example, mild symptoms of bacterial leaf spot were observed in baby leaf Swiss chard trials established during a dry and warm spring compared to the trial completed in cool and wet conditions that same year in the autumn (Derie et al. 2016). Similarly, Crane et al. (2023) observed that development of symptoms of bacterial leaf spot in four Swiss chard baby leaf crop trials in western Washington was strongly influenced by rainfall events in spring 2021.

The population size of rif-Pap010 detected in the 2021, 2022 and 2023 table beet seed crop trials varied over the duration of each trial. In each trial, the rif-Pap010 population increased following each inoculation but declined if conditions were dry despite the use of sprinkler irrigation to try and create more favorable conditions for bacterial leaf spot. The amount of rif-Pap010 recovered from the harvested table beet seed varied among the trials. In 2021, 200-fold more seedborne rif-Pap010 was detected on the harvested seed ($\log_{10}5.9 \pm 0.1$ CFU/g seed) compared to the 2022 harvested table beet seed ($\log_{10}2.5 \pm 0.4$ CFU/g), probably because the latter half of August and September 2021 when the seed was maturing, was wet and cool compared to the dry conditions over this period in the 2022 trial. In the 2023 trial, a 100-fold increase in rif-Pap010 was detected at $\log_{10}3.5 \pm 0.0$ CFU/g seed, reflecting the fact that late August was characterized by warm days and cool nights that resulted in heavy dews, with rains in September that lead to a greater recovery of seedborne rif-Pap010 compared to seed harvested in the 2022 trial but less than in the 2021 trial.

Results of the table beet seed crop trials in 2021, 2022, and 2023 highlight the complex interactions interplay between *P. syringae* pv. *aptata* and environmental conditions, as shown in previous studies. For example, the availability of nutrients such as amino acids, carbohydrates, and organic acids on leaf surfaces and abundant in pollen have been shown to influence epiphytic bacterial populations (Morris and Rouse 1985; Wilson and Lindow 1994a; 1994b). Mercier and Lindow (2000) demonstrated a relationship between *P. fluorescens* populations and the amount of sugars washed from individual leaves of greenhouse-grown snap beans. Other studies have demonstrated the significant role of environmental conditions in *P. syringae* population dynamics. Hirano and Upper (1991) confirmed that *P. syringae* populations tend to increase under prolonged moist conditions and high relative humidity, coupled with relatively cool temperatures. Rain also promotes bacterial growth on plant surfaces, although intense rains can reduce bacterial populations (Hirano et al. 1996). Under hot and dry conditions, *P. syringae* tend to decline substantially (Hirano and Upper 1991). The 2021 table beet seed crop trial exemplified this, as the rif-Pap010 population remained low over most of the duration despite frequent inoculations, i.e., the prevailing warm and dry conditions through mid-August did not favor development of rif-Pap010.

The lack of a significant correlation between CFU of rif-Pap010 recovered from leaf samples in the 2021and 2023 trials with daily RH, and minimum and maximum air temperatures over each trial duration indicates that other factors could have had more significant effects on rif-Pap010 development. The correlations of mean CFU of rif-Pap010/g tissue with the incidence and severity of bacterial leaf spot were negative in the 2021 trial, positive in the 2022 trial, and insignificant in the 2023 trial, reflecting the major influence of field conditions on both the pathogen and symptom expression. In 2021, symptoms remained relatively consistent over the

duration of the trial, but rif-Pap010 populations fluctuated widely. In 2022, symptoms were more prevalent than in 2021, and followed more closely the increase in rif-Pap010 population size. Symptoms were much less prevalent and very mild in 2023, which explains the lack of significant correlation with rif-Pap010 recovery. These observations highlight the complexity of the plant-pathogen interactions and the influence of environmental factors on pathogen and disease development. Also, the positive correlation between rif-Pap010 population and air temperature in the 2022 trial underscored the potential influence of temperature on *P. syringae* pv. *aptata* development on beet and chard.

In 2021 and 2022 field trials, detection of rif-Pap010 populations on the most prevalent weed species, indicated that lambsquarters, pigweed, and ladysthumb plants can serve as asymptomatic hosts of *P. syringae* pv. *aptata*. In the 2022 trial, the pathogen was detected at the highest density (~$\log_{10}$4 CFU/g tissue) and most frequently on lambsquarters, although the pathogen also reached this population once on pigweed and ladysthumb samples in August. The wide fluctuation in rif-Pap010 populations recovered across sampling periods on these three weed species suggests that the pathogen may not persist very long on these species or attain large enough populations to trigger symptom development, as foliar symptoms were never observed on any of the weed samples assayed.

Detection of rif-Pap010 on lambsquarters, pigweed, and ladysthumb highlights the potential role of weeds as asymptomatic reservoirs for inoculum of *P. syringae* pv. *aptata*. Therefore, weed control in table beet and Swiss chard seed crops may be important to minimize this risk. Other studies have highlighted the role of weeds in sustaining bacterial pathogen populations. Cafati and Saettler (1980) recovered *Xanthomonas campestris* pv. *phaseoli* from

inoculated plants, and even though the bacterial population declined three days after inoculation, colonies were still recovered 18 days post-inoculation.

In conclusion, this study demonstrated that strain Pap009 of *P. syringae* pv. *aptata*, which causes bacterial leaf spot symptoms on table beet and Swiss chard, was able to attain larger populations on beet and chard leaves as compared to Pap014, a strain that causes bacterial leaf spot symptoms only on table beet. However, both strains colonized the epidermis and the apoplast of beet and Swiss chard plants, so research is needed to understand the mechanisms that drive these differences in virulence and host range of the two strains. During the reproductive growth stage of beet seed crops, the population of *P. syringae* pv. *aptata* and bacterial leaf spot development was influenced significantly by environmental conditions. Table beet and Swiss chard seed growers should start with clean seed transplants to reduce the chances of introducing the pathogen into their seed crops, and maintain weed-free seed crops, as best as possible as this study demonstrated weeds can harbor *P. syringae* pv. *aptata* despite remaining asymptomatic. Seed growers in western Washington typically irrigate only 3 to 4 times a season. Therefore, there is limited capacity for growers to modify practices to manage bacterial leaf spot. One cultural management practice growers could consider is planting seed crops with rows in the predominant wind direction to facilitate air movement for drying the crop canopy after rains and irrigations, since table beet and Swiss chard seed crops usually develop very dense canopies. In warm and dry summers, symptoms may not be observed in beet or chard seed crops even if the crop is infected with *P. syringae* pv. *aptata*. However, if conditions became wet in late summer or fall when the seed is maturing, this increases the chances of infection of the developing seed. Practices that speed drying of the seed could help mitigate this. However, growers cannot swath and harvest seed crops too early, as this can adversely affect seed yield and quality, resulting in

reduction in seed to low germination for seeds that may not matured. In addition, postharvest seed treatments may be needed to eradicate the pathogen if harvested seed lots are infected. Storing seed for 12 to 24 months has been shown to reduce levels of *P. syringae* pv. *aptata*, particularly in seed lots with $<10^4$ CFU/g (Crane, 2023). This could be a viable option for seed companies, particularly for seed lots with high levels of *P. syringae* pv. *aptata*, provided there is prior knowledge of the local environmental conditions where the seed will be planted.

Crane (2023) also demonstrated that bactericides, including biological treatments such as Serenade Opti, Double Nickel, Regalia, Serenade ASO, and Lifegard, as well as copper products like ManKocide, Badge, Cueva, and Nordox, and the disinfectant KleenGrow, have limited efficacy in managing bacterial leaf spot. Therefore, these products are not a viable option in management of bacterial leaf spot in table beet and Swiss chard seed crops. Additionally, use of moderately resistant cultivars may help to minimize symptoms of bacterial leaf spot as Gaulke and Goldman 2022 demonstrated that table beet cv. Touchstone Gold and Swiss chard cv. Rainbow were the most resistant to bacterial leaf spot under greenhouse conditions. Similarly, Pratibha et al. (2024) illustrated that table beet cultivars Bohan and Bresko have low to moderate resistance to bacterial leaf spot, respectively, but were also susceptible to other foliar fungal diseases such as Cercospora leaf spot and Phoma leaf spot under New York climatic conditions. This underscores the need to screen table beet and Swiss chard cultivars in diverse environments to identify those resistant to foliar pathogens. Such cultivars can be used to produce seed for planting fresh and processing market crops, where healthy foliage and roots are essential.

Acknowledgements

We acknowledge the programs of Drs. Jonathan Jacobs and Carolee Bull for generating GFP-tagged and rifampicin resistant strains of *P. syringae* pv. *aptata* for use in this study. Thanks to the Vegetable Seed Pathology Program at the WSU Mount Vernon NWREC including Michael Derie, Babette Gundersen, Tomasita Villaroel, Alex Batson and Kayla Spawton for helping with the experiments. This work was funded by the United States Department of Agriculture (USDA) National Institute of Food and Agriculture NIFA Specialty Crops Research Initiative (SCRI) Project No. 2019-51181-30019, the Dick and Marcia Morrison Seed Production Pathology & Seed Health Fellowship, the Alfred Mark Christianson Memorial Fellowship, a Pacific Seed Association Scholarship, and the Raymond J. Tarleton Student Fellowship from the American Phytopathological Society.

Literature Cited

Abo-Elwafa, S. F. Abdel-Rahim, H. M., Abou-Salama, A. M., and Teama, E. A. 2006. Sugar beet floral induction and fertility. Effect of vernalization and day-length extension. Sugar Tech. 8:281-287.

AgWeatherNet. 2024. Washington State University. https://weather.wsu.edu/. Accessed 2 Feb. 2024.

Arabi, F., Nikravesh, Z., Babaeizad, V., Rezaeian, V., and Rahimian, H. 2006. Occurrence of bacterial leaf spot and blight of garden beet caused by *Pseudomonas syringae* pv. *aptata* in Iran. Iran. J. Plant Pathol. 42:655-671.

Arabiat, S., Chanda, A. K., Chittem, K., and Khan. M. F. R. 2016. First report of *Pseudomonas syringae* pv. *aptata* causing bacterial blight of sugar beet (*Beta vulgaris*) in Oregon. Plant Dis. 100:2334.

Bradbury, J. F. 1986. Guide to the Plant Pathogenic Bacteria. CAB International, Wallingford.

Brown, N. A., and Jamieson, C. O. 1913. A bacterium causing a disease of sugar beet and nasturtium leaves. J. Agric. Res. 1:189-210.

Cafati, C. R., and Saettler, A. W**.** 1980. Role of nonhost species as alternate inoculum sources of *Xanthomonas phaseoli*. Plant Dis. 64:194-196.

Cerutti, A., Jauneau, A., Auriac, M. C., Lauber, E., Martinez, Y., Chiarenza, S., Leonhardt, N., Berthomé, R., and Noël, L. D. 2017. Immunity at cauliflower hydathodes controls systemic infection by *Xanthomonas campestris* pv. *campestris*. Plant Physiol. 174:700-716.

Chancia, R., van Aardt, J., Pethybridge, S., Cross D., and Henderson, J. 2021. Predicting table beet root yield with multispectral UAS imagery. *Remote Sens.* 13:2180.

Choi, M. S., Kim, W., Lee, C., and Oh, C. S. 2013. Harpins, multifunctional proteins secreted by Gram-negative plant-pathogenic bacteria. Mol. Plant-Microbe Interact. 26:1115-1122.

Costerton, J. W., Stewart, P. S., and Greenberg, E. P. 1999. Bacterial biofilms: a common cause of persistent infections. Science 284:1318-1322.

Crane, A. S. 2023. Seed transmission of *Pseudomonas syringae* pv. *aptata*, and efficacy of bactericides for control of the pathogen in beet and Swiss chard seed production. MS thesis, Washington State University, Pullman. 63 pp.

Crosse, J. E. 1959. Bacterial canker of stone-fruits. Investigation of a method for measuring the inoculum potential of cherry trees. Ann. Appl. Biol. 47:306-317.

Cuppels, D. A., and Elmhirst, J. 1999. Disease development and changes in the natural *Pseudomonas syringae* pv. *tomato* populations on field tomato plants. Plant Dis. 83:759-764.

Danhorn, T., and Fuqua, C. 2007. Biofilm formation by plant-associated bacteria. Annu. Rev. Microbiol. 61:401-422.

Derie, M. L., Holmes, B. J., Safni, I., Bull, C. T., and du Toit, L. J. 2016. Seedborne inoculum thresholds of *Pseudomonas syringae* pv. *aptata*, causal agent of bacterial leaf spot, in 'baby leaf' Swiss chard crops. Phytopathology 106:S4.142 (Abstr.).

Donati, I., Cellini, A., Sangiorgio, D., Vanneste, J. L., Scortichini, M., Balestra, G. M., and Spinelli, F. 2020. *Pseudomonas syringae* pv. *actinidiae*: Ecology, infection dynamics and disease epidemiology. Microb. Ecol. 80:81-102.

du Toit, L. J. 2007. Crop Profile for Table Beet Seed in Washington. USDA Pest Management Centers. http://www.ipmcenters.org/CropProfiles/docs/WAbeetseed.pdf. Accessed 12 Mar. 2024.

du Toit, L. J., Crowe, F. J., Derie M. L., Simmons R. B., Pelter, G. Q. 2005. Bacterial blight in carrot seed crops in the Pacific Northwest. Plant Dis. 89:896-907.

Gaulke, E., and Goldman, I. L. 2022. Screening table beet and Swiss chard for resistance to *Pseudomonas syringae* pathovar *aptata*. HortScience 57:1436-1446.

Gowda, S. S., and Goodman, R. N. 1970. Movement and persistence of *Erwinia amylovora* in shoot, stem, and root of apple. Plant Dis. 54:576-580.

Harveson, R. M., Hanson, L. E., and Hein, G. L., Editors. 2009. Compendium of Beet Diseases and Pests, Second Edition. The American Phytopathological Society, St. Paul.

Hill, C. F. 1979. New plant disease records in New Zealand, N. Z. J. Agric. Res. 22:641-645.

Hirano S. S., and Upper, C. D. 2000. Bacteria in the leaf ecosystem with emphasis on *Pseudomonas syringae* - a pathogen, ice nucleus, and epiphyte. Microbiol. Mol. Biol. Rev. 64:624-653.

Hirano, S. S., Baker, L. S., and Upper. C. D. 1996. Raindrop momentum triggers growth of leaf-associated populations of *Pseudomonas syringae* on field-grown snap bean plants. Appl. Environ. Microbiol. 62:2560-2566.

Hirano, S.S., and Upper, C. D. 1991. Bacterial community dynamics. Pp. 271-294, In: Microbial Ecology of Leaves. J. H. Andrews and S.S. Hirano, editors. Springer-Verlag, New York.

Jacobsen, B. J. 2009. Bacterial leaf spot. Pp. 59-60. In: Compendium of Beet Diseases and Pests, Second Edition. R. M. Harveson, L. E. Hanson, and G. L. Hein, editors. The American Phytopathological Society, St. Paul.

Janse, J. D. 1979. A leaf spot disease of sugar beet caused by *Pseudomonas syringae*. Gewasbescherming 10:121-125.

Kado, C. I., and Heskett, M. G.1970. Selective medium for isolation of *Agrobacterium*, *Corynebacterium*, *Erwinia*, *Pseudomonas*, and *Xanthomonas*. Phytopathology 60:969-976.

King, E. O., Ward, M. K. and Raney, D. E. 1954. Two simple media for the demonstration of pyocyanin and fluorescin. J. Lab. Clin. Med. 44:301-307.

Kockelmann, A., Tilcher, R., and Fischer, U. 2010. Seed production and processing. Sugar Tech. 12:267-275.

Koike, S. T., Henderson, D. M., Bull, C. T., Goldman, P. H., and Lewellen, R. T. 2003. First report of bacterial leaf spot of Swiss chard caused by *Pseudomonas syringae* pv. *aptata* in California. Plant Dis. 87:1397.

Kubheka, G. C., Coutinho, T. A., Moleleki, N., and Moleleki, L. N. 2013. Colonization patterns of an mCherry-tagged *Pectobacterium carotovorum* subsp. *brasiliense* strain in potato plants. Phytopathology 103:1268-1279.

Laflamme, B., Dillon, M. M., Martel, A., Almeida, R. N. D., Desveaux, D., and Guttman, D. S. 2020. The pan-genome effector-triggered immunity landscape of a host-pathogen interaction. Science 367:763-768.

Lewis, S. M., and Goodman R. N. 1965. Mode of penetration and movement of fire blight bacteria in apple leaf and stem tissue. Phytopathology 55:719-723.

Lin, B.-H., Jayachandran, N. V., Jane, A., and John, C. 2003. Food and Agricultural Commodity Consumption in the United States: Looking Ahead to 2020. United States Department of Agriculture Economic Research Service AER-820. https://www.ers.usda.gov/webdocs/publications/42576/19268_aib792-7_1_.pdf?v=0 Accessed 1 Apr. 2024.

Lindemann, J., Arny, D. C., and Upper, C. D. 1984. Use of an apparent infection threshold population of *Pseudomonas syringae* to predict incidence and severity of brown spot of bean. Phytopathology 74:1334-1339.

Mac Faddin, J. F. 1985. Media for Isolation-Cultivation-Identification-Maintenance of Medical Bacteria. Baltimore, MD: Williams & Wilkins.

Melotto, M., Underwood, W., Koczan, J., Nomura, K., and He, S. Y. 2006. Plant stomata function in innate immunity against bacterial invasion. Cell 126:969-980.

Mercier, J., and Lindow, S. E. 2000. Role of leaf surface sugars in colonization of plants by bacterial epiphytes. Appl. Environ. Microbiol. 66:369-374.

Mohan, S. K., and Schaad, N. W. 1987. An improved agar plating assay for detecting *Pseudomonas syringae* pv. *syringae* and *Pseudomonas syringae* pv. *phaseolicola* in contaminated bean seed. Phytopathology 77:1390-1395.

Monier, J. M., and Lindow, S. E. 2004. Frequency, size, and localization of bacterial aggregates on bean leaf surfaces. Appl. Environ. Microbiol. 70:346-355.

Morris, C. E., and Rouse. D. I. 1985. Role of nutrients in regulating epiphytic bacterial populations. Pp. 63-82, In: Biological Control on the Phylloplane. C. E. Windels and S. E. Lindow, editors. American Phytopathological Society, St. Paul.

Morris, C. E., Sands, D. C., Vinatzer, B. A., Glaux, C., Guilbaud, C., Buffie`re, A., Yan, S., Dominguez, H., and Thompson, B. M. 2008. The life history of the plant pathogen *Pseudomonas syringae* is linked to the water cycle. ISME J. 2:321-334.

Morris, C., Glaux, C., Latour, X., Gardan, L., Samson, R., and Pitrat, M. 2000. The relationship of host range, physiology, and genotype to virulence on cantaloupe in *Pseudomonas syringae* from cantaloupe blight epidemics in France. Phytopathology 90:636-646.

Mutasa-Göttgens, E. S., Qi, A., Zhang, W., Schulze-Buxloh, G., Jennings, A., Hohmann, U., Müller, A. E., and Hedden, P. 2010. Bolting and flowering control in sugar beet: Relationships and effects of gibberellin, the bolting gene B and vernalization. AoB Plant. 2010: plq012

Nampijja, M., Derie, M. L., and du Toit, L. J. 2021. First report of bacterial leaf spot caused by *Pseudomonas syringae* pv. *aptata* on Swiss chard, *Beta vulgaris* subsp. *vulgaris*, in Arizona. Plant Dis. 105:3738.

Navazio, J., Colley, M., and Zyskowski, J. 2010. Principles and Practices of Organic Beet Seed Production in the Pacific Northwest. Organic Seed Alliance, Port Townsend.

Nikolić, I., Glatter, T., Ranković, T., Berić, T., Stanković, S., and Diepold, A. 2023. Repertoire and abundance of secreted virulence factors shape the pathogenic capacity of *Pseudomonas syringae* pv. *aptata*. Front. Microbiol. 14:1205257.

Nikolić, I., Stanković, S., Dimkić, I., Berić, T., Stojšin, V., Janse, J., and Popović, T. 2018. Genetic diversity and pathogenicity of *Pseudomonas syringae* pv. *aptata* isolated from sugar beet. Plant Pathol. 67:1194-1207.

Nottingham, S. 2004. Beetroot. Crimson Publishing, Bristol. Archived from the original (e-book) on 9 Feb. 2012.

Organic Seed Alliance. 2016. Climatic Considerations for Seed Crops: Guidelines and Field Trainings for Organic and Specialty Vegetable Seed Producers. https://seedalliance.org/. Accessed 21 Jan. 2022.

Pethybridge, S. J., Murphy, S., Branch, E., Sharma, P., and Kikkert, J. R. 2024. Manipulating table beet growth using exogeneous gibberellic acid 3 in New York, USA. Appl. Biol. Res. 184:196-209.

Pratibha, S., Murphy, S., Kikkert, J., and Pethybridge, S. 2024. Susceptibility of table beet cultivars to foliar diseases in New York. Plant Health Prog. *In Press*

Rackham, L. R. 2002. History of Specialty Seed Crop Production in the Pacific Northwest. Willamette Valley Specialty Seed Crops Association, Corvallis.

Ranković, T., Nikolić, I., Berić, T., Popović, T., Lozo, J., Medić, O., and Stanković, S. 2023. Genome analysis of two *Pseudomonas syringae* pv. *aptata* strains with different virulence capacity isolated from sugar beet: Features of successful pathogenicity in the phyllosphere microbiome. Microbiol. Spectr. 11:e0359822.

Rico, A., and Preston, G. M. 2008. *Pseudomonas syringae* pv. *tomato* DC3000 uses constitutive and apoplast-induced nutrient assimilation pathways to catabolize nutrients that are abundant in the tomato apoplast. Mol. Plant-Microbe Inter. 21:269-282.

Riffaud, C. M. H., and Morris, C. E. 2002. Detection of *Pseudomonas syringae* pv. *aptata* in irrigation water retention basins by immuno-fluorescence colony staining. Eur. J. Plant Pathol. 108:539-545.

Safni, I., Ramos-Sepulveda, L., Goldman, P., Derie, M., du Toit, L., Koike, S., Stockwell, V., and Bull, C. 2016. Genetic diversity of *Pseudomonas syringae* causing bacterial leaf spot on table beet (*Beta vulgaris*) and Swiss chard (*Beta vulgaris* subsp. *cicla*). Phytopathology 106:S4.143 (Abstr.).

Schaad, N. W., Jones, J. B., and Chun, W. 2001. Laboratory Guide for Identification of Plant Pathogenic Bacteria. 3rd ed. American Phytopathological Society, St. Paul, MN.

Schrader, L. W., and Mayberry S. K. 2003. Beet and Swiss chard production in California. Univ. of California Agric. Nat. Res. No. 8096. https://doi.org/10.3733/ucanr.8096. Accessed 16 Feb. 2024.

Schreiber, A., and Ritchie, L. 1995. Washington Minor Crops. Food and Environmental Quality Laboratory, Washington State University, Richland.

Sedighian, N., Shams-Bakhsh, M., Osdaghi, E., and Khodaygan, P. 2014. Etiology and host range of bacterial leaf blight and necrosis of squash and muskmelon in Iran. Plant Pathol. 96:507-514.

Stojšin, V., Balaž, J., Budakov, D., Stanković, S., Nikolić, I., Ivanović, Ž., and Popović, T. 2015. First report of *Pseudomonas syringae* pv. *aptata* causing bacterial leaf spot on sugar beet in Serbia. Plant Dis. 99:281.

Tymon, L. S., and Inglis, D. A. 2017. Identification and pathogenicity of *Pseudomonas syringae* genomospecies 1 phylogroup 2b causing leaf spots and fruit warts on cucurbits in western Washington U.S. Plant Pathol. 99:713-722.

Walker, J. C. 1952. Diseases and pests, Plant diseases. Pp. 190-191. In: Diseases of Vegetable Crops. McGraw-Hill Book Co., Inc., New York City.

Walter, T., Shattuck, D. W., Baldock, R., Bastin, M. E., Carpenter, A. E., Duce S., Ellenberg, J, Fraser, A., Hamilton, N., Pieper, S., Ragan, M. A., Schneider, J. E., Tomancak, P., Hériché, J. K. 2010. Visualization of image data from cells to organisms. Nat. Methods 7:S26-S41.

Wang, K., Kang, L., Anand, A., Lazarovits, G., and Mysore, K. S. 2007. Monitoring in planta bacterial infection at both cellular and whole-plant levels using the green fluorescent protein variant GFPuv. New Phytol. 174:212-223.

Weller, D. M., and Saettler, A.W. 1978. Rifampin-resistant *Xanthomonas phaseoli* var. *fuscans* and *Xanthomonas phaseoli*: Tools for field study of bean blight bacteria. Phytopathology 68:778-781.

Wilson, M., and Lindow, S. E. 1994a. Ecological similarity and coexistence of epiphytic ice-nucleation (Ice1) *Pseudomonas syringae* strains and a non-ice nucleating (Ice2) biological control agent. Appl. Environ. Microbiol. 60:3128-3137.

Wilson, M., and Lindow, S. E. 1994b. Coexistence among epiphytic bacterial populations mediated through nutritional resource partitioning. Appl. Environ. Microbiol. 60:4468-4477.

Table 2.1. Analysis of variance (ANOVA) for the amount of *Pseudomonas syringae* pv. *aptata* tagged with a green fluorescent protein (GFP) recovered 24, 48, 72, and 96 h after inoculation of 4-week-old table beet and Swiss chard seedlings in two greenhouse trials to evaluate why strain Pap009 causes bacterial leaf spot on table beet and Swiss chard whereas strain Pap014 only causes bacterial leaf spot on table beet

	Trial 1[a]		**Trial 2**[a]	
Factor	**Non-surface-sterilized leaves**	**Surface-sterilized leaves**	**Non-surface-sterilized leaves**	**Surface-sterilized leaves**
Host[b]	0.358	0.925	0.826	0.742
Inoculation[c]	0.980	0.251	0.976	0.173
Host*Inoculation	0.396	0.193	0.238	0.172
Time[d]	0.100	**0.069**	0.141	**0.089**
Host*Time	0.195	0.569	0.799	0.985
Inoculation*Time	0.115	**0.041**	**0.041**	**0.005**
Host*Inoculation*Time	0.354	0.276	0.211	0.118

[a] Each trial included a randomized complete block design with two (Trial 1) or three (Trial 2) replications. The ANOVA was calculated for the population of GFP-Pap009 and GFP-Pap014 recovered (CFU/g leaf tissue) from leaf disks sampled from 6 (Trial 1) and 12 (Trial 2) leaves of table beet and Swiss chard seedlings per replication per treatment. Bold font indicates statistical significance at $P \leq 0.10$.

[b] Swiss chard seedlings of the cv. Silverado and table beet seedlings of the cv. Red Ace.

[c] Inoculation treatments included: 1) GFP-Pap009, 2) GFP-Pap014, and 3) non-inoculated control plants. However, control plants were excluded from the ANOVA as the pathogen was not recovered from those plants.

[d] Plants were sampled 24, 48, and 72 h after inoculation in Trial 1; and 24, 48, 72, and 96 h after inoculation in Trial 2.

Table 2.2. Analysis of variance (ANOVA) for the amount of green fluorescent protein (GFP)-tagged *Pseudomonas syringae* pv. *aptata* recovered 24, 48, 72, and 96 h after inoculation of table beet and Swiss chard seedlings in two trials in a greenhouse to evaluate the differential pathogenicity of strain Pap009, which causes bacterial leaf spot on table beet and Swiss chard, vs. strain Pap014, which only causes bacterial leaf spot on table beet

	Trial 1[a]						**Trial 2**[a]							
	Non-surface-sterilized leaves			**Surface-sterilized leaves**			**Non-surface-sterilized leaves**				**Surface-sterilized leaves**			
Factor	**24 h**	**48 h**	**72 h**	**24 h**	**48 h**	**72 h**	**24 h**	**48 h**	**72 h**	**96 h**	**24 h**	**48 h**	**72 h**	**96 h**
Host[b]	0.618	0.393	0.240	0.930	0.277	0.215	0.483	0.393	0.442	0.427	0.441	0.620	0.943	0.436
Inoculation[c]	0.800	**0.018**	**0.049**	0.667	0.101	**0.020**	0.449	**<0.001**	**0.082**	**0.030**	0.447	**0.021**	**0.042**	**0.027**
Host*Inoculation	0.424	0.341	0.807	0.338	0.414	0.512	0.258	0.865	0.563	0.325	0.296	0.198	0.766	0.244

[a] Each trial included a randomized complete block design with two (Trial 1) or three (Trial 2) replications. Analyses were split by sampling time because of a significant interaction between inoculation and time (**Table 1**). Each ANOVA was calculated for the population of GFP-Pap009 and GFP-Pap014 recovered (CFU/g leaf tissue) from leaf disks sampled from 6 (Trial 1) and 12 (Trial 2) leaves from table beet and Swiss chard plants for each treatment in Trials 1 and 2, respectively. Bold font indicates statistical significance at $P \leq 0.10$.

[b] Swiss chard seedlings of the cv. Silverado and table beet seedlings of the cv. Red Ace.

[c] Inoculations treatments included: 1) GFP-Pap009, 2) GFP-Pap014, and 3) non-inoculated control plants. However, control plants were excluded from the ANOVA as the pathogen was not recovered from those plants.

Table 2.3. Mean amount of green fluorescent protein (GFP) tagged *Pseudomonas syringae* pv. *aptata* (log_{10} CFU/g tissue) recovered 24, 48, 72, and 96 h after inoculation of table beet and Swiss chard seedlings in two trials in a greenhouse to evaluate why strain Pap009 causes bacterial leaf spot on table beet and Swiss chard whereas Pap014 only causes bacterial leaf spot on table beet

Sampling time after inoculation[b]	Trial 1[a]						Trial 2[a]							
	Non-surface-sterilized leaves			Surface-sterilized leaves			Non-surface-sterilized leaves				Surface-sterilized leaves			
	24 h	48 h	72 h	24 h	48 h	72 h	24 h	48 h	72 h	96 h	24 h	48 h	72 h	96 h
GFP-Pap009	5.85 a	7.12 a	6.92 a	5.33 a	5.33 a	6.85 a	5.65 a	7.34 a	7.29 a	7.77 a	5.26 a	6.98 a	7.00 a	7.58 a
GFP-Pap014	5.70 a	5.35 b	5.72 b	5.58 a	5.58 a	5.47 b	5.25 a	5.46 b	5.06 b	5.02 b	4.38 a	5.62 b	4.27 b	4.87 b
Control[c]	0	0	0	0	0	0	0	0	0	0	0	0	0	0

[a] Each trial included a randomized complete block design with two (Trial 1) or three (Trial 2) replications. Table beet and Swiss chard leaves were rub-inoculated with a suspension of GFP-Pap009 and GFP-Pap014. Colonization of each strain was quantified by dilution plating a leaf maceration onto nutrient agar medium amended with 50 µg kanamycin/ml, and calculating CFU/g fresh weight. Means were separated using Fisher's protected least significant difference (LSD) at $P<0.10$. In each column, means with the same letters are not statistically significant.

[b] Plants were sampled 24, 48, and 72 h after inoculation in Trial 1; and 24, 48, 72, and 96 h after inoculation in Trial 2.

[c] The control plants consisted of table beet and Swiss chard rub-inoculated with phosphate buffer and Carborundum. Control plants were excluded from the analysis of variance and means separation because the pathogens was not recovered from these plants.

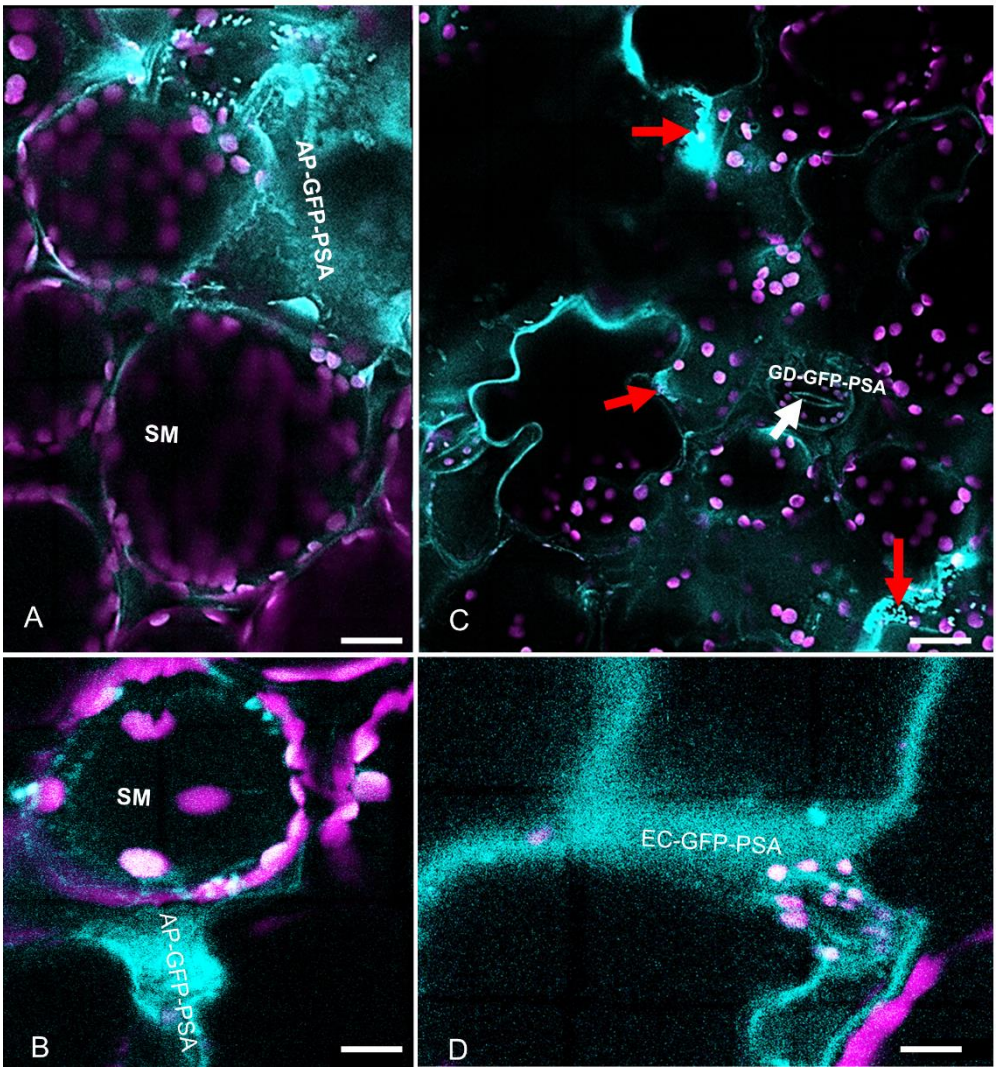

Fig. 2.1. Internal (A and B) and external (C and D) colonization of table beet leaves by a green fluorescent protein (GFP)-tagged strain of *Pseudomonas syringae* pv. *aptata* (GFP-Psa), viewed using a Leica confocal microscope (25x magnification). Chloroplasts are shown by magenta autofluorescence. GFP-tagged Psa cells are cyan in color. AP = apoplast; SM = spongy mesophyll cells with chloroplasts; AP-GFP-Psa = apoplast colonized by GFP-Psa; EC-GFP-Psa = epidermal cell walls colonized by GFP-tagged Psa; GD-GFP-PSA = guard cells colonized by GFP-tagged Psa. White arrow (C) shows GFP-Psa around a stomatum. Red arrows from top to bottom (C) show clusters of GFP-Psa, cytoplasmic localization of GF-Psa, and GFP-Psa clusters.

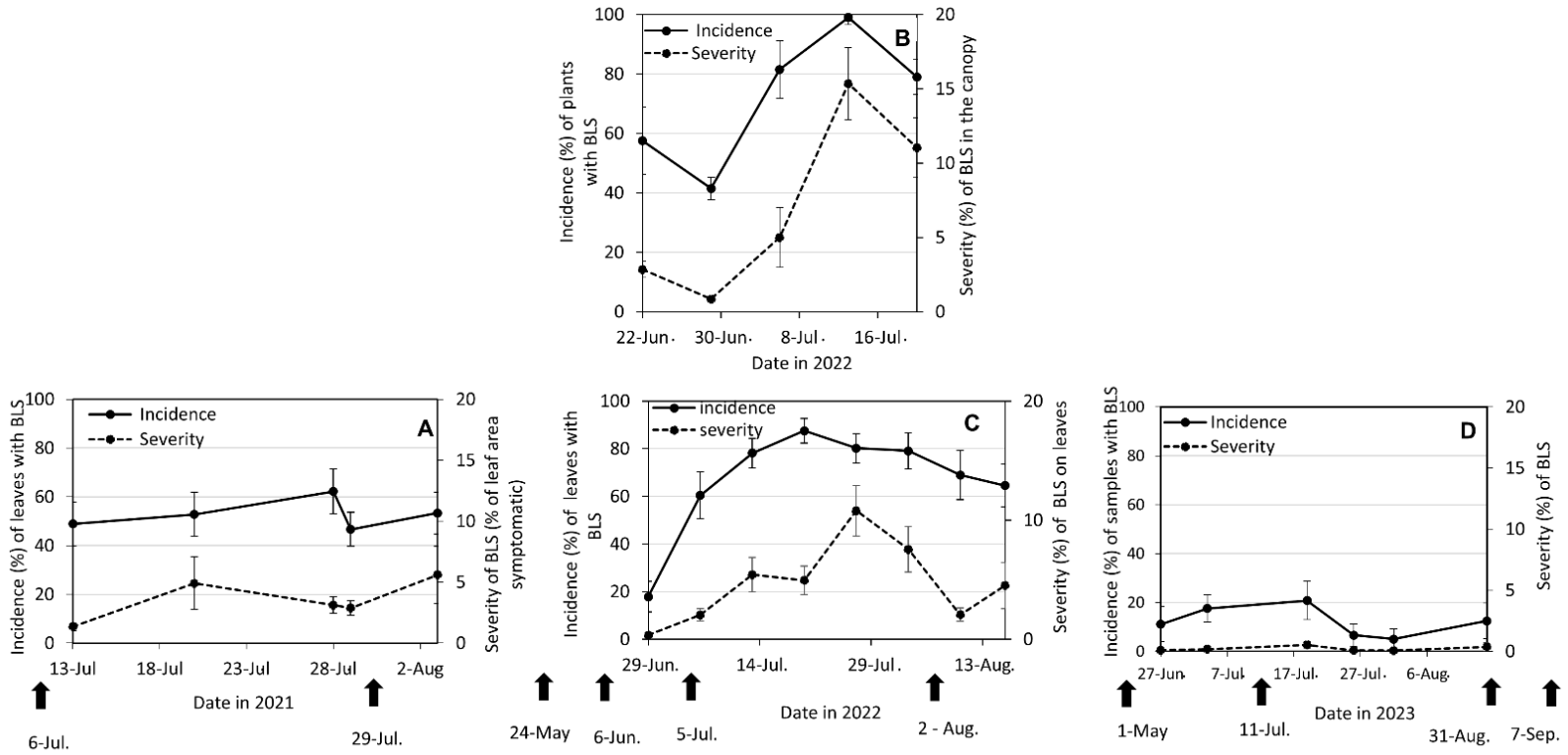

Fig. 2.2. A) Mean incidence (presence or absence) and severity (percentage of leaf area with symptoms) of bacterial leaf spot (BLS) on table beet leaves sampled in a 2021 table beet seed crop trial in Skagit Co., WA, following inoculation with a rifampicin-resistant strain of *Pseudomonas syringae* pv. *aptata* (rif-Pap010). Each data point shows the mean ± standard error for 90 leaf samples. B) Mean incidence (%) of 200 plants with symptoms and severity of BLS (percentage of canopy with symptoms) in a 2022 table beet seed crop trial in Skagit Co., WA following inoculation with rif-Pap010. C) Incidence and severity of BLS symptoms on leaf samples collected periodically during the 2022 trial. Each data point is the mean ± standard error of 200 plants (B) or 96 leaf samples (C). D**)** Mean incidence (percentage of leaves) and severity (percentage of leaf surface area) with symptoms of BLS for leaves sampled from a

2023 table beet seed crop trial in Skagit Co., WA, following inoculation of plants with rif-Pap010. Each data point shows the mean ± standard error for 96 leaves sampled periodically throughout the trial. Arrows indicate when the plants were inoculated in each trial.

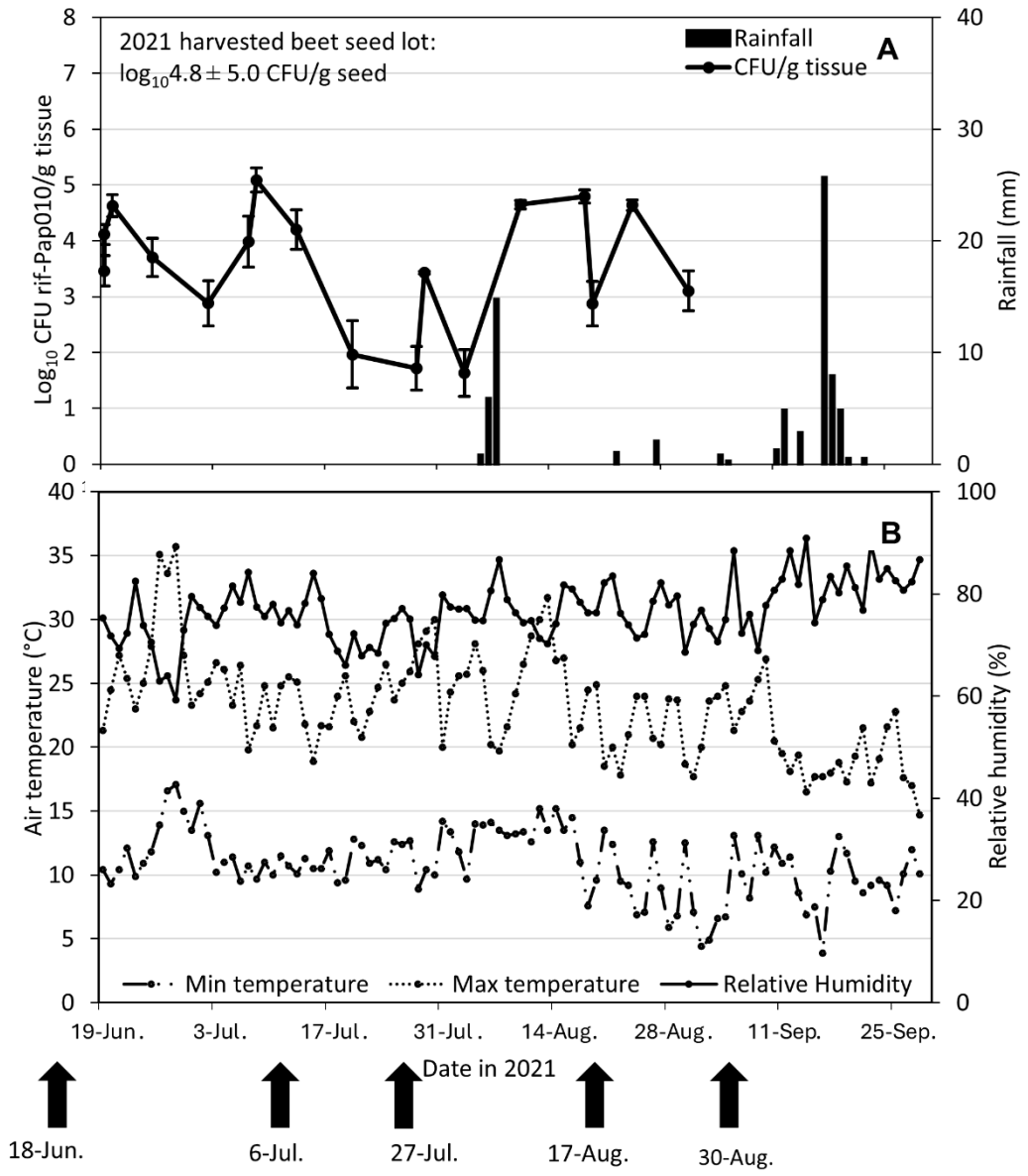

Fig. 2.3. A) Population of rifampicin resistant-*Pseudomonas syringae* pv. *aptata* strain Pap010 (rif-Pap010) recovered from leaf, stem, and flower samples collected from a table beet seed crop in 2021. Rainfall is shown by the black bars**.** B) Relative humidity and daily minimum and maximum air temperatures over the duration of the trial. The arrows indicate dates of inoculation with rif -Pap010. Each data point in A shows the mean ± standard error for 15 leaf samples used to quantify rif-Pap010 at each sampling time.

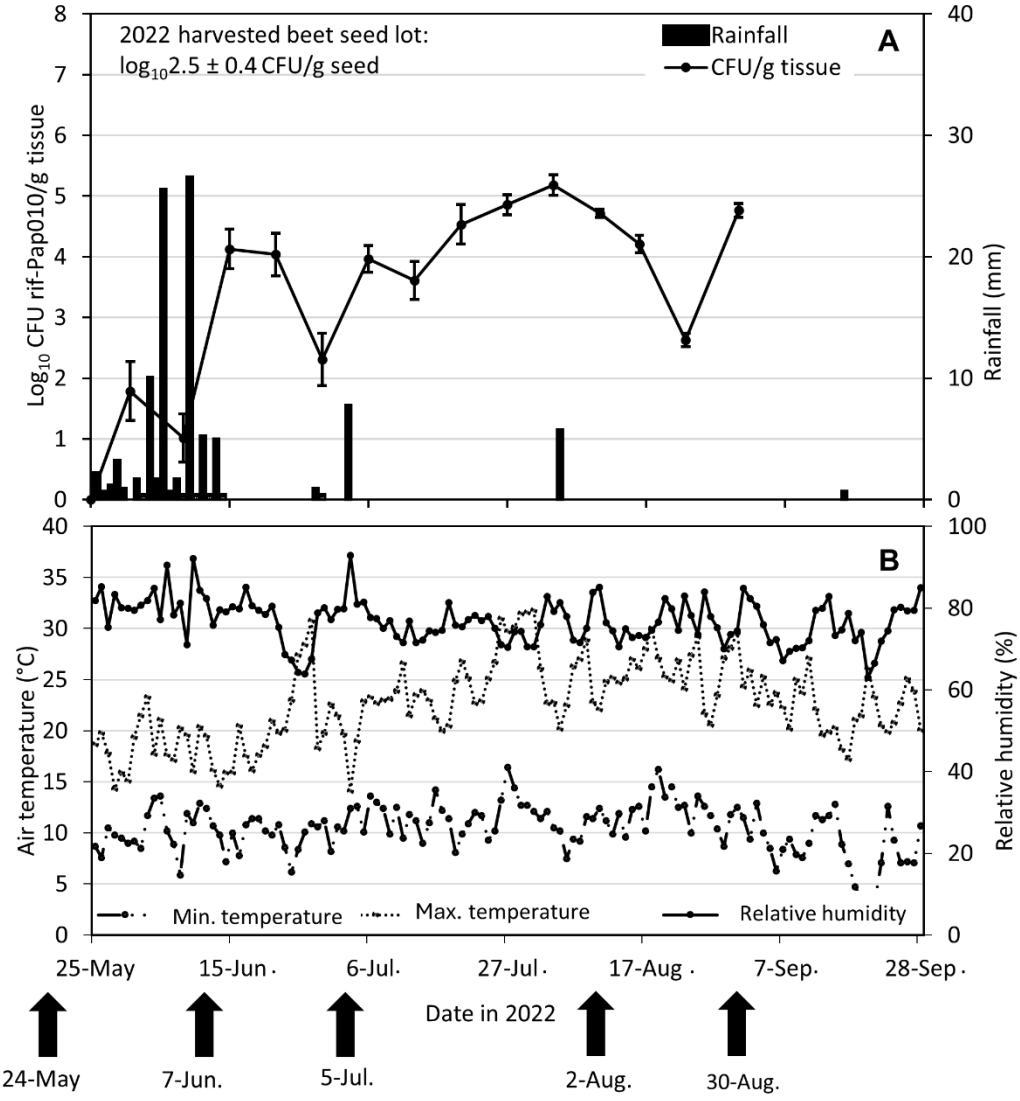

Fig. 2.4. A) Population of rifampicin resistant-*Pseudomonas syringae* pv. *aptata* strain Pap010 (rif-Pap010) recovered from leaf samples collected from a table beet seed crop in Skagit Co., WA in 2022, and rainfall over the duration of the trial. Each data point shows the mean ± standard error for 16 replicate leaf or seed stalk samples. B) Relative humidity, and daily minimum and maximum air temperatures over the duration of the trial. The arrows show dates of inoculation with rif -Pap010.

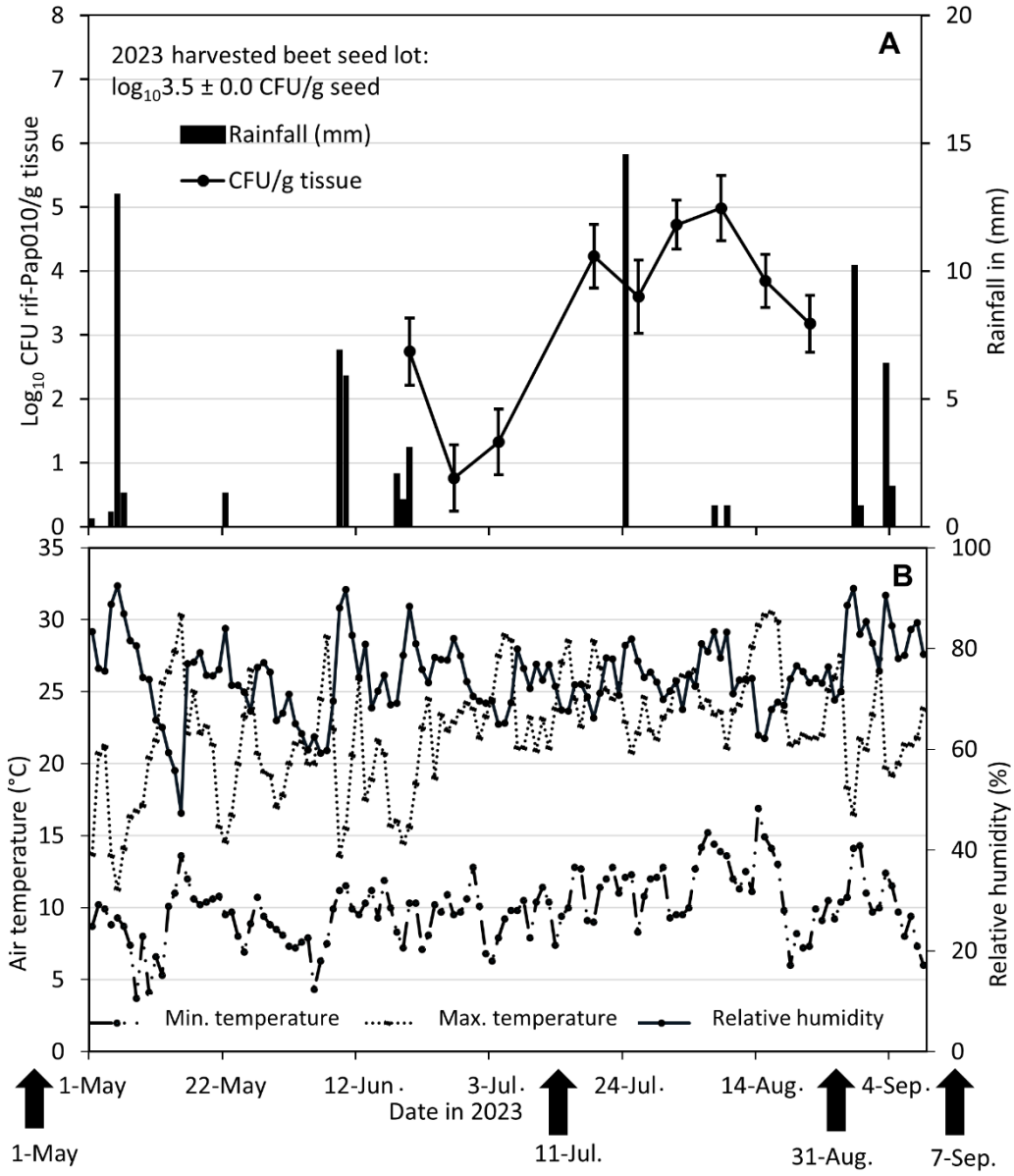

Fig. 2.5. A) Population of a rifampicin-resistant strain of *Pseudomonas syringae* pv. *aptata* (rif-Pap010) recovered from a table beet seed crop in Skagit Co., WA in 2023. Each data point shows the mean ± standard error for 16 plant leaf samples. B) Relative humidity %, and daily minimum and maximum air temperatures (°C) over the duration of the trial. Arrows show dates of inoculation of plants in the trial with rif-Pap010.

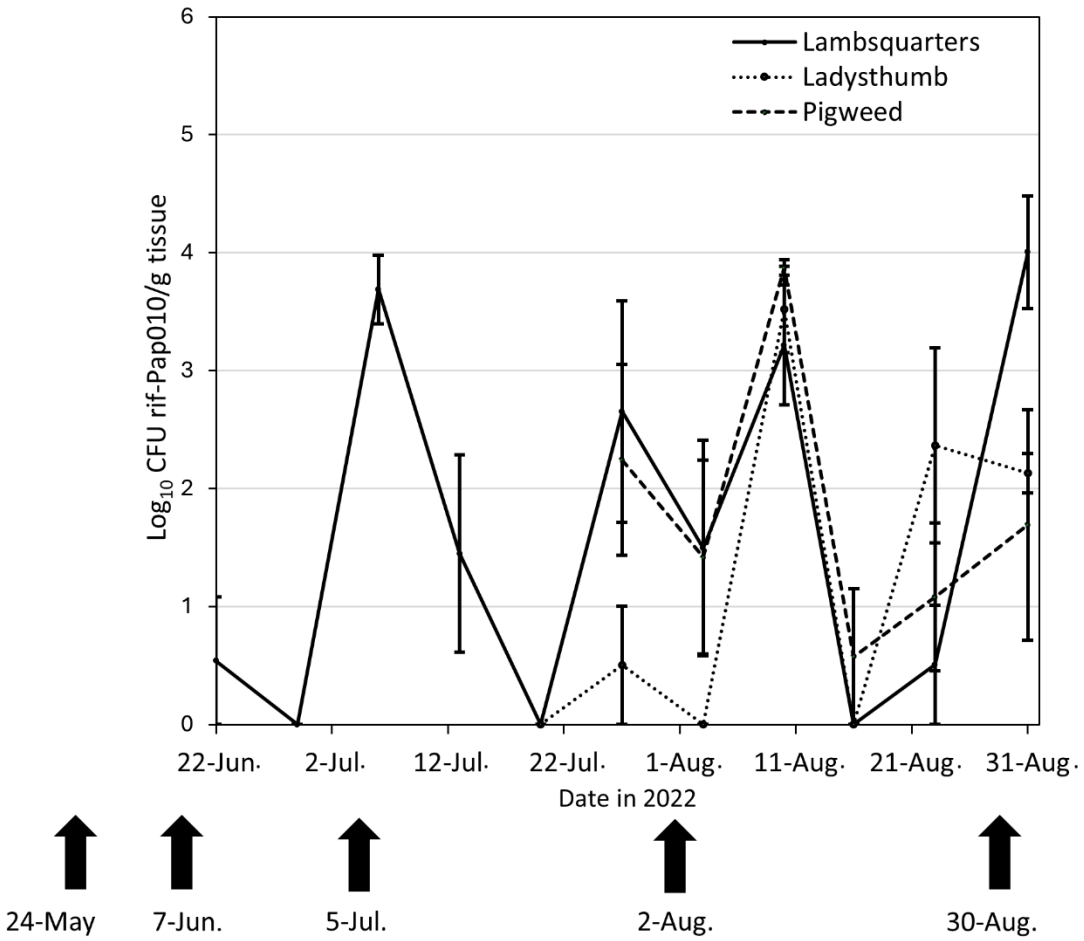

Fig. 2.6. Population of rifampicin resistant-*Pseudomonas syringae* pv. *aptata* strain Pap010 (rif-Pap010) recovered from lambsquarters (*Chenopodium album*), ladysthumb (*Persicaria maculosa*), and pigweed (*Amaranthus retroflexus*) weed samples in a 2022 table beet seed crop trial inoculated with rif-Pap010 in Skagit Co. Arrows show the dates of inoculation of the trial with rif -Pap010. Each data point shows the mean ± standard error of rif-Pap010 recovered from four replicate plant samples of that weed species.

CHAPTER THREE: EFFICACY OF HOT WATER AND SODIUM HYPOCHLORITE TREATMENT OF TABLE BEET SEED FOR MANAGEMENT OF SEEDBORNE *PSEUDOMONAS SYRINGAE* PV. *APTATA*

Introduction

Pseudomonas syringae pv. *aptata* is a seedborne and seed transmitted pathogen that causes bacterial leaf spot of Swiss chard (*Beta vulgaris* subsp. *vulgaris* Cicla Group), table beet (*Beta vulgaris* subsp. *vulgaris* Condivita Group), and sugar beet (*Beta vulgaris* subsp. *vulgaris* Altissima Group) (Jacobsen 2009). The disease is favored by prolonged cool to warm (10 to 25°C) and wet conditions (Brown and Jamieson 1913; Jacobsen 2009). Symptoms include dark brown to black lesions, ranging from 2 to 3 mm in diameter or larger when lesions coalesce, each with a distinct brown to black border (Crane 2023; Derie et al. 2016; Jacobsen 2009; Koike et al. 2003; Nampijja et al. 2021). The lesions are water-soaked during periods of high relative humidity, and coalesce during extended wet conditions, giving infected leaves a blighted appearance. *P. syringae* pv. *aptata* can infect cotyledons, leaves, stems, petioles or seed stalks via hydathodes, stomata, and wounds (Jacobsen 2009; Nikolić et al. 2018). Besides being moved on infected seed, *P. syringae* pv. *aptata* can spread in wind-blown infected plant particles, and is splash-dispersed. The bacterium also can persist as an epiphyte without causing symptoms of bacterial leaf spot (Riffaud and Morris 2002).

B. vulgaris subspecies are biennials (du Toit 2007; Harveson et al. 2009). Seed production requires photothermal induction for bolting (transition from vegetative to reproductive growth stages), i.e., vernalization and exposure to long days (Abo-Elwafa et al. 2006; du Toit 2007; Kockelmann et al. 2010; Navazio et al. 2010). Vernalization requirements

include subjecting the plants to temperatures between 0 and 15°C for 5 to 20 weeks, depending on the cultivar, to trigger bolting. The maritime area of western Oregon and western Washington in the Pacific Northwest (PNW) is the only region of the United States with the environmental conditions required for producing high quality table beet, sugar beet, and Swiss chard seed crops (du Toit 2007, Rackham 2002). Approximately 95% of the nation's table beet and Swiss chard seed production takes place in this region (du Toit 2007; Organic Seed Alliance 2016; Rackham 2002; Schreiber and Ritchie 1995).

Over the past few decades, bacterial leaf spot has become a more significant concern in the production of table beet and Swiss chard seed crops in the PNW (Derie et al. 2016; Safni et al. 2016). This is linked to the growing demand for seed to plant the expanding acreage of baby leaf beet and chard crops in the United States, fueled by increasing public awareness of the health benefits of vegetables and the convenience of pre-packaged salads (Lin et al. 2003). The high risk of bacterial leaf spot outbreaks in baby leaf crops is associated with dense plantings (7 to 9 million seeds/ha), overhead irrigation, and sequential plantings which create a highly favorable environment for seed transmission of *P. syringae* pv. *aptata* and development of bacterial leaf spot (Crane 2023; Derie et al. 2016). Incidences of bacterial leaf spot as low as 5% can result in rejection of baby leaf crops due to the difficulty of sorting and removing symptomatic leaves. In Swiss chard baby leaf field trials completed in western Washington in 2015 to evaluate thresholds for seed transmission of *P. syringae* pv. *aptata*, as little as 10^3 CFU/g seed resulted in seed transmission and development of bacterial leaf spot, with prevailing weather conditions influencing disease severity (Derie et al. 2016). Additional field trials in the same region in 2020 and 2021 showed that the threshold for seedborne inoculum that resulted in ≥5% disease incidence ranged from 0 to ~6 x 10^4 CFU/g seed, depending on environmental

conditions (Crane 2023). These trials suggest it may be necessary to plant seed free of *P. syringae* pv. *aptata* under favorable conditions to prevent development of bacterial leaf spot in baby leaf crops.

Since high quality beet and Swiss chard seed crops can be grown only in countries that have the appropriate climatic conditions, i.e., Argentina, Denmark, Chile, Germany, Peru, South Africa, and the PNW region of the United States, seed production and trade has become increasingly global as seed has to be moved from the areas of seed production to the many regions of the world where the seed is planted for commercial crop production (du Toit 2007; Rackham 2002). This global movement of seed exacerbates the risk of moving seedborne pathogens around the world (McGee 1995). To minimize losses associated with infected seed lots, some seed companies have invested in the use of proprietary seed treatments to reduce or eradicate infection by *P. syringae* pv. *aptata*, e.g., the ProBio Gopure treatment developed by Germains Seed Technology (Gilroy, CA) and the Clean Start organic disinfection process developed by Universal Seed, LLC (Independence, OR). However, these seed treatments are proprietary, and therefore result in additional expense and time due to the need to transport large volumes of seed to approved seed treatment facilities. In conventional table beet and Swiss chard seed production in the United States, captan (N-trichloro methylthio-4-cyclohexane-1,2-dicarboximide), thiram (N, N-dimethyl dithiocarbamic acid), and mefenoxam have been used widely to seed to manage damping-off caused by seedborne and soilborne fungal and oomycete pathogens (Babadoost 1992; Maude et al. 1969). These fungicides are not effective against *P. syringae* pv. *aptata*. There is a need for alternative effective seed treatments for this pathogen, which can be used in conventional and certified organic beet and Swiss chard production. Disinfectants such as sodium hypochlorite, calcium hypochlorite, hydrogen peroxide, and

calcium hydrogen carbonate, and hot water treatments have been used to treat seed infected with various seedborne bacterial pathogens, such as *Xanthomonas campestris* pv. *campestris* and *X. hortorum* pv. *carotae*, the causal agents of black rot of crucifers and bacterial blight of carrot, respectively (Hakalová et al. 2024; Miller and Lewis Ivey 2024; Sakudo et al. 2020; Temple et al. 2013; Vicente and Holub 2013).

Decortication, which involves removing part of the pericarp of seed, is used in the table beet and Swiss chard seed industry to enhance the uniformity in flow of seeds in planters, and to speed seed germination, leading to faster emergence and improved plant stands (Peck et al. 1967). Decortication facilitates quicker and more uniform germination by allowing moisture to penetrate the seed more effectively. Decortication also facilitates more uniform application of seed treatments. In addition, this treatment simplifies the processing and cleaning of seeds, making them more suitable for storage and distribution (Bainer and Leach 1946). Moreover, decortication can reduce the level of infection of some seedborne pathogens that reside primarily in the pericarp (TeKrony 1967), and minimizes the presence of chemical inhibitors in the pericarp that impede seed germination (Dekock et al. 1953; Miyamoto 1957).

Several factors influence the efficacy of seed treatments for control of seedborne pathogens, including the amount of infection in seed lots, incidence of the pathogen on seed, location of the pathogen in or on the seed, seed moisture level, seed size, seed vigor, age of seed, and tolerance of pathogen(s) to the specific physical, chemical, or biological treatments (Leben 1974; Maude 1996). For example, seed treatments that entail heat are more effective at eradicating bacteria from seed lots with higher moisture content compared to lots with low moisture content because moisture conducts heat, and bacteria in more moist seeds typically are more active metabolically (Leben 1974). Bacteria in dry seeds typically are in a state of

hypobiosis (reduced metabolism) and, therefore, harder to kill. Additionally, bacteria located deeper in the seed, e.g., in the embryo, are more difficult to reach and eliminate with heat without potentially damaging the embryo (Leben 1974, 1983; Maude 1996). It is also crucial that seed treatments do not damage seed germination or shelf life, i.e., seed treatments must be optimized for maximum efficacy and minimum phytotoxicity.

Beet and Swiss chard plants and seed can be colonized by *P. syringae* pv. *aptata* as well as non-pathogenic strains of *P. syringae* (Crane 2023). Currently, there is no molecular (DNA-based) diagnostic assay, such as a real-time or regular PCR assay, that can be used to differentiate non-pathogenic *P. syringae* isolates from isolates of *P. syringae* pv. *aptata* and, therefore, quantify the amount of the pathogen in infected seed lots. In numerous studies, antibiotic-resistant strains of bacterial pathogens that are capable of growing on media amended with the antibiotic to which they are resistant, have been employed to study and quantify plant pathogenic bacteria. For example, rifampicin-resistant strains of *X. phaseoli* pv. *phaseoli* (formerly *X. phaseoli*) and *X. citri* pv. *fuscans* (formerly *X. fuscans*) were generated to monitor these pathogens in common bean (*Phaseolus vulgaris*) under field conditions (Weller and Saettler 1978). In this study, we used a rifampicin-resistant strain of *P. syringae* pv. *aptata* (rif-Psa) to inoculate beet seed crop field trials in Skagit Co., WA in each of the three seasons, to generate beet seed lots infected with the pathogen (Chapter 2). The seed lots were used to evaluate the efficacy of hot water and bleach seed treatments for eradicating *P. syringae* pv. *aptata* from beet seed. The objectives of this study were to: 1) determine the location of infection of the table beet seed lots by the rif-Psa strain, 2) evaluate hot water and bleach seed treatments for management of seedborne *P. syringae* pv. *aptata*, and 3) evaluate potential use of decortication for control of seedborne rif-Psa.

Materials and Methods

A rifampicin-resistant strain of *P. syringae* pv. *aptata* strain Pap010 (rif-Pap010), that originated from a naturally infected seed lot from Washington State and is pathogenic to table beet and Swiss chard, was generated by Carolee Bull's program at The Pennsylvania State University in 2020. Rif-Pap010 was used to inoculate a table beet seed crop field trial in each of 2021, 2022, and 2023 at the Washington State University (WSU) Mount Vernon Northwestern Washington Research and Extension Center (NWREC) to generate a seed lot each year that could be used to address the objectives of this study. Seed in each of 2021, 2022, and 2023 were dried to 5.8% moisture content. Other details of each trial, including inoculations, disease assessments, harvest, and conditioning of the harvested seed are provided in Chapter 2.

Seed health assays. Seeds from each trial was thoroughly mixed before sampling, and three replicate samples of 10,000 seeds harvested from each trial were tested to quantify rif-Pap010 infection, following a modified version of the seed wash assay described by Mohan and Schaad (1987). Briefly, each 10,000-seed subsample was soaked in 1,800 ml of 0.85% saline in a sterile poly bag (22.9 cm x 30.5 cm, 6 Mil flat; Uline, Pleasant Prairie, WI) to which three drops of Tween 20 were added, and held at room temperature (22 ± 2°C) for 4 h with manual agitation every hour. Each bag of seed was then placed on a gyratory shaker operated at 150 rpm for 10 minutes. The seed rinsate was then decanted and a 900-µl aliquot diluted 10-fold four times. Each of three 100-µl aliquots of each dilution was spread onto a plate of nutrient agar (NA) medium amended with 10 ml of 10 mM rifampicin and 2 ml of 355 mM cycloheximide (rif-NA) (Weller and Saettler 1978). The remaining 600 µl of each dilution was spiked with 10^5 CFU of rif-Pap010/ml and incubated for 30 minutes to assess if any inhibitors might be present in each

seed lot that could affect detection and quantification of rif-Pap010. A 100-µl aliquot of the second dilution (10^5 CFU/ml) of rif-Pap010 also was plated onto rif-NA directly as a standard for calibration when counting rif-Pap010 colonies from the seed wash dilution plates. The plates were incubated at 27°C for 7 days, colonies counted, and CFU rif-Pap010/g seed calculated.

Location of seed infection. The rif-Pap010 infected table beet seed lot generated each year was used to determine the location of infection of the seed by rif-Pap010 (Fig. 3.1). For each of six replicate samples of 50 table beet seed from each rif-Pap010 infected seed lot, the pericarps and embryos were separated manually using a scalpel. Each pericarp and embryo was then soaked individually in 400 and 200 µl of 0.85% NaCl, respectively, in microcentrifuge tubes for 4 h. Each pericarp and embryo wash was then plated onto rif-NA, and the plates incubated for 7 days at 25°C. Rif-Pap010 colonies were counted to calculate the incidence of each of the pericarps and embryos infected as well as the amount of rif-Pap010 detected from each pericarp and embryo.

Chlorine seed treatments. The 2021 and 2023 beet seed lots infected with rif-Pap010, were used to evaluate the efficacy of chlorine seed treatments for eradication of seedborne inoculum. The seed lot generated in 2022 was not used due to the low levels of rif-Pap010 recovered from that lot. For each of the 2021 and 2023 seed lots, seed treatments with 1.2% NaOCl were evaluated using a randomized complete block design (RCBD) with four replications of each of four durations of treatment: 5, 15, 25, and 35 minutes. For each replication of each treatment, 5,000 seeds were soaked in 1,500 ml of 1.2% NaOCl to which four drops of Tween 20 were added in a sterile poly bag, and placed on a gyratory shaker operated at 200 rpm at room temperature (22 ± 1°C) for the appropriate duration. The seed wash was then decanted, and the seed triple-rinsed with 1,500 ml of deionized water for each rinse. For the control treatments,

four replicate samples of 5,000 seeds were each soaked in 1,500 ml of deionized water for each of the same durations to assess the impact of soaking alone for each duration on recovery of *P. syringae* pv. *aptata*. Four replicate samples of 5,000 seeds not soaked in 1.2% NaOCl or water served as an additional control treatment. After treatment and rinsing, the seeds were dried on brown Kraft paper in a fume hood for 4 days, and the dried to 5.8% moisture content, and seed stored at 6°C and 45% relative humidity (RH).

A subsample of 100 seeds from each replicate of each treatment was tested using the blotter germination assay of the Association of Official Seed Analysts (AOSA 2008) to assess potential impacts of the treatments on seed quality. The seeds were incubated in the dark at 20°C for 16 h and at 30°C for 8 h each day for 14 days, and the cumulative incidence of seed with normal germination, abnormal germination, rot, or dormancy recorded based on evaluations after 3, 7, and 14 days. The remaining 4,900 seeds from each replicate of each treatment were subjected to the same seed health assay described above, by placing the seed in a sterile poly bag with 800 ml of 0.85% NaCl and soaking the seed for 4 h at room temperature. A 900-µl aliquot of the resultant seed wash from each replication of each treatment was diluted serially 10-fold three times, a 100-µl aliquot of each dilution plated onto rif-NA in triplicate, and the plates incubated for 7 days at 27°C to determine the efficacy of each duration of bleach treatment on eradication of rif-Pap010 from the seed by quantifying the number of viable rif-Pap010 (CFU/g seed) recovered.

Hot water seed treatments. Samples of the rif-Pap010-infected beet seed lots harvested in 2021 and 2023 were used to evaluate hot water seed treatments for eradication of seedborne inoculum. From August through December 2022, a subsample of 2,500 seeds of the 2021 seed lot was used for each of four replications per treatment combination, rather than 5,000 seeds

because of the limited amount of seed available. The 6-by-5 factorial treatment design included five durations of exposure (10, 20, 30, 40, and 50 minutes) to each of six water temperatures (25, 40, 45, 50, 55, and 60°C), set up in a split-plot RCBD with temperature treatments assigned to whole plots and durations of treatment to split plots. Each subsample of 2,500 seeds was placed in a nylon mesh sock and immersed for the appropriate duration in deionized water that had been pre-heated to the appropriate temperature in a sterilized hot water bath (microprocessor controlled 280 series water bath, Precision Scientific Inc., Chicago, IL). The seeds were then rinsed in running tap water for 5 minutes immediately after treatment. The hot water bath equipment was disinfected with 70% ethyl alcohol between treatments to prevent cross-contamination. For the control treatments, four replicate samples of 2,500 seeds were soaked in water at 25°C for each of the same durations to determine the effect of the soaking dilutions alone on recovery of rif-Pap010, and four replicate samples of 2,500 seeds were not soaked in water. The treated seeds were then dried and stored as described for the chlorine seed treatment trials.

Seed germination assays were completed for a subsample of 100 seeds of each replicate of each treatment combination within 14 days of the hot water treatments, as described for the chlorine seed treatments. For the seed health assays, the remaining ~2,400 seeds for each replication of each treatment combination were placed in 600 ml of 0.85% NaCl and 100 µl of Tween 20 in a poly bag, soaked for 4 h at room temperature, a 900-µl aliquot of the seed wash diluted serially 10-fold three times, and a 100-ul aliquot of each dilution plated in triplicate on rif-NA medium. The plates were incubated and the rif-Pap010 colonies counted to calculate CFU/g seed, as described above.

The same hot water treatment combinations were evaluated using the rif-Pap010 infected seed lot harvested in 2023, except that 5,000 seeds were used for each treatment combination because of the larger amount of seed available. The treatments were tested within 3 months of harvesting that seed lot. The seed germination and seed health assays were conducted as described for the 2021 seed lot except that the remaining ~4,900 seeds of each replicate of each treatment combination were soaked in 800 ml of 0.85% NaCl for the seed health assay.

Effect of decortication on seedborne rif-Pap010. Using the rif-Pap010 infected seed lot generated in 2021, three subsamples of 5,000 seeds were decorticated using electric seed scarifier with a belt-driven fan and blower motor (6K030G, Forsberg, Inc., Thief River Falls, MN) operated for 30 s. The resultant powder and the decorticated seed were placed in separate poly bags (same as those used for the chlorine and hot water treatments) for each subsample. Ethyl alcohol was used to disinfect the fan and blower motor between subsamples to prevent cross-contamination. The control treatment included three replicate samples of 5,000 non-decorticated seeds. The powder from the removed pericarps was soaked in 600 ml of 0.85% NaCl for each replication, and the decorticated and non-decorticated seed samples were each soaked in 900 ml of 0.85% NaCl for 4 h at room temperature. The pericarp powder suspension was filtered through 4 layers of cheesecloth and a 900-µl aliquot of the wash diluted 10-fold three times. Similarly, a 900-µl aliquot of the seed wash from each replicate of the decorticated and non-decorticated seed samples was diluted serially three times. A 100-µl aliquot of each dilution of the wash from the powdered pericarps, decorticated seeds and non-decorticated seeds, was plated in triplicate onto rif-NA medium, and the plates incubated at 27°C for 7 days. Colonies recovered from the pericarp powder, decorticated seeds, and non-decorticated seeds were counted to determine the CFU rif-Pap010/g powder or seed. The seed germination assay

was completed as described above for the decorticated and non-decorticated seed samples. The same seed health assay for *P. syringae* pv. *aptata* method was followed using the rif-Pap010 infected table seed lot harvested in 2023, except six subsamples of 5,000 seeds were used, with each subsample of powdered pericarps, decorticated seeds, and non-decorticated seeds soaked in 800 ml of 0.85% NaCl.

Data analysis. Analyses of variance (ANOVA) for the dependent variables measured for chlorine and hot water seed treatments evaluated with the 2021 and 2023 table beet seed lots were calculated in R version 4.1.3. Data were subjected to transformations if the assumptions of normality of residuals and/or homogeneity of variances were not met. For the chlorine seed treatment trials, replications were treated as a random effect while the durations of chlorine or water treatment were fixed effects. Means separations were calculated using Tukey's honestly significant difference (HSD) at $P \leq 0.10$. For the hot water seed treatments with the 2021 and 2023 table beet seed lots, data for variables that did not meet the assumption of normality of residuals and/or homogeneity of variance were subjected to a non-parametric test in SAS on Demand for Academics or R version 4.1.3 if transformations did not resolve these violations. Replications were treated as a random effect whereas temperatures and durations of treatment were fixed effects. In the decortication trial with the 2021 and 2023 seed lots, an ANOVA was calculated to assess if decortication affected seed germination and the amount of rif-Pap010/g seed recovered after decortication.

Results

Location of seed infection. The amount of rif-Pap010 recovered from the harvested table beet seed from field trials in 2021, 2022, and 2023 averaged $\log_{10}4.9 \pm 0.1$ (mean ± standard

error), $\log_{10}2.5 \pm 0.4$, $\log_{10}3.5 \pm 0.0$ CFU/g seed, respectively (Fig. 3.1A, B, and C). No rif-Pap010 was not recovered from any of 300 embryos tested in each year. In 2021, rif-Pap010 was recovered from 27.8%, 6.0% and 16.4% of the pericarps from the 2021, 2022, and 2023 seed lots, respectively. The amount of rif-Pap010 recovered from the pericarps also differed among subsamples within trials. The amount of rif-Pap010 recovered from the pericarps also differed among subsamples within trials. The highest amount of rif-Pap010 recovered from a single pericarp was 20,000 CFU in 2021 and <1000 CFU in 2022 and 2023. More than half of the positive pericarps, had <1000 CFU in 2021 and <10 CFU in 2022 and 2023 (Fig. 3.1A, B, and C).

Chlorine seed treatments. Treatment of the 2021 rif-Pap010-infected table beet seed lots with 1.2% NaOCl significantly impacted the amount of rif-Pap010 recovered from the seed (Table 3.1, and Fig. 3.2A and B). No rif-Pap010 was recovered from any of the NaOCl-treated seeds, regardless of the duration of chlorine treatment (Fig. 3.2A). However, rif-Pap010 was recovered consistently from seeds soaked in water for all four durations, with no difference among the durations of water soaking ($P = 0.3916$, $\log_{10}2.4 \pm 0.3$ to $\log_{10}2.8 \pm 0.3$ CFU rif-Pap010/g seed). The non-treated control seed (no water soaking) had $\log_{10}2.7 \pm 0.4$ CFU rif-Pap010/g seed (Fig. 3.2A). In the 2023 seed lot, the non-treated seed had $\log_{10}3.2 \pm 0.2$ CFU rif-Pap010/g seed and none of the NaOCl treatments significantly reduce rif-Pap010 compared to soaking the seeds in water when averaged over all four durations of treatment ($P = 0.364$). Although not significant, there was almost a 10-fold reduction in amount of pathogen recovered from seeds soaked in 1.2% NaOCl vs. water for 35 minutes (Fig. 3.2C).

For the 2021 seed lot, there was no main effect of treatment (water vs. 1.2% NaOCl) on incidence of normal seed germination. However, duration of treatment ($P = 0.0660$) and

treatment- by -duration interaction effects (P = 0.0770) were significant. Non-treated seeds had 86.8 ± 2.3% normal germination, and the incidence of normal germination increased for seeds treated with 1.2% NaOCl for 25 minutes (88.7 ± 1.7%) and 35 minutes (88.0 ± 2.6%), based on Tukey's HSD test (Fig. 3.2B). For the 2023 seed lot, the main effects of water vs. 1.2% NaOCl treatments (P = 0.3922) and duration of treatment (P = 0.3332), as well as the treatment- by -duration interaction effect (P = 0.9887) were not significant (Table 3.1). The incidence of normal germination ranged from 82.0 ± 3.7 to 85.5 ± 2.9% for the durations of 1.2% NaOCl treatment and from 83.3 ± 3.4 to 89.8 ± 1.8% for the durations of water treatment in the 2023 trial (Fig. 3.2C). In the 2021 trial, the incidence of seed with abnormal germination did not differ significantly between the 1.2% NaOCl vs. water treatments (P = 0.6020), among the durations of treatment (P = 0.7850) and for the treatment- by -duration interaction (P = 0.1470) (Table 3.1, Fig. 3.2B). Similarly, in the 2023 trial, there was no significant (P = 0.4101) for treatments and P = 0.5063 for durations and the treatment- by -duration interaction was not significant (P = 0.6446) (Table 3.1 and Fig. 3.2D). In the 2021 trial, the incidence of non-germinated seeds was affected significantly by the main effects of water vs. NaOCl treatments (P = 0.0310) and duration of treatment (0.0270). However, the treatment- by -duration interaction was not significant (0.3780) (Table 3.1). The incidence of non-germinated seeds in the 2021 trial was greatest for seeds treated with 1.2% NaOCl for 5 minutes (9.8 ± 0.9%) and least for seeds soaked in water for 35 minutes (2.5 ± 0.6%) based on Tukey's HSD, with no significant difference among the rest of the water or NaOCl durations of treatments. For the 2023 trial, the main effects of treatment (P = 0.2090) and duration (0.7760), and the treatment- by -duration interaction (0.7760) were not significant. In both trials, the incidence of decayed seed was not affected by the main effects of treatment (P = 0.6360 and 0.5910) in the 2021 trial and 2023 trial,

respectively and duration (P = 0.8530 and 0.2360, respectively), or the treatment- by -duration interaction (P = 0.6590 and 0.970, respectively) (Table 3.1, Figs. 3.2B and 3.2D).

Hot water seed treatments. In the 2021 trial, the main effects of water temperature (P <0.00016) and durations (P = 0.0015) of hot water treatment, but the interaction between temperature and duration of hot water treatment was not significant (P = 0.5889) (Table 3.2). Non-treated seed averaged $\log_{10}4 \pm 0.1$ CFU rif-Pap010/g seed (mean ± standard error). Soaking of seeds in water at 25°C for 10 to 50 minutes averaged 2.7 ± 0.4 CFU/g seed. Soaking seeds in water at 40°C for 10 minutes resulted in the greatest rif-Pap010 recovery ($\log_{10}3.3 \pm 0.1$ CFU/g seed), compared to higher temperatures and longer durations of treatment (Fig. 3.3A). The amount of rif-Pap010 recovered for seeds treated at 40°C decreased slightly the longer the duration of treatment reading $\log_{10}2.4 \pm 0.9$ CFU/g seed for seeds treated for 50 minutes, but the duration effect was not significant (Fig. 3.3A). Treating seeds at 45°C for 10 and 20 minutes resulted in a significant decrease in amount of rif-Pap010 recovered compared to these durations at 40°C. Increasing the duration of treatment at 45°C decreased rif-Pap010 recovery further, to $\log_{10}1.3 \pm 0.8$, $\log_{10}1.7 \pm 0.8$ and $\log_{10}0.5 \pm 0.5$ after 30, 40, and 50 minutes of treatment at 45°C, respectively (Fig. 3.3A). Hot water treatment of the 2021 seed lot at 50°C reduced rif-Pap010 recovery significantly for all durations, ranging from $\log_{10}1.7 \pm 1.0$ at 10 minutes to $\log_{10}0.9 \pm 0.9$ CFU/g seed at 50 minutes, with greater reductions in rif-Pap010 recovery than the 40°C and 45°C treatments. For seeds treated at 55°C, rif-Pap010 was detected at <1.0 CFU/g seed for durations of 10 to 30 minutes of treatment ($\log_{10}0.9 \pm 0.9$ to $\log_{10}0.7 \pm 0.7$ CFU/g seed from 10 to 30 minutes, respectively) and treatment of seeds at 55°C for 40 and 50 minutes eradicated rif-Pap010 from the seed (Fig. 3.3A). Likewise, seed treatment at 60°C for all durations resulted in no recovery of rif-Pap010 (Fig. 3.3A).

In the 2023 trial, the main effects of water temperature and duration of treatment were highly significant (P <0.0001), as was the interaction between temperature and duration (P = 0.0010) (Table 3.2). Non-treated seed averaged $\log_{10}3.8 \pm 0.1$ CFU rif-Pap010/g seed. For seed treated in water at 25°C for all durations, rif-Pap010 was recovered at $\geq \log_{10}2.9$ (Fig. 3.3D). Even for seed treated at 40°C, the amount of rif-Pap010 recovered did not differ significantly from that recovered for seed treated in water at 25°C (Fig. 3.3D). For seeds treated at 45°C, the amount of rif-Pap010 detected was less for 40- and 50-minute durations of treatment, with only $\log_{10}1.5 \pm 0.6$ CFU/g seed detected on seeds treated for 50 minutes. For the 50°C treatment, the amount of rif-Pap010 detected in the seed health assay decreased from $\log_{10}3.2 \pm 0.3$ CFU/g seed with 10 minutes of treatment to $\log_{10}0.8 \pm 0.4$ CFU/g seed after 40 minutes of treatment. For seeds treated at 55°C, rif-pap010 detection decreased the longer the duration of treatment, with a significant reduction in rif-Pap010 recovery for the 30-minute treatment ($\log_{10}0.5 \pm 0.5$), and no recovery of the pathogen from seeds treated for 40 and 50 minutes (Fig. 3.3D). For seeds treated at 60°C, rif-Pap010 was not recovered at all durations of treatment, even the 10-minute treatment (Fig. 3.3D).

For seed quality assay of the hot water treatment trial with the 2021 seed lot, the incidence of seed with normal germination was affected significantly by temperature (P = 0.0650) but not duration (0.3330), and the interaction was significant (P < 0.0001) (Table 3.2). Non-treated seed had an average normal germination of 77.3 ± 4.2%. Rif-Pap010 at 25°C for 10 to 50 minutes ranged from (75.3 ± 4.0 to 81.5%). For seeds treated at 40°C, the percentage of normal germination did not differ significantly across the durations of treatment, and ranged from 73.8 ± 8.9 to 82.5 ± 5.7% (Fig. 3.3B). Results were similar for seeds treated at 45°C (range of 73.3 ± 11.8 to 80.3 ± 9% normal germination), with a slight increase in germination from the

20- to 30-minute duration and no differences for the 40- and 50-minute durations of treatment (Fig. 3.3B). Similarly, at 50°C, the incidences of normal seed germination for all durations of treatment were similar to those of the lower hot water treatment. In contrast, for seeds treated at 55°C, the incidence of seeds with normal germination was significantly greater for 20- to 50-minute durations of treatment, ranging from 86 ± 2.9 to 90.3 ± 1.7% (Fig. 3.3B). When seeds were treated at 60°C, the incidence of normal germination was greater for the three shortest durations (86.3 ± 2.6, 86.5 ± 3.1, and 81.8 ± 2.2% for 10, 20, and 30 minutes, respectively), which were similar statistically to those of the 55°C treatments. However, for the 40-minute duration of treatment at 60°C, there was a significant reduction in germination (to 68.0 ± 7.3%), and even further reduction for seeds treated for 50 minutes to 41.3 ± 5.8% (Fig. 3.3B).

For the 2023 lot, the main effect of temperature was highly significant ($P = 0.0002$), duration was not significant ($P = 0.6090$), and the interaction term was significant ($P < 0.0001$) for the effects on normal germination (Table 3.2). Rif-Pap010 at 25°C for 10 to 50 minutes ranged from 75 ± 4.4 to 86 ± 1.6%. Normal germination was greatest for seeds treated at 55°C for 30 minutes (92.0 ± 2.2%), which was significantly higher than for non-treated seeds (77.3 ± 4.2%), but not significantly different than for seeds treated at 55°C for 20 minutes (87.8 ± 1.0%) or at 60°C for 10 minutes (88.8 ± 1.8%) (Fig. 3.3E). Incidence of normal seed germination was not significantly different for seeds treated at 50°C for 50 minutes (87.5 ± 2.1%) and 55°C for 40 minutes (88 ± 0.8%) (Fig. 3.3E). In addition, no significant differences were detected at 25, 40, and 45°C treatments at all durations at 50°C for 10, 20, 30, and 40 minutes; at 55°C for 10, 40, or 50 minutes, and at 60°C for 20 and 30 minutes. Normal germination was reduced very significantly for seeds treated at 60°C for 40 and 50 minutes (to 60.5 ± 6.3 and 43.8 ± 7.1%, respectively) (Fig. 3.3E).

For the 2021 seed lot tested, the incidence of seeds with abnormal germination was not affected by the main effects of temperature (0.1441) or duration (0.7290), but there was a significant interaction (P = 0.08750) (Table 3.2). This is because abnormal germination was greater for seeds treated at 60°C for 50 minutes (35.0 ± 7.3%) (Fig. 3.3B). The non-treated seed had 17.8 ± 1.9%. Abnormal germination for seeds treated at 25°C averaged 17.5 ± 2.2% (Fig. 3.3B). The incidence of abnormal seed germination was least for seeds treated at 60°C for 20 minutes (7.8 ± 3.3%) or 55°C for 50 minutes (6.3% ± 2.1). For the 2023 trial, the main effect of temperature was significant (P = 0.0030) and the interaction of temperature and duration was highly significant (P <0.0001, Table 3.2) because treatment of the seeds at 60°C for 40 or 50 minutes significantly increased the incidence of abnormal germination to 19.8 ± 3.8 and 27.5 ± 5.1%, respectively, compared to 14.0 ± 2.4% for non-treated seed and 12.1 ± 1.7% for seed soaked in water at 25°C (Fig. 3.3E). The incidence of seeds with abnormal germination ranged from (8.0 ± 0.7 to 12.5 ± 3.4%) for seeds treated at 40°C for 10 to 50 minutes, 45°C for 10 to 50 minutes, 50°C for 10 to 40 minutes, 55°C for 10 minutes, and 60°C for 10 minutes. Treatment at 50°C for 50 minutes reduced the incidence of abnormal germination to 7.0 ± 1.5%, treatment at 55°C for 40 minutes reduced this to 6.0 ± 0.6%, treatment at 55°C for 30 minutes reduced abnormal germination to 3.8 ± 1.5% and treatment at 55°C for 50 minutes resulted in 4.3 ± 0.9% abnormal germination, with the latter significantly less than for all other treatments.

For the incidence of non-germinated seeds in the 2021 trial, there was a significant temperature main effect of (P = 0.0170) but the duration main effect and temperature-by-duration interaction effect were not significant (Table 3.2). Seed soaked at 25°C for 10 to 50 minutes had an incidence of non-germinated seed averaging 6.5 ± 2.1%. The incidence of non-germinated seeds increased to 13.3 ± 4.9 and 22 ± 4.4% for seeds treated at 60°C for 40 and 50

minutes, respectively, compared to 5.4 ± 0.9% for the non-treated seed (Fig. 3.3C). The incidence of non-germinated seeds was not significantly different for most of the other hot water treatments ranging from 3.3 ± 0.5 to 4.8 ± 1.1% for seeds treated at 40°C for 40 minutes, 45°C for 50 minutes, 50°C for 10 and 30 minutes, 55°C for 20 and 30 minutes, and 60°C for 10 minutes. The lowest incidence of non-germinated seeds was for the 55°C treatment for 50 minutes (3.0 ± 0.8%). For the 2023 trial, the main effect of temperature (P = 0.0040) and the temperature-by-duration effects (P = 0.0150) had significant incidences on the incidence of non-germinated seeds (Table 3.2). The incidence of non-germinated seeds was 7.5 ± 1.7% for non-treated seed. The highest incidence of non-germinated seeds for seeds treated at 60°C for 50 minutes (28.0 ± 2.7%) or 40 minutes (18.8 ± 3.0%), which were significantly greater than for the other hot water treatments (Fig. 3.3E). The incidence of non-germinated seeds was similar across the other treatments except for seeds treated at 55°C for 20 and 30 minutes (4.0 ± 0.8 and 4.0 ± 0.7%, respectively) (Fig. 3.3F).

The incidence of decayed seed in the 2021 trial was not affected significantly by temperature, duration, or the interaction of temperature and duration of hot water treatment (Table 3.3) and ranged from 0 to 2 ± 0.9%, with a mean of 0.6 ± 0.1% for the 2021 seed lot (Fig. 3.3C). In the 2023 trial, the incidence of decayed seed for the 2023 seed lot averaged 1.0 ± 0.4% for the control treatment at 25°C, while the non-treated seed had an incidence of 1.2 ± 0.5%, and was affected by temperature (P = 0.0250) only, not duration or the interaction effect (Table 3.2). The incidence of decayed seeds did not differ among hot water treatments (Fig. 3.3F).

Effect of decortication on seedborne rif-Pap010. For the decortication trial with 2021 seed lot, the highest amount of rif-Pap010 was recovered from the powder removed from the seed by decortication of the table beet seed samples with an average of $\log_{10}$4.9 ± 0.0 CFU/g

powder recovered compared to (log_{10}4.7 ± 0.1 CFU/g seed for the non-decorticated seed), and (log_{10}3.9 ± 0.1 CFU/g seed) for the decorticated seeds (P = <0.001). For the 2023 seed lot, the powder removed from the table beet seed pericarps by the decortication process averaged log_{10}4.77 ± 0.06 CFU/g powder compared to log_{10}3.1 ± 0.3 CFU/g seed for the non-decorticated seeds and log_{10}2.6 ± 0.1 CFU/g seed for the decorticated seeds (P <0.0001). The incidence of seeds with normal germination was significantly higher for the non-decorticated seeds than the decorticated seeds for both the 2021 and 2023 seed lots (Fig. 3.4). For the 2021 seed lot, non-decorticated seeds had a mean of 84.2 ± 1.9% normal germination whereas decorticated seeds had 69.0 ± 1.5% normal germination (P = 0.0034). Similarly, for the 2023 lot, non-decorticated seeds averaged 77.5 ± 2.5% normal germination vs. 41.8 ± 3.3% for decorticated seeds (P <0.001) (Fig. 3.4). The incidence of seeds with abnormal germination was greater for decorticated vs. non-decorticated for both seed lots (Fig. 3.4) with 11.3 ± 4.8 vs. 8.6 ± 1.7% for the 2021 lot, respectively (P = 0.6220); and 23.2 ± 2.76 vs. 10.8 ± 1.25% for the 2023 lot, respectively P = 0.0023. Similarly, the incidence of non-germinated seeds was greater for decorticated seeds with both seed lots (Fig. 3.4), with 16.3 ± 3.4% vs. 6.5 ± 2.0% for the 2021 seed lot, respectively (P = 0.0748), and 32.3 ± 2.9% vs. 5 ± 1.3% for the 2023 lot, respectively (P = 0.0023). The amount of decayed table beet seeds was greater for decorticated seeds (3.0 ± 0.6%) than non-decorticated seeds (1.0 ± 0.0%) for the 2021 lot (P = 0.068), but not for the 2023 seed lot (P = 0.7820), at 2.67 ± 0.76% vs. 3.00 ± 0.89%, respectively.

Discussion

Rif-Pap010 was not recovered from the embryos of 300 seed tested from infected table beet lots generated in each of 2021, 2022, and 2023 but was recovered from the pericarps of

these seed lots, demonstrating that rif-pap010 infection was limited to the pericarps of these lots. The amount of rif-Pap010 recovered from the pericarps differed among the three seed lots harvested from inoculated table beet seed crop field trials, most likely as a result of differences in weather conditions in the three seasons (Chapter 2). For the 2021 seed lot, 200-fold more seedborne rif-Pap010 was detected ($\log_{10}5.9 \pm 0.1$ CFU/g seed) compared to the 2022 lot ($\log_{10}2.5 \pm 0.4$ CFU/g), probably because the latter half of August and September 2021 was wetter and cooler compared to the 2022 season (Chapter 2). For the 2023 seed lot, a 100-fold increase in rif-Pap010 was recovered ($\log_{10}3.5$ CFU/g seed) compared to the 2022 seed lot, reflecting the fact that late August 2023 was characterized by warm days and cool nights that resulted in heavy dews, with rains in September creating conducive conditions for infection of the seed by rif-Pap010 compared to 2022, but less conducive than in 2021 (Chapter 2). Nonetheless, all three seed lots had comparatively low levels of infection based on some naturally infected lots having infection levels of $\log_{10}5$ to $\log_{10}7$ CFU/g seed (Crane 2023).

Treatment of the table beet seed lots generated in 2021 and 2023 with 1.2% NaOCl produced distinctly different results. For the 2021 seed lot, treatment with 1.2% NaOCl for as little as 5 minutes completely eradicated rif-Pap010 from the beet seed. On the contrary, treatment of the table beet seed generated in 2023 with 1.2% NaOCl for durations of 5, 15, 25, or 35 minutes did not eradicate the pathogen and did not reduce the amount of infection significantly compared to soaking the seeds in water for 5, 15, 25, or 35 minutes. The difference in rif-Pap010 recovery after NaOCl treatment for the two seed lots suggest that infection of the seed lot generated in 2021 was more limited to the surface of the pericarps, resulting in eradication of rif-Pap010 with as little as 5 minutes of treatment in 1.2% NaOCl, whereas infection of the seed generated in 2023 may have been located deeper within the pericarps. These

results indicate that chlorine seed treatment may only be effective for eradicating *P. syringae* pv. *aptata* when infection is limited to the seed surface. Studies with other seedborne bacterial pathogens and some fungal pathogens have shown that NaOCl can reduce infection located on the surface of seed (Carisse et al. 2000; Miller and Lewis Ivey; Toporek and Hudelson 2024). For example, Carisse et al. (2000) demonstrated that treating lettuce seeds infected with *Xanthomonas campestris* pv. *vitians* using 1% NaOCl for 5 and 20 minutes effectively reduced the incidence of infection without affecting seed germination adversely. However, the response of seeds to chlorine treatment can vary among crop species due to differences in seed size, structure, and architecture as well as the location of infection in the seed. As a result, chlorine seed treatments effective for one seed lot or for seed of one plant species may not yield the same results for other seed lots or seeds of other plant species (Maude 1996). This has been demonstrated also for some fungal seedborne pathogens (e.g., du Toit and Hernandez-Perez 2005).

Treatment of the rif-Pap010-infected table beet seed lots generated in 2021 and 2023 for 40 or 50 minutes in water heated to 55℃ or for as little as 10 minutes (the shortest duration tested) at 60℃ resulted in no recovery of rif-Pap010 from both lots. These results align with previous studies that demonstrated that temperatures >50℃ can eliminate some bacterial seed contaminants by causing protein denaturation, membrane disruption, and metabolic failure (Minchinton 1995; Sherf and MacNab 1986; Sutherland 1987). Hot water treatment of brassica seeds infected with *Xanthomonas campestris* pv. *campestris*, the causal agent of black rot, at 50℃ for 20 or 25 minutes, reduced the pathogen infection level 10,000-fold (Minchinton 1995). Similarly, hot water treatment of carrot seed at 53℃ for 10 minutes was effective at eradicating *X. campestris* pv. *carotae* (Nega et al. 2003; Temple et al. 2013). Treatment of the table beet

seed lots in this study at 60°C for longer than 30 minutes significantly reduced seed germination as a result of increasing the amount of abnormal germination and non-germination of seeds. While this length of time is much longer than required to eradicate rif-Pap010 in our tests, this demonstrates the potential risk of excessive head seed treatment at affecting seed quality adversely, as demonstrated in other studies on seedborne plant pathogens (e.g., du Toit and Hernandez-Perez). Higher seed moisture content enhances heat conductivity, increasing bacterial mortality while minimizing the need for prolonged seed exposure (Maude 1996).

While this study with beet seed lots infected with *P. syringae* pv. *aptata* supports the use of hot water seed treatment as a non-chemical, environmentally friendly seed sanitation method for management of seed lots infested with *P. syringae* pv. *aptata*, further studies are needed to assess the impact of these temperatures and durations on seed lots that are infected with higher levels of *P. syringae* pv. *aptata*. These studies need to include work to identify the minimum duration of treatment required to eradicate this pathogen, differences in the potential tolerances of different cultivars to hot water treatment, and if hydration of seed prior to treatment enhances the efficacy of hot water treatments.

Decortication of the 2021 and 2023 beet seed lots in this study, resulted in significant reductions in the amount of rif-Pap010 recovered from the decorticated seed. The decorticated table beet seeds consistently had less rif-Pap010 than decorticated seeds with ~1 and ~2-fold reduction in rif-Pap010 for the 2021 and 2023 seed lots, respectively. This indicates that seedborne inoculum resided primarily on the outer surface of the pericarps of the table beet seed lots, as has been demonstrated for several other seedborne bacterial pathogens (Maude 1996; Schuster and Coyne 1974), and potentially supported by the chlorine seed treatment trial for the 2021 seed lot. While the removal of the outer part of the pericarp in beet seed has the potential

can be effective to reduce seedborne inoculum levels and potential to enhance the effectiveness of some types of seed treatments (Tekrony 1967). The greater reduction in the amount of rif-Pap010 recovered from the 2023 seed lot vs. the 2021 lot was likely due to the lower infection level of the seed lot generated in 2023 (log_{10}3.5 CFU/g seed) vs. 2021 (log_{10}5.9 CFU/g seed).

Decortication of the two table beet seed lots negatively affected seed germination. The non-decorticated seeds had significantly more normal germination than the decorticated seeds. This is contrary to what has been documented in some other studies in which decortication improved seed germination by facilitating quicker and more uniform germination as a result of facilitating the seeds to imbibing moisture more rapidly (TeKrony 1967). The reduction in seed germination of the decorticated table beet seed in this study might reflect the duration and severity of decortication having damaged the seed mechanically. Previous studies have shown that removal of the pericarp can expose seeds to mechanical damage and increase susceptibility to desiccation (Bewley et al. 2013). The incidence of abnormal seed germination was greater for the decorticated seeds compared to non-decorticated seeds, which further supports the likelihood of the decortication protocol used in this study having caused physical damage that impacted germination (Copeland and McDonald 2012).

In summary, this study provided valuable insights into the location of rif-Pap010 infection in three table beet seed lots generated in inoculated table beet seed crop field trials, the efficacy of hot water and bleach seed treatments for reducing seedborne inoculum, and the impact of decortication on seedborne *P. syringae* pv. *aptata*. Rif-Pap010 infection was restricted to the pericarp for all three seed lots. Environmental factors during seed crop development, such as temperature and humidity, appear to have had a significant influence on rif-Pap010 infection of the seed. The efficacy of 1.2% NaOCl seed treatments for eradicating rif-Pap010 varied

between the two seed lots, indicating that the location of infection by the pathogen plays a major role in efficacy of disinfectant seed treatment for control of seedborne inoculum. For the 2021 seed lot, rif-Pap010 was eradicated from the seed within as little as 5 minutes of treatment with 1.2% NaOCl, but treatment of the 2023 lot with 1.2% NaOCl for 5, 15, 25, or 35 minutes failed to eradicate the pathogen, likely due to rif-Pap010 being embedded deeper within the pericarps of the 2023 seed lot.

Hot water treatment at 55°C for 40 to 50 minutes or at 60°C for 10 to 30 minutes was effective at eradicating rif-Pap010 populations from the two beet seed lots tested without adversely affecting seed quality, reinforcing prior studies on hot water treatment to disrupt bacterial survival on seed (Minchinton 1995; Sherf and MacNab 1986; Sutherland 1987). However, exposure of table beet seed to hot water treatment at 60°C for >30 minutes significantly reduced seed germination, confirming that higher temperatures can compromise seed quality and viability (Nega et al. 2003). Future studies could focus on evaluating hot water treatments with more severely infested seed lots, as seed companies have reported that table beet seed lots with high levels of *P. syringae* pv. *aptata* are difficult or impossible to clean without also adversely affecting seed quality.

The effect of decortication on rif-Pap010 recovery and seed germination highlighted both the benefits and potential drawbacks of partial pericarp removal. Decorticated seeds consistently harbored less rif-Pap010 than non-decorticated seeds (Maude 1996; Schuster and Coyne 1974), but the level of decortication of the table beet seeds in this study reduced normal germination and increased abnormal germination as a result of mechanical damage to the seed (Bewley et al. 2013; Copeland and McDonald 2012). These findings underscore the need to balance pathogen reduction with seed integrity when considering decortication as a sanitation strategy.

Acknowledgements

We acknowledge the program of Dr. Carolee Bull for generating a rifampicin resistant strain of *P. syringae* pv. *aptata* Pap010 for this study. We thank members of the Vegetable Seed Pathology Program at the WSU Mount Vernon NWREC, including Alex Batson, Babette Gundersen, Michael Derie, Kayla Spawton, and Tomasita Villaroel, for technical assistance. This work was funded by the United States Department of Agriculture National Institute of Food and Agriculture Specialty Crops Research Initiative Project No. 2019-51181-30019, the Dick and Marcia Morrison Seed Production Pathology & Seed Health Fellowship, the Alfred Mark Christianson Memorial Fellowship, a Pacific Seed Association Scholarship, and the WSU College of Agricultural, Human, and Natural Resource Sciences Hatch Project No. WNP0001.

Literature Cited

Abo-Elwafa, S. F., Abdel-Rahim, H. M., Abou-Salama, A. M., and Teama, E. A. 2006. Sugar beet floral induction and fertility. Effect of vernalization and day-length extension. Sugar Tech. 8:281-287.

Association of Official Seed Analysts. 2008. Principles and procedures. Pp. 6-57, In: Germination Tests. Rules for Testing Seeds. AOSA, Ithaca, NY.

Babadoost, M. 1992. Vegetable seed treatment. University of Illinois at Urbana-Champaign, Department of Crop Sciences. RPD No. 915. http://ipm.illinois.edu/diseases/rpds/915.pdf. Accessed 1 Apr. 2024.

Bainer, R., and Leach, L. D. 1946. Processing sugar beet seed by decortication, burr reduction and segmentation. Proc. Am. Soc. Sugar Beet Tech. 4:625-639.

Bewley, J. D., Bradford, K. J., Hilhorst, H.W.M., and Nonogaki, H. 2013. Seeds: Physiology of Development, Germination and Dormancy, Third Edition. Springer, New York.

Brown, N. A., and Jamieson, C. O. 1913. A bacterium causing a disease of sugar beet and nasturtium leaves. J. Agric. Res. 1:189-210.

Carisse, O., Ouimet, A., Toussaint, V., and Philion, V. 2000. Evaluation of the effect of seed treatments, bactericides, and cultivars on bacterial leaf spot of lettuce caused by *Xanthomonas campestris* pv. *vitians.* Plant Dis. 84:295-299.

Copeland, L. O., and McDonald, M. B. 2012. Principles of Seed Science and Technology, Fourth Edition. Springer, New York.

Crane, A. S. 2023. Seed transmission of *Pseudomonas syringae* pv. *aptata*, and efficacy of bactericides for control of the pathogen in beet and Swiss chard seed production. MS thesis. Washington State University, Pullman. 63 pp.

Dekock, P. C., Hunter, P. F., and MacDonald, I. 1953. A germination inhibitor in sugarbeet. J. Exp. Bot. 4:272-282.

Derie, M. L., Holmes, B. J., Safni, I., Bull, C. T., and du Toit, L. J. 2016. Seedborne inoculum thresholds of *Pseudomonas syringae* pv. *aptata*, causal agent of bacterial leaf spot, in 'baby leaf' Swiss chard crops. Phytopathology 106:S4.142 (Abstr.).

du Toit, L. J. 2007. Crop Profile for Table Beet Seed in Washington. USDA Pest Management Centers. http://www.ipmcenters.org/CropProfiles/docs/WAbeetseed.pdf. Accessed 12 Mar. 2024.

du Toit, L. J., and Hernandez-Perez, P. 2005. Efficacy of hot water and chlorine for eradication of *Cladosporium variabile*, *Stemphylium botryosum*, and *Verticillium dahliae* from spinach seed. Plant Dis. 89:1305-1312.

Germains Seed Technology. https://germains.com/us/product-category/seed-health-us/. Accessed 12 Nov. 2024.

Hakalová, E., Tekielska, D. A., Wohlmuth, J., and Čechová, J. 2024. Management of bacterial blight of carrots by phenolic compound treatments. PloS One 19:e0299105.

Harveson, R. M., Hanson, L. E., and Hein, G. L., Editors. 2009. Compendium of Beet Diseases and Pests, Second Edition. The American Phytopathological Society, St. Paul.

Jacobsen, B. J. 2009. Bacterial leaf spot. Pp. 59-60, In: Compendium of Beet Diseases and Pests, Second Edition. R. M. Harveson, L. E. Hanson, and G. L. Hein, editors. The American Phytopathological Society, St. Paul.

Kockelmann, A., Tilcher, R., and Fischer, U. 2010. Seed production and processing. Sugar Tech. 12:267-275.

Koike, S. T., Henderson, D. M., Bull, C. T., Goldman, P. H., and Lewen, R. T. 2003. First report of bacterial leaf spot of Swiss chard caused by *Pseudomonas syringae* pv. *aptata* in California. Plant Dis. 87:1397.

Leben, C. 1974. Survival of plant pathogenic bacteria. Ohio Agric. Res. Dev. Cent. Spec. Circ. 100. 21 pp.

Leben, C. 1983. Chemicals plus heat as seed treatments for control of angular leaf spot of cucumber seedlings. Plant Dis. 67:991-993.

Lin, B. H., Jayachandran, N. V., Jane, A., and John, C. 2003. Food and Agricultural Commodity Consumption in the United States: Looking Ahead to 2020. USDA Economic Research Service, AER-820. https://www.ers.usda.gov/webdocs/publications/42576/19268_aib792-7_1_.pdf?v=0. Accessed 1 Apr. 2024.

Maude, R. B. 1996. Seedborne Diseases and Their Control: Principles and Practice. CAB International, Wallingford.

Maude, R. B., Vizor, A. S., and Shuring, C. G. 1969. The control of fungal seedborne diseases by means of a thiram seed soak. Ann. Appl. Biol. 64:245-257.

McGee, D. C. 1995. Epidemiological approach to disease management through seed technology Annu. Rev. Phytopathol. 33:445-466.

Miller, S. A., and Lewis Ivey, M. L. 2024. Hot water and chlorine treatments to eradicate bacterial plant pathogens from vegetable seeds. The Ohio State University Extension Factsheet HYG 5818. https://ohioline.osu.edu/factsheet/hyg-5818. Accessed 10 Jan. 2025.

Minchinton, E. J. 1995. Control of black rot contamination in *Brassica* seeds. Horticultural Research and Development Corp. https://ausveg.com.au/app/data/technical-insights/docs/VG204. Accessed 23 Jan. 2025.

Miyamoto, T. 1957. The germination inhibitor in sugarbeet seedballs. Quart. Bull. Mich. Agric. Expt. Sta. 39:518-525.

Mohan, S. K., and Schaad, N. W. 1987. An improved agar plating assay for detecting *Pseudomonas syringae* pv. *syringae* and *Pseudomonas syringae* pv. *phaseolicola* in contaminated bean seed. Phytopathology 77:1390-1395.

Nampijja, M., Derie, M. L., and du Toit, L. J. 2021. First report of bacterial leaf spot caused by *Pseudomonas syringae* pv. *aptata* on Swiss chard, *Beta vulgaris* subsp. *vulgaris*, in Arizona. Plant Dis. 105:3738.

Navazio, J., Colley, M., and Zyskowski, J. 2010. Principles and Practices of Organic Beet Seed Production in the Pacific Northwest. Organic Seed Alliance, Port Townsend.

Nega, E., Ulrich, R., Werner, S., and Jahn, M. 2003. Hot water treatment of vegetable seed – an alternative seed treatment method to control seed-borne pathogens in organic farming. J. Plant Dis. Prot. 110:220-234.

Nikolić, I., Stanković, S., Dimkić, I., Berić, T., Stojšin, V., Janse, J., and Popović, T. 2018. Genetic diversity and pathogenicity of *Pseudomonas syringae* pv. *aptata* isolated from sugar beet. Plant Pathol. 67:1194-1207.

Organic Seed Alliance. 2016. Climatic Considerations for Seed Crops: Guidelines and Field Trainings for Organic and Specialty Vegetable Seed Producers. https://seedalliance.org/. Accessed 16 Jul. 2024.

Peck, N. H., Clark, B. E., and Natti, J. J. 1967. Effect of decortication and fungicide on performance of table beet seed. Agron. J. 59:78-80.

Rackham, L. R. 2002. History of Specialty Seed Crop Production in the Pacific Northwest. Willamette Valley Specialty Seed Crops Association, Corvallis.

Riffaud, C. M. H., and Morris, C. E. 2002. Detection of *Pseudomonas syringae* pv. *aptata* in irrigation water retention basins by immuno-fluorescence colony staining. Eur. J. Plant Pathol. 108:539-545.

Safni, I., Ramos-Sepulveda, L., Goldman, P., Derie, M., du Toit, L., Koike, S., Stockwell, V., and Bull, C. 2016. Genetic diversity of *Pseudomonas syringae* causing bacterial leaf spot on table beet (*Beta vulgaris*) and Swiss chard (*Beta vulgaris* subsp. *cicla*). Phytopathology 106:S4.143 (Abstr.).

Sakudo, A., Haritani, M., Furusaki, K., Onishi, R., and Onodera, T. 2020. Electrically charged disinfectant containing calcium hydrogen carbonate mesoscopic crystals as a potential measure to control *Xanthomonas campestris* pv. *campestris* on cabbage seeds. Microorganisms 8:1606.

Schreiber, A., and Ritchie, L. 1995. Washington Minor Crops. Food and Environmental Quality Laboratory, Washington State University, Richland.

Schuster, M. L. and Coyne, D. P. 1974. Survival and transmission of seedborne bacterial pathogens in crops. Annu. Rev. Phytopathol. 12:199-221.

Sherf, A. F. and MacNab, A. A. 1986. Vegetable Diseases and Their Control. John Wiley and Sons, New York.

Sutherland, J. 1987. Control of seed-borne diseases with a hot-water bath. Agnote Order No. 3660/87. 2 pp.

TeKrony, D. M. 1967. Germination potential in monogerm seed of *Beta* v*ulgaris* L. MS thesis, Oregon State University, Corvallis. 51 pp.

Temple, T. N., du Toit, L. J., Derie, M. L., and Jonson, K. B. 2013. Quantitative molecular detection of *Xanthomonas hortorum* pv. *carotae* in carrot seed before and after hot water treatment. Plant Dis. 97:1585-1592.

Toporek, S., and Hudelson, B. 2024. Hot-water seed treatment for disease management. University of Wisconsin-Madison Plant Disease Factsheet D0064. https://hort.extension.wisc.edu/articles/hot-water-seed-treatment-for-disease-management/. Accessed 28 Feb. 2025.

Universal Seed LLC. 2024. Seed disinfection. https://universalseed.com/disinfection.html. Accessed 12 Nov. 2024.

Vicente, J. G., and Holub, E. B. 2013. *Xanthomonas campestris* pv. *campestris* (cause of black rot of crucifers) in the genomic era is still a worldwide threat to brassica crops. Mol. Plant. Pathol.14:2-18.

Weller, D. M., and Saettler, A.W. 1978. Rifampin-resistant *Xanthomonas phaseoli* var. *fuscans* and *Xanthomonas phaseoli*: Tools for field study of bean blight bacteria. Phytopathology 68:778-781.

Table 3.1. Analyses of variance for seed germination assays and seed health assays of table beet seed infected with a rifampicin resistant strain of *Pseudomonas syringae* pv. *aptata* (rif-Ppa010) and treated with 1.2% sodium hypochlorite or water for 5, 15, 25, and 35 minutes[a]

Assay and dependent variables	Trial 1						Trial 2					
			P value						*P* value			
	R^{2b}	CV (%)[c]	Rep	Trt	Dur	Trt × Dur	R^{2b}	CV (%)[c]	Rep	Trt	Dur	Trt × Dur
Seed health assay[e]	-	-	-	-	-	-	0.3000	52.11	1.0000	0.3030	0.2410	0.3640
Seed germination assay (%)[d]												
Normal germination	0.570	7.14	-	0.4540	**0.0660**	**0.0770**	0.3080	7.12	-	0.3922	0.3332	0.9887
Abnormal germination	0.480	57.57	-	0.6020	0.7850	0.1470	0.2750	40.13	-	0.4101	0.5063	0.6446
Non-germinated seed	0.660	63.81	-	**0.0310**	**0.0270**	0.3780	0.2750	50.80	-	0.2090	0.7760	0.7760
Decayed seed[e]	0.110	49.12	1.000	0.6360	0.8530	0.6590	0.1950	36.00	1.0000	0.5910	0.2360	0.9700

[a] Each trial consisted of a randomized complete block design with four replications (Rep) of 5,000 seeds from a seed lot infected with a rifampicin resistant strain of *P. syringae* pv. *aptata* (rif-Pap010). The seeds were treated with1.2% NaOCl or deionized water (Trt) for durations (Dur) of 5, 15, 25, and 35 minutes. Infected table beet seed lots were generated in 2021 (Trial 1) and 2023 (Trial 2). Analysis of variance was not conducted for seed samples treated with 1.2% NaOCl in Trial 1 because colonies were not recovered from any of the seed. Non-treated seed was excluded from the analysis.

[b] R^2 = coefficient of determination.

[c] CV = coefficient of variation.

[d] For each replication of each treatment, 100 seeds were subjected to the blotter germination assay of the Association of Official Seed Analysts (2008).

[e] Data for Trials 1 and 2 that were analyzed using Friedman's nonparametric rank test because of non-normal residuals and heterogeneous variances. Bold font indicates significance at $P \leq 0.10$.

Table 3.2. Analyses of variance for seed germination assays and seed health assays of table beet seed lots infected with a rifampicin resistant strain of *Pseudomonas syringae* pv. *aptata* (rif-Pap010) and treated with water heated to 25, 40, 45, 50, 55, and 60°C for durations ranging from 0 to 50 minutes

			***P* value**				
Trial, assay and dependent variable[a]	***R*²[c]**	**CV (%)[d]**	**Rep**	**Temp**	**Rep × Temp**	**Dur**	**Dur × Temp**
Trial 1[b]							
Seed health assay							
CFU rif-Pap010/g seed[eg]	0.795	95.59	**<0.0001**[g]	**<0.0016**	**0.0002**	**0.0015**	0.5889
Germination assay (%)							
Normal germination	0.800	18.40	**0.0001**	**0.0650**	-	0.3330	**<0.0001**
Abnormal germination[g]	0.480	51.40	1.0000	0.1440	0.2205	0.7296	**0.0875**
Non-germinated seed	0.492	28.10	**0.0156**	**0.0170**	-	0.9140	0.1280
Decayed seed[g]	0.507	37.30	0.9694	0.1969	**0.0809**	0.2021	0.2285
Trial 2[b]							
Seed health assay							
CFU rif-Pap010/g seed[g]	0.850	27.50	1.000	**<0.0001**	**0.058**	**<0.0001**	**0.0010**
Germination assay (%)[g]							
Normal germination	0.750	35.20	1.000	<**0.0002**	**0.0370**	0.6090	**<0.0001**
Abnormal germination	0.690	39.70	1.000	**0.0030**	0.1050	0.6330	**<0.0001**
Non-germinated seed	0.490	50.70	1.000	**0.0040**	0.8930	0.2210	**0.0150**
Decayed seed	0.470	40.50	1.000	**0.0250**	0.4310	0.1720	0.2970

[a] Each trial consisted of a split-plot, randomized complete block design with four replications. Temp = water temperatures of 25, 40, 45, 50, 55, or 60ºC (whole plots); Rep = replication; Dur = durations of 10, 20, 30, 40, or 50 minutes of treatment (split plots); data for seeds not treated were excluded from the analysis.

[b] Table beet seed lot generated in 2021 (Trial 1) and 2023 (Trial 2).

[c] R^2 = coefficient of determination.

[d] CV = coefficient of variation.

[e] For Trial 1, CFU of rif-Pap010 recovered from seeds treated at 25ºC were not included in the analysis due to inadequate seed available, so only one replication of those treatments were included.

[f] For each replication of each treatment combination, 100 seeds were subjected to the blotter germination assay of the Association of Official Seed Analysts (2008).

[g] Data in Trials 1 and 2 were analyzed using Friedman's nonparametric rank test because of non-normal residuals and/or heterogeneous variances. Bold font indicates significance at $P \leq 0.10$.

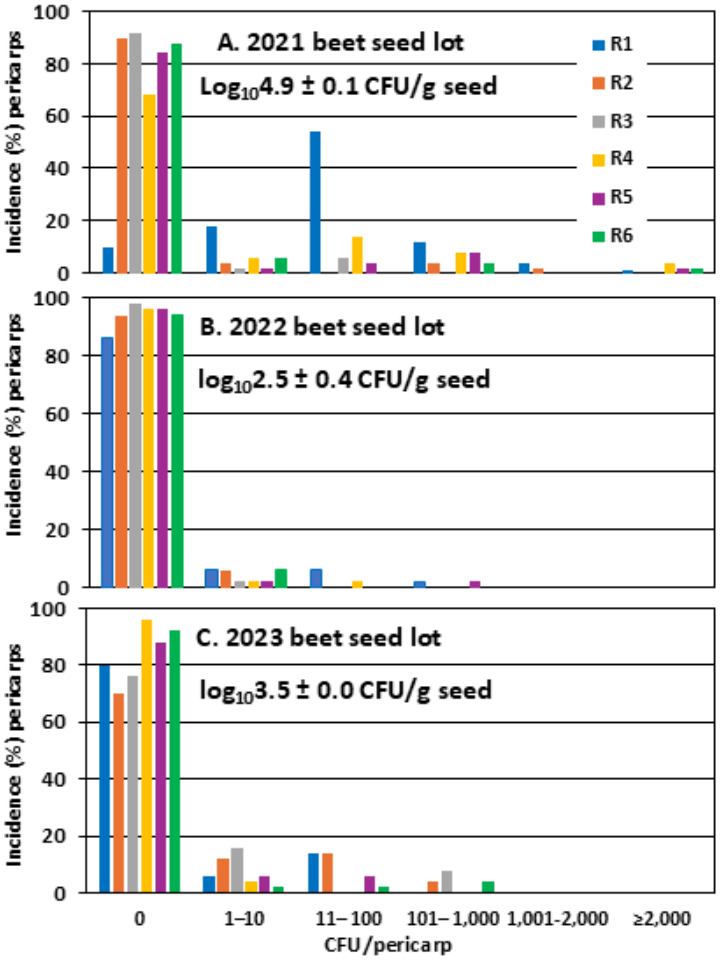

Fig. 3.1. Incidence (%) of six replications of 50 table beet seed pericarps and embryos infected with a rifampicin-resistant strain of *Pseudomonas syringae* pv. *aptata* (rif-Pap010) from seed lots of a proprietary cultivar harvested from an inoculated beet seed crop field trial in each of 2021 (A), 2022 (B), and 2023 (C). Rif-Pap010 was not recovered from any of the 300 embryos tested from each of the 2021, 2022, and 2023 seed lots. R1 to R6 represent the six replications of 50 seeds assayed for each seed lot. CFU/pericarp = range in colony forming units (CFU) recovered per pericarp.

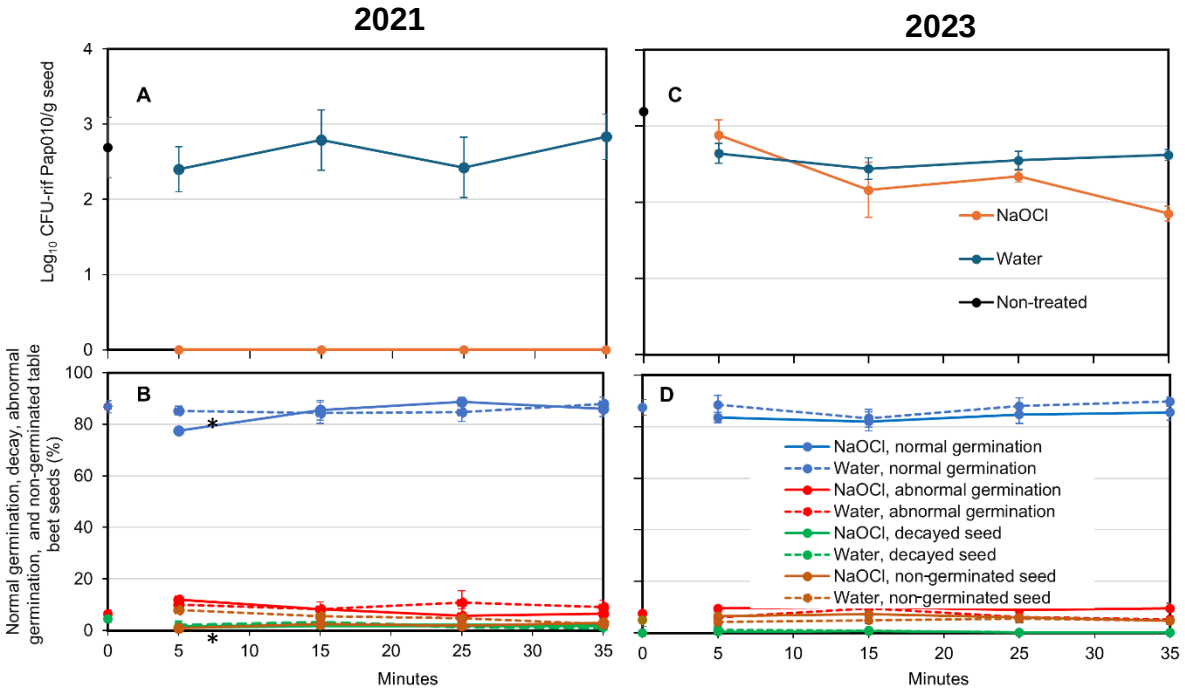

Fig. 3.2. Efficacy of seed treatment with 1.2% NaOCl or deionized water for 0, 5, 15, 25, and 35 minutes on eradication of a rifampicin resistant strain of *Pseudomonas syringae* pv. *aptata* (rif-Pap010) from two table beet seed lots of a proprietary cultivar (A and C). The infected seed lots were generated in 2021 (A and B) and 2023 (C and D). Percentage of treated seed with normal germination, abnormal germination, decay, or non-germination (B and D). For the seed health assays (A and C), each data point shows the mean ± standard error (SE) for 4 replications of 5,000 seeds. For the seed germination assays (B and D), each 4 data point represents the mean ± SE for 4 replications of 100 seeds subjected to the blotter germination assay of the Association of Official Seed Analysts (2008). Asterix indicate means that were significantly different.

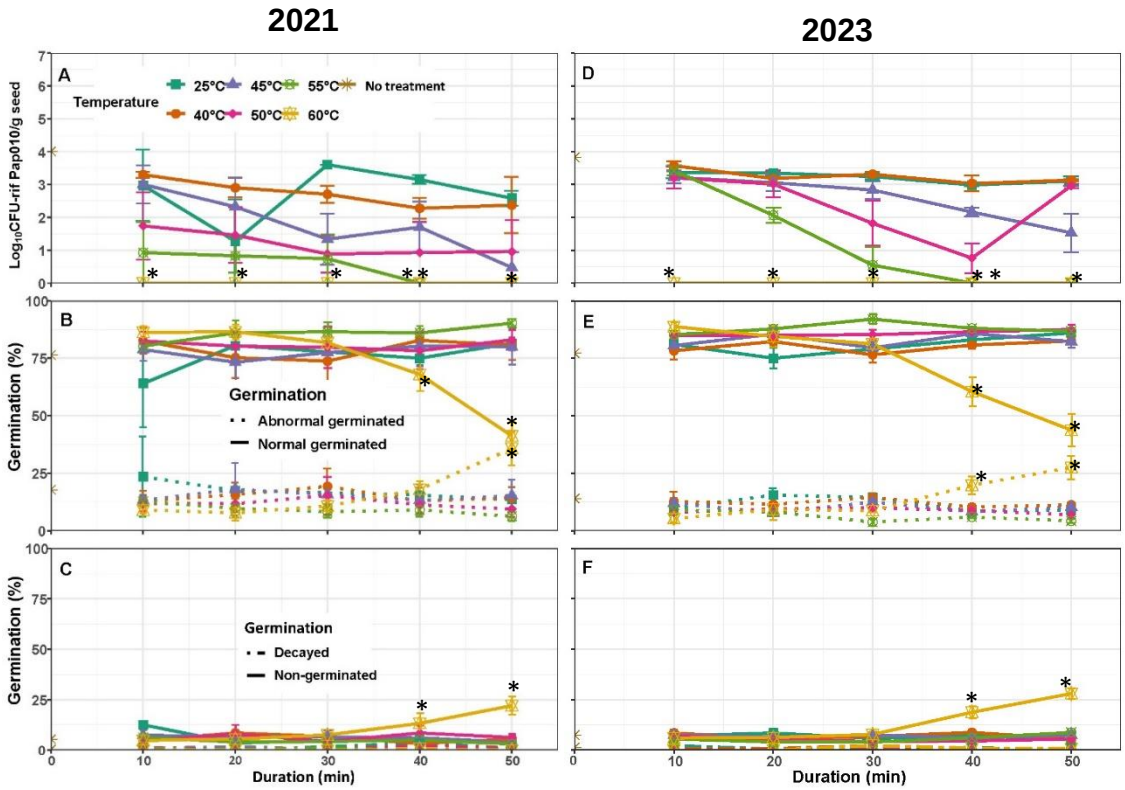

Fig. 3.3. Efficacy of hot water treatment for eradication of a rifampicin-resistant strain of *Pseudomonas syringae* pv. *aptata* (rif-Pap010) from table beet seed lots of a proprietary cultivar generated in 2021 and 2023 after hot water treatment at 25, 40, 45, 50, 55, and 60°C for durations of 0, 10, 20, 30, 40, and 50 minutes (A and D). Percentage of normal and abnormal seed germination (B and E), and non-germinated and decayed seed (C and F) following treatment. For each replication of each treatment combination, 100 seeds were subjected to the blotter germination assay the Association of Official Seed Analysts (2008). Each data point shows the mean ± standard error for 4 replications of 2,500 (A) or 5,000 (D) seeds in the seed health assays and 100 seeds for the germination assay (B, C, E, and F). Asterisks indicate the means that were significantly different.

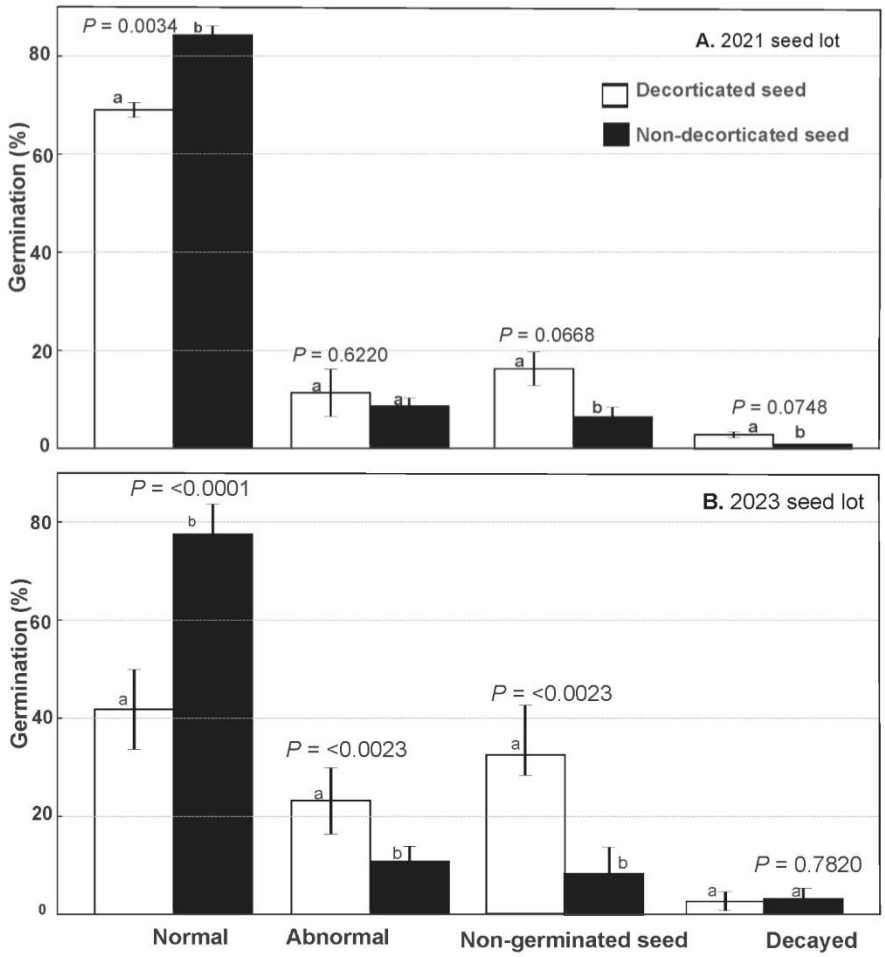

Fig. 3.4. Percentage of seed with normal germination, abnormal germination, decay, or non-germinated for decorticated and non-decorticated seeds of a table beet seed lot infected with a rifampicin-resistant strain of *Pseudomonas syringae* pv. *aptata* (rif-Pap010), harvested from an inoculated table beet seed crop trial in 2021 (A) and 2023 (B). Each bar represents the mean ± standard error of 3 (A) and 6 (B) replicate samples of 100 decorticated and 100 non-decorticated seeds that were subjected to the blotter germination assay of the Association of Official Seed Analysts (2008). Means with the same letters are not significantly different based on Tukey's honestly significant difference (HSD) at $P \leq 0.10$.